UNIVERSIDADE DO PORTO

INSTITUTO DE CIÊNCIAS BIOMÉDICAS DE ABEL SALAZAR

INSIGHTS ON SIGNAL TRANSDUCTION PATHWAYS INVOLVED IN FAMILIAL AMYLOIDOTIC POLYNEUROPATHY NEURODEGENERATION

FILIPE ALMEIDA MONTEIRO

Dissertação de doutoramento em Ciências Biomédicas

2006

UNIVERSIDADE DO PORTO

INSTITUTO DE CIÊNCIAS BIOMÉDICAS DE ABEL SALAZAR

INSIGHTS ON SIGNAL TRANSDUCTION PATHWAYS INVOLVED IN FAMILIAL AMYLOIDOTIC POLYNEUROPATHY NEURODEGENERATION

FILIPE ALMEIDA MONTEIRO

Dissertação de doutoramento em Ciências Biomédicas

2006

UNIVERSIDADE DO PORTO

INSTITUTO DE CIÊNCIAS BIOMÉDICAS DE ABEL SALAZAR

INSIGHTS ON SIGNAL TRANSDUCTION PATHWAYS INVOLVED IN FAMILIAL AMYLOIDOTIC POLYNEUROPATHY NEURODEGENERATION

FILIPE ALMEIDA MONTEIRO

Dissertação de Candidatura ao grau de Doutor em Ciências Biomédicas submetida ao Instituto de Ciências Biomédicas de Abel Salazar

Orientador: Maria João Gameiro de Mascarenhas Saraiva, Professora Catedrática, Departamento de Biologia Molecular, Instituto de Ciências Biomédicas de Abel Salazar, Universidade do Porto.

Co-orientador: Mónica Luísa Ribeiro Mendes de Sousa, Investigadora Auxiliar, Instituto de Biologia Molecular e Celular; e Professora Auxiliar Convidada, Departamento de Biologia Molecular, Instituto de Ciências Biomédicas de Abel Salazar, Universidade do Porto.

Preceitos legais

De acordo com o disposto no Decreto-Lei nº216/92 de 13 de Outubro e no Regulamento de Doutoramento pela Universidade do Porto, esclarece-se serem da nossa responsabilidade a execução das experiências que permitiram a obtenção dos resultados apresentados, excepto quando referido em contrário, assim como a sua interpretação e discussão.
Nesta dissertação foram apresentados os resultados contidos nos artigos publicados ou em vias de publicação seguidamente mencionados:

Monteiro FA, Cardoso I, Sousa MM, Saraiva MJ. (2006). In vitro inhibition of transthyretin aggregate-induced cytotoxicity by full and peptide derived forms of the soluble receptor for advanced glycation end products (RAGE). *FEBS Lett.* 580:3451-3456.

Monteiro FA, Sousa MM, Cardoso I, do Amaral JB, Guimarães A, Saraiva MJ. (2006). Activation of ERK1/2 MAP kinases in familial amyloidotic polyneuropathy. *J Neurochem.* 97:151-161.

Monteiro FA and Saraiva MJ. High mobility group protein 1: a marker of cytotoxicity in familial amyloidotic polyneuropathy. *In preparation.*

Monteiro FA and Saraiva MJ. Transcription factors interplay in familial amyloidotic polyneuropathy. *In preparation.*

À Nanda por tudo o que vivemos juntos...

Sem ti não teria sido tão especial!

Acknowledgements

À minha orientadora, Profª Maria João Saraiva, por todo o apoio e orientação científica. Gostaria de salientar o facto de ter sempre a porta aberta para nos ouvir e a sua capacidade e energia inesgotável para acompanhar de perto o desenvolvimento do nosso trabalho, apesar dos inúmeros afazeres.

À minha co-orientadora, Mónica Sousa, sempre presente e empenhada ajudando-me a vencer cada obstáculo. Um exemplo em ciência!

À Isabel Cardoso, cuja contribuição foi decisiva para que parte do trabalho aqui desenvolvido se traduzisse em duas publicações científicas.

Ao professor Miguel Soares, pela revisão desta dissertação a qual melhorou significativamente este documento.

Ao laboratório da Neurobiologia Molecular, a todos os que aqui estão e aos que por aqui passaram deixo expresso o meu reconhecimento de que ao compartilharem comigo todos estes anos, dia após dia, contribuíram para esta tese. Vocês são a minha segunda família!!!

Às pessoas dentro e fora do IBMC que de alguma forma contribuíram para esta tese, agradeço o vosso apoio.

Ao laboratório do Prof. Edgar e da Profª Odete, que me acompanharam nas minhas primeiras incursões laboratoriais.

Au laboratoire du Dr Jean-Michel Drezen de m'avoir accueilli comment élève de ERASMUS et avoir réveillé dans moi le goût par l'investigation scientifique. Un remerciement très spécial pour Dr Elisabeth Huguet.

À Nanda, cujo amor, dedicação e incentivo nunca faltaram ao longo destes anos tornando esta tese possível!

Um agradecimento muito especial aos meus pais e irmã, por me terem incutido os valores que me permitem ser... como sou.

Agradeço o apoio financeiro disponibilizado pela Fundação para a Ciência e a Tecnologia (SFRH/BD/4563/2001) e Fundação Luso-Americana para o Desenvolvimento, a qual me deu a oportunidade de trabalhar durante 5 meses no laboratório do Dr David Stern em Nova Iorque.

Table of contents

Summary

The hallmark of familial amyloidotic polyneuropathy (FAP) is the deposition of amyloid in the peripheral nervous system. Transthyretin (TTR) is the major component of amyloid fibrils, which have a systemic extracellular distribution throughout the connective tissue of several organs, being the brain and liver parenchyma spared. Several point mutations in TTR have been described and most are associated with FAP, an autosomal dominant disease. Physiologically, TTR is a plasma tetrameric protein of four 14 kDa identical subunits that functions as a carrier for thyroxine (T_4) and retinol (vitamin A) by formation of a 1:1 molar complex with retinol binding protein (RBP). The precise mechanisms underlying TTR amyloid fibril formation and neurodegeneration in FAP are poorly understood.

In FAP pathological process, the receptor for advanced glycation end products (RAGE) has been implicated in signal transducing cytotoxic effects of extracellular deposited TTR. The structural basis of the RAGE-ligand interaction is currently not well defined. Here we have shown that TTR interaction with RAGE is conserved across mouse and human species and is not dependent on RAGE glycosylation. Moreover, strand D of TTR structure seems important for the TTR-RAGE interaction as well as a motif in RAGE (residues 102-118) located within the V-domain; this motif suppressed TTR aggregate-induced cytotoxicity in cell culture. These studies might allow the design of therapeutical strategies aiming to block TTR access to RAGE.

Previous studies demonstrated that nerves from asymptomatic carriers of TTR Val30Met variant, present TTR deposited in an aggregated non-fibrillar form prior to the formation of amyloid fibrils and signs of oxidative/inflammatory stress were already evident. Subsequent studies showed that non-fibrillar TTR aggregates, but not mature fibrils, are toxic to cells *in vitro*. However, the molecular signaling mechanisms related to neurodegeneration in FAP are largely unknown. We have addressed this issue using several methodologies aiming to search for differentially expressed genes and proteins in FAP pathology. FAP salivary gland (SG) biopsies were used to perform antibody microarrays. From the differentially expressed proteins, a few candidates were selected for further analysis. Up-regulation of chondroitin sulfate proteoglycans (CSPG) in FAP SG was observed. These preliminary data on CSPG up-regulation are interesting as it suggests a likely role in the inflammation process and/or in facilitating amyloidogenesis in FAP.

Previously, mRNA microarray analysis was performed in SG from FAP patients and displayed mitogen-activated protein (MAP) kinase phosphatase 1 (MKP-1) down-

regulation. We further validated this result by other techniques. MKP-3 was also down-regulated in FAP SG biopsies. Given the relationship between MKPs and MAPKs, the later were investigated. Only extracellular signal-regulated kinases 1/2 (ERK1/2) displayed increased activation in FAP SG and nerves. ERK1/2 kinase (MEK1/2) activation was also up-regulated in FAP nerves. In addition, a FAP transgenic mouse model revealed increased ERK1/2 activation in peripheral nerve affected with TTR deposition when compared to control animals. Treatment of a Schwannoma cell line with TTR aggregates stimulated ERK1/2 activation, which was partially mediated by RAGE suggesting the possible involvement of other cellular receptors. Moreover, caspase-3 activation triggered by TTR aggregates was suppressed by U0126, a MEK1/2 inhibitor, indicating that ERK1/2 activation is essential for TTR aggregate-induced cytotoxicity. Taken together, these data suggest that abnormally sustained activation of ERK in FAP may represent an early signaling cascade leading to neurodegeneration.

Previous studies have shown that TTR aggregates interaction with RAGE induces activation of NFκB, a transcription factor most likely involved in induction of inflammatory and oxidative stress-related genes in FAP. We have pursued to unravel the participation of other transcription factors, such as the ones activated by MAPKs. We have shown that activation of Elk-1 is down-regulated in FAP SG and nerves from asymptomatic carriers, which is possibly related to ERK1/2 negative feedback modulation. Other transcription factors, such as ATF-2 and c-Jun presented different activations in FAP SG and nerves from asymptomatic carriers, suggesting tissue specific pathways to be further investigated. Our preliminary data suggest a complex interplay between selected transcription factors in FAP, but give guidance for further investigation on pathways not addressed herein.

Recently, high mobility group box 1 (HMGB1) protein was reported to be implicated in Alzheimer's disease (AD) pathology, another amyloid-related disorder. Here we investigated whether HMGB1 expression is altered in FAP. We have found that HMGB1 was relocated from the nucleus to the cytosol of epithelial cells of FAP SG. In FAP nerves, HMGB1 expression was up-regulated in axons. To access HMGB1 subcellular localization in sensorial neurons, we have used dorsal root ganglia (DRG) from a FAP transgenic mouse model. In this model, neuronal cell bodies in DRG affected with TTR deposition revealed HMGB1 up-regulation in the cytoplasm when compared with non-affected DRG. HMGB1 was not detected in serum of FAP patients, whereas it was found in saliva from a small number of FAP patients. Thus, HMGB1 appears to be an early marker for cytotoxicity elicited by deposited TTR in FAP and future studies should elucidate the mechanisms behind HMGB1 relocation towards the cytosol.

Taken together, our studies provided insights on signal transduction pathways involved in FAP neurodegeneration and identified structural motifs important for RAGE-TTR

interaction. These findings offer new targets for the design of FAP therapeutical approaches.

Sumário

A polineuropatia amiloidótica familiar (PAF) é caracterizada principalmente pela deposição de amilóide no sistema nervoso periférico. A PAF é uma doença hereditária de transmissão autossómica dominante tendo sido descritas várias mutações pontuais no gene da transtirretina (TTR), a maioria das quais associada a esta patologia. A TTR é o componente principal das fibras de amilóide, as quais têm uma distribuição extracelular sistémica por todo o tecido conjuntivo de vários órgãos, excepto o cérebro e o fígado. A TTR é uma proteína sérica tetramérica constituída por quatro subunidades idênticas de 14 kDa. Fisiologicamente, transporta a tiroxina (T_4) e o complexo formado pelo retinol (vitamina A) ligado à proteína de ligação ao retinol (RBP). Relativamente à patologia, os mecanismos detalhados que estão na base da formação de fibras de amilóide pela TTR e da neurodegeneração na PAF são ainda pouco compreendidos.

No processo patológico da PAF, a deposição extracelular da TTR induz efeitos tóxicos no interior da célula que se pensa serem mediados pelo receptor para produtos finais glicosilados (RAGE). Actualmente, os aspectos estruturais da interacção RAGE-ligando não estão definidos. No entanto, os estudos que realizamos mostram que a interacção da TTR com o RAGE é conservada ao longo das espécies humana e de ratinho, e que não depende da glicosilação do RAGE. Verificamos ainda que a cadeia D da estrutura da TTR parece relevante para a interacção TTR-RAGE assim como um motivo no RAGE (resíduos 102-118) com localização compreendida no domínio-V. Estudos num sistema celular mostraram que este motivo é capaz de suprimir a citotoxicidade exercida pelos agregados da TTR. Este trabalho pode permitir o planeamento de estratégias terapêuticas que tenham como objectivo bloquear o acesso da TTR ao RAGE.

Estudos anteriores demonstraram que os nervos de portadores assintomáticos de TTR Val30Met apresentavam deposição da TTR sob a forma de agregados não fibrilares antes da formação de fibras de amilóide e que nessa fase eram já evidentes, sinais de stress oxidativo/inflamatório. Estudos subsequentes demonstraram ainda que os agregados de TTR não fibrilar, ao contrário das fibras, são tóxicos para as células *in vitro*. Todavia, os mecanismos moleculares de sinalização associados à neurodegeneração que ocorre na PAF são na sua maior parte desconhecidos.

Com o objectivo de procurar genes e proteínas diferencialmente expressos na PAF, foram usadas várias abordagens experimentais. "Microarrays" de anticorpos foram realizados usando biopsias de glândulas salivares (GS) de doentes PAF. Das proteínas diferencialmente expressas encontradas, só algumas foram seleccionadas para posterior análise tendo-se observado sobre-expressão de proteoglicano de sulfato de condroitina

(CSPG) em GS de doentes PAF. Estes resultados preliminares são muito interessantes porque sugerem que o CSPG pode desempenhar um papel no processo inflamatório e/ou na formação de amilóide na PAF. Anteriormente, uma análise de "microarrays" feita a partir de mRNA purificado de GS de doentes PAF mostrou sub-expressão do gene para a proteína fosfatase "mitogen-activated protein (MAP) kinase phosphatase 1" (MKP-1). Este resultado foi ainda validado em tecidos, por imuno-histoquímica. A proteína fosfatase MKP-3 é também sub-expressa em GS de doentes PAF. Dado a relação existente entre as proteínas fosfatases MKPs e as proteínas cinases MAPKs, estas últimas foram investigadas. Somente as cinases "extracellular signal-regulated kinases 1/2" (ERK1/2) mostraram sobre-activação em GS e nervos de doentes PAF. As cinases responsáveis pela activação das cinases ERK1/2, ou seja as cinases MEK1/2, também mostraram sobre-activação em nervos de doentes PAF. Além disso, estudos em ratinhos transgénicos que expressam a TTR Val30Met evidenciaram sobre-activação das cinases ERK1/2 em nervos periféricos afectados pela deposição de TTR, quando comparados com animais controlo. O tratamento de uma linha celular de Schwannomas com agregados de TTR estimulou a activação das cinases ERK1/2. Esta activação foi parcialmente mediada pelo RAGE sugerindo assim o possível envolvimento de outros receptores celulares. Por outro lado, a activação da caspase-3, desencadeada pelos agregados de TTR, foi suprimida pelo uso do composto U0126, um inibidor das cinases MEK1/2, indicando que a activação das cinases ERK1/2 é essencial para a indução de citotoxicidade por parte dos agregados de TTR. Em conjunto, estes resultados sugerem que a activação anormal e persistente das cinases ERK1/2 pode representar um passo inicial na cascata de sinalização levando posteriormente à neurodegeneração.

Estudos anteriores demonstraram que a interacção dos agregados de TTR com o RAGE desencadeia a activação do NFκB, um factor de transcrição muito provavelmente envolvido na indução de genes relacionados com o processo de inflamação e de stress oxidativo da PAF. Na sequência desses estudos, procuramos descobrir se existe participação de outros factores de transcrição, tais como os que são activados pelas vias MAPK. Verificamos que o factor de transcrição Elk-1 está sub-activado em GS de doentes PAF e em nervos de portadores assintomáticos. Esta diminuição de activação está possivelmente relacionada com um processo de modulação de feedback negativo da via ERK1/2. Outros factores de transcrição, tais como ATF-2 e o c-Jun apresentaram activações diferentes em GS de doentes PAF e nervos de portadores assintomáticos, sugerindo a existência de vias de sinalização específicas para cada tecido. Estes resultados preliminares sugerem uma inter-relação complexa entre os factores de transcrição seleccionados na PAF fornecendo pistas para investigações futuras em vias de sinalização que não foram abordadas neste trabalho.

Recentemente, a proteína "high mobility group box 1" (HMGB1) foi implicada na patologia da doença de Alzheimer (AD), uma doença relacionada com a deposição de amilóide. Neste estudo investigamos se a expressão da proteína HMGB1 está alterada na PAF. Observou-se que em células epiteliais de GS de doentes PAF, a proteína HMGB1 passa a ter uma localização citosólica em vez de nuclear. Por outro lado, em nervos de doentes PAF, a expressão da proteína HMGB1 mostrou-se aumentada nos axónios. Para aceder à localização subcelular da proteína HMGB1 em neurónios sensoriais, usamos gânglios raquidianos dorsais (DRG) de ratinhos transgénicos TTRVal30Met. Neste modelo, os corpos celulares de neurónios presentes nos DRG afectados pela deposição da TTR evidenciaram sobre-expressão no citosol quando comparados com DRG não afectados. A proteína HMGB1 não foi detectada no soro mas foi encontrada na saliva de um número limitado de doentes PAF. Assim, a proteína HMGB1 parece ser um marcador precoce da citotoxicidade desencadeada pelos depósitos da TTR em doentes PAF. Estudos futuros deverão elucidar os mecanismos que estão por detrás da translocação da proteína em direcção ao citosol.

Em suma, estes estudos forneceram conhecimentos em vias de transdução de sinal envolvidas na neurodegeneração associada à PAF tendo sido ainda identificados os motivos estruturais importantes na interacção entre a TTR e o RAGE. Estas descobertas propõem novos candidatos para a planificação de abordagens terapêuticas na PAF.

Résumé

La caractéristique principale de la polyneuropathie amyloïde familiale (PAF) est le dépôt d'amyloïde dans le système nerveux périphérique. La transthyrétine (TTR) est le composant principal des fibrilles amyloïdes, qui ont une distribution extracellulaire systémique dans tout le tissu connectif de plusieurs organes, seuls les parenchymes du cerveau et du foie sont épargnés. Plusieurs mutations ponctuelles dans le gène de la TTR ont été décrites et la plupart sont associées à la PAF, une maladie dominante autosomale. Physiologiquement, la TTR est une protéine tétramérique du plasma composée de quatre sous-unités identiques de 14 kDa et qui fonctionne comme transporteur de la thyroxine (T_4) et également du rétinol (vitamine A) par formation d'un complexe molaire de 1:1 avec la protéine de liaison au rétinol (RBP). Les mécanismes précis fondamentaux à la base de la formation de fibrilles de TTR amyloïdes et la neurodégénérescence associée à la PAF sont mal compris.

Dans le processus pathologique de la PAF, le récepteur pour les produits finaux de glycosylation avancée (RAGE) a été impliqué dans la transduction de signaux cytotoxiques induite par la TTR déposée extracellulairement. La base structurale de l'interaction de RAGE-ligand n'est actuellement pas bien définie. Ici, on a démontré que l'interaction de la TTR avec RAGE est conservée chez l'Homme et la souris et ne dépend pas du niveau de glycosylation de RAGE. D'ailleurs, la chaîne D de la structure de TTR semble importante pour l'interaction TTR-RAGE aussi bien qu'un motif du RAGE (résidus 102-118) située dans le V-domaine; ce motif est capable de supprimer la cytotoxicité induite par les agrégats de TTR dans des cellules en culture. Ces études pourraient permettre la conception de stratégies thérapeutiques visant à bloquer l'accès de TTR à la RAGE.

Des études précédentes ont démontré que les nerfs des porteurs asymptomatiques de la variante de TTR Val30Met, présentent la TTR sous une forme non-fibrillaire agrégée avant la formation des fibrilles amyloïdes et des signes de stress oxydatif/inflammatoire étaient déjà évidents. Les études suivantes ont prouvé que les agrégats non-fibrillaires de TTR, et non pas les fibrilles mûres, sont toxiques aux cellules *in vitro*. Cependant les mécanismes de signalisation moléculaires liés à la neurodégénérescence de la PAF sont en grande partie inconnus. On a abordé ces questions en utilisant plusieurs méthodologies visant à rechercher les gènes et les protéines différentiellement exprimés au cours de la pathologie de la PAF. Des biopsies de glandes salivaires (GS) de patients atteints de PAF ont été employées pour réaliser des "microarrays" d'anticorps. À partir des protéines différentiellement exprimées, quelques candidats ont été choisis pour

poursuivre l'analyse. On a observé une sur-expression des proteoglycans de sulfate de chondroïtine (CSPG) dans les GS de malades PAF. Ces résultats préliminaires sur la sur-expression de CSPG sont très intéressants car ils suggèrent un rôle probable dans le processus d'inflammation et/ou dans la facilitation de l'amyloïdogénèse de la PAF.

Précédemment, une analyse "microarrays" réalisée à partir d'ARNm purifié des GS de malades PAF a montré la sous-expression de la "mitogen-activated protein" (MAP) kinase phosphatase (MKP-1). On a de plus validé ce résultat par immunohistochimie. MKP-3 est également sous-exprimée dans des biopsies de GS de malades PAF. Etant donné la relation entre MKPs et MAPKs, ces dernières ont été étudiées. Seule l'activation des protéine kinases "extracellular signal-regulated kinases 1/2" (ERK1/2) a été augmentée dans des biopsies de GS et nerfs de malades PAF. L'activation des kinases des ERK1/2 (MEK1/2) est également augmentée dans les nerfs de malades PAF. De plus, un modèle de PAF de souris transgéniques a indiqué l'activation des kinases ERK1/2 accrue dans les nerfs périphériques touchés par le dépôt de TTR, en comparaison à des animaux contrôles. Le traitement d'une lignée de cellules de Schwannoma avec des agrégats de TTR a stimulé l'activation des kinases ERK1/2, et ceci partiellement par intermédiaire du récepteur RAGE suggérant la participation possible d'autres récepteurs cellulaires. D'ailleurs, l'activation de la caspase-3 déclenchée par des agrégats de TTR a été supprimée par U0126, un inhibiteur des kinases MEK1/2, indiquant que l'activation des kinases ERK1/2 est essentielle pour la cytotoxicité induite par les agrégats de TTR. Pris ensemble, ces résultats suggèrent que l'activation anormalement soutenue des kinases ERK au cours de la PAF constitue une cascade précoce de signalisation menant à la neurodégénéréscence.

Des études précédentes ont prouvé que l'interaction d'agrégats de TTR avec RAGE induit l'activation de NFκB, un facteur de transcription très probablement impliqué dans l'induction des gènes relatifs aux processus inflammatoires et oxydants de la PAF. On a poursuivi ces études et on a découvert la participation d'autres facteurs de transcription, tels que ceux activés par des kinases MAPKs. On a prouvé que l'activation d'Elk-1 est diminuée dans des biopsies de GS de malades PAF et dans les nerfs des porteurs asymptomatiques, ce qui est probablement lié à une boucle de rétroaction négative sur les kinases ERK1/2. D'autres facteurs de transcription, tels que ATF-2 et c-Jun présentent des activations différentiels dans des biopsies de GS de malades PAF et dans les nerfs des porteurs asymptomatiques, suggérant des voies de signalisation spécifiques à chaque tissu qu'il sera intéressant d'étudier à l'avenir. Les résultats préliminaires suggèrent une interconnexion complexe entre les facteurs de transcription activés au cours de la PAF, mais cela donne des directions pour la recherche future sur des voies de signalisation non étudiées jusque là.

Récemment, il a été rapporté que la protéine "high mobility group box 1" (HMGB1) est impliquée dans la pathologie de la maladie d'Alzheimer (AD), une autre maladie amyloïde. Dans cette étude on a étudié si l'expression de la protéine HMGB1 est changée au cours de la PAF. On a constaté que la protéine HMGB1 est déplacée du noyau vers le cytosol dans des cellules épithéliales de biopsies de GS de malades PAF. Dans des nerfs de malades PAF, la protéine HMGB1 est sur-exprimée dans les axones. Pour accéder à la localisation de la protéine HMGB1 dans les neurones sensoriels, on a utilisé des ganglions dorsaux rachidiens (DRG) d'un modèle PAF de souris transgéniques. Dans ce modèle, les corps cellulaires de neurones des DRG avec le dépôt de TTR ont indiqué la sur-expression de la protéine HMGB1 dans le cytoplasme en comparaison avec des DRG non-atteints. La protéine HMGB1 n'a pas été détectée dans le sérum de malades PAF, tandis qu'on l'a trouvée dans la salive d'un nombre restreint de malades PAF. Ainsi, la protéine HMGB1 semble être un marqueur précoce pour la cytotoxicité déclenchée par la TTR déposée au cours de la PAF et les études futures devraient élucider les mécanismes impliqués dans la relocalisation de la protéine HMGB1 vers le cytosol.

Dans l'ensemble, nos études ont fourni des connaissances sur des voies de transduction du signal impliquées dans la neurodégénéréscence associée à la PAF et ont identifié des motifs structuraux importants pour l'interaction entre la TTR et le RAGE. Ces résultats offrent de nouveaux candidats pour la conception de nouvelles approches thérapeutiques pour la PAF.

Abbreviations

Aβ: Amyloid β-peptide

AD: Alzheimer's disease

AGEs: Advanced glycation end products

ASK-1: Apoptosis signal-regulating kinase 1

ATF-2: Activating transcription factor-2

BDNF: Brain derived neurotrophic factor

CaM: Ca^{2+}-binding protein calmodulin

CaM-K: CaM-dependent protein kinase

Cdc42: Cell division control protein 42

CHOP: C/EBP homologous protein

CNS: Central nervous system

Cox-III: Cytochrome c oxidase III

CREB: cAMP response element binding protein

CSF: Cerebrospinal fluid

CSPG: Chondroitin sulfate proteoglycan

DD: Differential display

DN-RAGE: Dominant negative-RAGE

DRG: Dorsal root ganglion

ECM: Extracellular matrix

Elk-1: ETS-domain transcription factor 1

ERK1/2: Extracellular signal-regulated kinase 1/2

FAC: Familial amyloidotic cardiomyopathy

FAP: Familial amyloidotic polyneuropathy

GAG: Glycosaminoglycan

HAT: Histone acetyltransferase

HD: Huntington's disease

HDAC: Histone deacetylase

HMGB1: High mobility group box 1 protein or amphoterin

IL-1β: Interleukin-1β

IL-10: Interleukin-10

iNOS: Inducible nitric oxide synthase

JAK: Janus kinase

JNK: c-Jun N-terminal kinase

LPS: Lipopolysaccharide

MAPK: mitogen-activated protein kinase

M-CSF: Macrophage-colony stimulating factor

MEF-2C: Myocyte enhancer factor 2C

MEK/MKK: MAPK kinase

MEKK: MAPKK kinase

MKP: MAP kinase phosphatase

MSK: Stress-activated protein kinase

ND7/23: Mouse neuroblastoma x rat neurone hybrid cell line

NFκB: Nuclear transcription factor κB

NGAL: Neutrophil gelatinase-associated lipocalin

NGF: Nerve growth factor

PD: Parkinson's disease

PG: Proteoglycan

PNS: Peripheral nervous system

PP: Serine/threonine protein phosphatase

PTP: Protein tyrosine phosphatase

RAGE: Receptor for advanced glycation end products

RBP: Retinol-binding protein

RN22: Rat Schwannoma cell line

RNS: Reactive nitrogen species

ROS: Reactive oxygen species

RSK: Ribosomal p90 S6 kinase

SAP: Serum amyloid P component

SG: Salivary gland

SH2BP1: SH2-binding protein 1

sRAGE: Soluble RAGE

SSA: Systemic senile amyloidosis

STAT: Signal transducer and activator of transcription

TF: Transcription factor

TLR-2/-4: Toll-like receptors-2 or -4

TM-1α: Tropomyosin-1α

TNFα: Tumor necrosis factor α

TTR: Transthyretin

TTR Leu55Pro (L55P): Leucine for proline exchange at position 55 of transthyretin.

TTR Val30Met (V30M): Valine for methionine exchange at position 30 of transthyretin

PART I

General Introduction

General introduction

Familial amyloidotic polyneuropathy (FAP) is a neurodegenerative disease characterized by pathological tissue deposition of amyloidogenic variant transthyretin (TTR) in non-fibrillar and amyloid fibrillar forms. Our research project aims at unravelling signal transduction pathways by which TTR deposits cause the pathological features associated with FAP, namely neurodegeneration.

In the following sections, we present a general introduction dealing with several concepts that we find to be relevant to the understanding of the hypotheses raised on neurodegeneration and for experimental research work carried out in this thesis.

1. Transthyretin (TTR)

TTR, formerly called prealbumin because of migrating ahead of albumin in an electrical field, was discovered in 1942 in the cerebrospinal fluid (CSF) (Kabat et al. 1942) and shortly after in the plasma (Seibert and Nelson 1942). Plasma TTR is mainly produced by the liver (Soprano et al. 1985); on the other hand, TTR in CSF is synthesized by the choroid plexus of the brain, though its expression is regulated differentially from liver (Dickson et al. 1986). The word TransThyRetin discloses its dual physiological role as a transporter for thyroxine (Woeber and Ingbar 1968) and retinol (Raz et al. 1970).

1.1. TTR gene structure and regulation

The TTR gene is located in chromosome 18, more specifically in 18q11.2-q12.1 (Whitehead et al. 1984; Wallace et al. 1985) and is codified by single copy gene (Tsuzuki et al. 1985). The gene is composed by 6.9 kilobases (kb) comprising four exons (E1 to E4) and three introns (I1 to I3) (Sasaki et al. 1985; Tsuzuki et al. 1985) (Figure 1). E1, with 95 basepairs (bp) long, encodes a signal peptide of 20 amino acids (aa) and the first three aa of the mature protein; E2 (131 bp), E3 (136 bp) and E4 (253 bp) hold the rest of the coding sequences for aa 4-47, 48-92 and 93-127, respectively.

Introns I1, I2 and I3 are 934 bp, 2090 bp and 3308 bp long, respectively. Introns I1 and I3 contain two independent open reading frames (ORFs) but their function, if any, is unknown (Soares et al. 2003). Several consensus sequences were found upstream of the transcription initiation site, which were the following: a TATA box at position –30 to –24 bp

followed by a GC rich region of approximately 20 bp, a CAAT box at position –101 to –96 bp and overlapping sequences homologous to glucocorticoid responsive elements at positions –224 and –212 bp. A polyadenylation signal (AATAAA) was identified 123 bp downstream from the coding sequence (Sasaki et al. 1985).

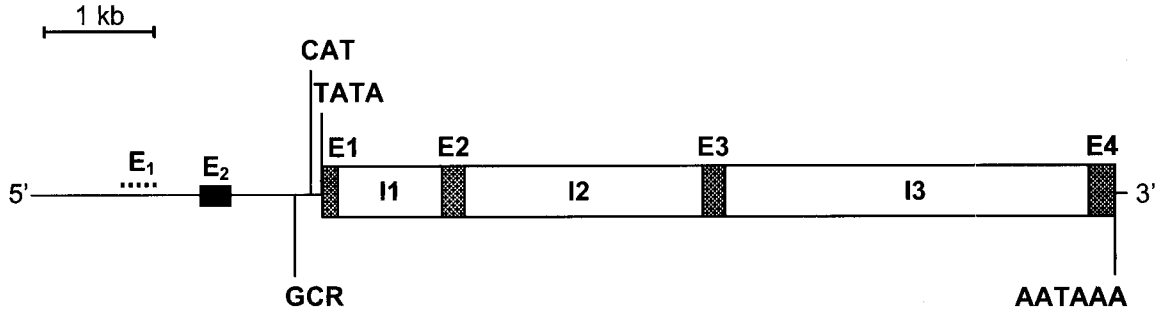

Figure 1. Human TTR gene structure.
Exons 1 to 4 (E1 to E4) and introns 1 to 3 (I1 to I3); E_1: sequence homogous to mouse enhancer; E_2: human specific enhancer; GCR: glucocorticoid responsive element; CAT: CAAT box; AATAAA: polyadenylation signal. Adapted from (Sasaki et al. 1985).

Regarding *ttr* gene regulation, two major regulatory regions were found in mouse *ttr* gene: a proximal promoter sequence at -50 to -150 bp and a distal enhancer element located between 1.6 and 2.15 kb upstream (Costa et al. 1986). By comparative analyses the same regulatory sequences were found in the human gene. The promoter region of the human *ttr* gene contains DNA binding sites for hepatocyte nuclear factors (HNF-1, HNF-3, HNF-4 and C/EBP), which are present in the liver but not in most other adult tissues (Costa et al. 1990). Characterization of transgenic mice carrying the human *ttr* gene containing either 6 kb or 0.6 kb of the upstream region, suggested that choroid plexus and liver *ttr* expression are differentially regulated, possibly due to the action of different cis and/or trans-acting factors (Costa et al. 1990; Nagata et al. 1995).

The *ttr* gene transcription originates a ~0.7 kb mRNA that is composed by the following regions: a 5'-untranslated region (26-27 nucleotides), the coding region (441 nucleotides), and a 3'-untranslated region (145-148 nucleotides) preceding the poly(A) tail (Mita et al. 1984; Soprano et al. 1985). Mouse cDNA is 82% and 90% homologous to the human and rat cDNA, respectively; and the amino acid sequence homology is higher: 91% homology to the human and 96% to the rat amino acid sequence (Costa et al. 1986). Therefore, TTR protein is highly conserved through evolution.

1.2. TTR expression

In humans, the liver is the main producer of plasma TTR, more than 90%, which is secreted into the bloodstream. TTR concentration in plasma ranges from 170 to 420 µg/mL (Vatassery et al. 1991). Plasma TTR concentration is age dependent and in healthy newborns it is about half of that found in adults (Vahlquist et al. 1975). In addition, plasma TTR levels begin to decline after age 50 (Ingenbleek and De Visscher 1979).

The choroid plexus is the major site for TTR synthesis, when expressed as tissue/mass ratio, and corresponds to a ~30-fold higher expression per gram of tissue as compared to liver (Weisner and Roethig 1983). Epithelial cells lining the ventricular surface of the choroid plexus secrete TTR into the CSF where TTR concentration varies from 5 to 20 µg/mL (Vatassery et al. 1991). In fact, TTR represents 20% of the total CSF proteins (Weisner and Roethig 1983).

In addition, several other sites of TTR expression have been identified in mammals, such as the retinal pigment epithelium of the eye (Martone et al. 1988), the islets of Langerhans in the pancreas (Jacobsson 1989) and in minor amounts the stomach, heart, skeletal muscle and spleen (Soprano et al. 1985).

During embryonic development in humans, TTR is expressed first in the thela choroidea, the precursor of the choroid plexuses, around the eighth week, and later in the liver (Richardson et al. 1994). In mice, after the tenth day of gestation, TTR expression is found in hepatocytes, tela choroidea and visceral yolk sac (Murakami et al. 1987).

In a phylogenetic view, TTR synthesis is present in fish (Santos and Power 1999), birds and mammalian ancestors (Richardson et al. 1994). In fish, TTR is produced mainly by the liver whereas in reptiles TTR is produced by the choroid plexus but not by the liver (Achen et al. 1993), while birds and mammals produce in both tissues (Harms et al. 1991).

Recently, an increasing number of functional sequences homologous to TTR, called TTR-like, are being reported for prokaryote and lower eukaryote organisms (Eneqvist et al. 2003; Hennebry et al. 2006).

1.3. TTR structure

TTR is a non-glycosylated tetrameric protein displaying tetrahedral symmetry. It consists of four identical subunits, each containing 127 amino acids (13,725 Da), and it has a molecular mass of 54,980 Da (Kanda et al. 1974).

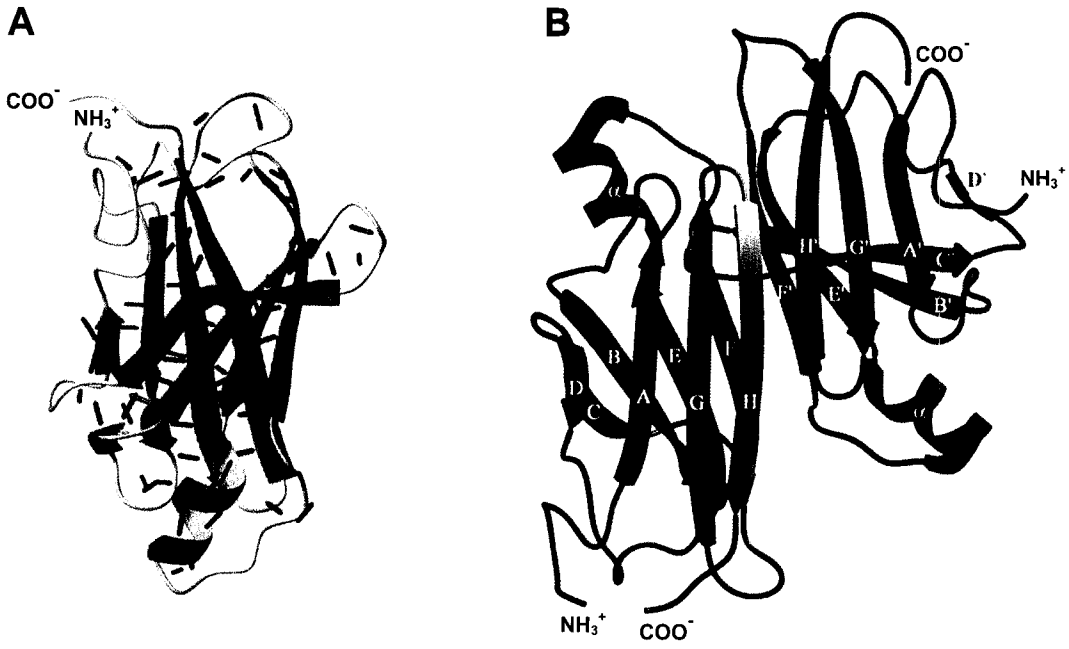

Figure 2. Representation of the TTR monomer and dimer.
A, TTR monomer. Adapted from PDB entry 1ETB (Hamilton et al. 1993). **B**, TTR dimer; each monomer contains two β-sheets composed of strands DAGH and CBEF, which extend to two 8-stranded β-sheets when two monomers associate forming a dimer. Adapted from PDB entry 1ETB (Hamilton et al. 1993).

The secondary and tertiary structures of each monomer were solved using X-ray diffraction studies of the crystallized protein at a resolution of 1.8 Å (Blake et al. 1978). Approximately 55% of the amino acids in each monomer are implicated in the formation of β-sheet structure and 5% are situated in a single α-helix segment. The TTR monomer contains eight β-strands, A throughout H, of seven to eight amino acids in length. The exception is β-strand D, which comprises three amino acids in length. The eight strands form two sheets of four strands each, DAGH and CBEF, arranged in a topology similar to the classic Greek key barrel (Figure 2A). The single α-helix segment encompasses amino acids 75 to 83 at the end of β-strand E (Blake et al. 1978).

Two TTR monomers associate to form one dimer by the interaction of chains F and H of each monomer. The dimer is composed of two eight-stranded β-sheets and the strands arrangement is the following: DAGHH'G'A'D' and CBEFF'E'B'C', knowing that strands A-H belong to one monomer and A'-H' to the other (Figure 2B).

The tetramer results from the assembly of two dimers by opposing their inner β-sheets and interacting mainly at loop regions adjoining β-strands G and H and β-strands A and B. The quaternary structure of TTR has the shape of a globular protein whose overall size is 70 Å x 55 Å x 50 Å. The arrangement of the four subunits forms a central hydrophobic channel through the molecule where two binding sites for thyroid hormones are located (Blake et al. 1978), as represented in figure 3.

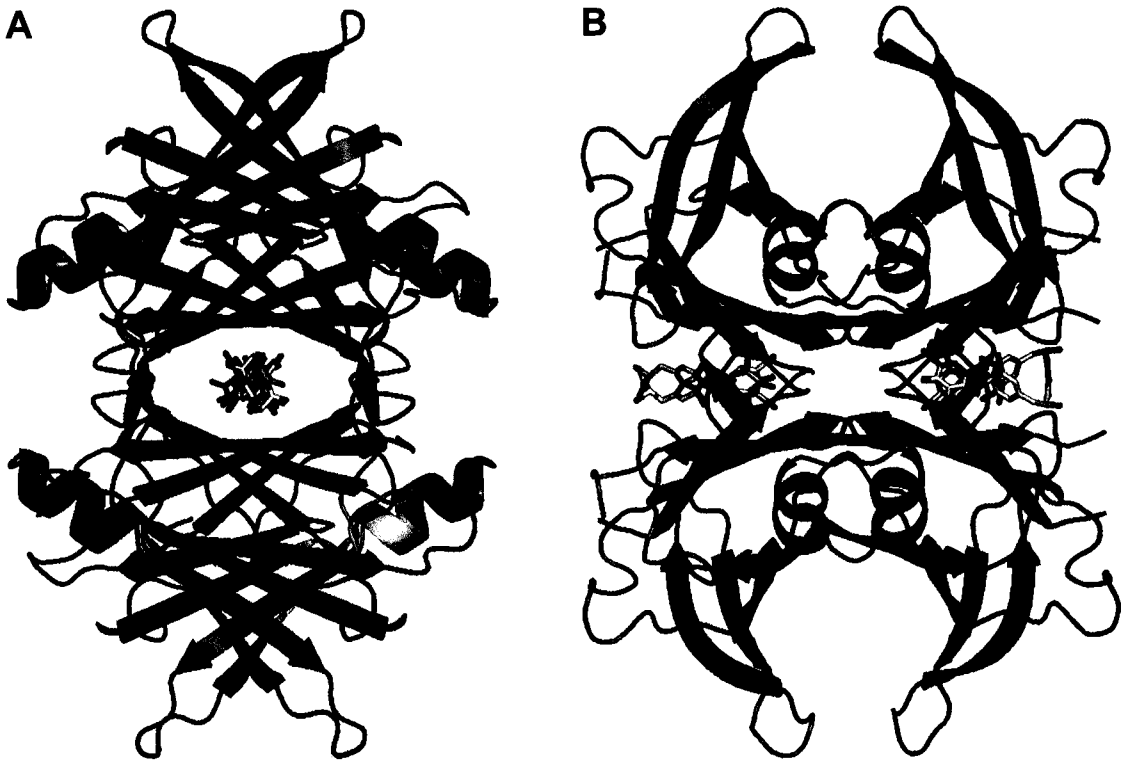

Figure 3. Representations of the quaternary structure of TTR bound to two molecules of T_4. **A**, View showing the central hydrophobic channel with T_4 molecules in front of each other. **B**, View showing both T_4 molecules; because of the two fold axis along the binding channel there are two symmetry-related binding modes for both T_4 molecules (shown in grey and pink) (Almeida et al. 2005). (Kindly provided by Dr Luís Gales, Molecular Structure Group, IBMC).

1.4. TTR physiological functions

The two major physiological functions known for TTR are the transport of T_4 (3, 5, 3', 5'-tetraiodo-L-thyronine) and retinol (vitamin A), the later through the formation of a complex with retinol-binding protein (RBP) (Raz et al. 1970).

1.4.1. Thyroxine (T_4) transport

In mammals, thyroid hormones are essential for normal development and metabolism. The thyroid gland synthesizes thyroxine (T_4), which gives rise to the biologically active hormone, triiodothyronine (T_3), by a deodination process that occurs in the target tissues (Kohrle 1994). Once secreted, thyroid hormones are bound to plasma proteins. There are three proteins responsible for the transport of T_4 in human plasma, i) TTR, ii) thyroxine-binding globulin (TBG) and iii) albumin (Robbins 1991). Although TBG is the main thyroxine-binding protein in the plasma of humans, TTR is the major thyroxine carrier in the plasma of rodents and in the CSF of both rodents and humans. In humans, TTR transports ~15% of T_4 in plasma and 80% in the CSF (Robbins 1991).

The TTR tetramer has two structurally identical binding sites for T_4 located in its central hydrophobic channel (Nilsson and Peterson 1971; Blake et al. 1978), depicted in figure 3. These two thyroxine-binding sites have very different affinities for T_4, which is explained by an allosteric effect upon occupation of the first site by T_4 (Andrea et al. 1980). Therefore, each TTR tetramer carries no more than one T_4 molecule (Robbins 1991). As TTR has much higher affinity for T_4 than for T_3, TTR binds virtually no T_3 (Andrea et al. 1980).

1.4.2. Retinol (vitamin A) transport

Retinol (vitamin A) is essential for several physiological functions, namely for vision, reproduction, growth and development. TTR is a retinol plasma carrier, through binding to retinol-binding protein (RBP) (Kanai et al. 1968). RBP is a 21 kDa monomeric protein consisting of 182 amino acids (Rask et al. 1979). The conformational structure of RBP bound to retinol was determined by x-ray crystallography (Newcomer et al. 1984). Despite the presence of four binding sites for RBP in TTR, only one molecule is bound to TTR under physiological conditions, because RBP concentration in plasma is limiting (van Jaarsveld et al. 1973). *In vitro,* TTR does not bind four RBP molecules also due to steric hindrance of the two bound RBP molecules (Monaco et al. 1995). Each RBP molecule binds to one of the TTR dimers, as represented in figure 4. The dissociation constants for the two RBP molecules were estimated as $1.9 \pm 1.0 \times 10^{-7}$ M for the first and 3.5×10^{-5} M for the second one. In most circumstances, TTR:RBP:retinol complexes are present in the plasma in a 1:1:1 equimolar ratio (Blaner 1989). This process allows holo-RBP to stabilize and prevent its rapid renal or intestinal leakage (Raz et al. 1970). Moreover, retinol is also protected from oxidation and plasma insolubility by this complex. Once retinol is taken up by peripheral tissues, the resulting apo-RBP (devoid of retinol) has a significantly

shortened half-life of ~3.5 h (Peterson et al. 1974). The main amino acids of TTR involved in the interaction with RBP are Arg^{21}, Val^{20}, Leu^{82} and Ile^{84}, which are contributed by two monomers; in addition, Gly^{83} forms hydrogen bound with the OH group of retinol and interacts with Leu^{35} of RBP. This interaction reinforces the relevance of retinol in the stabilization of TTR:RBP complex (Naylor and Newcomer 1999).

Figure 4. TTR in a complex with RBP/Retinol (●).
Adapted from PDB entry 1QAB (Naylor and Newcomer 1999).

In summary, given that both thyroid hormones and retinoids are essential for normal embryonic development, it was thought that the disruption of *ttr* gene could result in development impairment and in a severe phenotype. However, this was not the case; TTR-knockout mice display no obvious phenotypic abnormalities (Episkopou et al. 1993). In TTR-knockout mice, circulating levels of T_4, retinol, and RBP are about 35%, 6%, and 5%, respectively of those observed for wild-type mice (Episkopou et al. 1993; Palha et al. 1994; Wei et al. 1995). Nevertheless, TTR is not needed for thyroid hormone to be delivered to tissues (Palha et al. 1997; Palha et al. 2000b; Palha et al. 2002) even in conditions of increased hormone demand (Sousa et al. 2005a). Thus TTR most likely is a redundant protein in thyroid hormone homeostasis. Similarly, TTR-knockout mice do not show signs of retinoid deficiency in tissues (Wei et al. 1995), but present lower circulation levels of RBP possibly due to increased renal filtration of the RBP-retinol complex (van Bennekum et al. 2001). Therefore, other proteins and/or alternative pathways for tissue delivery might overcome TTR's function as a carrier. It is possible that the major function of TTR remains to be elucidated.

1.4.3. Other TTR functions

Apart from the already mentioned TTR-binding properties related to thyroid hormones and to vitamin A, TTR has been reported to have other functions.

TTR has been reported to bind pterins, that are cofactors in the synthesis of catecholamines (Ernstrom et al. 1995), norepinephrine oxidation products (Boomsma et al. 1991), polyhalogenated compounds (Brouwer 1989), retinoic acid (Smith et al. 1994), and plant flavonoids (Lueprasitsakul et al. 1990); however the physiological importance of these interactions is still unknown.

By computer analysis it was observed that the external surface of the TTR tetramer presents structural complementarity to double-helical DNA. This suggested a possible common ancestor origin for TTR and the thyroid hormone nuclear receptors (Blake and Oatley 1977), but no further studies have been published on this issue. There is some structural homology between TTR and the family of glucagon-secretin gastrointestinal peptide hormones (Jornvall et al. 1981); the importance of such homology is unknown.

TTR was found to be associated with lipoproteins in human plasma (Tanaka et al. 1994), in particular, with high density lipoproteins (HDL) through interaction with apoliprotein AI (apoAI). In addition, the amount of TTR that circulates bound to HDL was estimated as 1-2% of total plasma TTR. Noteworthy, TTR was not detected in other lipoprotein fractions and the HDL fraction contained TTR in a non-RBP bound form (Sousa et al. 2000a). Moreover, TTR is capable to process proteolytically apoAI by cleaving its C-terminus. Thus, TTR can act as a novel plasma cryptic protease that might have a potential important role under physiological and/or pathological biological settings (Liz et al. 2004).

It has been described that TTR binds soluble amyloid β-peptide (Aβ), thus sequestrating Aβ and preventing the formation of amyloid fibrils in the brain of patients with Alzheimer's disease (AD) (Schwarzman et al. 1994). In agreement, decreased levels of CSF TTR were reported in AD patients (Riisoen 1988). However, no mutations in the *ttr* gene have been found associated with AD (Palha et al. 1996). Moreover, lower CSF TTR concentrations have been also found in depressed patients (Hatterer et al. 1993).

Recently, it was shown that TTR-knockout mice display increased exploratory activity and reduced signs of depressive-like behaviour (Sousa et al. 2004a). Although this behaviour might result from increased norepinephrine levels that were found in the limbic forebrain of TTR-knockout mice, the precise mechanism underlying these phenotypes and the relationship to TTR still remains to be elucidated (Sousa et al. 2004a). Very recently, it was reported that neuropeptide Y (NPY), which has among others anti-depressant

properties, is significantly increased in TTR-knockout mice (Nunes et al. 2006), therefore giving new molecular insights to its less depressive behaviour. In this study, it was shown that the nervous system of the TTR-knockout mice presents over-expression of peptidylglycine α-amidating monooxygenase (PAM), the rate-limiting enzyme in amidated neuropeptide maturation, and increased NPY levels, which correlate with the increase in lipoprotein lipase (LPL) expression and activity. It was proposed that TTR modulates neuropeptide maturation through down-regulation of PAM expression, thus providing a new physiologic function for TTR in the homeostasis of the nervous system (Nunes et al. 2006). Sensorimotor functions of TTR-knockout mice were impaired as determined by functional evaluation, when compared to wild-type littermates (Fleming et al. 2005). Upon nerve injury, TTR-knockout mice displayed a lower total number of myelinated fibers and unmyelinated fibers after 15 days or 1 month of recovery, respectively. Moreover, expression of Nogo, a regeneration inhibitor, was found increased in the nerve distal stump of TTR-knockout mice when compared to wild-type littermates (Fleming et al. 2005). All together, these data strongly indicate that TTR has an essential function in the physiology of the nervous system and in the regeneration of the peripheral nerve.

1.5. TTR metabolism

In the rat, the major sites of TTR degradation, both of liver and choroids plexus origin, are the liver (36-38%), followed by the muscle (12-15%) and skin (8-10%). Other tissues, namely the kidneys, adipose tissue, testes, and gastrointestinal tract account each for 1-8% of body TTR degradation. Minor amounts (less than 1%) of TTR degradation occur in other tissues analyzed. The mean fractional turnover of plasma TTR is 0.15/h, and that of the total body TTR 0.04/h. Moreover, the estimated turnover of CSF TTR was about 0.33/h. No specific transfer and degradation in the nervous system was observed if labelled TTR was injected in the plasma (Makover et al. 1988).

Although different evidences suggest a receptor-mediated uptake of TTR (Divino and Schussler 1990; Vieira et al. 1995), no mechanism has been reported. Later studies provided evidence for the involvement of megalin, a multiligand receptor, in renal uptake of TTR. Because RBP is also a megalin ligand, TTR might be more relevant for the renal uptake of T_4, given that TTR carries about 15% of T_4 present in human plasma. Therefore, this mechanism of TTR uptake in the kidney might play a role in thyroid hormone homeostasis (Sousa et al. 2000b). Since liver is the major site of TTR degradation, its cellular uptake was also investigated using a Hepatoma cell line and primary hepatocytes. This study provided evidence for TTR internalization mediated by a yet unidentified receptor-associated protein

(RAP)-sensitive receptor. As TTR uptake was inhibited by lipoproteins it is likely that a common pathway might exist between TTR and lipoprotein metabolism (Sousa and Saraiva 2001).

1.6. TTR molecular variants

So far 84 amyloidogenic TTR variants have been described (Table 1). All except one result from point mutations in the polypeptide chain; the only exception is the deletion of one amino acid at position 122 (Table 1, # 83). The majority of the amyloidogenic TTR variants are associated with peripheral neuropathy as the main clinical manifestation. Often, cardiomyopathy, carpal tunnel syndrome and vitreopathy occur as well.

Table 1. TTR mutations in amyloidoses.
Adapted from (Saraiva 2004).

#	Mutation	Codon change →		Predominant Clinical Features	Origin
1	Cys10Arg	TGT	CGT	PN, AN, Eye	Hungary
2	Leu12Pro	CTG	CCG	LM, PN, AN	UK
3	Asp18Glu	GAT	GAG	PN, AN	Columbia
4	Asp18Gly	GAT	GGT	LM	Hungary
5	Asp18Asn	GAT	AAT	Heart	USA
6	Val20Ile	GTC	ATC	Heart	Germany
7	Ser23Asn	AGT	AAT	Heart	Portugal
8	Pro24Ser	CCT	TCT	Heart, CTS, PN	USA
9	Ala25Thr	GCC	ACC	LM, PN	Japan
10	Ala25Ser	GCC	TCC	Heart, PN	USA
11	Val28Met	GTG	ATG	PN, AN	Portugal
12	Val30Met	GTG	ATG	PN, AN, Eye	several
13	Val30Ala	GTG	GCG	Heart, AN	Germany
14	Val30Leu	GTG	CTG	PN, AN	Japan
15	Val30Gly	GTG	GGG	LM, Eye	France
16	Phe33Ile	TTC	ATC	PN, Eye	Poland
17	Phe33Leu	TTC	CTC	PN, AN	Poland
18	Phe33Val	TTC	GTC	PN, AN	UK
19	Phe33Cys	TTC	TGC	CTS, Heart	USA
20	Arg34Thr	AGA	ACA	PN, Heart	Italy
21	Lys35Asn	AAG	AAC	PN, AN, Heart	France
22	Ala36Pro	GCT	CCT	PN, Eye	Greece
23	Asp38Ala	GAT	GCT	PN, Heart	Japan
24	Trp41Leu	TGG	TTG	Eye	Russia
25	Glu42Gly	GAG	GGG	PN, AN	Japan
26	Glu42Asp	GAG	GAT	Heart	France
27	Phe44Ser	TTT	TCT	PN, AN, Heart	Ireland
28	Ala45Asp	GCC	GAC	Heart	Italy
29	Ala45Ser	GCC	UCC	Heart	Sweden
30	Ala45Thr	GCC	ACC	Heart	Italy
31	Gly47Arg	GGG	CGG	PN, AN	Japan
32	Gly47Ala	GGG	GCG	Heart, PN, AN	Italy
33	Gly47Val	GGG	GTG	PN, AN, Heart	Sri Lanka
34	Gly47Glu	GGG	GAG	PN	Germany
35	Thr49Ala	ACC	GCC	Heart, PN	Italy
36	Thr49Ile	ACC	ATC	PN, Heart	Japan
37	Ser50Arg	AGT	AGG	PN, AN	Japan/Portugal

#	Mutation	Codon change →		Predominant Clinical Features	Origin
38	Ser50Ile	AGT	ATT	Heart, PN, AN	Japan
39	Glu51Gly	GAG	GGG	Heart	USA
40	Ser52Pro	TCT	CCT	PN, AN, Heart	UK/Portugal
41	Gly53Glu	GGA	GAA	LM, Heart	France
42	Glu54Gly	GAG	GGG	PN, AN	UK
43	Glu54Lys	GAG	GAA	PN, AN, Heart	Japan
44	Leu55Arg	CTG	CGG	LM, PN	Germany
45	Leu55Pro	CTG	CCG	PN, Heart, AN	Taiwan
46	Leu55Gln	CTG	CAG	AN, PN	USA
47	His56Arg	CAT	CGT	Heart	USA
48	Leu58His	CTC	CAC	CTS, Heart	Germany
49	Leu58Arg	CTC	CGC	CTS, AN, Eye	Japan
50	Thr59Lys	ACA	AAA	Heart, PN	Italy
51	Thr60Ala	ACT	GCT	Heart, CTS	Ireland
52	Glu61Lys	GAG	AAG	PN	Japan
53	Phe64Leu	TTT	CTT	PN, CTS, Heart	Italy
54	Phe64Ser	TTT	TCT	LM, PN, Eye	Italy
55	Ile68Leu	ATA	TTA	Heart	Germany
56	Tyr69His	TAC	CAC	Eye	Scotland
57	Tyr69Ile	TAC	ATC	CTS, Heart	Japan
58	Lys70Asn	AAA	AAC	CTS, PN, Eye	Germany
59	Val71Ala	GTG	GCG	PN, Eye	Spain
60	Ile73Val	ATA	GTA	PN, AN	Bangladesh
61	Ser77Phe	TCT	TTT	PN	France
62	Ser77Tyr	TCT	TAT	PN	Germany
63	Tyr78Phe	TAC	TTC	Heart, PN	Italy
64	Ile84Ser	ATC	AGC	Heart, CTS, Eye	Switzerland
65	Ile84Asn	ATC	AAC	Eye, Heart	Italy
66	Ile84Thr	ATC	ACC	Heart, PN, AN	Germany
67	Glu89Gln	GAG	CAG	PN, Heart	Italy
68	Glu89Lys	GAG	AAG	PN, Heart	USA
69	Ala91Ser	GCA	TCA	PN, CTS, Heart	France
70	Gln92Lys	GAG	GCT	Heart	Japan
71	Ala97Gly	GCC	GGC	Heart, PN	Japan
72	Ala97Ser	GCC	TCC	PN, Heart	France
73	Ile107Val	ATT	GTT	Heart, CTS, PN	Germany
74	Ile107Met	ATT	ATG	PN, Heart	Germany
75	Ala109Ser	GCC	TCC	PN	Japan
76	Leu111Met	CTG	ATG	Heart	Denmark
77	Ser112Ile	AGC	ATC	PN, Heart	Italy
78	Tyr114Cys	TAC	TGC	PN, AN, Eye	Japan
79	Tyr114His	TAC	CAC	CTS	Japan
80	Tyr116Ser	TAT	TCT	PN, CTS	France
81	Ala120Ser	GCT	TCT	Heart, PN, AN	Africa
82	Val122Ile	GTC	ATC	Heart	Africa
83	Val122del	GTC	loss	Heart, PN, CTS	Equator/Spain
84	Val122Ala	GTC	GCC	Heart, Eye, PN	UK

Legend: AN, autonomic neuropathy; CTS, carpal tunnel syndrome; Eye, vitreous deposition; PN, peripheral neuropathy; LM, leptomeningeal amyloid; Heart, cardiomyopathy.

Several TTR mutations without clinical manifestations have also been described (Table 2). The allele frequency has been estimated in different populations. For instance, Gly6Ser, present in about 12% of the Caucasian population (Jacobson et al. 1995), and Thr119Met, present in 0.8% of the Portuguese and German populations (Alves et al. 1997), are non-amyloidogenic polymorphisms.

Table 2. Non-amyloidogenic TTR mutations.
Adapted from (Saraiva 2004).

#	Mutation	Codon change →		Frequency*
1	Gly6Ser	GGT	AGT	33/558
2	Met13Ile	ATG	ATC	ND
3	Asp74His	GAC	CAC	ND
4	His90Asn	CAT	AAT	16/12,400
5	Gly101Ser	GGC	AGC	ND
6	Pro102Arg	CCC	CGC	1/8,000
7	Arg104Cys	CGC	TGC	ND
8	Arg104His	CGC	CAC	ND
9	Ala108Ala**	GCC	GCT	ND
10	Ala109Thr	GCC	ACC	1/10,000
11	Ala109Val	GCC	GTC	ND
12	Thr119Met	ACG	ATG	35/10,000
13	Pro125Ser	CCC	TCC	ND

Legend: *, refers to mutant allele frequency; **, silent mutation; ND, not determined.

Also, several compound heterozygotes, carriers of two different TTR mutations, have been reported (Table 3). Interestingly, the combination of non-amyloidogenic and amyloidogenic mutations, usually present in different alleles, sometimes influences the clinical outcome. For example, the polymorphic Gly6Ser mutation in Val30Met patients does not influence the clinical manifestation of the disease (Jacobson et al. 1995), whereas the Thr119Met and the Arg104His non-pathogenic mutations exert a significant protective effect among Portuguese and Japanese Val30Met patients, respectively (Longo Alves et al. 1997; Terazaki et al. 1999). The study of pathogenic and non-pathogenic TTR variants is important for the understanding of TTR-related amyloidosis and also to establish a relationship between the structure and function of the molecule.

Table 3. TTR compound heterozygotes.
Adapted from (Saraiva 2004).

#	Mutation	Frequency*
1	Gly6Ser/Val30Met	7/160
2	Gly6Ser/Phe33Ile**	ND
3	Gly6Ser/Ala45Asp	ND
4	Gly6Ser/Ser77Tyr	ND
5	Gly6Ser/Tyr114Cys	ND

6	Gly6Ser/Thr119Met	ND
7	Gly6Ser/Val122Ala	ND
8	His90Asn/Val30Met	ND
9	His90Asn/Glu42Gly**	ND
10	His90Asn/Thr119Met	ND
11	Arg104His/Val30Met	ND
12	Arg104His/Thr59Lys	ND
13	Thr119Met/Val30Met	ND

Legend: *, refers to mutant allele frequency; **, mutations on the same allele; ND, not determined.

1.6.1. TTR variant: Leu55Pro

Leu55Pro TTR variant was first described in a family from West Virginia that developed an unusually aggressive form of widespread TTR amyloidosis (Jacobson et al. 1992). Later, another family from Taiwan was reported to have subjects carrying the same mutation and developed familial amyloidotic polyneuropathy (FAP) with an early-onset and a fatal outcome before age 30 (Yamamoto et al. 1994). The main clinical features evidenced by Leu55Pro patients were peripheral and autonomic neuropathy and cardiomyopathy.

Biochemical studies characterized the structure, ligand-binding properties, tetrameric stability and amyloidogenicity of this particular TTR variant. TTR Leu55Pro has lower tetramer stability towards dissociation into monomers when compared to the wild-type (wt) molecule and is more prone to form amyloid fibrils (McCutchen et al. 1993; Lashuel et al. 1998). TTR Leu55Pro/TTR wt heterotetramers obtained from plasma revealed a very low binding affinity for T_4, while recombinant TTR Leu55Pro did not bind T_4 (Almeida and Saraiva 1996).

X-ray crystallographic studies have shown that, with the exception of the Leu55Pro mutation, all amyloidogenic mutations failed to show drastic structural changes, however, all of them appear to lead to the destabilization of the TTR tetrameric structure. The x-ray crystal structure of Leu55Pro TTR variant showed a major change in the secondary structure by the disruption of β-strand D which becomes a long loop that bridge β-strands C and E (Figure 5). The proline for leucine substitution also disrupts the hydrogen bonds between β-strand D and β-strand A, resulting in the exposure of new surfaces involved in aggregation of monomeric TTR (Sebastiao et al. 1998). Indeed, two constructed mutants containing either a deletion or a substitution in β-strand D (spanning amino acids 53-55) were unstable and spontaneously formed aggregates (Goldsteins et al. 1997).

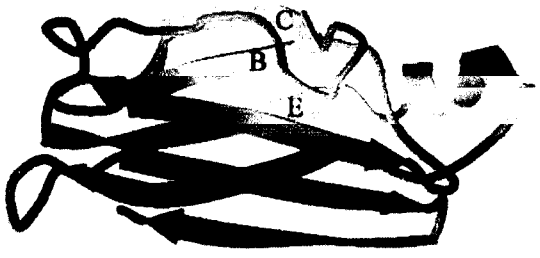

Figure 5. Representation of the Leu55Pro TTR monomer.
Observe the long loop CE originated from the disruption of hydrogen bonds between β-strands D and A. Adapted from PDB entry 5TTR (Sebastiao et al. 1998).

Based on the observation that the amyloidogenicity of the variants was inversely correlated with the stability of the tetramer (Bonifacio et al. 1996), it is likely that the Leu55Pro TTR variant exists in an amyloidogenic conformation, with an enhanced tendency to assemble into amyloid fibrils, while wild-type protein remains stable at the same conditions (Sebastiao et al. 1998). Thus, it was proposed that Leu55Pro TTR monomer resembles the amyloidogenic intermediate in the pathway leading to insoluble amyloid fibril formation. This work also proposed a model for oligomeric TTR consisting of a tubular structure with inner and outer diameters of 30 and 100 Å and four monomers per cross-section (Sebastiao et al. 1998). In sum, the disruption of strand D or abnormal dimer-dimer interactions may provide the driving force for TTR polymerization into amyloid fibrils.

2. Familial Amyloidotic Polyneuropathy (FAP)

In 1952, Corino de Andrade described, for the first time in the Portuguese population, familial amyloidotic polyneuropathy (FAP) as "a peculiar form peripheral neuropathy; familiar atypical generalized amyloidosis with special involvement of the peripheral nerves". The disease has an usually onset between 20 and 35 years of age, is progressive, life conditioning and ultimately fatal within 10 to 15 years (Andrade 1952).
FAP is a form of systemic amyloidosis inherited in an autosomal dominant mode. The main component of amyloid fibrils consists of TTR in which the most common mutation found is a valine replacement by methionine at position 30 (TTR Val30Met) (Saraiva et al. 1984). The main focus of FAP occurs in Northern Portugal affecting about 500 families. Worldwide diverse foci of populations with FAP exist, being Japan and Sweden the second and third largest foci.

2.1. FAP clinical features

After onset of the clinical symptoms, there is a progressive and severe sensory, motor and autonomic polyneuropathy leading to death. FAP clinical symptoms are characterized by early sensory impairment of temperature and pain sensations in the feet. Later, motor involvement occurs with disease progression causing wasting and weakness. A progressive loss of reflexes of upper limbs may occur years later progressing in a similar fashion. Early nervous system autonomic dysfunction is manifested by impotence, urinary bladder dysfunction, motility disturbances in the gastro-intestinal tract and paresis. Malabsorption of nutrients, cardiac insufficiency and vitreous opacities are also common (Andrade 1952).

More than 80 amyloidogenic mutations in TTR have been described (see table 1), displaying some different clinical features but, the majority, is associated with peripheral nervous system involvement. Some mutations give rise to FAP clinical symptoms that do not differ from the original description of the disease; others show different clinical manifestations that may include cardiomyopathy, carpal tunnel syndrome, and vitreous and leptomeningeal TTR deposition (Sousa and Saraiva 2003). Genetic testing is helpful not only for identifying possible carriers of TTR mutations but also for the diagnosis of axonal neuropathies of unknown etiology. Nevertheless, the same pathological TTR variant sometimes gives rise to different clinical manifestations, therefore presenting heterogeneous FAP phenotypes that are addressed in the following section.

2.2. FAP phenotypic heterogeneity

Among TTR Val30Met patients of different origins, namely Portugal, Sweden, Japan, Greece, France and England, there is some heterogeneity in FAP both in age of onset and clinical presentation. For instance, the Swedish kindreds have a later onset, around 56 years of age, and also differ from Portuguese patients by presenting often vitreous opacities. Within Portuguese Val30Met kindreds, significant differences in clinical features and severity of symptoms are rare. However, in a few cases a more benign course of the disease was observed. Genetic analysis of these patients, presenting mild symptoms, revealed that they were compound heterozygotes having, besides Val30Met pathogenic mutation, a second mutation in a different allele of the *ttr* gene resulting in a Thr119Met variant. Hence, Thr119Met TTR is considered a non-pathogenic mutation with protective effects in Val30Met patients (Alves et al. 1997). Interestingly, anticipation of age of clinical onset in successive generations of some TTR Val30Met families has been observed

(Yamamoto et al. 1998). In fact, within Japanese TTR Val30Met FAP patients there is a wide range of clinical features. For instance, Japanese cases of late-onset show different features from those with typical early-onset of Val30Met FAP (Misu et al. 1999). Genetic and/or environmental factors responsible for clinicopathological differences between the early and the late ages of onset of FAP need to be identified.

TTR mutations, such as Leu55Pro and Leu12Pro, are the most aggressive in terms of onset and severity of symptoms, probably due to high instability of the protein conformation (Jacobson et al. 1992; Brett et al. 1999). TTR Val122Ile and Leu111Met are variants associated with cardiomyopathy without neuropathy, named familial cardiac amyloidosis (FAC) (Gorevic et al. 1989; Nordvag et al. 1992). Heart deposition of non-mutated TTR also occurs in elderly people, designated by senile systemic amyloidosis (SSA) (Westermark et al. 1990). SSA reflects the intrinsic amyloidogenic tendency of TTR, which is more susceptible with age. Apart from the amyloidogenic potential of the transthyretin variants accounting for the variable phenotypic expression of FAP, other modulator factors may contribute for amyloid fibril deposition and specificity of the tissue affected.

2.3. TTR amyloidogenesis

TTR amyloidogenesis has been object of intense investigation; however, the precise mechanisms underlying TTR amyloid fibril formation remain to be elucidated. Although TTR has a tendency to self-assemble into amyloid fibrils probably related to its high β-sheet content, other factors are believed to be implicated in this process *in vivo*.

2.3.1. Hypotheses for TTR amyloidogenesis

Three hypotheses have been proposed to explain the mechanism that triggers amyloidogenesis in FAP, which are the following:

1) *The proteolytic hypothesis.* Some amyloidogenic peptides are released from precursors by proteolysis, for instance, amyloid β-peptide (Aβ) is found in senile plaques of AD patients. Similarly, TTR peptides in addition to the intact protein, have been found in extracted amyloid fibrils from SSA and some FAP patients, raising the hypothesis that proteolysis could initiate fibril formation by the release of amyloidogenic fragments (Gustavsson et al. 1995). However, Val30Met TTR fibrils do not always present the referred proteolytic fragments (Tawara et al. 1983; Saraiva et

al. 1984), therefore the role of proteolysis in TTR amyloidogenesis is still debatable and needs further confirmation to be established.

2) *The nucleation or seeding hypothesis.* Amyloid formation via nucleation-dependent oligomerization has been proposed (Harper and Lansbury 1997; Lansbury 1997). The ordered nucleus is formed after a lag phase and then, fibrils grow rapidly following a sigmoid curve (Kisilevsky 2000). The administration of isolated amyloid fibrils in animal models was reported to accelerate amyloid deposition, thus functioning as an amyloid-enhancing factor (Kisilevsky and Boudreau 1983; Johan et al. 1998). In the case of TTR, some reports contradicted the seeding theory *in vitro* (Hurshman et al. 2004) and *in vivo*. For example, the administration of amyloid fibrils, extracted from the heart of a FAP patient, did not accelerate TTR amyloid deposition in a FAP mouse model (Wei et al. 2004). Apparently, these results suggest that TTR amyloid fibril formation does not seem to follow the pathway involving a nucleation or seeding mechanism, as amyloidogenic peptides (such as Aβ and islet amyloid polypeptide) do.

3) *The conformational hypothesis.* It is based on the exposure of new structural conformations due to mutations. Most amyloidogenic proteins present an extensive β-sheet structure, such as TTR, and are prone to form amyloid fibrils (Blake et al. 1978). It is currently accepted that amyloidogenic proteins must undergo destabilization into a partial unfolded state, in order to initiate the amyloidogenic pathway. In the case of TTR, mutations would favour the formation and/or exposure of new structural motifs that would lead to tetramer dissociation and formation of partial unfolded intermediates (Figure 6).

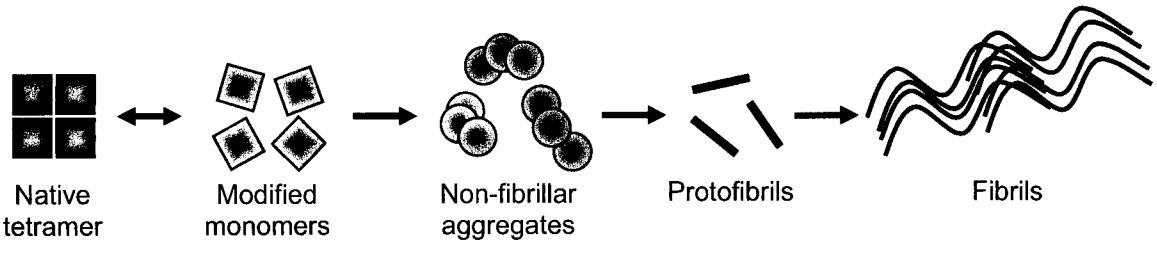

Figure 6. Hypothetical pathway of TTR amyloid fibril assembly.
Native TTR tetramer molecule dissociates into modified monomers that self-aggregate producing non-fibrillar TTR aggregates, protofibrils and amyloid fibrils; adapted from (Sousa and Saraiva 2003).

2.3.2. Intermediate species in TTR amyloidogenesis

Different TTR species have been proposed as intermediates in the pathway of fibril formation, which are the following:

1) *Monomeric intermediates*. Based on recent studies performed at physiological conditions to understand the process that occurs *in vivo*, it was reported that TTR dissociates into non-native monomeric species, which cannot re-associate into tetramers (Quintas et al. 1997, 1999). The formation of non-native monomeric species, with low conformational stability, give rise to partially unfolded monomeric species with a high tendency for ordered aggregation into amyloid fibrils (Quintas et al. 2001). In fact, TTR amyloid fibril formation is favored by amyloidogenic mutations due to the native tetrameric destabilization. *Ex vivo* TTR amyloid fibrils were compared with *in vitro* assembled TTR fibrils for their morphological appearance and it was suggested that the later may represent immature fibrillar species (Cardoso et al. 2002). The proposed model suggests the molecular arrangement of TTR monomers within fibrils and suggests early fibril assembly events.
2) *Dimeric intermediates*. Dimeric TTR intermediate species have also been proposed to be the building blocks leading to fibril formation (Olofsson et al. 2001; Serag et al. 2001). However, an other study showed that mutant stable dimers were unable to polymerize into amyloid, unless they were dissociated into monomers (Redondo et al. 2000b). Thus, this theory is still debatable.
3) *Tetrameric intermediates*. Several studies have implied an altered tetramer as an intermediate in the process of TTR fibril formation (Goldsteins et al. 1997; Eneqvist et al. 2000; Ferrao-Gonzales et al. 2000). To note that these studies were based either in speculative mutants or used insensitive methods to detect monomeric species.

2.3.3. Other components in TTR amyloid deposits

In vivo, amyloid deposits are composed of the disease-specific protein component, and other components. These include serum amyloid P component (SAP), proteoglycans (of the heparan sulfate and/or chondroitin sulfate types), apolipoprotein E (ApoE) and several basement membrane constituents such as fibronectin, laminin and collagen type IV, among others (Kisilevsky 2000). The precise role of these components in the amyloidogenesis process is not clear. However, local components must influence both amyloid fibril formation and tissue-specific deposition. For instance, glycosaminoglycan (GAG) moieties of proteoglycans (PG) seem to favour fibrillogenesis: first, by stabilizing or inducing conformational changes in amyloidogenic precursors that promote fibril formation

or by increasing fibril stability, and secondly, by protecting from proteolysis during fibril formation and after tissue deposition (Dember 2005). Significant amounts of GAGs were detected associated with isolated myocardial TTR amyloid fibrils. The GAGs were identified as 50% chondroitin sulfate, 33% heparin/heparan sulfate, and 17% hyaluronan. The proportion of different GAGs in amyloid deposits may depend both on the organ or tissue affected and on the fibril type (Magnus et al. 1991).

SAP, a plasma glycoprotein, is always present in amyloid deposits, because it has a single calcium-dependent binding site that recognizes a structural motif common to all types of amyloid fibrils, regardless of their component subunits. Thus, SAP is a universal amyloid fibril ligand. SAP contributes to amyloidogenesis, probably due to stabilization of amyloid fibrils and retardation of their clearance (Pepys 2001).

Ultrastructural immunoelectronmicroscopy analysis of FAP amyloid deposits revealed that fibrils are composed of a surface layer and a core. The surface layer is composed of heparan sulfate PG that is externally associated with a loose assembly of TTR filaments. The core contained a microfibril-like structure in which SAP is enclosed in a tight helical structure of chondroitin sulfate PG (Inoue et al. 1998). Despite the fact that SAP and heparin sulfate PG are always present in tissues associated with amyloid fibrils, *in vitro* amyloid fibrils can be formed from several natural polypeptides in their absence.

2.3.4. FAP animal models

The generation of animal models that mimic the human pathological features are of the utmost importance to study *in vivo* mechanisms related to the disease process and to develop therapeutic strategies. In order to investigate the TTR amyloidogenesis process *in vivo*, different transgenic mice carrying the human *ttr* Val30Met gene were generated.

In 1986, the first FAP mouse model was generated (Sasaki et al. 1986). These mice contained a DNA fragment composed of the mouse metallothionein-I (MT) promoter fused to the gene coding sequence for human TTR Val30Met. The expression of the transgene was zinc-inducible and secreted into the plasma but at low levels (2.5 - 12 µg/mL). No amyloid deposition was found, probably due to TTR low plasma levels (Sasaki et al. 1989).

Meanwhile, a distal enhancer element in the mouse *ttr* gene was discovered (Costa et al. 1990). Subsequently, other transgenic mice containing a DNA fragment composed of about 6 kb of the upstream region and the entire human *ttr* Val30Met gene (6-TTRMet30) were generated (Nagata et al. 1995). These mice showed similar TTR expression levels in the plasma as found in man (200-600 µg/ml) and 10 fold increased relatively to 0.6-TTRMet30 mice. TTR was not only expressed in the liver and yolk sac but also in the

choroid plexus. Amyloid deposition started at 9 months of age in the gastrointestinal tract, cardiovascular system and kidneys, extending to other organs and tissues with aging. At 24 months of age the pattern of amyloid deposition was similar to FAP autopsied cases, except for the absence of TTR deposition in the peripheral and autonomic nervous systems (Takaoka et al. 1997).

In 1993, the TTR-knockout mice became available (Episkopou et al. 1993) and were crossed to the 6-TTRMet30 mice, generating animals lacking the endogenous *ttr* gene but carrying the human TTR Val30Met mutant. The same pathological features were observed for these transgenic mice in a TTR-knockout background (Kohno et al. 1997).

To study the process of age-related fibrillogenesis, a feature of SSA, transgenic mice over-expressing human wild-type TTR were generated. 84% of mice older than 18 months developed TTR deposits primarily in the heart and kidney. In most of the animals, the deposits were non-fibrillar and non-congophilic, but 20% of the animals older than 18 months had TTR cardiac amyloid deposits identical to the lesions seen in SSA. Extraction of amyloid and non-amyloid deposits showed intact human TTR with no evidence of proteolysis or co-deposition of murine TTR. This work rose, for the first time, the hypothesis that the non-fibrillar deposits are either a precursor of amyloid fibrils or an alternate form of tissue deposition (Teng et al. 2001).

Very recently, a new FAP mouse model carrying human TTR Val30Met in a heat shock transcription factor 1 (HSF1) knockout background was generated (Santos 2005; Santos and Saraiva 2005). These transgenic mice presented an earlier and more extensive non-fibrillar TTR deposition in distinct organs; furthermore, deposition in the peripheral and autonomic nervous systems was for the first time reported. In the peripheral nervous system (PNS), the mice displayed signs of inflammatory and oxidative stress similarly to asymptomatic carriers of TTR Val30Met. Taken together, the data suggest that genes under HSF1 control might be involved in countering FAP pathogenesis; however, this mechanism remains to be elucidated. This new FAP animal model presents an opportunity to test pharmacological therapies and to address the influence of the stress response in protein misfolding-related diseases.

2.4. FAP pathological features

FAP is characterized by systemic extracellular deposition of amyloid fibrils throughout the connective tissue, especially in the PNS (Coimbra and Andrade 1971b, 1971a). The brain and liver parenchyma are spared. TTR was found to be the main protein constituent of amyloid deposits (Costa et al. 1978). The pattern of distribution of amyloid deposits in the

PNS is diffuse, involving nerve trunks, plexuses, sensory and autonomic ganglia. Immunohistochemical methods have shown the patchy but widespread deposition of non-fibrillar TTR aggregates in the PNS of FAP patients (Sousa and Saraiva 2003).

In peripheral nerves, amyloid deposits affect the epineurium, perineurium and more prominently the endoneurium. Endoneurium deposits occur near blood vessel walls, close to collagen fibrils and Schwann cells. Although amyloid deposits are found in close contact with Schwann cells, it appears that no morphological changes in Schwann cells occur. In later stages of FAP progression, endoneurial contents are replaced by amyloid, abundant collagen bundles, Schwann cells without axons and fibroblasts, and only a few nerve fibers are spared. To note that intracellular TTR deposits or labelling in neurons and Schwann cells were never found. Autonomic nerves are also affected by amyloid deposition leading to autonomic dysfunction involving gastrointestinal, urogenital and cardiovascular systems. In figure 7 is depicted TTR deposition in the peripheral nerve of FAP patients.

In dorsal root ganglia (DRG), amyloid deposition occurs in the stroma in close contact with satellite cells and there is a progressive loss of neuron population preferentially the small diameter ones (Sobue et al. 1990), which agrees with the clinically observed impairment of pain and temperature sensations and autonomic dysfunction. The number of efferent nerve fibers is greatly affected with amyloid deposition, whereas in afferent fibers where amyloid is scarce, only a slight reduction in the number occurs. Other ganglia show a similar pattern (Sousa and Saraiva 2003).

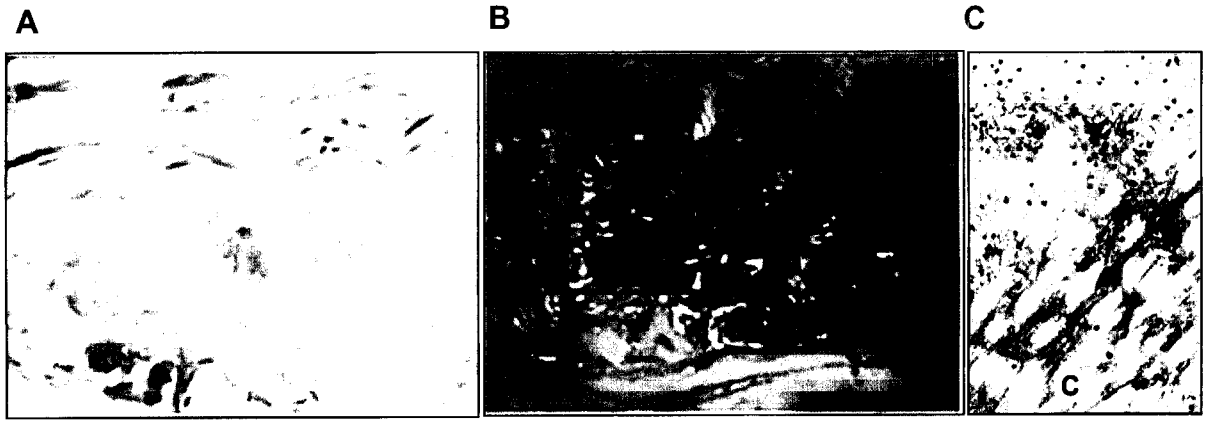

Figure 7. TTR deposition in the nerve of a FAP patient.
A, TTR immunohistochemistry. **B**, Congo Red staining. Adapted from Sousa et al. 2001a. **C**, TTR immunogold electromicroscopy; arrow head: TTR immunostaining; C: collagen bundles (kindly provided by Rui Fernandes, Molecular Neurobiology Group, IBMC).

2.4.1. FAP therapeutic strategies

TTR is synthesized mainly in the liver, and orthotopic liver transplantation (OLT) eliminates more than 95% of variant amyloidogenic TTR from the bloodstream. Currently, liver transplantation is the only potentially curative therapy in this disorder, particularly in younger patients with the most prevalent TTR Val30Met variant, with mild symptoms. Although excellent outcomes have been reported, including improvement in autonomic and peripheral nerve function along with regression of visceral amyloid deposits, the results of OLT are influenced by many factors; for example, properties of TTR variants, nutritional status, age, and severity of neuropathy and cardiac amyloid involvement. Paradoxical acceleration of TTR amyloid deposition following OLT may occur in the heart and certain other sites in some patients (Stangou and Hawkins 2004). This invasive therapy involves several risks for the patients; therefore, the development of non-invasive treatments is needed.

Another possible therapeutic approach is to suppress the expression of mutated *ttr* gene in the liver is gene therapy. In FAP, two strategies using this method were investigated. The first consists in the inhibition of variant TTR mRNA expression by antisense or RNA ribozymes; the second is the repair of mutated TTR gene by chimaeraplasts or single-stranded oligonucleotides. Target gene repair is thought to be a more promising method because the effect can last permanently and is more suitable for proteins with a short plasma half-life. These strategies were tested *in vitro* and *in vivo*, and despite promising results, perfect gene conversion is still not achieved (Nakamura et al. 2004; Ando 2005).

Given that SAP is present in all types of amyloid deposits and contributes for the pathogenesis by stabilization and protection of amyloid fibrils from proteolytic degradation, removal of SAP *in vivo* is likely to reduce the stability of amyloid deposits and promote their regression. Currently, this hypothesis is being tested by the administration of a drug, named CPHPC, that binds to SAP leading to a very rapid clearance by the liver, thus depleting SAP from circulation (Pepys et al. 2002). This drug potently removes SAP from human amyloid deposits in the tissues and has apparently no side effects, therefore, may serve as a therapeutic strategy for all forms of amyloidosis.

Other therapeutic strategies are based on the development and administration of compounds that inhibit amyloid fibril formation or promote fibril disruption. Considering a hypothetical pathway for TTR amyloid fibril formation (Figure 6) that consists in a multi-step process, potential molecular strategies to inhibit amyloid formation or to disrupt amyloid fibrils have been proposed. The mechanisms of drugs action include: TTR stabilizers (I), TTR fibril formation inhibitors (II) and TTR amyloid fibril disrupters (III).

Strategy (I) aims to stabilize and avoid TTR tetramer dissociation through binding of stabilizer molecules such as derivates of some non-steroidal anti-inflammatory drugs (NSAIDs), which include diflunisal, diclofenac, flufenamic acid, and derivates (Miller et al. 2004). In addition, among metal ions, Cr^{3+} has been reported to increase TTR tetrameric stability (Ando 2005). These drugs act by binding to TTR at T_4 binding sites, since T_4 binding to TTR *in vitro* has been demonstrated to stabilize the molecule (Miroy et al. 1996).

The objective of strategy (II) is to arrest fibril formation after the generation of unfolded monomers by the impairment of any of the multi-steps that lead to amyloid fibril formation. A study has been performed in this area. BSB, a Congo red derivate that binds to amyloid fibrils in FAP, suppressed TTR amyloid formation *in vitro*. Thus, BSB might prevent amyloid formation, although further evaluation is required *in vivo* (Ando 2005).

Strategy (III) has the goal of disrupting formed amyloid fibrils. 4'-Iodo-4'-deoxydoxorubicin (I-DOX), tetracycline derivates and nitrophenols have been described as amyloid fibril disrupters (Cardoso et al. 2003). Studies of the action of I-DOX in TTR amyloid demonstrated that it disrupts the fibrillar structure of TTR amyloid into amorphous material (Palha et al. 2000a). However, I-DOX is cardiotoxic, therefore, derivates or other compounds should be designed with similar activity but lacking toxicity. That is the case of tetracyclines, a class of antibiotics. From the tetracyclines tested, doxycycline was the most effective TTR fibril disrupter. To note that the disruption of TTR fibrils by I-DOX or doxycycline has originated non-toxic TTR species, as assessed in cell culture.

Very recently, TTR immunization was reported to have a potential application in immune therapy for FAP. Knowing that TTR Tyr78Phe mutant exposes a cryptic epitope recognized by an antibody that also reacts with amyloid fibrils (Redondo et al. 2000a), this variant was used for immunization. Indeed, immunization of transgenic mice expressing human TTR Val30Met in a TTR-knockout background resulted in the recruitment of lymphocytes and macrophages to sites related to amyloid deposition and in the clearance of amyloid deposits (Terazaki et al. 2006).

TTR aggregates are thought to be responsible for major neuronal dysfunction, for instance they are able to trigger inflammatory and apoptotic related pathways (Sousa and Saraiva 2003). In addition, oxidative stress occurs in FAP tissues with amyloid deposits (Nyhlin et al. 2002). Therefore, free radical scavengers, namely vitamin C and acetylcystein, were administrated to FAP patients. However, these treatments were unsuccessful as lipid peroxidation, a marker of oxidative stress, was not reduced (Nyhlin et al. 2002). Other strategies aiming to block the deleterious effects of TTR aggregates should be considered. The TTR stabilization strategy (I) appears to be the most interesting since it intervenes at the very first step in the process of amyloid formation and, therefore, in

principle impairs the formation of non-fibrillar TTR aggregates, which are the most cytotoxic species.

2.4.2. Hypotheses for neuronal loss

In FAP, nerve fiber loss is due to axonal degeneration. Morphological characterization revealed that axonal loss initially affects unmyelinated and low diameter myelinated fibers and later affects the largest myelinated fibers (Sousa and Saraiva 2003). Based on the pathological features, several hypotheses have been proposed to explain neurodegeneration in FAP: (i) ischemia caused by amyloid deposits around blood vessels; (ii) compression of nervous tissue by amyloid deposits; and (iii) lesions in the dorsal root ganglia (DRG) neurons or Schwann cells; the first two hypotheses were never clearly demonstrated and the third one needs to be further investigated (Sousa and Saraiva 2003).

2.4.3. The presence of toxic non-fibrillar TTR aggregates prior to TTR amyloid fibril formation

Early reports of FAP nerves suggested the presence of non-fibrillar aggregates, at the time of unknown origin, co-existing with fibrillar material (Coimbra and Andrade 1971b). Only recently, TTR deposition has been shown to occur locally as non-fibrillar aggregates prior to formation of amyloid fibrils (Sousa et al. 2001a). Nerve biopsy from asymptomatic TTR Val30Met carriers showed that TTR was already deposited as an aggregated non-fibrillar form, whereas amyloid fibrils were absent, as assessed by Congo red staining; these carrier individuals were termed FAP 0. To note that FAP 0 individuals showed no reduction in the number of nerve fibers, when compared to normal individuals, whereas the following stages of FAP progression displayed increase degrees of both amount of amyloid deposition and nerve fiber reduction (termed FAP 1, 2 and 3, respectively). TTR aggregates have an extracellular distribution, close to Schwann cells, in FAP 0 and in later stages of FAP coexist with mature fibrils (Sousa et al. 2001a). TTR aggregates and amyloid fibrils toxicity was subsequently tested in cell culture systems. Cytotoxicity was observed only with prefibrillar TTR, whereas the soluble counterpart and the longer fibrils, including *ex vivo* isolated amyloid, did not produce toxic effects (Sousa et al. 2001a; Andersson et al. 2002; Reixach et al. 2004). Thus non-fibrillar TTR aggregates are the major cytotoxic species in tissue culture and FAP 0 nerves. Toxicicity of TTR aggregates at the molecular level is next described.

2.4.3.1. Pro-inflammatory and anti-inflammatory mechanisms

Semi-quantitative analysis of immunohistochemical images for pro-inflammatory cytokines such as tumour necrosis factor α (TNFα), interleukin-1β (IL-1β) and macrophage-colony stimulating factor (M-CSF) was performed in FAP and control nerves. These cytokines were up-regulated in FAP nerves and immunostaining was specifically located in endoneurial axons. FAP 0 nerves already evidenced these inflammatory signs, which were sustained at later stages of FAP (Sousa et al. 2001a; Sousa et al. 2001b). Thus, increased levels of these cytokines occur already at asymptomatic stage (FAP 0), indicating that TTR aggregates exert a neuronal pro-inflammatory response. In fact, IL-1β mRNA transcripts were found mainly in FAP axons suggesting that neurons are the principal site of IL-1β synthesis. Moreover, treatment of primary cultures of DRG neurons and Schwann cells with TTR aggregates induced the expression of IL-1β and TNFα, whereas soluble TTR had no effect (Sousa et al. 2001b).

To test the hypothesis that pro- and anti-inflammatory events may exist during the course of FAP, the anti-inflammatory cytokine IL-10 has been selected. Indeed, IL-10 immunohistochemistry in FAP nerves showed increased expression in axons and Schwann cells but only at stages when amyloid was present (FAP 1-3). Thus, enhanced expression of IL-10 occurs concomitantly with over-expression of pro-inflammatory cytokines. However, the levels of IL-10 might not be sufficient to down-regulate pro-inflammatory cytokines during the later stages of disease progression (Sousa et al. 2005b).

In AD, the close interplay between the senile plaques, inflammatory mediators and activated microglia and astrocytes has indicated a relevant role for immune/inflammatory mechanisms in neurodegeneration (Veerhuis et al. 1999). An intriguing feature of FAP nerves is the absence of recruitment of immune/inflammatory cells, despite the production of pro-inflammatory cytokines by neuronal axons. To note that in PNS pro-inflammatory cytokines exhibit pleiotrophic effects on homeostasis and are produced locally by resident and infiltrating macrophages, lymphocytes, mast cells, Schwann cells, fibroblasts and sensory neurons (Skundric and Lisak 2003).

2.4.3.2. Oxidative stress

The involvement of oxidative stress in FAP was investigated on human colon biopsy samples by analysing markers of lipid peroxidation. For instance, anti-hydroxynonenal antibody reacted with amyloid deposits; in addition, the levels of thiobarbituric acid

reactive substances (TBARS), another marker of lipid peroxidation, and the levels of protein carbonyl, a maker of protein modifications by free radicals, were found significantly increased in FAP patient biopsies (Ando et al. 1997). Knowing the relation between cytokines and expression of the inducible form of nitric oxide synthase (iNOS), human nerves were examined for iNOS enzyme. iNOS immunostaining was increased in FAP nerves especially in axons (Sousa et al. 2001b). Moreover, increased iNOS was also present in FAP 0 stressing the influence of prefibrillar TTR aggregates as the causative agent. The capacity of TTR aggregates to induce synthesis of iNOS was further demonstrated in primary cultures of DRG neurons and Schwann cells (Sousa et al. 2001b). Elevated levels of nitric oxide (NO), produced by iNOS, favour the reaction with superoxide anion to generate the strong oxidant agent peroxynitrite (Ischiropoulos et al. 1992a; Ischiropoulos et al. 1992b; Combs et al. 2001). Peroxynitrite can nitrate aromatic residues such as tyrosine to form 3-nitrotyrosine, which is a useful marker of peroxynitrite production (Ischiropoulos et al. 1992a; Ischiropoulos et al. 1992b). In fact, 3-nitrotyrosine was increased in axons from FAP nerves including FAP 0 (Sousa et al. 2001b). The capacity of TTR aggregates to induce oxidative stress was further shown in a neuroblastoma cell line, where toxicity was blocked by catalase indicating a free oxygen radical dependent mechanism (Andersson et al. 2002). These studies provided the first insights into selective neuronal perturbation in FAP taking place prior to amyloid deposition; however, neuroprotective pathways that allow the nerve to survive in the initial stages of FAP, despite the noxious effects of TTR aggregates deposits, are unknown.

2.4.3.3. Extracellular matrix (ECM) remodeling

Recently, microarray analysis of FAP salivary glands, with amyloid deposits, revealed increased expression of two genes related to extracellular matrix (ECM) remodeling (Sousa et al. 2005b). These included biglycan and neutrophil gelatinase-associated lipocalin (NGAL), which exists in a complex with matrix metalloproteinase-9 (MMP-9). By semi-quantitative immunohistochemistry, up-regulation of the ECM-related proteins (i.e. biglycan, NGAL and MMP-9) was confirmed in FAP salivary glands and nerves. Interestingly, MMP-9 was able to degrade TTR aggregates and fibrils *in vitro*; however, in the presence of serum amyloid P component (SAP), a universal amyloid constituent, the ability of MMP-9 to degrade TTR fibrils was reduced (Sousa et al. 2005b). Given the relationship between ECM remodeling and inflammation (Tufvesson and Westergren-Thorsson 2000, 2002), over-expression of ECM-related proteins and inflammation-related molecules in FAP probably contribute to neurodegeneration.

2.4.3.4. Neuronal apoptosis

Neurons may die as a physiological process in development or as a pathological process in disease. Apoptosis is a common mechanism of neuronal cell death in neurodegenerative disorders, however there is evidence supporting the existence of alternative pathways leading to cell death, such as necrosis (Yuan et al. 2003). Apoptosis is characterized by mitochondrial dysfunction inducing activation of caspases, nuclear condensation, DNA degradation and cell death (Bamberger and Landreth 2002). Activation of caspase-3, a critical protease in the late execution phase of apoptosis, started at FAP 0 and augmented in later stages of FAP nerves (Sousa et al. 2001b). Supporting the toxic nature of non-fibrillar TTR aggregates, activation of caspase-3 was demonstrated in both neuronal and Schwann cell lines exposed to TTR aggregates; however, soluble TTR and mature fibrils did not activate caspase-3. In addition, TTR aggregates were also able to induce increased DNA fragmentation in a neuronal cell line (Sousa et al. 2001a; Sousa et al. 2001b). The ability of TTR aggregates to promote cytotoxicity was further demonstrated in a neuroblastoma and HeLa cell lines (Andersson et al. 2002; Olofsson et al. 2002; Reixach et al. 2004). These studies represent the first steps to disclose apoptotic neuronal death in FAP, however, if a necrosis mechanism also occurs is still unknown.

2.5. Cell surface receptors in FAP: the involvement of the receptor for advanced glycation end products (RAGE)

Recently it was proposed that TTR amyloid fibrils bind to plasma membranes through electrostatic interactions causing altered membrane fluidity, which might explain neurotoxicity (Hou et al. 2005); however, previous studies suggested interaction with cell surface receptors such as RAGE as a candidate mechanism involved in TTR aggregate-induced toxicity. The RAGE receptor has a broad repertoire of ligands; among them are amyloid fibrils composed of different subunits (Bucciarelli et al. 2002). In pathological settings, such as amyloidoses, where RAGE ligands accumulate, over-expression of the receptor itself and cellular perturbation occur often resulting in a sustained inflammatory response (Bucciarelli et al. 2002). When RAGE expression was analyzed in FAP nerves, increased levels of RAGE were present already at FAP 0 and especially located in axons (Sousa et al. 2001b). With the progression of the disease, RAGE levels were even more increased indicating that this receptor might be related with cellular perturbation in FAP. In cell culture, RAGE has been demonstrated to bind TTR aggregates inducing activation of

the transcription factor κB (NFκB) (Sousa et al. 2000c). FAP nerves and salivary glands have also shown NFκB activation and nuclear translocation (Sousa et al. 2000c; Sousa et al. 2005b). Induction of pro-inflammatory cytokine (i.e. TNFα and IL-1β) and iNOS expression together with NFκB and caspase-3 activation triggered by TTR aggregates was abrogated in cell culture by an anti-RAGE antibody or by soluble RAGE (Sousa et al. 2000c; Sousa et al. 2001b). Therefore, RAGE most likely plays a crucial role in mediating TTR aggregate-dependent deleterious signaling cascades, probably leading to FAP neurodegeneration. However, we should not exclude the possible involvement of other cellular receptors in FAP. Based on the available data, a general hypothesis for neurodegenerative signaling pathways in FAP is displayed in figure 8.

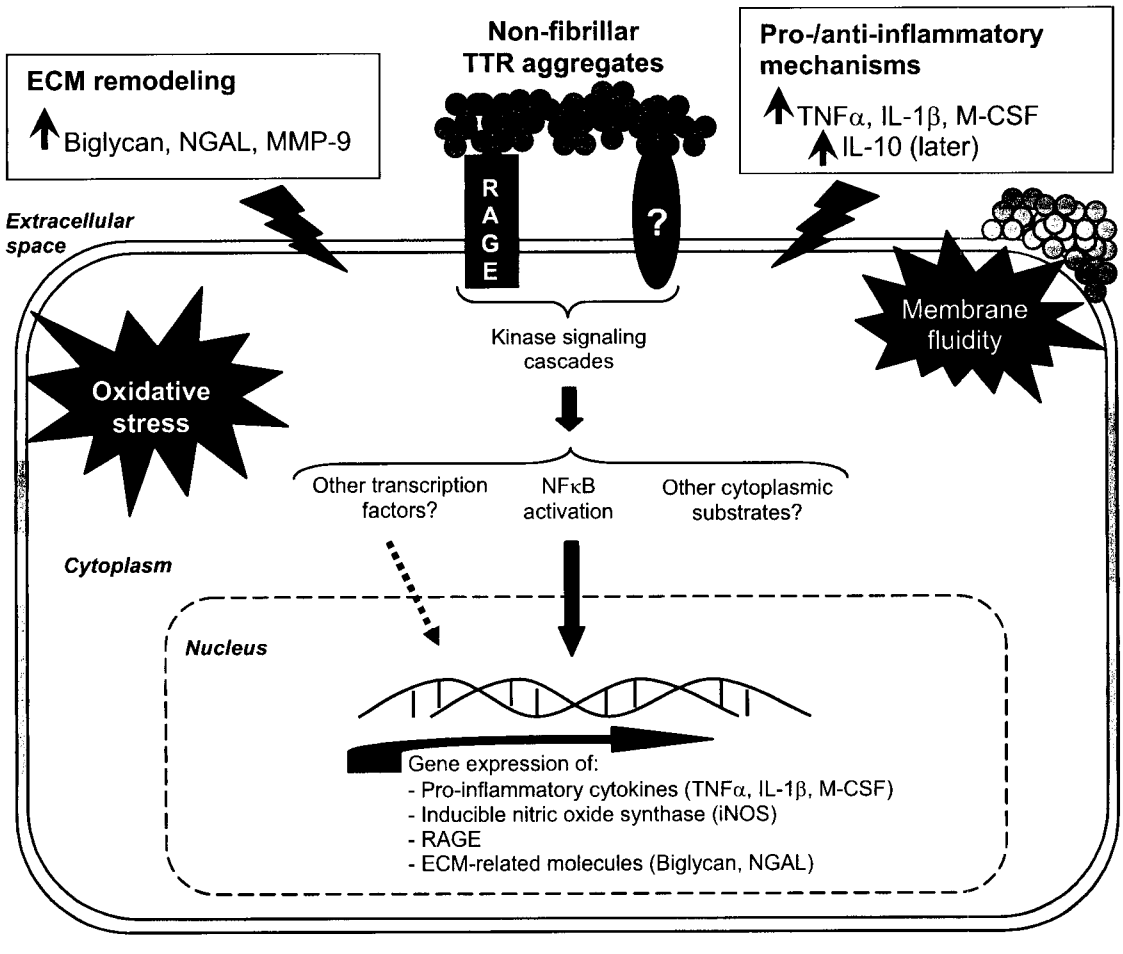

Figure 8. Hypothesis for the molecular signaling mechanisms triggered by non-fibrillar TTR aggregates leading to neuronal degeneration in FAP, as described in the text.

3. Receptor for advanced glycation end products (RAGE)

In 1992, when searching cell surface receptors for advanced glycation end products (AGEs) using bovine lung extract and radiolabelled AGE-BSA (AGE-modified bovine serum albumin), RAGE was isolated, cloned and fully characterized for AGEs binding (Neeper et al. 1992; Schmidt et al. 1992).

Homology analysis revealed that RAGE is a member of the immunoglobulin superfamily of receptors, because of its extracellular region containing one "variable" V-type immunoglobulin domain and two "constant" C-type immunoglobulin domains (Neeper et al. 1992). The RAGE gene encodes a 45 kDa protein that contains a 332 amino acid extracellular domain, a single transmembrane spanning region, followed by a short (43 amino acids), highly charged cytoplasmic tail (Neeper et al. 1992; Schmidt et al. 1992). Competitive binding studies using extracellular domains of RAGE demonstrated that V-type domain is the ligand-binding domain of RAGE (Kislinger et al. 1999).

3.1. RAGE ligands

Shortly after RAGE was recognized as a receptor for AGEs, it became evident that a number of other ligands also interacted with the receptor (Schmidt et al. 2001; Bucciarelli et al. 2002). Structural analysis of ligand-RAGE interaction revealed that the receptor recognizes three-dimensional conformational structures, such as β-sheets and fibrils, rather than specific amino acid sequences (Schmidt et al. 2001; Bucciarelli et al. 2002). This indicates the importance of understanding the structure of ligand recognition sites in RAGE and, therefore, x-crystallography data are expected. RAGE binds fibrils composed of Aβ (accumulating in AD) (Yan et al. 1996), amyloid A (accumulating in systemic amyloidosis) (Yan et al. 2000) and TTR (accumulating in FAP) (Sousa et al. 2000c). Further ligands of RAGE are S100/calgranulins, a family of closely related calcium-binding polypeptides that accumulates extracellularly at sites of chronic inflammation (Hofmann et al. 1999) and Mac-1, a β2-integrin able to mediate leukocyte adhesion (Chavakis et al. 2003). Another ligand of RAGE is high mobility group box 1 protein (HMGB1), which is described in more detail in the next section. RAGE multiligand properties are also seen with other receptors of the immunoglobulin family, including CD36 (Krieger 2001), another AGE receptor. One should note that all of the RAGE ligands studied so far appear to be multivalent, thus having other cell surface receptors in addition to RAGE (Schmidt et al. 2001).

3.1.1. High mobility group box 1 (HMGB1)

HMGB1 is a DNA-binding protein that, in addition to transcriptional regulatory functions within the cell, may also exist extracellularly and on the surface of cells (Muller et al. 2004). In the later, HMGB1-RAGE interaction has been studied in neurite outgrowth and tumor biology (Hori et al. 1995; Taguchi et al. 2000). HMGB1 is released extracellularly from activated monocytes/macrophages and is a mediator of inflammation (Andersson and Tracey 2003). Furthermore, an active secretion mechanism of HMGB1 from monocytes via secretory lysosomes has been described (Bianchi and Manfredi 2004). Blockade of HMGB1 *in vivo* resulted in survival to septic shock (Wang et al. 1999).
HMGB1 is released by cells upon necrosis but not after apoptosis, where it is irreversibly bound by chromatin (Bianchi and Manfredi 2004). Interestingly, HMGB1 has also a role in enhancing the toxicity of Aβ in Alzheimer's disease (AD). In AD brains, HMGB1 was enhanced and colocalized with Aβ in senile plaques associated with microglia. Diffuse deposits of HMGB1 were found around dying neurons in rat models of AD delaying clearance of Aβ by microglia (Takata et al. 2003; Takata et al. 2004).
Taken together, extracellular HMGB1 is a signal for tissue damage triggering inflammatory responses. Nevertheless, it has been described that besides RAGE, toll-like receptors 2 and 4 (TLR-2 and -4) also mediate inflammatory effects of HMGB1 (Park et al. 2004), but the precise roles of these or other unknown receptors remain to be elucidated.

3.2. RAGE expression and isoforms

RAGE transcription is controlled by several transcription factors, including specificity protein 1 (Sp1), activator protein-2 (AP-2), NFκB and nuclear factor of interleukin 6 (NF-IL6) (Li and Schmidt 1997). RAGE expression occurs in both a constitutive and inducible manner, depending on the cell type and developmental stage. Whereas RAGE is constitutively expressed during embryonic development, its expression is down-regulated in adult life. However, known exceptions are the skin and the lung, which constitutively express RAGE throughout life. RAGE is expressed at low levels in adults in a range of cell types, including monocytes/macrophages, lymphocytes, endothelial cells, smooth muscle cells, neurons, among others (Brett et al. 1993; Hori et al. 1995; Ritthaler et al. 1995). Biological stress such as mechanical vascular injury, diabetes, inflammation, and neurodegenerative disorders such as AD and FAP lead to striking up-regulation of RAGE

expression, correlating with increased ligand accumulation (Yan et al. 1996; Hofmann et al. 1999; Sousa et al. 2001b).

Recently, additional RAGE isoforms that encode several truncated forms of RAGE lacking the transmembrane region and the cytoplasmic tail were identified, but the functional significance of these secreted forms have not yet been described (Malherbe et al. 1999; Yonekura et al. 2003). The existence of truncated RAGE isoforms from the same gene (coexpressed with the full length RAGE transcript) implies that the pre-mRNA of RAGE can be subjected to alternative splicing under the control of yet unknown pathways (Schlueter et al. 2003). In mice, however, these truncated RAGE isoforms are likely produced by carboxyl-terminal truncation (Hanford et al. 2004).

3.2.1. Soluble RAGE (sRAGE)

In order to gain insights on the pathological role of RAGE, the interaction of ligands with cell surface RAGE was blocked using soluble RAGE (sRAGE). sRAGE is a truncated form of the receptor comprising the extracellular domain and thereby functions as a decoy that prevents ligands from interacting with the cell surface receptor. Application of sRAGE *in vitro* and *in vivo* resulted in effective blockade of RAGE. For instance, administration of sRAGE in a range of animal models has been shown to prevent accelerated diabetic atherosclerosis (Park et al. 1998), impaired wound healing (Goova et al. 2001), colitis (Hofmann et al. 1999), Aβ penetration of the blood-brain barrier (Deane et al. 2003), and tumour cell migration and invasion (Taguchi et al. 2000).

Since most of the data obtained with sRAGE was confirmed by application of neutralizing antibodies to the receptor and/or transfection with plasmids over-expressing dominant negative RAGE (DN-RAGE), the receptor has been suggested as a potentially effective therapeutic target (Hudson et al. 2003). At the same time, it seems unlikely that RAGE could mediate so many deleterious effects in such diverse models of disease. Since RAGE binds to a variety of ligands, the promising effects observed with sRAGE might not be specific as sRAGE might also block the interaction of ligands with other receptors. For example, S100 proteins and HMGB1 recognize cell surface receptors other than RAGE (Robinson et al. 2002; Erlandsson Harris and Andersson 2004). Indeed, in several animal models, protection from development of pathology, such as diabetic neuropathy, was more profound in wild-type mice treated with sRAGE than in RAGE-deficient mice (Bierhaus et al. 2004).

3.3. RAGE-dependent signaling

It is well established that RAGE acts as a signal transduction receptor after ligand engagement, as deletion of the cytosolic tail originates a dominant-negative effect on ligand-induced gene activation (Kislinger et al. 1999; Taguchi et al. 2000; Sakaguchi et al. 2003). RAGE cytosolic tail lacks known signaling motifs (i.e. phosphorylation sites, kinase domains, etc.), but it is critical for RAGE-dependent cellular activation.

AGEs elicit a toxic effect by generation of reactive oxygen species (ROS), which occurs mainly via activation of RAGE (Lander et al. 1997). Initial studies showed that intracellular signaling from AGE-RAGE interaction directly induce generation of ROS, which lead to activation of p21ras and extracellular signal-regulated kinases 1/2 (ERK1/2), a signaling cascade belonging to mitogen-activated protein kinases (MAPKs) group, and activation and nuclear translocation of NFκB, a transcription factor that regulates expression of multiple pro-inflammatory genes (Lander et al. 1997; Yeh et al. 2001). ROS may be originated via nicotinamide adenine dinucleotide phosphate (NADPH) oxidase and/or other mechanisms (Lander et al. 1997; Wautier et al. 2001).

Subsequent studies have identified that ligand binding of RAGE triggers several signaling cascades including the MAPKs (i.e. ERK1/2, p38 and c-Jun N-terminal kinases (JNKs)) (Taguchi et al. 2000), the Rho GTPases cdc42/rac that is a pathway involved in cell growth and migration (Huttunen et al. 1999), and stress-activated JAK/STAT (Janus kinase/signal transducer and activator of transcription), thereby reprogramming cellular properties (Huang et al. 2001; Sakaguchi et al. 2003). Upon RAGE engagement, other transcription factors might be activated, including Sp1 (Li et al. 1998) and cAMP response element binding protein (CREB), which depend on upstream ERK1/2-RSK2 activation (Huttunen et al. 2002b). The cytoplasmic domain of RAGE has been shown to interact directly with ERK1/2 (Ishihara et al. 2003), but it is possible that other signaling molecules may also interact, since RAGE signals through other pathways that do not involve ERK1/2.

The diversity of signaling cascades identified in RAGE-mediated cellular signaling (Figure 9) implies that different RAGE ligands might induce the activation of different signal transduction pathways (especially in different cell types) and thereby add a further level of complexity to the RAGE network. The consequences of such mechanisms may be critical in a scenario where endogenous negative feedback pathways, responsible for returning cellular settings to a steady state, are disturbed and pathways leading to cellular activation escalate (Bierhaus et al. 2005).

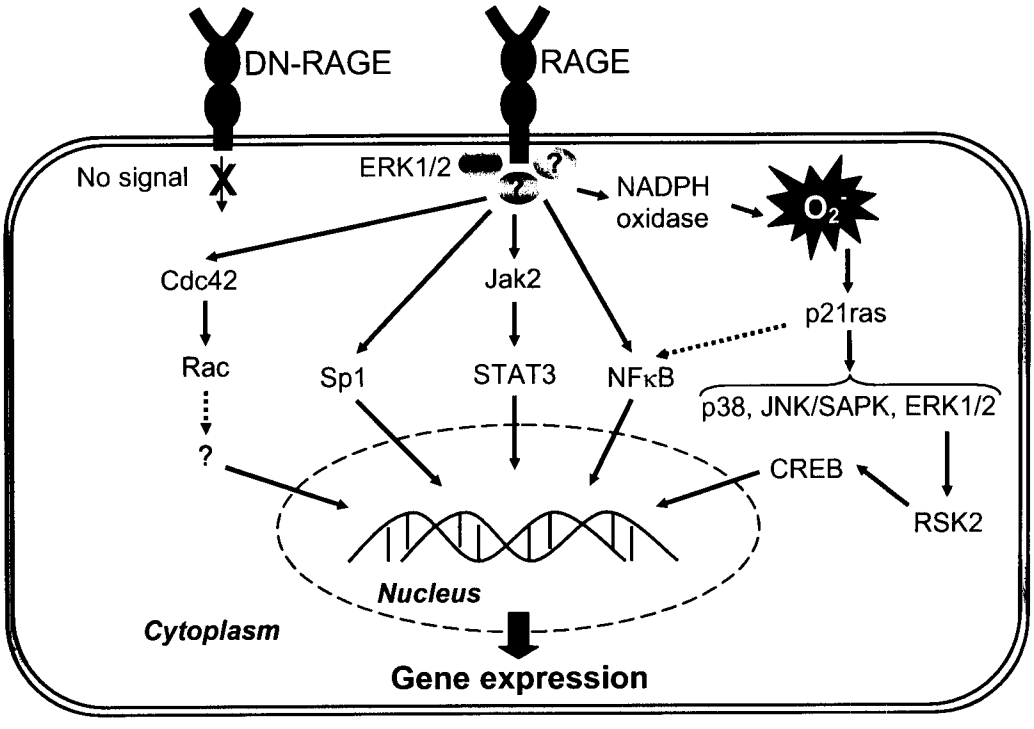

Figure 9. RAGE-induced signaling pathways.
The binding of ligands to RAGE, such as AGEs, S100/calgranulins and HMGB1, results in activation of a cascade of signaling pathways, including cdc42/rac, JAK/STAT and MAPKs leading to gene activation and cellular response. Expression of the dominant-negative (DN) form of RAGE, without the signaling tail, blocks signaling and gene expression. Solid arrows denote activation; the dashed arrows denote unknown intermediate signaling mediators.

3.4. RAGE physiological functions

The absence of a developmental phenotype in RAGE-deficient mice and the possibility that RAGE might impact in multiple chronic disease states have largely focused attention away from the physiological roles of this receptor. So far, only a few reports have suggested that RAGE expression might contribute to developmental paradigms. For example, in axonal sprouting which accompanies neuronal development, the RAGE-HMGB1 interaction may be important (Hori et al. 1995; Huttunen et al. 1999). The neurite outgrowth-promoting role of RAGE was recently confirmed *in vivo* in a unilateral sciatic nerve crush model, in which the blockade of RAGE, either by sRAGE or by blocking $F(ab')_2$ fragments of antibodies reduced functional regeneration of peripheral nerve (Rong et al. 2004a). It is of major importance to dissect RAGE physiological roles, in order to fully elucidate the safety of long-term blockade of RAGE in human subjects with chronic diseases.

3.5. RAGE in AD and amyloidoses

In a search for cell surface interaction sites for Aβ, RAGE was identified (Yan et al. 1996) and found to bind Aβ in a nanomolar range (50-150 nM). RAGE expression was enhanced in AD, particularly in affected neurons, microglia and vasculature. The outcome of the Aβ-RAGE interaction may vary accordingly with the cell type. For instance, in neurons it generates oxidative stress, activating NFκB and inducing expression of macrophage-colony stimulating factor (M-CSF) and after prolonged incubation with Aβ, neurons undergo RAGE-dependent apoptosis, whereas microglia demonstrates sustained cellular activation that includes expression of cytokines, i.e. TNFα and chemotaxis (Yan et al. 1996; Du Yan et al. 1997). Further studies suggested a positive feedback loop in which Aβ-RAGE-mediated microglial activation enhances expression of M-CSF and RAGE, possibly initiating an ascending spiral of cellular activation (Lue et al. 2001). Transgenic mice with targeted neuronal over-expression of RAGE were crossed with a murine model of AD. This double transgenic model displayed early abnormalities in spatial learning/memory, accompanied by increased neuropathologic findings, before such changes were found in AD mice. In contrast, transgenic mice bearing a DN-RAGE construct targeted to neurons crossed with an AD animal model displayed preservation of spatial learning/memory and diminished neuropathologic changes. These data implicates RAGE as a cofactor for Aβ-induced neuronal perturbation in a model of Alzheimer's-type pathology (Arancio et al. 2004).

Other studies have revealed that RAGE interacts more broadly with β-sheet fibrils regardless the composition of the subunits (amylin, serum amyloid A, prion-derived peptides, among others) (Yan et al. 2000), and deposition of amyloid results in enhanced expression of RAGE. A murine model for systemic amyloidosis induced by amyloid-enhancing factor/silver nitrate displayed accumulation of amyloid A in the spleen. Deposition of amyloid A correlated with cell stress markers, such as heme oxygenase type 1, interleukin 6, and M-CSF, as well as activation of NFκB. Blocking access of ligands to the receptor by administrating mice with sRAGE or blocking $F(ab')_2$ fragments of anti-RAGE IgG, resulted in a decreased accumulation of amyloid and decreased cellular stress in the spleen, as showed by diminished expression or activation of the above mentioned cell stress markers (Yan et al. 2000). These evidences indicate that RAGE is a signal transduction molecule for a variety of β-sheet fibrils.

4. Mitogen-activated protein kinases (MAPKs)

MAPKs are important players in signal transduction pathways activated by a range of stimuli and mediate a number of physiological and pathological responses in cell function. In the following section are described the mode of activation of MAPKs signaling cascades and some of their targets.

4.1. MAPK signal transduction pathways

MAPKs are a family of ubiquitous proline directed, serine/threonine protein kinases, which play a critical role in transducing multiple signals from the cell surface to the nucleus in all eukaryotic species. The three major subfamilies of MAPKs encompass extracellular signal-regulated kinases 1/2 (ERK1/2), p38 kinases and c-Jun N-terminal kinases (JNKs) (Chang and Karin 2001; Pearson et al. 2001). Multiple genes and splice variants for each MAPK as well as for a number of specific upstream kinases responsible for MAPK phosphorylation and activation have been reported; these are depicted in figure 10. All MAPK family members are terminal kinases of a three-tiered activation system in which successive members are phosphorylated by upstream dual kinases; therefore, MAPKs are regulated by phosphorylation signaling cascades (Pearson et al. 2001). MAPKs are phosphorylated by members of the upstream MAPK kinase (MAPKK) family (also known as MEKs or MKKs) on threonine and tyrosine residues within a conserved Thr-X-Tyr motif in the activation loop (where X represents glutamate in ERK, proline in JNK and glycine in p38) (Pearson et al. 2001). MAPKKs are, in turn, regulated by serine/threonine phosphorylation by a number of upstream MAPKKKs (or MEKK), which include Raf family, apoptosis signal-regulating kinase 1 (ASK-1), TGFβ-activated kinase 1 (TAK1), and members of mixed lineage kinases (MLKs) (Davis 2000; Chang and Karin 2001). Following phosphorylation and activation, each individual MAPK is capable of phosphorylating and regulating a number of specific substrates that include transcription factors (following translocation of the activated MAPK from the cytosol into the nucleus), cytoskeletal elements, cytosolic targets and other protein kinases; some of these are shown in figure 10. Such array of substrates indicates a key role for MAPKs in modulating diverse cell functions, which is supported by recent studies using pharmacological inhibitors and dominant inhibitory or active mutant kinases, as well as analysis of knockout mice. For instance, ERKs are involved in cellular chemotaxis, cell cycle progression and mitogenesis, oncogenic transformation and metastasis, neuronal differentiation and survival, and in processes related with memory and learning (Mansour et al. 1994; Xia et

al. 1995; Ferrell 1996; Kornhauser and Greenberg 1997; Reszka et al. 1997). On the other hand, JNKs and p38 are important in pathways controlling T cell differentiation, production of inflammatory cytokines and apoptotic cell death (Xia et al. 1995; Verheij et al. 1996; Ichijo et al. 1997; Yang et al. 1998).

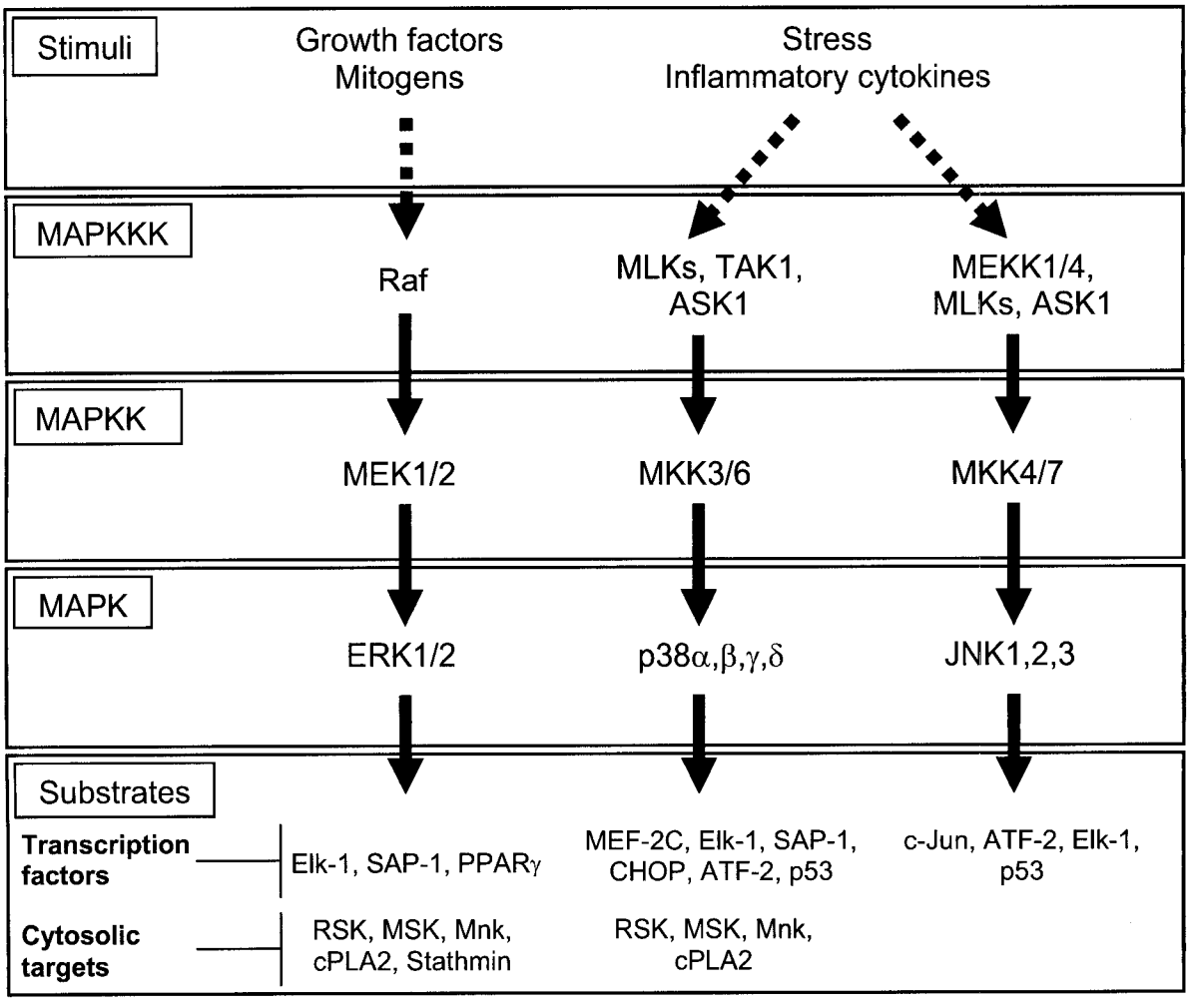

Figure 10. Schematic representation of the main mammalian MAP kinase signal transduction pathways.
MAPKs are boxed together and include extracellular signal-regulated kinases 1/2 (ERK1/2), c-Jun N-terminal kinases (JNKs) and p38 kinases. Each MAPK is activated after phosphorylation by specific upstream MAPKK as indicated by solid arrows. MAP/ERK kinase 1 (MEK1) and MEK2 activate the ERKs, MKK3 and MKK6 activate p38 kinases, and MKK4 and MKK7 activate JNKs. Raf family activates MEK1/2, mixed lineage kinases (MLKs) and apoptosis signal-regulating kinase 1 (ASK-1) activates both MKK3/6 and MKK4/7, whereas TGFβ-activated kinase 1 (TAK1) activates only MKK3/6 and MEKK1/4 activates MKK4/7. Generally, ERKs are activated strongly by growth factors, mitogens, among others. Conversely, JNK and p38 MAPKs are activated by cell stresses (e.g. UV light, oxidants, etc.), cytokines, among others. MAPKs phosphorylate serine or threonine residues preceding a proline, although additional docking sites outside of the kinase active site also appear to be important in defining substrate selectivity. Some established target substrates for MAPKs include transcription factors such as members of E-26-specific (ETS) domain proteins namely Elk-1 and serum response factor accessory protein 1 (SAP-1), c-Jun, activating transcription factor-2 (ATF-2) myocyte enhancer factor (MEF-2C), C/EBP homologous protein (CHOP), poly-(ADP-ribose)-polymerase γ (PPARγ) and p53 (Sionov and Haupt 1999), microtubule regulator stathmin, cytosolic substrate such as cytosolic phopholipase A2 (cPLA2) and downstream target kinases such as ribosomal p90 S6 kinase (RSK), mitogen- and stress-activated protein

kinase (MSK), MAP kinase-integrating kinase (Mnk). MAPKKK activation (dashed arrows) is mediated by numerous upstream kinases acting together with various GTP binding proteins as well as complex-forming adaptor proteins. Adapted from (Camps et al. 2000).

4.2. MAPK signal termination

Activation of MAPKs is a reversible process even in sustained presence of activating stimuli, indicating that protein phosphatases provide an important mechanism for MAPK control (Camps et al. 2000).

4.2.1. MAPK inactivation by threonine or tyrosine dephosphorylation

Dephosphorylation of either the threonine or tyrosine residue within the MAPKs activation loop Thr-X-Tyr motif alone results in their enzymatic inactivation. In cells, dephosphorylation and inactivation of MAPKs occur with kinetics ranging from minutes to several hours depending on the cell type and activating stimulus. For instance, ERKs can be rapidly inactivated by constitutive serine/threonine protein phosphatases (PPs), such as protein phosphatase 2A (PP2A) (Alessi et al. 1995). Members of the protein tyrosine phosphatase (PTP) family also bind and inactivate ERK MAPKs. However, little is known about their general importance in terminating MAPK signaling, such as specificity for different MAPKs and mechanisms that may control their phosphatase activity. In contrast, much progress has been made to understand the role of a subclass of PTPs that possess activity for dephosphorylating both phosphotyrosine and phosphothreonine residues, hereafter called dual specificity MAP kinase phosphatases (MKPs) (Camps et al. 2000).

4.2.2. MAPK inactivation by dual specificity MAP kinase phosphatases (MKPs)

To date, 13 dual specificity MKPs have been identified and characterized. These include dual specificity phosphatase 1/MAP kinase phosphatase 1 (DUSP1/MKP-1), DUSP4/MKP-2, DUSP6/MKP-3, DUSP9/MKP-4, DUSP10/MKP-5, MKP-6, DUSP16/MKP-7, DUSP2/phosphatase of activated cells 1 (PAC1), DUSP5/VH3, DUSP8/VH5, DUSP7/B59, DUSP3/VH-related (VHR) and DSP2 (Theodosiou and Ashworth 2002; Farooq and Zhou 2004). All MKPs mediate inactivation of MAPKs. Structurally, MKPs share some common features, including an active site sequence motif, two N-terminal CH2 domains that are homologous to the cell cycle regulator Cdc25 and a cluster of basic amino acids that are involved in binding of MAPKs (Theodosiou and Ashworth 2002). Most MPKs display wide tissue distribution but expression varies in subcellular locations

(Theodosiou and Ashworth 2002). For instance, MKP-1 is predominantly nuclear, whereas MKP-3 is found in the cytosol, whereas some other MKPs show both cytosolic and nuclear localizations. MKPs also display different substrate specificity towards MAPKs. For example, MKP-3 and PAC1 selectively dephosphorylate ERK1/2, whereas MKP-1, MKP-2 and MKP-4 show a broad phosphatase activity for all subfamilies of MAPKs (Farooq and Zhou 2004).

Another feature of MKPs is their tight and rapid transcriptional induction by growth factors and/or cellular stresses. In PC12 cells, for example, MKP-1, MKP-2 and VH5 all undergo fast induction as immediate early genes in response to mitogens (Martell et al. 1995; Misra-Press et al. 1995). Mechanisms controlling MKP gene transcription are likely to be complex, although expression of some MKP genes, such as MKP-1, MKP-2 and PAC1, were reported to be dependent at least in part of MAPK activation (Bokemeyer et al. 1996; Grumont et al. 1996; Brondello et al. 1997). This provides a mechanism of negative feedback of activated MAPK or a regulatory cross-talk between parallel MAPK pathways. Based on available data a model for MAPK inactivation by MKPs was proposed (Camps et al. 2000). In this model, cell stimulation by growth factors, cytokines or stresses leads to a rapid transcription of one or some MKP genes. Increase of MKPs transcription may derive from activation of specific MAPKs, however other pathways are possible. After translation of the MKP mRNA into protein, the catalytically inactive MKP migrates to a specific subcellular compartment within the nucleus and/or cytosol. Upon interaction with target MAPK, MKP binds tightly through its N-terminus, which triggers activation of the phosphatase catalytic domain. If the bound MAPK is activated, then it will become rapidly inactivated. By contrast, if the MAPK is not active, then its tight binding to an active MKP is predicted to disable kinase activation by subsequent stimulus (Camps et al. 2000). Together, tight control of MKP gene induction as well as substrate selectivity and catalytic activation by specific MAPKs, enable a mechanism for rapid and targeted inactivation of selected MAPK activities.

4.3. MAPKs activation in neurodegeneration

Given that abnormal cell death most likely occurs in many neurodegenerative diseases (Harper and Wilkie 2003), discovery of pharmacological targets that could halt cell death has been object of intense research. Before a cell is committed to die, it is believed that a balance between survival and death signals exists. Many of the pathways involved in these processes are regulated by mechanisms of phosphorylation and target gene transcription. The latter is controlled by transcription factors, which are regulated by a

number of kinases. Indeed, evidence for the activation of ERK1/2, JNK and p38 MAPK pathways in disease settings and in models of neurodegenerative disorders has been well documented (Harper and Wilkie 2003). For example, increased MAPK phosphorylation was observed in AD (Zhu et al. 2002b) and also in several sporadic and familial neurodegenerative diseases characterized by tau deposits (Ferrer et al. 2003). Furthermore, active ERK1/2 is increased in substancia nigra neurons of patients with Parkinson's disease (PD) and other Lewy body diseases (Zhu et al. 2002a), and in the vulnerable penumbra following acute ischemic stroke in humans (Slevin et al. 2000). Subsequently, we will solely focus on ERK1/2 roles in neuronal survival and death.

4.3.1. Opposing roles of ERK1/2 kinases in neuronal injury and disease.

Several reports suggest that ERK1/2 kinases mediate neuroprotective activity of extracellular factors, including neurotrophins (Xia et al. 1995). ERK1/2 kinases are also activated upon neuronal injury, and may serve as a defensive mechanism that helps to compensate for the deleterious effects of a damaging insult. For instance, ERK1/2 activation by brain derived neurotrophic factor (BDNF) was shown to protect cultured rat cortical neurons against apoptosis, induced by genotoxic compounds (Hetman et al. 1999). In addition, several other reports suggest that ERK1/2 may serve as a transducer for agents that protect from other forms of neuronal injury including excitotoxicity, calcium overload, oxidative injury, hypoxia or neurotoxic viruses (Hetman and Gozdz 2004). The emerging mechanisms of ERK1/2-mediated neuroprotection may involve transcriptional regulation that could induce production of anti-apoptotic mediators and/or direct inhibition of cell death machinery. For instance, ERK-dependent activation of its target kinase ribosomal p90 S6 kinase (RSK2) was suggested to activate the transcription factor CREB, which increases the expression of the anti-apoptotic *Bcl-2* gene, and to phosphorylate Bad, inhibiting its pro-apoptotic activity (Bonni et al. 1999). Furthermore, active ERK1/2 was also shown to directly phosphorylate and inhibit Bim (Biswas and Greene 2002), another pro-apoptotic member of bcl-2 family, and glycogen synthase kinase 3 β (GSK3β), a pro-apoptotic kinase (Hetman et al. 2002).

On the other hand, there is growing evidence implicating ERK1/2 in promoting of cell death in both neurons and other cell types, namely in neurodegenerative diseases (Harper and Wilkie 2003). These studies suggest a link between active ERK1/2 and diseased neurons, which is difficult to ascribe functionality from expression data alone, as kinase activation may simply reflect a cellular response to stress and not necessarily trigger cell death or survival pathways.

Neuroprotective effects of ERK1/2 inhibition were observed *in vivo*, for example, in models of cerebral ischemia-reperfusion. In these studies, blockade of ERK1/2 activation, using pharmacological inhibitors of MEK1/2, led to reduced neuronal injury and loss of function in mice and gerbils (Alessandrini et al. 1999). Several *in vitro* studies revealed protective effect of ERK1/2 activation blockade in both established cell lines and primary neurons subjected to a variety of insults. These include toxicity induced by peroxynitrite (Oh-hashi et al. 1999), mechanical trauma (Mori et al. 2002), glutathione depletion (Satoh et al. 2000; Stanciu et al. 2000), zinc (Seo et al. 2001), Aβ with iron (Kuperstein and Yavin 2002), the parkinsonian neurotoxin 1-methyl-4-phenylpyridinium (MPP+) (Gomez-Santos et al. 2002), among other insults (Cha et al. 2000; Du et al. 2002). Moreover, the potential contribution of ERK1/2 activation to cell death was not limited to neurons, as MEK1/2 inhibitors have been found to block cell death in a range of other cell types such as vascular smooth muscle cells (Gurjar et al. 2001), fibroblasts (Sakon et al. 2003) and renal epithelial cells (Ramachandiran et al. 2002). Together, these studies implicate a detrimental role for ERK signaling during injury when oxidative stress is present.

Interestingly, many model systems that suggest a detrimental role for ERK1/2 activation are associated with delayed and sustained kinetics of ERK1/2 activation (Colucci-D'Amato et al. 2003). It is well known that neurodegenerative diseases and ischemic-reperfusion injury have in common the generation of ROS/reactive nitrogen species (RNS). Indeed, ERK activation appears to be mediated by redox mechanisms in both neuronal injuries (Stanciu et al. 2000) and models of neurodegeneration (Kuperstein and Yavin 2002; Zhu et al. 2002a). Studies in transgenic mice (Noshita et al. 2002) and cell culture (Kulich and Chu 2003) suggest that inhibition of ERK1/2 signaling is an important mechanism by which antioxidants confer protection. There is a variety of potential targets of ROS and RNS that could contribute to ERK1/2 activation. These include upstream activators of ERK1/2, such as cell surface receptors (Zhang et al. 2000), adapter (Shc) (Vindis et al. 2001) and GTP-binding kinases (Ras) (Kamata and Hirata 1999), whose oxidation may result in activation of ERK1/2 signaling pathway. In addition, downstream inactivators of ERK1/2 include protein phosphatases and proteasome components that are susceptible to oxidative inactivation, thus leading to ERK1/2 activation. In fact, phosphatases capable of inactivating ERK1/2 include PPs, PTPs and dual specificity MKPs (Keyse 2000). PTPs and MKPs share a $HC(X)_5R$ motif that is critical for enzymatic activity, and this catalytic cysteine residue is particularly susceptible to oxidation (Gabbita et al. 2000). Indeed, transient oxidative inactivation of PTPs is a common mechanism in signal transduction, but higher oxidation states are usually irreversible, which may result in pathologically sustained ERK1/2 activity. In addition, oxidative modification of the metal binding residues of metallophosphatases could probably affect serine/threonine PP activity as well (Gabbita

et al. 2000). Likewise, ubiquitin-proteosome system impairment, which has been reported in neurodegenerative diseases, may delay degradation of ERK1/2 (Hashimoto et al. 2000). Together, the chronic ERK1/2 activity in injured neurons likely reflects abnormal activation of upstream signaling mediators, impairment of negative feedback regulators and/or alterations in degradation pathways (Chu et al. 2004).

Chronic activation of ERK1/2 in certain subcellular compartments, possibly by sequestration, most likely affects the accessibility of ERK1/2 to downstream targets, which can lead to neurotoxic responses that are driven by these kinases. For instance, in PD and AD, ERK1/2 appears to be localized within discrete cytoplasmic granules (Pei et al. 2002; Zhu et al. 2002a).

How can we reconcile the beneficial *vs* deleterious observations of ERK1/2 activation? The factors that are proposed to determine the survival or death outcome of these multifunctional transducers include differences in the activation intensity or duration, the subcellular localization of signaling molecules, the signaling context provided by other pathways or the cellular energetic state. In addition, the nature and extent of cellular injury may also change the final results for the same signaling events. Finally, chronic activation of a signaling pathway probably reflects impairment of negative feedback regulators that normally function to terminate signaling responses. Some or all these factors may also affect the ultimate outcome of ERK1/2 activation in the nervous system (Chu et al. 2004; Hetman and Gozdz 2004). The mechanisms that determine whether ERK1/2 activation stimulates or inhibits neuronal survival are an interesting target for research. Identification of these mechanisms is thought to be crucial to develop useful strategies for targeting ERK1/2 signaling cascade to intervene against neurodegenerative diseases (Hetman and Gozdz 2004).

5. Concluding remarks

The molecular signaling mechanisms triggered by toxic non-fibrillar TTR aggregates, which ultimately lead to neurodegeneration in FAP, remain poorly understood. Some molecular insights were given by investigation of the toxic nature of non-fibrillar TTR deposits in human FAP nerves and in cell culture studies. These included increased expression of inflammation and matrix remodeling-related molecules and signs of oxidative stress namely tyrosine nitration of proteins. Apart from the known involvement of the NFκB transcription factor, thought to mediate transcriptional induction of some of the above mentioned molecules, the involvement of other transcription factors implicated in

promoting the apoptotic death pathway leading to neurodegeneration are missing, as well as structural binding motifs responsible for RAGE-TTR interaction need to be further investigated.

In cell culture, RAGE has been demonstrated to serve as a cell surface signal transduction receptor for TTR aggregates eliciting early inflammation and oxidative stress and later apoptotic death. However, early intracellular signaling events triggered by RAGE engagement leading to activation of gene transcription are unknown. Besides, intervention of other still unknown receptors has to be considered.

The present study addressed some of these questions to provide new insights on molecular signaling mechanisms associated with FAP pathology.

PART II

Research Project

Objectives

The main propose of the research project described in the following chapters was to unravel unknown signaling mediators in FAP pathogenesis and to study RAGE-TTR interaction *in vitro*.

The designed experiments had the following goals:

1) Characterization of TTR interaction with RAGE *in vitro*. *Chapter 1*
2) Search for new molecular targets elicited by the presence of toxic non-fibrillar TTR aggregates. *Chapter 2*
3) Investigation of MAPK signaling pathways in FAP. *Chapter 3 – Part I*
4) Search for transcription factors in FAP. *Chapter 3 – Part II*
5) Assessment of HMGB1 involvement in FAP. *Chapter 4*

CHAPTER 1

In Vitro Inhibition of Transthyretin Aggregate-Induced Cytotoxicity by Full and Peptide Derived Forms of the Soluble Receptor for Advanced Glycation End Products (RAGE)

In Vitro Inhibition of Transthyretin Aggregate-Induced Cytotoxicity by Full and Peptide Derived Forms of the Soluble Receptor for Advanced Glycation End Products (RAGE)

Filipe Almeida Monteiro[1,2], Isabel Cardoso[1], Mónica Mendes Sousa[1] and Maria João Saraiva[1,2]

[1]Molecular Neurobiology, Instituto de Biologia Molecular e Celular, Porto, Portugal;

[2]Instituto de Ciências Biomédicas de Abel Salazar, University of Porto, Portugal.

Corresponding author: Maria João Saraiva; Molecular Neurobiology; Instituto de Biologia Molecular e Celular; R. Campo Alegre, 823. 4150-180 Porto, Portugal.

Tel. 351-226074900; Fax 351-226099157. E-mail: mjsaraiv@ibmc.up.pt

Running title: Transthyretin-receptor for advanced glycation end products interaction.

Abstract

Familial amyloidotic polyneuropathy (FAP) is a neurodegenerative disorder characterized by systemic extracellular deposition of transthyretin (TTR) amyloid fibrils. The latter have been proposed to trigger neurodegeneration through engagement of the receptor for advanced glycation end products (RAGE). The structural basis of RAGE-ligand interaction is currently poorly understood. Here we show that TTR interaction with RAGE is conserved across mouse and human species and is not dependent on RAGE glycosylation. Moreover, strand D of TTR structure seems important for the TTR-RAGE interaction as well as a motif in RAGE (residues 102-118) located within the V-domain; this motif suppressed TTR aggregate-induced cytotoxicity in cell culture.

Abbreviations: AGE, advanced glycation end products; FAP, familial amyloidotic polyneuropathy; HMGB1, high mobility group box 1 protein or amphoterin; RAGE, receptor for AGE; RAGEp, RAGE peptide; RBP, retinol-binding protein; SAP, serum amyloid P component; sRAGE, soluble RAGE; TTR, transthyretin.

Introduction

FAP is a hereditary neurodegenerative disorder characterized by systemic extracellular deposition of TTR amyloid fibrils in several organs, mainly in the peripheral nervous system (Coimbra and Andrade 1971b, 1971a). Several point mutations in TTR have been described to promote amyloidogenesis (Saraiva 2001), though the most common is a substitution of a Val for Met at position 30 (V30M) (Saraiva et al. 1984). Physiologically, TTR is a plasma homotetrameric protein of ~55 kDa that functions as a carrier for thyroxine (T_4) and retinol (vitamin A) (Raz et al. 1970) by formation of a 1:1 molar complex with retinol-binding protein (RBP).

RAGE is a member of the immunoglobulin superfamily of cell surface molecules (Neeper et al. 1992; Schmidt et al. 1992). RAGE has been described as a receptor for advanced glycation end products (AGEs) (Neeper et al. 1992; Schmidt et al. 1992), S100/calgranulins (Hofmann et al. 1999), HMGB1 (amphoterin) (Hori et al. 1995), amyloid β-peptide (Aβ) and for β-sheet fibrils composed of subunits such as Aβ, amylin, serum amyloid A or prion protein (Yan et al. 1996; Du Yan et al. 1997; Yan et al. 2000; Sasaki et al. 2002). Structurally, RAGE is composed of three extracellular immunoglobulin-like domains (V, C, C'-type domains), a single transmembranar domain, and a short cytoplasmic tail that is essential for RAGE-mediated signaling (Neeper et al. 1992; Schmidt et al. 1992; Huttunen et al. 1999). The V-type domain, at the amino terminal, has been shown to be involved in ligand binding (Kislinger et al. 1999).

The secreted RAGE isoform, named soluble RAGE (sRAGE), acts as a decoy to trap ligand and prevent interaction with cell surface receptors (Bucciarelli et al. 2002). sRAGE was shown to have important inhibitory effects in several cell culture and transgenic mouse models, in which it prevented or reversed full-length RAGE signaling. For instance, the administration of sRAGE has been shown to suppress accelerated diabetic atherosclerosis (Park et al. 1998), impaired wound healing (Goova et al. 2001), tumour cell migration and invasion (Taguchi et al. 2000), regeneration after nerve crush (Rong et al. 2004a), amyloid-β penetration in blood-brain barrier (Deane et al. 2003) and accumulation of amyloid (Yan et al. 2000).

Previous studies using recombinant sRAGE produced in baculovirus system showed interaction with soluble and aggregated TTR, with a K_d of approximately 120 nM (Sousa et al. 2000c); the interaction of TTR aggregates with RAGE triggers inflammatory and oxidative stress pathways (Sousa et al. 2000c; Sousa et al. 2001b). Caspase-3 was shown to be up-regulated in axons of FAP nerves. Activation of these markers was abrogated in cell culture by an anti-RAGE antibody or by sRAGE (Sousa et al. 2001b).

Because sRAGE is a glycoprotein (Srikrishna et al. 2002), it is likely that glycosylation is important for the ability of sRAGE to interact with its ligands. In fact, a reduction in amphoterin-RAGE binding after RAGE deglycosylation was observed using purified bovine RAGE (Srikrishna et al. 2002). The aim of this study was to characterize the TTR interaction with a non-glycosylated sRAGE by testing competitors such as TTR wild-type and mutants, RAGE ligands and amyloid fibril ligands. In addition, we identified a RAGE motif recognized by TTR, which might be useful for therapeutical intervention in some RAGE-related pathologies.

Materials and methods

Proteins and peptides

Recombinant TTRs (i.e. human and mouse wild-type (wt) TTR, and human TTR mutants: L55P, Y78F, V30M, T119M, E92C, S117C) were produced in an *E. coli* expression system and purified as previously described (Almeida et al. 1997). TTR mutants E92C and S117C were designed by AM Damas *in silico* based of specific structural domains to stabilize TTR, whereas L55P, Y78F, V30M and T119M are naturally occurring mutations. Purified soluble TTR was dialyzed against PBS, pH 7.4, prior to use in binding assays. RBP was isolated using a TTR affinity column. TTR aggregates were generated by acidification of wtTTR (2 mg/mL) (Bonifacio et al. 1996). TTR fibrils were produced by incubation of the aggregates for 15 days at 37°C. TTR aggregates and fibrils were positive by Thioflavin T spectrofluorometric assays. Protein concentrations were determined by the Lowry method (Lowry et al. 1951). Human sRAGE produced in the baculovirus system was a kind gift of Dr Shi Du Yan. The human sRAGE cDNA (i.e. the extracellular domain comprising residues 23-340) cloned in a pET32b expression vector (Novagen) was kindly provided by Dr Larry Denner. sRAGE with an amino terminal His-tag was expressed and isolated from *E. coli* using HisTrap HP column (Amersham), following manufacturer's recommendations. sRAGE-His-tag was digested with enterokinase (Invitrogen) and passed through a nickel affinity column to remove the His-tag product and undigested fusion protein. A DNA fragment encoding mouse sRAGE (NCBI accession no. BC061182) encompassing residues 1-307 (without signal peptide) was amplified from mouse lung cDNA with primers 5'-CACCATGCAGAACATCACAGCCCGGAT-3' and 5'-GCCTTCAGCTGGCCCCTCATCGCCGGT-3' and subsequently cloned and expressed using the pET101/D-TOPO expression system (Invitrogen). Mouse sRAGE fusion protein with a carboxyterminal His-tag (msRAGE-His-tag) was isolated from bacteria inclusion bodies. Briefly, msRAGE-His-tag was purified and refolded by exchange to non-denaturating buffer conditions prior to elution with imidazole (Sigma) from the HisTrap HP column (Amersham), following the manufacturer's instructions. Fractions containing pure sRAGE proteins were combined and concentrated using Ultrafree-15 Concentrators from Milipore. Functional activity of purified human and mouse sRAGE produced in a prokaryotic system were assessed by binding assays to wtTTR. A RAGE peptide encompassing residues 102-118 of human RAGE extracellular ligand-binding domain (Yeh et al. 2001) was synthesized by Alta Bioscience (Birmingham). Human TTR peptides spanning β-strand A (residues 10-22), β-strand H (residues 100-118) and α-helix (residues c71-93) (Jarvis et al. 1994) were synthesized by Alta Bioscience. Bovine serum

albumin (BSA, fraction V; Sigma) was glycated by incubation with 0.5 M glucose at 37°C for 6 weeks (Schmidt et al. 1992) and characterized by AGE fluorescence and absorbance methods as previously described (Valencia et al. 2004). Recombinant HMGB1 (amphoterin), > 90% pure, was obtained from Sigma and human serum amyloid P component (SAP), ≥ 99% pure, was purchased from Calbiochem.

Radioligand binding assays

Recombinant proteins were iodinated with $Na^{125}I$ (NEN) using the Iodogen (Sigma) method following the supplier's instructions. The reaction mixture was subsequently desalted by Sephadex G50 gel filtration. ^{125}I-labelled proteins were > 90% precipitable in 20% trichloroacetic acid and homogeneous by SDS-PAGE. Where indicated 96 well plates (Maxisorp, Nunc) were coated with sRAGE, RAGE peptide and fibrillar (f) TTR (5 µg/well) in coating buffer (0.1 M bicarbonate/carbonate buffer, pH 9.6) and incubated overnight at 4°C. Unoccupied sites were blocked by incubation with 5% non-fat dried milk in PBS for 2 h at 37°C. K_d assays were performed as described elsewhere (Sousa et al. 2000c). For competition studies, a constant amount of ^{125}I-labelled proteins (either sRAGE or TTR) was added to each well alone or in the presence of the indicated molar excess of unlabelled competitors. Specific binding was defined as that observed with ^{125}I-labelled protein alone minus ^{125}I-labelled protein in the presence of 100-fold molar excess unlabelled protein. Binding data were fit to a one-site model and analyzed by the method of Klotz and Hunston (Klotz and Hunston 1984) using nonlinear regression analysis with the Prism program (GraphPad Software Inc.). Results are shown as percent of maximal binding ± SD and are representative of a minimum of two independent experiments.

Cell culture assays

RN22 cells (rat Schwannoma cell line) were purchased from the European Collection of Cell Cultures. RN22 were propagated for experiment as described elsewhere (Sousa et al. 2001a). Activation of caspase-3 was measured using the fluorometric caspase-3 assay kit (Sigma), following the manufacturer's recommendations. Briefly, 80% confluent cells were incubated in assay media (DMEM containing 1% dialyzed FBS) with 2 µM of soluble or aggregated TTR for 24 h. Where indicated 10 µM of soluble RAGE or RAGE peptide were pre-incubated with 2 µM TTR aggregates in assay media for 3 h at 37°C with agitation, and subsequently added to cells. Then, cells were trypsinized and the cell pellet was lysed in 100 µL of kit lysis buffer; cell lysate samples were assayed as described previously (Sousa et al. 2001a). Values shown are the mean of quadruplicates of two independent experiments. Student's *t* test statistical analysis was used to determine statistical

significance between cells exposed to assay media and cells exposed to different regulators and *P* values of less than 0.05 were considered significant.

Results

Characterization of TTR-sRAGE interaction

To test the hypothesis that TTR binding to RAGE depends on glycosylation of the receptor, we expressed human and mouse sRAGE in a bacterial expression system. Microtiter wells with adsorbed human sRAGE produced in either bacteria or baculovirus bound ^{125}I-TTR in a dose-dependent and saturable manner, with K_d = 376.0 ± 67.50 nM and 385.5 ± 175.8 nM, respectively (Figure 1A). Similarly, mouse sRAGE produced in bacteria bound ^{125}I-TTR, with K_d = 105.8 ± 53.45 nM (data not shown). These binding affinities are similar to values previously found for glycosylated sRAGE i.e. a K_d of approximately 120 nM (Sousa et al. 2000c). Therefore, TTR binding affinity to RAGE is not influenced by post-transcriptional modifications, such as glycosylation which occurs in proteins expressed using the baculovirus system.

In the attempt to identify the region of TTR that binds to sRAGE we performed radioligand binding assays using as unlabelled competitors TTR peptides (TTRp) within the β-strands A and H, and an α-helix. However, none of the analyzed TTRp competed with TTR for interaction with non-glycosylated human sRAGE, showing no binding affinity towards sRAGE (Figure 1B). Another TTR region must be interacting with RAGE, thus further TTRp should be designed.

To analyze whether structural changes in TTR could affect binding affinity to RAGE (both from human and mouse origins), we tested several TTR mutants and mouse TTR for non-glycosylated RAGE binding. Among these human mutants (described in materials and methods), L55P significantly lost a competition effect, showing a ~10-fold lower affinities to both human (Figure 1C) and mouse (data not shown) sRAGE, as compared to human wtTTR. Cross competition curves of human and mouse TTR for human (Figure 1C) and mouse sRAGE binding were not significantly different (data not shown). These data suggest that the L55P region of TTR is relevant for RAGE binding and that it is likely that TTR-RAGE interaction is unchanged across mouse and human species.

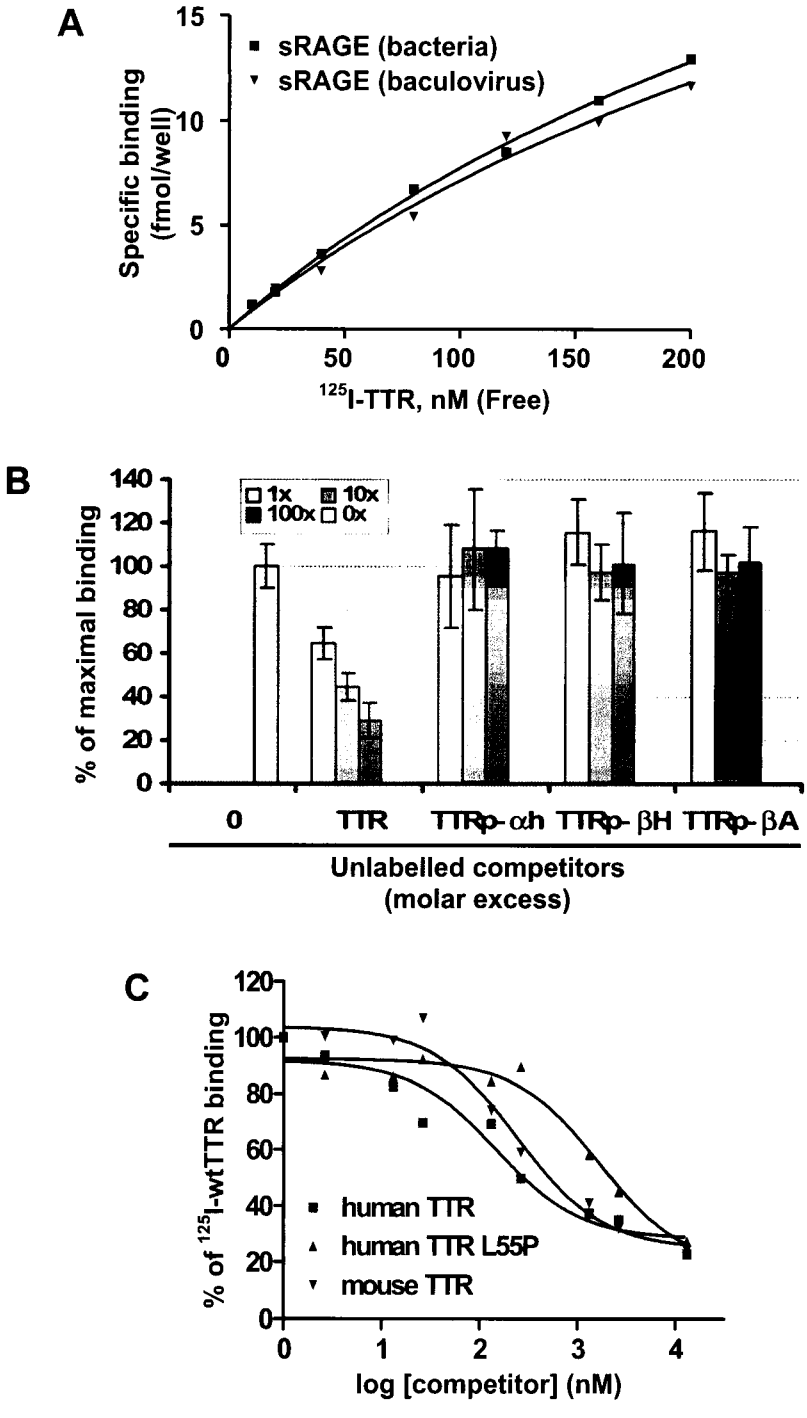

Figure 1. Characterization of TTR-sRAGE interaction.
A, Binding of human wild-type (wt) ^{125}I-TTR to human sRAGE produced in either bacteria or baculovirus expression systems; specific binding was assessed as described in materials and methods. **B**, Binding of human ^{125}I-wtTTR to human sRAGE produced in bacteria. 4 nM of ^{125}I-TTR was added to each well in the presence of 1, 10, or 100-fold molar excess of the following unlabelled competitors: TTR, TTR peptide α-helix (TTRp-αh), TTR peptide β-strand H (TTRp-βH) and TTR peptide β-strand A (TTRp-βA). 0 denotes no addition. **C**, Displacement curves of human ^{125}I-wtTTR from human sRAGE produced in bacteria by mouse and mutant TTR. 25 nM of ^{125}I-wtTTR was added to each well in the presence of increased molar excess of one of the following unlabelled competitors: human wtTTR, human TTR L55P and mouse wtTTR.

It was previously shown that soluble and aggregated TTR bind glycosylated sRAGE. We now observed that aggregated and fibrillar TTR competed with soluble TTR having similar affinities towards human sRAGE produced in bacteria (Figure 1D). We then questioned whether TTR and RAGE ligands could compete for the interaction between TTR and non-glycosylated sRAGE. sRAGE did not bind the TTR-RBP complex and RBP alone was not a ligand (Figure 1D), consistent with previous observations for RBP inhibition of TTR binding to glycosylated sRAGE (Sousa et al. 2000c). AGE albumin, a RAGE ligand (Neeper et al. 1992; Schmidt et al. 1992), competed with TTR for sRAGE binding, suggesting that TTR and AGE-BSA share the same RAGE binding site (Figure 1D). Finally, HMGB1 (amphoterin) another RAGE ligand (Hori et al. 1995), did not compete with TTR for sRAGE binding (Figure 1D). All the above binding data obtained with human sRAGE were further confirmed with mouse sRAGE, both produced in bacteria (data not shown).

The serum amyloid P component (SAP), usually present in amyloid deposits (Pepys et al. 1994), competed in a dose-dependent manner with human sRAGE for fibrillar TTR binding, which is most probably related to the binding of SAP to amyloid fibrils (Figure 1E). Indeed, SAP did not bind either soluble TTR or sRAGE (data not shown).

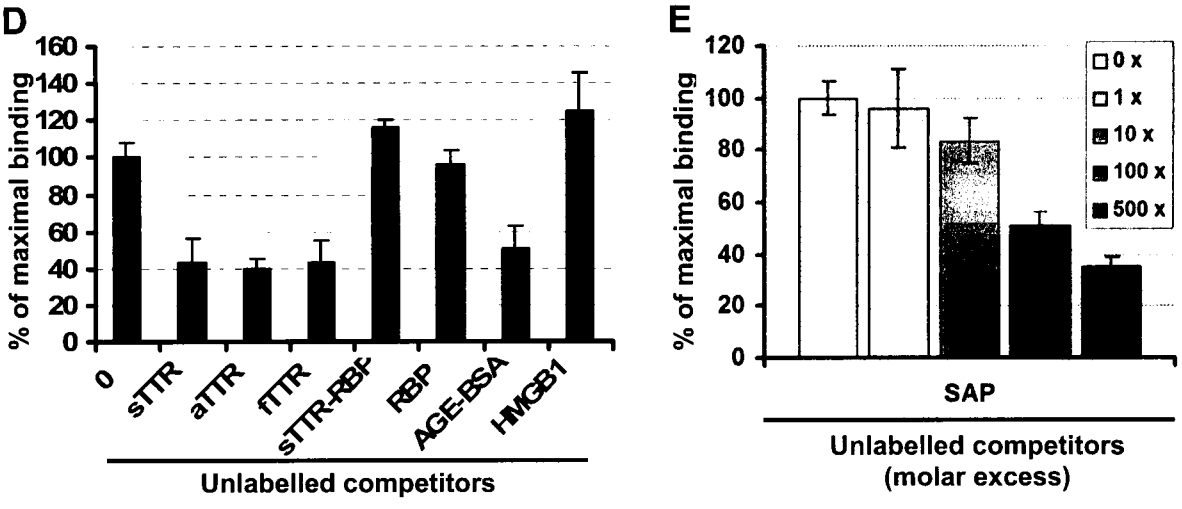

Figure 1 (cont.). Characterization of TTR-sRAGE interaction.
D, Binding of soluble ^{125}I-TTR to human sRAGE produced in bacteria. 4 nM of ^{125}I-TTR was added to each well in the presence of one of the following unlabelled competitors (100-fold molar excess): soluble TTR (sTTR), aggregated TTR (aTTR), fibrillar TTR (fTTR), sTTR combined with retinol-binding protein (RBP) (sTTR-RBP), RBP alone (RBP), AGE albumin (AGE-BSA), HMGB1, and 0 denotes no addition. **E**, Binding of human ^{125}I-sRAGE produced in bacteria to fibrillar wtTTR. 6 nM of ^{125}I-sRAGE was added to each well in the presence of 1, 10, 100, or 500-fold molar excess of unlabelled serum amyloid P component (SAP).

TTR binding to RAGE peptide

A human RAGE peptide, corresponding to the 102-118 amino acid region of the RAGE V-domain, was previously reported to block N^{ε}-(carboxymethyl)lysine (CML)-induced NFκB-driven reporter gene expression in human monocytic THP-1 cells (Yeh et al. 2001). Thus, we hypothesized that this region could be involved in TTR binding. Indeed, ^{125}I-sTTR bound to the RAGE peptide in a dose-dependent, specific and saturable manner, with K_d = 91 ± 44 nM (Figure 2A), which is not significantly different from observations reported using human sRAGE produced in baculovirus (Sousa et al. 2000c). We next studied the TTR binding properties to the RAGE peptide using different RAGE and TTR ligands. RAGE peptide bound by decreasing order of affinity to: soluble, aggregated and fibrillar TTR (Figure 2B). In addition, it bound to the TTR-RBP complex. This was unexpected, since TTR-RBP did not bind to either human sRAGE produced in baculovirus or bacteria (Sousa et al. 2000c) (Figure 1D); RBP alone did not bind (Figure 2B). AGE-BSA competed for TTR binding to RAGE peptide, further indicating that TTR and AGE-BSA may have similar RAGE binding sites (Figure 2B). Finally, amphoterin (HMGB1) did not compete (Figure 2B).

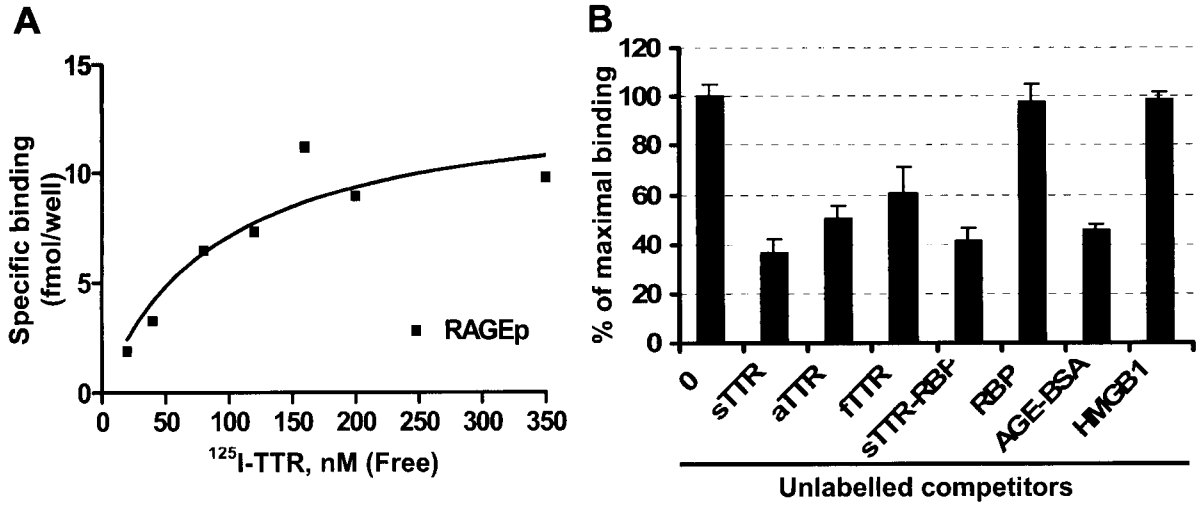

Figure 2. TTR binding to RAGE peptide.
A, Binding of soluble wild-type ^{125}I-TTR to human RAGE peptide (RAGEp); specific binding was assessed as described in materials and methods. **B**, Binding of soluble ^{125}I-TTR to RAGEp. 4 nM of ^{125}I-TTR was added to each well in the presence of one of the following unlabelled competitors (100-fold molar excess): soluble TTR (sTTR), aggregated TTR (aTTR), fibrillar TTR (fTTR), sTTR combined to retinol-binding protein (RBP) (sTTR-RBP), RBP alone (RBP), AGE albumin (AGE-BSA), HMGB1, and 0 denotes no addition.

Inhibition of TTR aggregate-induced cytotoxic effects by non-glycosylated sRAGE and RAGE peptide

A Schwannoma cell line used previously to demonstrate RAGE mediated neurotoxicity triggered by TTR aggregates (Sousa et al. 2001b), was used to determine whether non-glycosylated sRAGE and RAGE peptide could block induction of caspase-3 by TTR aggregates. Here we show that both non-glycosylated human sRAGE and RAGE peptide impaired TTR aggregate-induced caspase-3 activation in RN22 cells (Figure 3). Therefore, RAGE peptide is biologically functional to block TTR aggregate-induced cytotoxic effects.

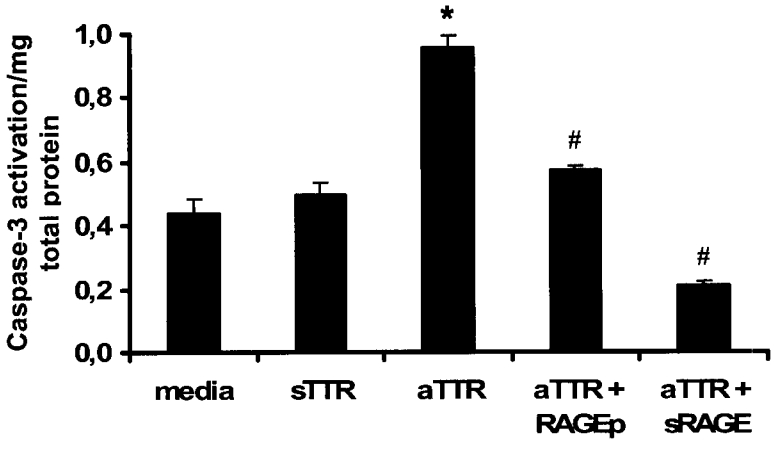

Figure 3. Induction of caspase-3 by TTR aggregates is inhibited by both non-glycosylated sRAGE and RAGE peptide.
Induction of caspase-3 activity in RN22 cells exposed for 24 h to 2 μM of either soluble TTR (sTTR) or aggregated TTR (aTTR). Where indicated, cells were incubated with 10 μM of either soluble RAGE (sRAGE) or RAGE peptide (RAGEp). $^{*}P < 0.01$, compared with untreated control. $^{\#}P < 0.01$, compared with cells treated with TTR aggregates.

Discussion

The detailed nature of RAGE-ligands interactions is presently unknown. Despite the cross competition of RAGE ligands for binding to the receptor (Hofmann et al. 1999), it is unclear whether ligands interact with the same regions of the V-domain, or whether a large binding pocket with several subdomains arranged in a way to optimally fit different ligand-bearing structures exists. It is important to note that all RAGE ligands described so far appear to be multivalent, and that in each case, other cell surface receptors with which they interact have been reported (Schmidt et al. 2001). It was shown that RAGE serves as a receptor for amyloid, as it binds fibrils composed of different subunits with K_d ~50-150 nM, such as Aβ (Schmidt et al. 2000; Yan et al. 2000). This is in accordance with the idea that RAGE recognizes conformational structures rather than specific amino acid sequences (Schmidt et al. 2000, 2001). Such is the case of SAP, an universal amyloid ligand (Pepys et al. 1994). SAP was capable of competing in a dose-dependent manner with sRAGE for fibrillar TTR binding, suggesting that RAGE and SAP recognize the same general motif/s of amyloid fibrils.

RAGE has two potential *N*-glycosylation sites: residues Asn^{2} and Asn^{57}, which were shown to have *N*-linked carbohydrate (Hanford et al. 2004). The residue Asn^{57} is located within the ligand-binding V-domain; however, it is not known whether RAGE glycosylation is needed for the interaction with β-sheet structures. In the present study we investigated the interaction of TTR (soluble, aggregated and fibrillar) with non-glycosylated sRAGE *in vitro* using an established radioimmunoassay in plastic wells (Sousa et al. 2000c) and found binding to all TTR species.

After screening several TTR mutants as unlabelled competitors, only human L55P TTR variant displayed a 10-fold decreased binding affinity towards human and mouse sRAGE. This result suggests that the TTR β-strand region encompassing residues 54-56 (strand D) is important in TTR-RAGE interaction. Indeed, the L55P mutation alters the TTR secondary structure by disruption of the β-strand D, which becomes a long loop that connects β-strands C and E, therefore exposing new surfaces when compared to the wild-type TTR (Sebastiao et al. 1998). TTR crystal structure revealed that each TTR monomer contains eight β-strands, which form two sheets of four strands each, DAGH and CBEF, arranged in a topology similar to the classic Greek key barrel (Blake et al. 1974; Sebastiao et al. 1998). Due to its high β-sheet content, soluble TTR is a good model to study the interaction of RAGE with β-sheet ligands.

Advanced glycation end products (AGEs), the products of nonenzymatic glycation and oxidation of proteins and lipids, accumulate in a wide variety of biological settings such as

diabetes, inflammation, and aging (Ramasamy et al. 2005). AGE-BSA and TTR appear to have the same RAGE binding region, which is independent of glycosylation, as AGE-BSA competed for TTR-RAGE ligation; moreover, it was previously shown that when V, C, and C'-type domains were generated separately in bacteria (without glycosylation modifications), solely the V-domain inhibited binding of AGE-BSA to RAGE (Kislinger et al. 1999).

HMGB1 interaction with RAGE has been studied in models such as neurite outgrowth (Hori et al. 1995), tumour cell invasion and metastasis (Taguchi et al. 2000) and sepsis (Liliensiek et al. 2004). A C-terminal motif of HMGB1 (amino acids 150-183) that contains an α-helix had been suggested to be responsible for RAGE binding (Huttunen et al. 2002a). This observation prompted us to test a fragment peptide of TTR that comprises a short α-helix (c71-93) for sRAGE binding. Similarly to TTR peptides spanning β-strands A and H this TTR peptide did not bind sRAGE. In the present study, we show that HMGB1 did not inhibit TTR binding to sRAGE, which lead us to rise the hypothesis that HMGB1 has a different RAGE binding site and supports the notion that glycosylation is relevant for HMGB1 binding to RAGE (Srikrishna et al. 2002).

Studies with RAGE peptide recapitulated the competition results of AGE-BSA and HMGB1 with non-glycosylated RAGE, except for TTR-RBP complex. TTR is known to circulate in plasma bound to RBP and it is likely that the TTR-RBP complex does not interact with RAGE, as suggested by our and previous data (Sousa et al. 2000c). Sousa et al (2000) hypothesised that this might be caused either by steric hindrance of the RBP molecule on the surface of TTR or by the fact that RAGE and RBP might share overlapping binding sites on TTR. Our data suggest that the TTR binding sites for both RBP and RAGE are close, since in contrast to sRAGE, the RAGE peptide could interact with TTR even when in a complex with RBP. Previously, this RAGE peptide was reported to block the induction of NFκB-driven reporter gene expression in human monocytic THP-1 cells stimulated by human serum albumin modified with N^{ε}-(carboxymethyl)lysine adducts (CML-HSA), which is a predominant AGE that accumulates *in vivo* (Yeh et al. 2001). Another group reported that full-length RAGE and sRAGE bind glyceraldehyde-modified BSA, in contrast to a N-truncated RAGE splice variant (Yonekura et al. 2003). This N-truncated RAGE splice variant starts precisely with the amino acid sequence of the RAGE peptide used in our studies that comprises residues 102 to 118 of RAGE extracellular domain, which is within the V-domain (V-domain sequence lies from residue 41 to 126). One explanation to these apparently contradictory data is the different type of AGEs used that can possibly interact with different subdomains within the V-domain. In cell culture, incubation of sRAGE or RAGE peptide, which sequestrate RAGE ligands

acting as a decoy, were able to suppress the activation and signaling of full-length RAGE. sRAGE inhibition of RAGE-dependent signaling may involve besides its action as a decoy, inhibition of fibrillogenesis as suggested recently for Aβ (Chaney et al. 2005). The different forms of TTR (soluble and aggregate) are known ligands of RAGE, and signal transduction through RAGE is believed to play a potential important role in the TTR pathogenesis observed in FAP (Sousa et al. 2000c; Sousa et al. 2001b; Monteiro et al. 2006). Future studies should aim at administrating RAGE counteracting agents in FAP transgenic mouse models.

In summary, these studies indicate that not only TTR interaction with RAGE is not dependent on RAGE glycosylation but also it is conserved across mouse and human species. In addition, TTR β-strand D is important to the TTR-RAGE interaction as well as a RAGE motif spanning residues 102-118 located within the V-domain responsible for RAGE ligand binding. Moreover, this RAGE motif is not involved in HMGB1-RAGE binding; furthermore, RAGE peptide was able to suppress TTR aggregate-induced cytotoxicity in cell culture which may be useful for therapeutical proposes.

ACKNOWLEDGEMENTS

We thank Paul Moreira for the production and purification of recombinant wild-type and mutant TTRs, Dr Pedro Pereira for helpful discussions on recombinant human sRAGE purification and Dr Ana Margarida Damas for providing TTR peptide α-helix and *in silico* design of TTR mutants. This work was supported by grants from POCTI and POCI programs of Fundação para a Ciência e Tecnologia – FCT, Portugal (M. J. S.) and fellowships SFRH/BPD/9416/2002 (to I. C.) and SFRH/BD/4563/2001 (to F. A. M.) from Fundação para a Ciência e Tecnologia, Portugal.

CHAPTER 2

Search for Differentially Expressed Genes and Gene Products in Familial Amyloidotic Polyneuropathy

Search for Differentially Expressed Genes and Gene Products in Familial Amyloidotic Polyneuropathy

Filipe Almeida Monteiro[1,2], Mónica Mendes Sousa[1]

and Maria João Saraiva[1,2]

[1]Molecular Neurobiology, Instituto de Biologia Molecular e Celular, Porto, Portugal;

[2]Instituto de Ciências Biomédicas de Abel Salazar, University of Porto, Portugal.

Corresponding author: Maria João Saraiva; Molecular Neurobiology; Instituto de Biologia Molecular e Celular; R. Campo Alegre, 823. 4150-180 Porto, Portugal.

Tel. 351-226074900; Fax 351-226099157. E-mail: mjsaraiv@ibmc.up.pt

Running title: New targets in familial amyloidotic polyneuropathy.

Abstract

Familial amyloidotic polyneuropathy (FAP) is a hereditary autosomal dominant neurodegenerative disease characterized by the systemic deposition of transthyretin (TTR) amyloid fibrils with special involvement of the peripheral nervous system (PNS). Previous studies demonstrated that early in FAP, TTR is already deposited in an aggregated non-fibrillar form prior to the formation of TTR amyloid fibrils. Moreover, it was shown that TTR non-fibrillar aggregates, but not mature fibrils, are toxic to cells *in vitro*. However, the molecular signaling mechanisms related to neurodegeneration in FAP are still largely unknown. Here, we addressed this issue using several methodologies, such as differential display (DD), antibody and mRNA microarrays. By DD, candidate genes triggered upon TTR aggregates treatment of ND7/23 neuronal cell line turned out to be false positives, as assessed by Northern blot analysis. Next, FAP salivary gland (SG) biopsies were used to perform antibody microarrays. From the differentially expressed proteins, a few candidates were selected for further analysis. Down-regulation of apoptosis regulator Bcl-x_L expression in FAP was not a valid change as assessed by immunoblot and immunohistochemistry of SG. Up-regulation of Smad4 and GRB2 expression was confirmed by immunoblot but not by immunohistochemistry; however, these markers need further investigation in the future given the potential role for the former, in anti-inflammatory mechanism occurring in FAP and for the latter, in mediating the Ras signaling pathway which leads to the activation of ERK/MAPK cascade. Up-regulation of chondroitin sulfate proteoglycans (CSPG) in FAP SG was confirmed both by immunoblotting and semi-quantitative immunohistochemistry. These preliminary data on CSPG is interesting as it suggests a potential role in inflammation process and/or in facilitating amyloidogenesis in FAP. Finally, SG from FAP patients were used previously in mRNA microarray analysis and displayed mitogen-activated protein (MAP) kinase phosphatase 1 (MKP-1) down-regulation. This result was validated by RT-PCR and suggests that MAPK cascades might be up-regulated in FAP. Taken together, these new targets found differentially expressed in FAP might provide guidance for future investigation aiming to develop novel therapeutic approaches for FAP.

Abbreviations: CSPG, chondroitin sulfate proteoglycans; DD, differential display; ERK, extracellular signal-regulated kinase; FAP, familial amyloidotic polyneuropathy; GRB2, growth factor receptor-bound protein 2; MAPK, mitogen-activated protein kinase; MKP-1, MAP kinase phosphatase 1; RAGE, receptor for advanced glycation end products; SG, salivary gland; Smad4, mothers against decapentaplegic (DPP) homolog 4; TTR, transthyretin.

Introduction

The hallmark of familial amyloidotic polyneuropathy (FAP) is the deposition of amyloid in the peripheral nervous system (PNS) (Sousa and Saraiva 2003). The pattern of deposition consists of amyloid deposits diffusely distributed, involving nerve trunks, plexuses, sensory and autonomic ganglia (Said et al. 1984; Hanyu et al. 1989; Sobue et al. 1990; Takahashi et al. 1997). Transthyretin (TTR) is the major component of amyloid fibrils, which have a systemic extracellular deposition throughout the connective tissue of several organs, with the exception of the brain and liver parenchyma and affecting particularly the PNS (Coimbra and Andrade 1971b, 1971a). Neurodegeneration in FAP is characterized by axonal fiber degeneration accompanied with neuron loss in dorsal root ganglia (DRG). Several hypotheses have been raised to explain axonal and neuronal loss: 1) compression of the nervous tissue by amyloid; 2) nerve ischemia secondary to lesions caused by perivascular amyloid; however, these two hypotheses were never demonstrated; and 3) lesions in the DRG or Schwann cells. Regarding the latter hypothesis, the existence of toxic non-fibrillar TTR aggregates in early FAP nerves was reported in the absence of amyloid fibrils and fiber degeneration (Sousa et al. 2001a). *In vitro,* using a Schwannoma cell line, treatment with prefibrillar (i.e. aggregates) TTR preparations induced activation of caspase-3, whereas the soluble form and the longer fibrils had no significant effect, suggesting that non-fibrillar TTR aggregates are toxic to cells (Sousa et al. 2001a). Since then, several studies corroborated that non-fibrillar TTR aggregates are the major toxic species in cell culture (Olofsson et al. 2002; Reixach et al. 2004; Matsubara et al. 2005). This finding raised the following question: how do TTR aggregates cause toxicity to cells? Recently, it was proposed that TTR amyloid fibrils bind to plasma membrane through electrostatic interactions causing altered membrane fluidity, which might explain the observed cytotoxic effects (Hou et al. 2005). Another possible candidate mechanism is the interaction with cell surface receptors, namely, the receptor for advanced glycation end products (RAGE). RAGE has been shown to interact with TTR aggregates eliciting activation of the transcription factor κB (NFκB) (Sousa et al. 2000c). In addition, blockade of RAGE in cell culture abrogated increased expression of pro-inflammatory cytokines and activation of caspase-3 triggered by TTR aggregates (Sousa et al. 2001b). In FAP tissues, RAGE expression is increased in sites related to amyloid deposition (Sousa et al. 2000c). Moreover, asymptomatic FAP nerves (with non-fibrillar TTR aggregates but without amyloid deposits) already show increased expression of pro-inflammatory cytokines and oxidative stress-related molecules in neuronal axons that is maintained throughout the course of FAP, possibly driving neurons into apoptotic death as

suggested by the up-regulation of proteolytically activated caspase-3 (Sousa et al. 2001b). These studies represented the first steps to unravel molecular signaling mechanisms related to neurodegeneration in FAP.

Therefore, the identification of genes and proteins differentially expressed during the pathological changes that occur throughout the course of FAP is needed. However, the invasiveness and the limited amount of mRNA and protein that is possible to obtain from nerve biopsies are limiting the performance of studies of gene and protein expression. Labial SG biopsies have been reported as a sensitive and specific tool for the diagnosis of several amyloidoses (Lechapt-Zalcman et al. 1999); this tissue not only has extensive TTR deposition that correlates well with deposition observed in the PNS, but also represents a minimally invasive method (Lechapt-Zalcman et al. 1999). Moreover, SG biopsies were demonstrated to be a sensitive way to investigate molecular events related to TTR deposition during the pathogenesis of FAP that were validated in nerve biopsies, considered to be the golden standard for the clinical evaluation of FAP (Sousa et al. 2005b). In the present study, we searched for differentially expressed genes and proteins by approaches such as DD using a cell culture system, and antibody and mRNA microarrays using SG biopsies to gain insights on molecular signaling pathways affected by cytotoxic TTR aggregates in FAP.

Materials and methods

Subjects

Labial minor SG biopsies were obtained from V30M FAP patients prior to performing liver transplantation, the only available treatment for this disorder. Control SG were from age- and gender-matched non-FAP volunteer individuals that had no evidence of infection. The collection of biopsies material was approved by ethical committee of Hospital Geral de Santo António, Porto, Portugal, and participant subjects were volunteers. For protein extracts, SG were collected and immediately frozen at -80°C until usage. For immunohistochemical analysis, SG were collected to 4% paraformaldehyde in PBS. The general characterization of SG consisted of TTR immunohistochemistry and analysis of presence of amyloid deposits by Congo red staining. SG with TTR deposition along with amyloid deposits were classified as FAP (Sousa et al. 2005b).

Proteins

Wild-type recombinant TTR was produced from *E. coli* BL21 expression system and purified as previously described (Almeida et al. 1997). For preparation of TTR aggregates, TTR was dialyzed against water, pH 7.0, and then incubated with 0.05 M sodium acetate, pH 3.6, for 48 h at room temperature i.e. 22°C. The preparation was then centrifuged at 15,000 *g* for 30 min, the pellet washed and resuspended in phosphate-buffered saline (PBS), pH 7.4. Protein concentration was determined by the Lowry method (Lowry et al. 1951). TTR aggregates are composed of short fibrils and amorphous aggregates as assessed by ultrastructural analysis (Sousa et al. 2001a).

Cell culture assays and RNA preparation

ND7/23 cells (mouse neuroblastoma x rat neurone hybrid) were from the European Collection of Cell Culture. ND7/23 were propagated in 10 cm dishes in monolayer and maintained at 37°C in a humidified atmosphere of 95% and 5% CO_2. Cells were grown in Dulbecco's minimal essential media (DMEM) (Gibco) supplemented with 10% fetal bovine serum (FBS) (Gibco), 2 mM glutamine (Sigma) and 100 U/mL penicillin/streptavidin (Gibco) (complete media). When cells reached ~80% confluence in 10 cm tissue culture dishes, they were incubated in assay media (DMEM without FBS) with 1 μM of soluble or aggregated TTR for 24 h. After treatment, cells were washed with PBS, lysed with 1 mL of Trizol (Invitrogen) and total RNA was isolated according to manufacturer's instructions. RNA integrity was visually confirmed by running a sample in an ethidium bromide stained

gel composed by 7% formaldehyde/1% agarose in MOPS buffer and was ready for DD analysis. To determine the involvement of RAGE in differential expression of genes induced by TTR aggregates, as displayed by DD, we performed transient transfections of ND7/23 cells with Lipofectamine (Gibco) according with the manufacturer's recommendations. Briefly, cells were at ~60% confluence in 10 cm tissue culture dishes. pcDNA3 plasmid carrying human RAGE cDNA (12 µg) was used for transfection. Mock transfections with pcDNA3 alone were performed as a control. Cells were exposed to a mixture of Lipofectamine and plasmid for 5 h. After removal of the transfection reagent, fresh medium was added and the incubation continued for 24 h. Assessment of RAGE expression in RAGE-transfected ND7/23 cells was done by reverse transcriptase PCR (RT-PCR) with Superscript kit (Invitrogen) following the manufacturer's instructions. Primers to amplify human RAGE cDNA were 5' ATGGCAGCCGGAACAGCAG 3' (sense) and 5' TCAAGGCCCTCCAGTACTACTC 3' (anti-sense). Subsequently, RAGE-transfected ND7/23 cells were treated in assay media with 1 µM of soluble or aggregated TTR for 24 h. Mock-transfected cells were incubated in assay media alone. After treatment, total RNA was extracted as described above.

mRNA Differential Display (DD)

DD was performed as described elsewhere (Liang and Pardee 1992; Liang et al. 1993). Total RNA (20 µg) was subjected to DNase I treatment using the MessageClean kit (GenHunter Corp, Nashville, TN). Subsequently, RNA was extracted with phenol/chloroform (3:1) followed by ethanol precipitation. Next, RNA was quantified and quality assessed as described above. cDNA was synthesized from equal amounts of total RNA (0.2 µg) in a 20 µL reaction containing 20 µM dNTP mix, 0.2 µM one-base-anchored H-T_{11}M primer (M = G, A or C), reverse transcriptase buffer and 100 units of Moloney Murine Leukemia Virus (MMLV) reverse transcriptase (GenHunter). Reverse transcription (RT) was performed at 37°C for 1 h and finished with a 5 min step at 75°C. cDNA was frozen at -20°C until usage.

Radiolabeling of DD-PCR reactions was carried out using RNAspectra kit (GenHunter), according to supplier's instructions. Briefly, 2 µL from the previous RT reactions were used for PCR employing different combinations of H-T_{11}M primers (0.2 µM) and arbitrary primers 13-mers (0.2 µM each), 2 µM dNTP mix, along with 0.2 µL α-[^{33}P]-dATP and 1 unit of Taq polymerase (Qiagen) in a 20 µL volume reaction. PCR was performed as indicated by the supplier: 40 cycles at 94°C for 30 sec, 40°C for 2 min (for low stringency annealing of primers) and 72°C for 1 min; one additional last step of extension at 72°C for 5 min was performed. PCR products were separated by electrophoresis in 6% denaturing polyacrylamide gel. The gel was blotted in 3MM paper, dried in a gel dryer for 1 h at 80°C

and exposed to Kodak BioMax MR films. Bands of interest were excised from gel, boiled in 50 µL water, and the eluted cDNAs were re-amplified with the corresponding primer pairs used in the original PCR reaction. The re-amplified cDNAs fragments were run and purified from agarose gel with the Qiaex II gel extraction kit (Quiagen), cloned into the pCR-TRAP vector (GenHunter), and used to transform GenHunter competent cells. Cloned cDNA fragments were sequenced after plasmid extraction with Qiaprep Miniprep kit (Qiagen). The identification of cDNAs was determined by sequence homology by using Blastn software from the National Centre for Biotechnology Information (NCBI) database.

Northern Blotting

Northern blot analysis was performed for validation of differential gene expression results. Total RNA was extracted following the above described protocol. Total RNA (20 µg) was separated by electrophoresis in a 7% formaldehyde/1% agarose gel and blotted to a nylon membrane (Amersham Biosciences). RNA blot was stained with 0.03% methylene blue in 0.3 M sodium acetate, pH 5.0, to check integrity and loading. The membrane was probed using the cloned DD fragments that were radiolabelled with α-[^{32}P]-dCTP by random priming applying the Stratagene Labeling kit following the manufacturer's instructions. NuncTrap probe purification columns (Stratagene) were used to remove unincorporated nucleotides. Bands were visualised using either the Molecular Dynamics Typhoon 9200 imager (Amersham Biosciences) or exposed Hyperfilms MP (Amersham Biosciences).

Antibody microarray analysis

SG biopsies from six FAP patients and four control individuals, age and gender matched, were collected and immediately frozen at -80°C until usage. All of the procedures were performed according to Panorama Antibody Microarray recommendations (Sigma) with minor adjustments. Briefly, SG biopsies were homogenized in two pools (FAP and control) with lysis buffer (Sigma). For labelling, 1 mL of each protein extract (1 mg/mL) was conjugated with both Cy3 and Cy5 monofunctional reactive dye (Amersham Biosciences). Dye excess was removed applying labelled sample on a SigmaSpin column. Subsequently, protein concentration was determined by Bradford method; the dye to protein molar ratio (D/P) was between 2.1 and 2.5. Next, 10 µg/mL of each sample FAP-Cy5 and Control-Cy3 were mixed in 5 mL of Array incubation buffer (Sigma) and incubated with Panorama Antibody Slide (Slide #1; Sigma) for 30 min at room temperature. Simultaneously, the sample mixture of FAP-Cy3 and Control-Cy5 was incubated with Slide #2. Subsequently, the slides were completely dried and protected from light. Scanning was performed using ScanArray Express, Packard BioScience

(Perkin-Elmer), and image acquisition was done with ScanArray Express software using a 10 µm resolution. For fluorescence signal quantification, we used the QuantArray software version 3.0 and the histogram method for measuring the pixels. Each slide array contains 224 different antibodies each one spotted in duplicate on nitrocellulose coated glass slides. These antibodies are representative of biological pathways including apoptosis, cell cycle, neurobiology, cytoskeleton, signal transduction, and nuclear proteins. The array was used for comparing protein expression profiles in control and FAP SG samples labelled with different dyes (Cy3 or Cy5). The two slides approach with the dyes reversed addresses the majority of variability that could be introduced. For data analysis, the Cy3/Cy5 fluorescent signal ratio for each antigen was calculated and these values were used to calculate Internally Normalized Ratios (INRs) by the following formula: $INR = \sqrt{\frac{Ratio\ 1}{Ratio\ 2}}$, where the Ratio 1 is obtained from slide #1 and the ratio 2 from slide #2. Next, an Average INR for each antibody-antigen duplicate was calculated. These values were averaged to calculate the Average INR for the experiment. The experimental Average INR value was multiplied by 1.3 and 0.77 to obtain the upper and lower threshold values, respectively. Any value out of this range could be a valid change, as described by (Anderson et al. 2003). We have not obtained any INR value out of this range; therefore, we used less stringent thresholds by multiplying experimental Average INR by 1.040 and 0.924. INR values based on Cy3/Cy5 ratios in which the antigen signals were less than twice the background signal were excluded.

Immunoblots

To validate the antibody microarray data, we assessed protein expression by immunoblot using the same protein extract pools of SG from control and FAP individuals used for microarray analysis. Equal amounts of protein were separated in 15% SDS-PAGE and transferred to nitrocellulose Hybond-C Extra (Amersham Biosciences) using a semidry transfer system. Blots were incubated with blocking buffer (5% nonfat dried milk in Tris-buffered saline (TBS) with 0.1% tween-20 (T)) for 1 h at room temperature. Subsequently, incubation with primary antibodies, at the appropriate dilution, was performed overnight at 4°C in 5% bovine serum albumin (BSA) in TBS-T. The primary antibodies used were mouse monoclonal anti-Bcl-x_L (1:200; Sigma), rabbit polyclonal anti-Bcl-2 (1:500; Santa Cruz Biotech), mouse monoclonal anti-Smad4 (1:1000; Sigma), mouse monoclonal anti-GRB2 (1:250; Sigma), anti-Chondroitin sulfate (1:500; Sigma); and mouse monoclonal anti-β-actin (1:5000; Sigma). After incubation with secondary sheep anti-rabbit IgGs peroxidase conjugate (1:5000; The Binding Site), goat anti-mouse IgGs peroxidase

conjugate (1:5000; Pierce) or anti-sheep/goat IgGs peroxidase conjugate (1:5000; The Binding Site) in 1% nonfat dried milk TBS-T for 1 h, blots were developed using the SuperSignal West Pico Chemiluminescent Substrate kit (Pierce) and exposed to Hyperfilm ECL (Amersham Biosciences).

Immunohistochemistry

For immunohistochemical analysis, SG paraffin sections were deparaffinated, hydrated in a modified alcohol series, endogenous peroxidase activity was blocked with 3% hydrogen peroxide in methanol for 15 min and incubated in blocking buffer (4% FBS and 1% BSA in PBS) for 30 min at 37°C in a moist chamber. Incubation with primary antibody, at the appropriate dilution in blocking buffer, was performed overnight at 4°C in a humidified chamber. Primary antibodies were mouse monoclonal anti-Bcl-x_L (1:500; Sigma) and rabbit polyclonal anti-Bcl-2 (1:200; Santa Cruz Biotech), mouse monoclonal Smad4 (1:500; Sigma), mouse monoclonal anti-GRB2 (1:1000; Sigma), anti-Chondroitin sulfate (1:10000; Sigma). Antigen visualization was performed with biotin-extravidin-peroxidase kits (Sigma), using 3-amino-9-ethyl carbazole (Sigma) as substrate. On parallel control sections, primary antibody was replaced by blocking buffer alone. Semi-quantitative immunohistochemistry (SQ-IHC) analysis was performed using Scion Image software. This application enables the measurement of the area occupied by pixels corresponding to the immunohistochemical substrate's color that is normalized relatively to the total area. Each slide used in the SQ-IHC was analyzed in 4 different representative areas. Results shown represent % occupied area (± SD).

RNA microarray and semi-quantitative RT-PCR analysis

SG from four FAP patients and four control individuals, age and gender matched, were collected and hybridization to the U95A oligonucleotide array (Affymetrix) which represents ~12,000 human sequences was performed as previously described (Sousa et al. 2005b). Genes scored as increased or decreased in all pairwise comparisons were selected. A gene was considered to have modified expression if it averaged ≥ ± 2.5 fold change. To validate the microarray data at the RNA level, total RNA from SG from 3 control individuals and 3 FAP patients was isolated with Trizol (Invitrogen) and subjected to RT-PCR with the Superscript II kit (Invitrogen). PCR was performed for 30 cycles at 95°C for 30 sec, 56°C for 45 sec and 72°C for 1 min. Specific primers were designed using PRIMER3 (http://frodo.wi.mit.edu/cgi-bin/primer3/primer3_www.cgi) and the sequence from the NCBI database. Sense and antisense primers were: for human MKP1, 5'-CTTGATCAACGTCTCAGCCA-3' and 5'-AGAGGTCGTAATGGGGCTCT-3' and for

human β-actin, 5'- AGAAAATCTGGCACCACACC-3' and 5'-CCATCTCTTGCTCGAAG TCC-3'. PCR products were quantified from 1% agarose gels by densitometry using the Scion Image software (Scion Corporation). Density values of RT-PCR products were normalized with β-actin PCR product. Results are presented as normalized density ± SD.

Statistical analysis

Group values, expressed as the mean ± SD, were compared by Student's *t* test, and *P* values of less than 0.05 were considered significant.

Results

Analysis of gene expression by DD in ND7/23 cell line exposed to TTR aggregates

In an attempt to identify altered gene expression induced by TTR aggregates cytotoxic species, we used DD analysis to compare ND7/23 neuronal cells exposed or unexposed to TTR aggregates. DD showed several up- and down-regulated genes in treated ND7/23 cells when compared with non-treated cells (Figure 1 A). Combining 1 anchor primer with 7 arbitrary primers, covering about 8% of the genes expressed in a cell (Liang et al. 1995), we cloned and sequenced nine fragments containing portions of candidate genes affected by the presence of TTR aggregates. From these, four corresponded to sequences that are not assigned to any gene, whereas three corresponded to SH2-binding protein 1 (SH2BP1), one to cytochrome c oxidase III (Cox-III), and finally, one to tropomyosin 1 alfa (TM-1α). Thus, we identified three genes whose expression was different in TTR aggregate-treated ND7/23 cells by the DD methodology (Table 1 and Figure 1 A, B). Although the function of SH2BP1 is not known, it interacts with proteins containing the Src homology 2 (SH2) domain and, therefore, mediates the assembly of diverse multicomponent signaling complexes (Malek et al. 1996). Regarding Cox-III, it is part of the catalytic core of the cytochrome c oxidase enzyme, which is the terminal component of the mitochondrial respiratory chain and plays a vital role in cellular energy transformation (Hosler 2004).

Table 1. Summary of differentially expressed genes in TTR aggregate-treated ND7/23 cells, identified by DD.

Gene	Function	Change
SH2-binding protein 1 (SH2BP1)	Unknown function; interacts with Src homology 2 (SH2)-containing proteins[1]	Decrease
Cytochrome c oxidase III (Cox-III)	Subunit III of cytochrome c oxidase is part of the catalytic core of the enzyme[2] and is encoded by mitochondrial DNA (mtDNA)[3]	Decrease
Tropomyosin 1 alfa (TM-1α)	Integral component of the thin filament in muscle fibers and is involved in regulating actin-myosin interactions[4]	Decrease

[1](Malek et al. 1996); [2](Hosler 2004); [3](Taanman 1997); [4](Rethinasamy et al. 1998).

Given the involvement of receptor for advanced glycation end products (RAGE) in mediating inflammatory and apoptotic pathways exerted by TTR aggregates (Sousa et al. 2000c; Sousa et al. 2001b), we transfected ND7/23 cells with RAGE to evaluate whether the differential expression of the selected genes could be mediated by RAGE. RAGE expression in RAGE-transfected ND7/23 cells was confirmed by RT-PCR (data not

shown). After cell treatment with soluble and aggregated TTR, total RNA was analyzed by Northern blot using radiolabelled cloned sequences as probes. In fact, neither SH2BP1 nor Cox-III displayed down-regulation of expression upon treatment with aggregated TTR in both RAGE-transfected and non-transfected cells (Figure 2 C). Then, we went back to total RNA used for DD analysis and found that only Cox-III appeared down-regulated in treated cells (Figure 2 D). Finally, we found no interest in the study of TM-1α because it has a structural function in the cytoskeleton and most likely is constitutively expressed (Table 1 and Figure 2 A, B).

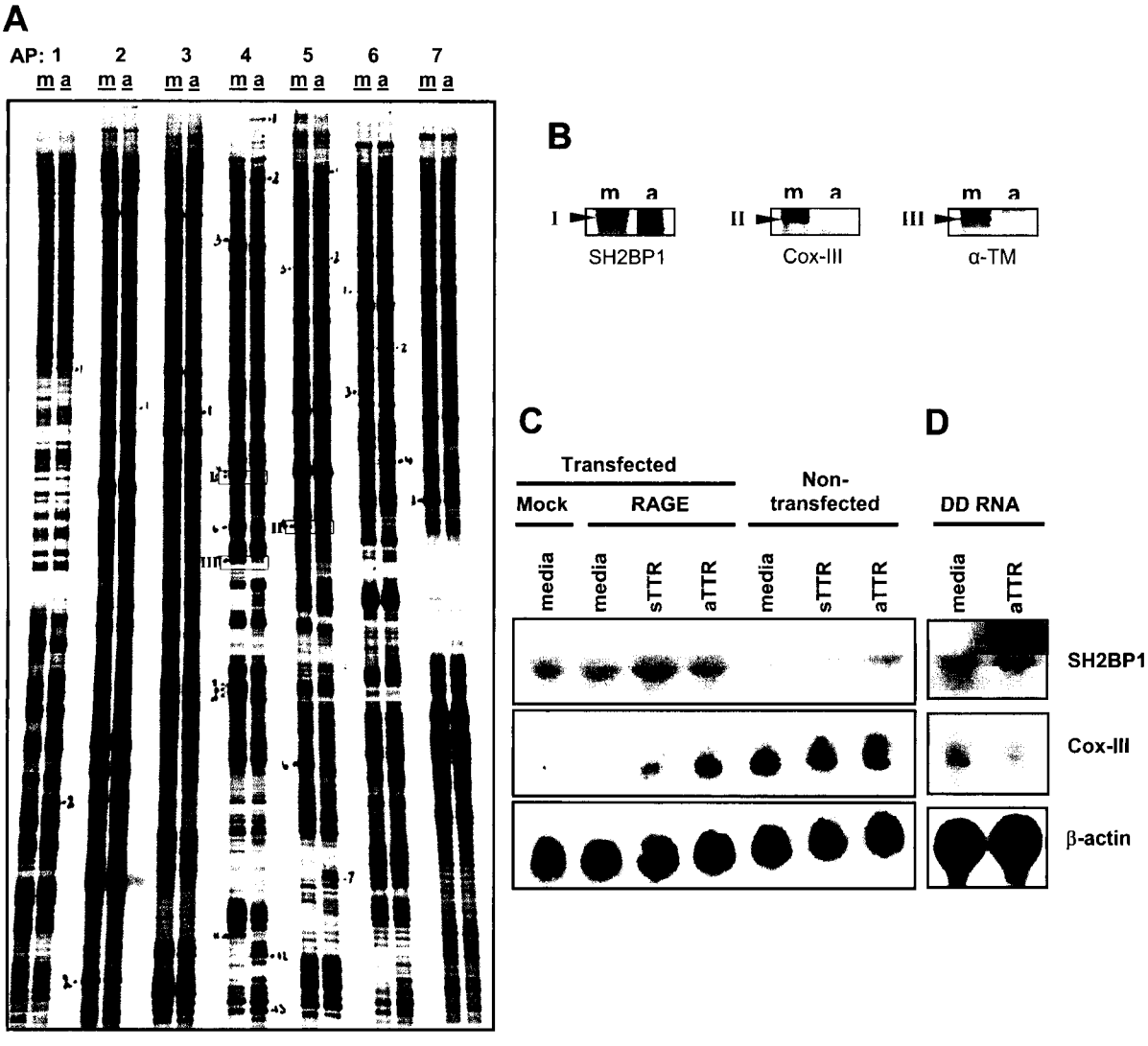

Figure 1. DD analysis of ND7/23 cells exposed to TTR aggregates displayed altered expression of candidate genes.
A, Representative DD gel picture that indicates several genes whose expression might be altered. Excised bands of identified genes are inside rectangles (I-III); AP, arbitrary primers; absence (m) and presence (a) of TTR aggregates. **B**, Comparison of gene expression of non-treated (m) and treated ND7/23 cells with 1 μM aggregated TTR (a). DD result of some of the cloned genes is shown. **C**, Assessment of RAGE mediation in altered gene expression displayed by DD. Northern blot analysis of Cox-III and SH2BP1 gene expression in RAGE-transfected and non-transfected ND7/23 cells treated with either 1 μM soluble TTR (sTTR) or 1 μM aggregated TTR (aTTR) for 24 h.

D, Northern blot analysis of Cox-III and SH2BP1 gene expression, using original RNA samples of DD, for validation of DD results.

Analysis of protein expression in FAP SG extracts

To search for differentially expressed proteins in FAP, we used SG biopsies that are known to follow similar signaling pathways as those found in the nerve, namely the activation of NFκB transcription factor (Sousa et al. 2000c; Sousa et al. 2005b). To undertake this study an antibody microarray approach was chosen. Microarrays of SG-labelled proteins were performed as described in the materials and methods section. According to the selection criteria eight proteins were differentially expressed and covered areas such as apoptosis, cell cycle, signal transduction and components of cytoskeleton and extracellular matrix (ECM) (Table 2).

Table 2. Summary of differentially expressed proteins in FAP SG, identified by antibody microarrays.

Protein	Function	Change
Bcl-x_L	Promotes cell survival[1]	Decrease
Cdc27	Regulation of cell cycle[2]	Increase
Smad4	Transcriptional activation upon TGF-β-induced signaling[3]	Increase
Connexin 43	Component of gap junctions (cytoskeleton)[4]	Increase
Chondroitin sulfate (CS)	Extracellular matrix (ECM) proteoglycan compound[5]	Increase
Cofilin	Essential for cellular processes involving actin remodelling[6]	Increase
GRB2	Signal transduction upon receptor-type tyrosine kinase-induced signaling[7]	Increase
Phosphothreonine	Signal transduction[8]	Increase

[1](Farrow et al. 1995); [2](Barinaga 1995); [3](Liu et al. 1997);[4](Dermietzel and Spray 1993); [5](Avnur and Geiger 1984);[6](Suzuki et al. 1995); [7](Cheng et al. 1998); [8](Heffetz et al. 1991).

We next validated the microarray data by immunoblotting analysis of human SG lysates and immunohistochemistry of SG from controls and FAP patients. Microarrays of FAP SG revealed that cyclin Cdc27, connexin 43, cofilin and phosphothreonine protein expression was up-regulated, but thus far they were not validated. Down-regulation of Bcl-x_L was not confirmed by immunoblot analysis of the same samples, which showed the inverse expression (Figure 2 A). Given that Bcl-x_L and Bcl-2 promote cell survival by forming heterodimers with pro-apoptotic Bax (Hsu and Youle 1997), we also analyzed Bcl-2 by immunoblot. Bcl-x_L and Bcl-2 were increased in FAP SG extracts (Figure 2 A).

Immunohistochemical analysis of Bcl-x_L and Bcl-2 in SG showed no differences between FAP and control groups, as evidenced by the similar staining pattern (Figure 2 B). As expected, in both cases the immunostaining was exclusively cytoplasmic and was present in epithelial cells in SG excretory ducts. Taken these results together, differential expression of Bcl-x_L observed in microarrays and immunoblot is contradictory.

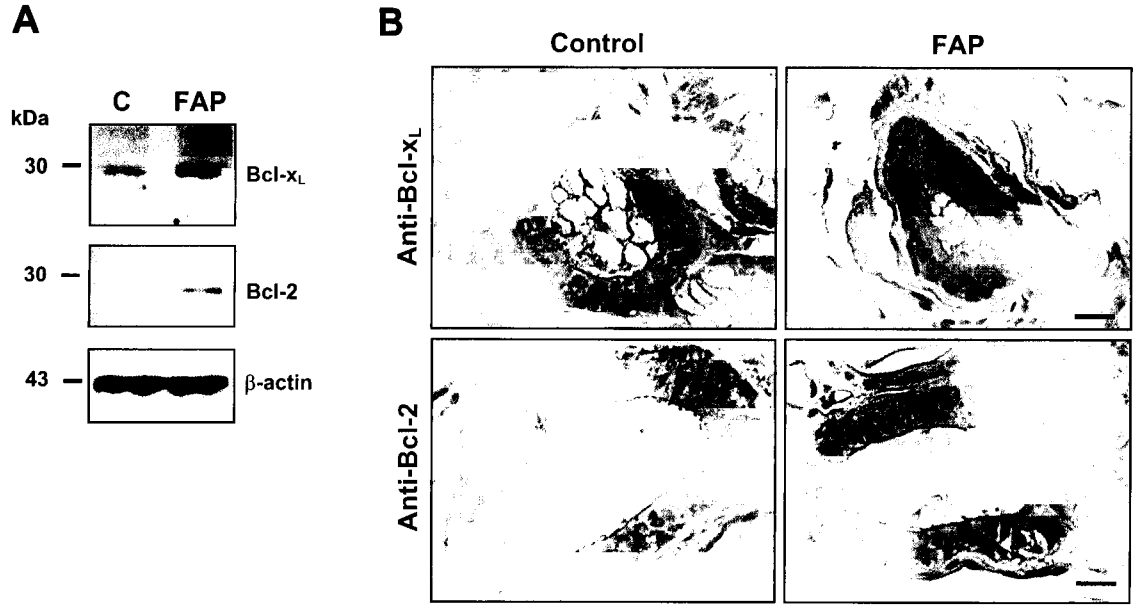

Figure 2. Bcl-x_L and Bcl-2 expression in human FAP SG.
A, Immunoblots representing expression of Bcl-x_L (upper lane), Bcl-2 (middle lane) and β-actin (lower lane) in SG pool extracts from control and FAP individuals. 40 µg of total protein was loaded per lane. **B**, Bcl-x_L (upper panels) and Bcl-2 (lower panels) immunohistochemistry of representative SG from control individuals (left panels; n=6) and FAP patients (right panels; n=6). Bar, 20 µm.

Up-regulation of Smad4 in FAP SG was confirmed by immunoblot (Figure 3 A). However, immunohistochemistry of Smad4 in SG revealed no differences in immunostaining between control and FAP individuals (Figure 3 B). Smad4 is a component of the complex responsible to activate transcription upon ligand binding to the receptors of the transforming growth factor beta (TGF-β) family (Lagna et al. 1996). Previously, it was suggested the existence of a balance between pro-inflammatory and anti-inflammatory mechanisms during the course of FAP (Sousa et al. 2005b), however TGF-β as an anti-inflammatory cytokine has never been addressed. In addition, expression of growth factor receptor-bound protein 2 (GRB2) was also up-regulated in FAP SG, which was validated by immunoblot (Figure 3 A). As for Smad4, GRB2 increased expression in FAP SG was not confirmed by immunohistochemistry (Figure 3 B). For both, the immunostaining was present predominantly in the cytoplasm of epithelial cells of SG excretory ducts.

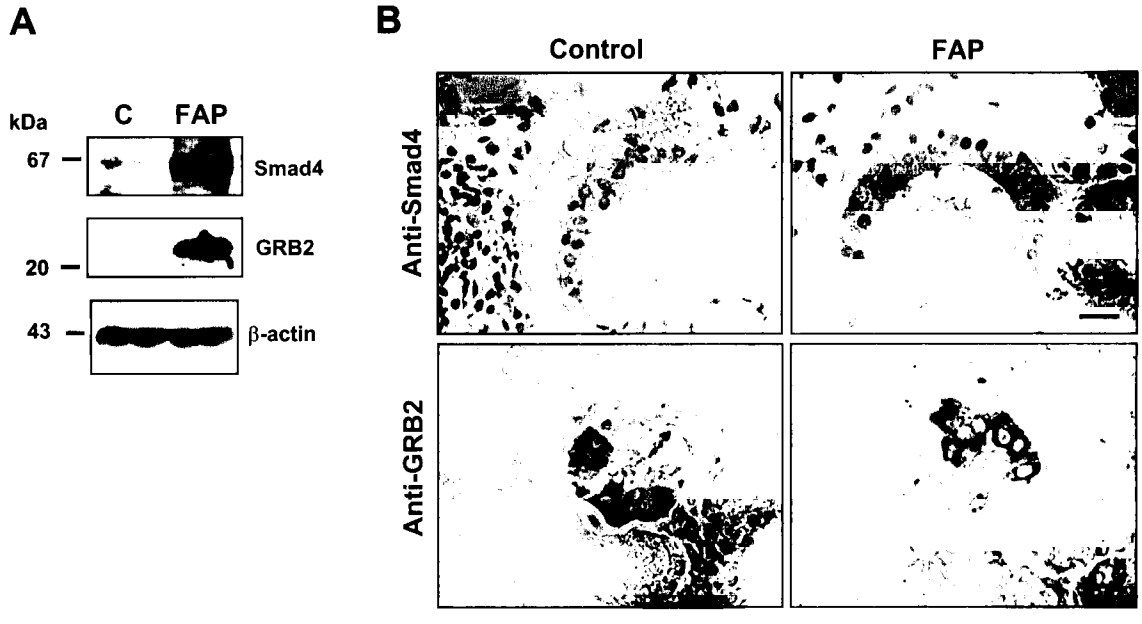

Figure 3. Smad4 and GRB2 expression in human FAP SG.
A, Immunoblots representing expression of Smad4 (upper lane) and GRB2 (middle lane) and β-actin (lower lane) in SG pool extracts from control and FAP individuals. 40 μg of total protein was loaded per lane. **B**, Smad4 (upper panels) and GRB2 (lower panels) immunohistochemistry of representative SG from control individuals (left panels; n=6) and FAP patients (right panels; n=6). Bar, 20 μm.

Finally, up-regulation of chondroitin sulfate proteoglycans (CSPG) was found in FAP SG. We validated the microarray data both by immunoblot and semi-quantitative immunohistochemistry. Immunoblot analysis of SG extract pools of indicated an up-regulated expression of CSPG in FAP when compared to control SG pool extract (Figure 4 A). By semi-quantitative immunohistochemistry, amyloid laden SG from FAP patients showed a significant up-regulation of CSPG expression, when compared with control and asymptomatic SG (Figure 4 B and chart). CSPG immunostaining was distributed extracellularly in the connective tissue around gland acini, excretory ducts and blood vessels. Interestingly, CSPG has been found associated with amyloid fibrils in FAP and in other amyloid related-disorders (Inoue et al. 1998)

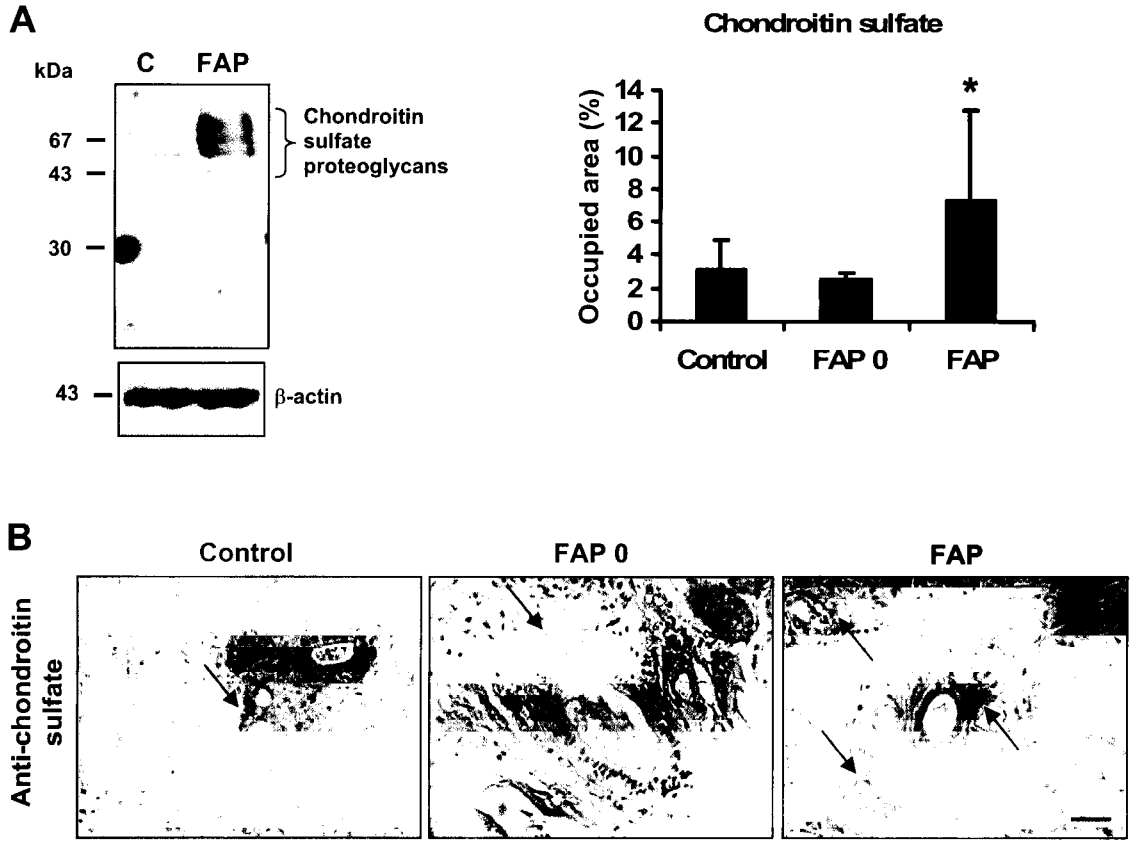

Figure 4. Chondroitin sulfate expression in human FAP SG.
A, Immunoblot representing expression of chondroitin sulfate (upper lane) and β-actin (lower lane) in SG pool extracts from control and FAP individuals. 40 µg of total protein was loaded per lane. **B**, Chondroitin sulfate immunohistochemistry of representative SG from control individuals (left panel) and FAP 0 (middle panel) and FAP patients (right panel). Arrows, extracellular localization. Bar, 40 µm. **Chart**, Quantification of immunohistochemical images of chondroitin sulfate staining in SG. Data are represented as percentage of occupied area in squared pixels ± SD for SG controls (n=9), FAP 0 (n=3) and FAP patients (n=9). *$P < 0.05$, compared to control group.

Analysis of gene expression in FAP SG

Gene expression microarray data from human FAP SG showed a down-regulation (6.2-fold ± 1.4) of mitogen-activated protein (MAP) kinase phosphatase 1 (MKP-1/CL100). To note that other genes differentially expressed were reported (Sousa et al. 2005b). RT-PCR of MKP-1 mRNA in human SG indicated a down-regulated expression in FAP when compared to controls, as shown in figure 5 and chart, confirming the microarray results. This result suggests a possible up-regulation of MAP kinases activation in FAP SG.

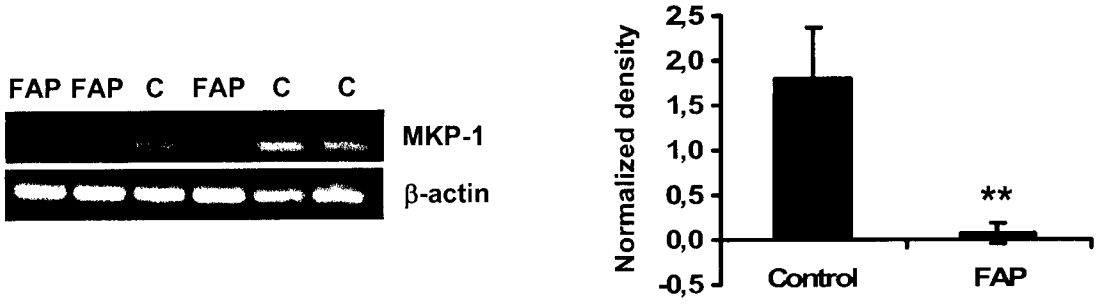

Figure 5. MKP-1 mRNA is down-regulated in FAP SG.
RT-PCR analysis of RNA extracted from SG of control (C) individuals and FAP patients. MKP-1 (upper lane) and β-actin (lower lane). **Chart**, Densitometry of MKP-1/β-actin RT-PCR amplifications in control (n=3) and FAP (n=3) SG biopsies. $^{**}P < 0.008$, compared to control group.

Discussion

The molecular mechanisms by which TTR deposits exert toxic effects driving cells into death are not fully understood. This lack of knowledge prompted us to search for new molecules involved in FAP pathology with the goal of giving insights for the development of new therapeutic strategies.

Using DD as a tool to detect altered gene expression in a neuronal cell line exposed to cytotoxic TTR aggregates, we found down-regulation of SH2BP1, Cox-III and TM-1α genes. However, the candidate genes SH2BP1 and Cox-III were false positives, since this result was not confirmed by Northern blot analysis of a replicate experiment.

Subsequently, we shifted to search for differentially expressed proteins in FAP SG biopsies by antibody microarrays methodology. Since we have not obtained any valid change in accordance with the criteria proposed previously (Anderson et al. 2003), we used a less stringent analysis for the selection of differentially expressed proteins. Thus, this fact might account for the unsuccessful validation of some of the candidate proteins. From the differentially expressed proteins analyzed, down-regulation of Bcl-x_L in FAP was not confirmed neither by immunoblotting or immunohistochemistry. Up-regulation of Smad4 and GRB2 was confirmed by immunoblotting, whereas immunohistochemical analysis displayed no differences between controls (n=6) and FAP patients (n=6); however, the immunostaining was located mainly in SG excretory ducts that represent only a small fraction of the total biopsy in contrast to the total lysate levels assessed by immunoblotting. Therefore, these markers need further investigation in a larger number of individual control and FAP SG biopsies by immunoblotting and in other clinical tissues for validation. If confirmed, Smad4 altered expression might be involved in an anti-inflammatory mechanism occurring in FAP, given that Smad4 is activated upon the action of transforming growth factor β (TGF-β), an anti-inflammatory cytokine (Lagna et al. 1996). Regarding GRB2 over-expression, if confirmed, might be related to FAP pathological process, since GRB2 is an adaptor protein and mediates the Ras signaling pathway (Cheng et al. 1998), which leads to the activation of ERK/MAPK cascade. Finally, up-regulation of CSPG in FAP SG was validated both by immunoblotting and semi-quantitative immunohistochemistry. This result is in accordance with previous observations that CSPG is associated with amyloid fibrils in amyloid-related diseases (Inoue et al. 1998). Proteoglycans (PG) that may be modified by a chondroitin sulfate (CS) type of glycosaminoglycans (GAGs) chain include aggrecan, neurocan, brevican, bamacan, a CD44 isoform, and in certain instances, syndecans, betaglycan, and serglycin. Several reports have been implicating GAGs in inflammation process by participation as

both pro-inflammatory and anti-inflammatory mediators (Taylor and Gallo 2006). Recently, an over-expression of ECM remodelling genes, namely biglycan, neutrophil gelatinase-associated lipocalin (NGAL) and matrix methaloproteinase-9 (MMP-9) in FAP was reported (Sousa et al. 2005b). It is well established the relationship between ECM components and inflammatory cascades. In FAP, a balance between the increased expression of pro-inflammatory cytokines followed by increase of anti-inflammatory cytokine IL-10 exists. However the levels of IL-10 may be insufficiently increased to shutdown inflammatory cytokines during the latter course of FAP, as has been suggested (Sousa et al. 2005b). Therefore, CSPG may be playing a role in the inflammation process and/or contributing to amyloidogenesis by helping in fibril assembly (Snow et al. 1987); this issue warrants however further investigation.

Previously, SG from FAP patients were used in mRNA microarray analysis (Sousa et al. 2005b); MKP-1 gene expression was down-regulated in FAP, which was here confirmed by RT-PCR. MKP-1 is known to dephosphorylate and inactivate all MAPKs (i.e. ERK, p38 and stress-activated protein kinases or Jun amino-terminal kinases (SAPKs/JNKs)). This data suggest that MAPK cascades might be up-regulated in FAP. We will evaluate in the following chapter the relevance of this preliminary result in FAP.

ACKNOWLEDGEMENTS

We are grateful to Dr. João Sousa (Life and Health Sciences Research Institute (ICVS), School of Health Sciences, University of Minho, Portugal) for helpful discussions on DD analysis.

We thank to Dr. Manuel Santos and Dr. Laura Cristina Carreto (Laboratório de Genómica Funcional, Centro de Biologia Celular, Universidade de Aveiro, Portugal) for scanning Antibody Microarray slides and helpful discussions on obtained data.

We thank Dr Barbas do Amaral (Estomatology, Maxillofacial Surgery, Hospital Geral de Santo António, Porto, Portugal) for SG collection and Rossana Correia (Molecular Neurobiology, IBMC) and Rui Fernandes (Advanced Tissue Analysis Facility, IBMC) for tissue processing.

CHAPTER 3 – PART I

Activation of ERK1/2 MAP Kinases in Familial Amyloidotic Polyneuropathy

Activation of ERK1/2 MAP Kinases in Familial Amyloidotic Polyneuropathy

Filipe Almeida Monteiro[1,2], Mónica Mendes Sousa[1], Isabel Cardoso[1], José Barbas do Amaral[3], António Guimarães[4] and Maria João Saraiva[1,2]

[1]Molecular Neurobiology, Instituto de Biologia Molecular e Celular, Porto, Portugal;

[2]Instituto de Ciências Biomédicas de Abel Salazar, University of Porto, Portugal;

[3]Estomatology, Maxillofacial Surgery, Hospital Geral de Santo António, Porto, Portugal;

[4] Neuropathology, Hospital Geral de Santo António, Porto, Portugal.

Corresponding author: Maria João Saraiva; Molecular Neurobiology; Instituto de Biologia Molecular e Celular; R. Campo Alegre, 823. 4150-180 Porto, Portugal.

Tel. 351-226074900; Fax 351-226099157. E-mail: mjsaraiv@ibmc.up.pt

Running title: Extracellular signal-regulated kinases 1/2 in familial amyloidotic polyneuropathy.

Abstract

Familial amyloidotic polyneuropathy (FAP) is a neurodegenerative disorder characterized by the extracellular deposition of transthyretin (TTR), especially in the PNS. Given the invasiveness of nerve biopsy, salivary glands (SG) from FAP patients were used previously in microarray analysis; mitogen-activated protein (MAP) kinase phosphatase 1 (MKP-1) was down-regulated in FAP. Results were validated by immunohistochemistry both in SG and in nerve biopsies of different stages of disease progression. MKP-3 was also down-regulated in FAP SG biopsies. Given the relationship between MKPs and MAPKs, the later were investigated. Only extracellular signal-regulated kinases 1/2 (ERK1/2) displayed increased activation in FAP SG and nerves. ERK1/2 kinase (MEK1/2) activation was also up-regulated in FAP nerves. In addition, a FAP transgenic mouse model revealed increased ERK1/2 activation in peripheral nerve affected with TTR deposition when compared to control animals. Cultured rat Schwannoma cell line treatment with TTR aggregates stimulated ERK1/2 activation, which was partially mediated by the receptor for advanced glycation end products (RAGE). Moreover, caspase-3 activation triggered by TTR aggregates was abrogated by U0126, a MEK1/2 inhibitor, indicating that ERK1/2 activation is essential for TTR aggregate-induced cytotoxicity. Taken together, these data suggest that abnormally sustained activation of ERK in FAP may represent an early signaling cascade leading to neurodegeneration.

Abbreviations: ERK, extracellular signal-regulated kinase; FAP, familial amyloidotic polyneuropathy; IL-1β, interleukin-1β; iNOS, inducible nitric oxide synthase; MAPK, mitogen-activated protein kinase; M-CSF, macrophage-colony stimulating factor; MEK, MAPK/ERK kinase; MKP-1, MAP kinase phosphatase 1; NFκB, nuclear transcription factor κB; pERK, phosphorylated ERK; RAGE, receptor for advanced glycation end products; SAPK/JNK, stress-activated protein kinase or jun amino-terminal kinase; SG, salivary gland; tERK: total ERK; TNFα, tumor necrosis factor α; TTR, transthyretin.

Introduction

Familial amyloidotic polyneuropathy (FAP) is an autosomal dominant neurodegenerative disorder characterized by the extracellular deposition of transthyretin (TTR) amyloid fibrils throughout the connective tissue of several organs, particularly in the peripheral nervous system (PNS) (Coimbra and Andrade 1971b, 1971a). Morphologically, FAP is characterized by distal axonal loss of fibers that leads to the pathophysiological condition associated with this disorder. In FAP, the most common TTR variant presents a substitution of methionine for valine at position 30 – TTR V30M. In the peripheral nerve, TTR aggregates and amyloid fibrils appear mainly in the endoneurium in proximity of blood vessels and near Schwann cells and collagen fibrils (Coimbra and Andrade 1971b, 1971a). In later stages of disease progression, severely affected nerves present endoneurium contents replaced by amyloid, abundant collagen bundles, Schwann cells without axons and fibroblasts, and only a few nerve fibers retain viability. In ganglia, TTR amyloid deposits are present in the stroma in close contact with satellite cells and a progressive loss of neurons is observed (Hofer and Anderson 1975; Ikeda et al. 1987; Hanyu et al. 1989; Takahashi et al. 1991).

Recently, it was shown that TTR aggregates bind to the receptor for advanced glycation end products (RAGE) and that FAP tissues have increased expression of this receptor in sites related to amyloid deposition (Sousa et al. 2000c). The TTR aggregates-RAGE interaction exerts cytotoxic effects as it triggers activation of the nuclear transcription factor κB (NFκB) (Sousa et al. 2000c). FAP nerves show increased expression of pro-inflammatory cytokines such as tumor necrosis factor α (TNFα), interleukin-1β (IL-1β) and macrophage-colony stimulating factor (M-CSF). Oxidative stress also arises in FAP nerves by up-regulation of inducible nitric oxide synthase (iNOS) (Sousa et al. 2001b), which produces NO. Furthermore, caspase-3, a critical protease in the late execution phase of apoptosis, was shown to be up-regulated in axons of FAP nerves. Activation of these markers was abrogated in cell culture by an anti-RAGE antibody or by the soluble domain of RAGE.

These studies represented the first step to understand the involvement of RAGE in the pathophysiological changes in FAP. The signaling mechanisms that mediate TTR aggregates-RAGE interaction and NFκB activation are presently unknown. The engagement of RAGE by a ligand triggers activation of key cell signaling pathways, such as p21ras, mitogen-activated protein kinases (MAPKs), NF-κB and cdc42/rac, thereby reprogramming cellular properties (Yan et al. 1994; Lander et al. 1997; Huttunen et al. 1999). For example, the inhibition of RAGE-amphoterin interaction suppressed activation

of extracellular signal-regulated kinase 1/2 (ERK1/2), p38 and stress-activated protein kinases or jun amino-terminal kinases (SAPKs/JNKs) MAPKs in rat C6 glioma cells (Taguchi et al. 2000).

ERK1/2 are serine-threonine kinases and are activated by dual phosphorylation of threonine and tyrosine residues at the activation domain carried out by MAPK kinase 1/2 (MEK1/2) (Pearson et al. 2001). Active-ERK1/2 targets include several transcription factors, signaling mediators, cytoskeletal proteins and protein kinases. Because ERK1/2 substrates are found in various subcellular compartments (Grewal et al. 1999), the biological outcome of ERK1/2 activation will depend in part of the localization of ERK1/2 and its accessibility to potential substrates within that compartment. ERK1/2 cytoplasmic substrates are of particular importance in neurons, in which ERK1/2 activation may occur at a considerable distance from the nucleus. ERK1/2 activity is decreased by either phosphotyrosine phosphatases or dual specificity (serine-threonine and tyrosine) phosphatases also known as MAPK phosphatases (MKPs) (Pearson et al. 2001).

Differential gene expression microarray data from human FAP SG has shown differences in genes expressed in control and FAP SG, which included extracellular matrix (ECM) remodelling genes; microarray results were validated in nerve biopsies (Sousa et al. 2005b). In the microarray data, MAPK phosphatase 1 (MKP-1/CL100) expression was ~6-fold down-regulated in FAP. MKP-1 is an inducible nuclear dual specificity phosphatase that can dephosphorylate and inactivate ERK1/2, SAPK/JNK and p38 MAPKs (Camps et al. 2000). In the present study we questioned whether MKPs and MAPKs are associated with FAP pathology.

Materials and methods

Subjects

Labial minor SG biopsies were obtained from V30M FAP patients prior to performing liver transplantation, the only available treatment for this disorder. Control SG were from age- and gender-matched non-FAP volunteer individuals that had no evidence of infection. The collection of biopsies material was approved by ethical committee of Hospital Geral de Santo António, Porto, Portugal, and participant subjects were volunteers. SG collection and characterization was described previously (Sousa et al. 2005b). For immunohistochemical analysis, SG were collected to 4% paraformaldehyde in phosphate-buffered saline (PBS). The general characterization of SG consisted of TTR immunohistochemistry and analysis of presence of amyloid deposits by Congo red staining. SG with TTR deposition but without amyloid deposits were classified as FAP 0, and SG with TTR deposition along with amyloid deposits were classified as FAP. Sural nerve biopsy specimens from FAP patients, asymptomatic carriers (FAP 0) and controls (near relatives of FAP patients who ultimately turned out not to have mutations in TTR) were available at the Hospital Geral de Santo António, Porto, Portugal, since this material was obtained as part of the clinical diagnosis and evaluation of FAP, prior to the current use of molecular diagnostic methods.

Immunohistochemistry

For immunohistochemical analysis, nerve and SG paraffin sections were deparaffinated, hydrated in a modified alcohol series, antigens were unmasked by microwaving in 10 mM sodium citrate buffer pH 6.0 (except for anti-human TTR immunohistochemistry), endogenous peroxidase activity was blocked with 3% hydrogen peroxide in methanol for 15 min and incubated in blocking buffer [4% fetal bovine serum (FBS) and 1% bovine serum albumin (BSA) in PBS] for 30 min at 37°C in a moist chamber. Incubation with primary antibody, at the appropriate dilution in blocking buffer, was performed overnight at 4°C in a humidified chamber. Primary antibodies were rabbit polyclonal anti-phospho-MEK1/2 (Ser217/221) (1:50-nerves; 1:100-SG), rabbit polyclonal anti-MEK1/2 (1:100-nerves), mouse monoclonal anti-phospho-p44/42 MAP kinase (Thr202/Tyr204) (1:20-nerves; 1:100-SG), rabbit polyclonal anti-p44/42 MAP kinase (1:100-nerves and SG), mouse monoclonal anti-phospho-p38 (Thr180/Tyr182) (1:20-nerves; 1:50-SG), mouse monoclonal anti-phospho-JNK/SAPK (Thr183/Tyr185) (1:20-nerves; 1:50-SG), all purchased from Cell Signaling Tecn.; rabbit polyclonal anti-MKP-1 (V-15) (1:100-nerves; 1:500-SG), goat polyclonal anti-MKP-3 (N-18) (1:20-nerves; 1:100-SG), mouse

monoclonal anti-phospho-JNK (G-7) (1:20-nerves) were from Santa Cruz Biotech and rabbit polyclonal anti-human TTR (1:1000) was from DAKO. On parallel control sections, primary antibody was replaced by blocking buffer alone and in the case of TTR immunohistochemistry, anti-TTR antibody was pre-adsorbed with recombinant TTR (10 µg TTR/3.9 µg of primary antibody incubated overnight at room temperature). Subsequent immunohistochemistry was performed with either affinity-purified alkaline phosphatase- or peroxidase- conjugated secondary antibody (Sigma). Antigen visualization was performed with either biotin-extravidin-alkaline phosphatase or biotin-extravidin-peroxidase kits (Sigma), using Fast Red (Sigma) or 3-amino-9-ethyl carbazole (Sigma), respectively, as substrates. Semi-quantitative immunohistochemistry (SQ-IHC) analysis was performed using Scion Image software (freely downloaded from Scion Corporation website). This application enables the measurement of the area occupied by pixels corresponding to the immunohistochemical substrate's color that is normalized relatively to the total area. Each slide used in the SQ-IHC was analyzed in 5 different representative areas. To assess kinase activation, data is shown as the ratio between the stained areas occupied by phospho-specific and total-specific antibodies, within the same nerve biopsy. Results are shown as % of occupied area (± SD).

Proteins

Wild-type recombinant TTR was produced from *E. coli* BL21 expression system and purified as previously described (Almeida et al. 1997). Purified soluble TTR was detoxified using Endotoxin Removing Gel (Pierce). For preparation of TTR aggregates, TTR was dialyzed against water, pH 7.0, and then incubated with 0.05 M sodium acetate, pH 3.6, for 48 h at room temperature. The preparation was then centrifuged at 15,000 *g* for 30 min, the pellet washed and resuspended in PBS, pH 7.4. Protein concentration was determined by the Lowry method (Lowry et al. 1951). TTR aggregates are composed of short fibrils and amorphous aggregates as assessed by ultrastructural analysis (Sousa et al. 2001a).

Cell culture assays

RN22 cells (rat Schwannoma cell line) were from the European Collection of Cell Cultures. RN22 were propagated in 10 cm dishes in monolayer and maintained at 37ºC in a humidified atmosphere of 95% and 5% CO_2. Cells were grown in Dulbecco's minimal essential media (DMEM) (Gibco) supplemented with 10% FBS (Gibco), 2 mM glutamine (Sigma) and 100 U/mL penicillin/streptavidin (Gibco) (complete media). For ERK1/2 activation assays, cells were grown in complete media in six-well plates. When ~50% confluence was reached, cells were washed with PBS and starved in DMEM containing

1% dialyzed FBS for ~16 h. Subsequently, cells were treated with 1 μM of soluble or aggregated TTR for the indicated time periods. For studies using goat polyclonal anti-RAGE antibody (N-16) (αRAGE) (Santa Cruz Biotech) and non-immune (NI) purified IgGs from goat serum (Sigma), following starvation, cells were pre-incubated for 3 h with 30 μg/mL of αRAGE or NI, and then treated with 1 μM TTR aggregates plus 10 μg/mL of αRAGE or NI in DMEM containing 0.5% dialyzed FBS for 30 min. For caspase-3 activation assays, cells were grown in 25 cm^2 flasks. Activation of caspase-3 was measured using the Fluorometric Caspase-3 Assay kit (Sigma), following the manufacturer's instructions. Briefly, 80% confluent cells were incubated in assay media (DMEM containing 1% dialyzed FBS) with 2 μM of soluble or aggregated TTR for 24 h. Where indicated cells were pre-incubated for 1 h with 1 μM U0126 (Calbiochem), a MEK1/2 inhibitor, and subsequently cells were incubated with 5 μM U0126 alone or 5 μM U0126 with 2 μM TTR aggregates. Next, cells were trypsinized and the cell pellet was lysed in 100 μL of kit lysis buffer; 40 μL of each cell lysate sample was used in duplicates for determination of caspase-3 activation. The remaining cell lysate was used to determine total cellular protein concentration with the Bio-Rad protein assay, using BSA as standard. Values shown are the mean of quadruplicates of two independent experiments. Student's *t* test statistical analysis was used to determine statistical significance between cells exposed to assay media and cells exposed to different regulators.

Immunoblots

Following treatment with TTR, cells were washed twice with ice-cold PBS, and lysed with 100 μL of lysis buffer (Cell Signaling Tecn.) containing a protease inhibitor cocktail (Calbiochem). Cell lysates were centrifuged at 11,000 *g* and protein in the supernatant was quantified with the Bio-Rad protein assay. Equal amounts of protein were loaded in 12% SDS-PAGE and transferred to nitrocellulose Hybond-C Extra (Amersham Biosciences) using a semidry transfer system. Blots were incubated with blocking buffer (5% nonfat dried milk, and 50 mM NaF, to inhibit phosphatases, in Tris buffered saline (TBS) with 0.1% tween-20 (T)) for 1 h at room temperature. Subsequently, incubation with primary antibodies, at the appropriate dilution, was performed overnight at 4ºC in 5% BSA/TBS-T with 50 mM NaF. The primary antibodies used were rabbit polyclonal anti-phospho-p44/42 MAP kinase (Thr202/Tyr204) (1:1000), rabbit polyclonal anti-p44/42 MAP kinase (1:1000), purchased from Cell Signaling Tecn., and rabbit polyclonal anti-ERK 1 (C-16) (1:1000) from Santa Cruz Biotech. After incubation with secondary sheep anti-rabbit IgGs peroxidase conjugate (1:5000; The Binding Site) in 1% nonfat dried milk TBS-

T for 1 h at room temperature, blots were developed using the SuperSignal West Pico Chemiluminescent Substrate kit (Pierce) and exposed to Hyperfilm ECL (Amersham Bioscieneces). Blots were first incubated with phospho-specific antibodies, stripped with Re-Blot Plus Mild Solution (Chemicon) according to manufacturer's instructions, reblocked, and then incubated with the respective anti-total protein antibody for total protein normalization. Quantitative analysis of immunoblot images was performed using the Scion Image software (Scion Corporation). Results are shown as the squared pixels ratio between phospho-p44/42 and total-p44/42 MAPK, and represented as fold activation relatively to cells exposed to assay media.

Mice nerve preparation

Transgenic mice bearing the human TTR V30M in a TTR-knockout background (Kohno et al. 1997) were compared to TTR-knockout (Episkopou et al. 1993) and wild-type mice. Mice were killed by cervical distension. Nerves were rapidly excised and frozen in dry ice. In order to analyze ERK1/2 activation, peripheral nerves were ground into powder with a frozen pestle in dry ice and homogenized in lysis buffer (5 mM EDTA, 2 mM EGTA, 20 mM MOPS pH 7.0, 30 mM sodium fluoride, 20 mM sodium pyrophosphate, 1 mM sodium orthovanadate, 40 mM β-glycerophosphate, 0.5% triton X-100, pH 7.2) supplemented with protease inhibitor cocktail set III (Calbiochem). Homogenate samples were centrifuged at 16,000 *g* for 30 min, and supernatants assayed for protein concentration by the Bio-Rad method.

Statistical analysis

Group values, expressed as the mean ± SD, were compared by Student's *t* test, and *P* values of less than 0.05 were considered significant.

Results

MKP-1 and MKP-3 expression is down-regulated in FAP

As shown in the previous chapter 2, gene expression microarray from human FAP SG displayed down-regulation (6.2-fold ± 1.4) of mitogen-activated protein (MAP) kinase phosphatase 1 (MKP-1/CL100). We validated the microarray data both by RT-PCR (data shown in the previous chapter) and semi-quantitative immunohistochemistry. In the later, amyloid laden SG from FAP patients showed a significant down-regulation of MKP-1 (Figure 1A upper panels and chart), validating the microarray results. MKP-1 immunostaining was more abundant in the cytoplasm of the stratified cuboidal epithelial lining present in excretory ducts than in the nucleus. We then performed immunohistochemical analysis for MKP-1 in FAP nerve biopsies in different stages of disease progression. At later stages of FAP progression, when compared with controls and asymptomatic carriers (FAP 0), MKP-1 expression was down-regulated in axons (as documented in Figure 1A lower panels and chart). To test whether the expression of other dual specificity MAP kinase phosphatases (MKPs) could be affected in FAP, we studied MKP-3, which specifically inactivates ERK1/2 when compared with JNK and p38 MAPKs. MKP-3 was down-regulated in FAP 0 SG as well as in SG from FAP patients (Figure 1B upper panels and chart). The immunostaining was exclusively cytoplasmatic in the epithelial lining of excretory ducts. However, in human nerve biopsies, MKP-3 was up-regulated in axons of the FAP 0 asymptomatic stage as compared to controls, but MKP-3 levels at the symptomatic stage did not differ from controls (Figure 1B lower panels and chart).

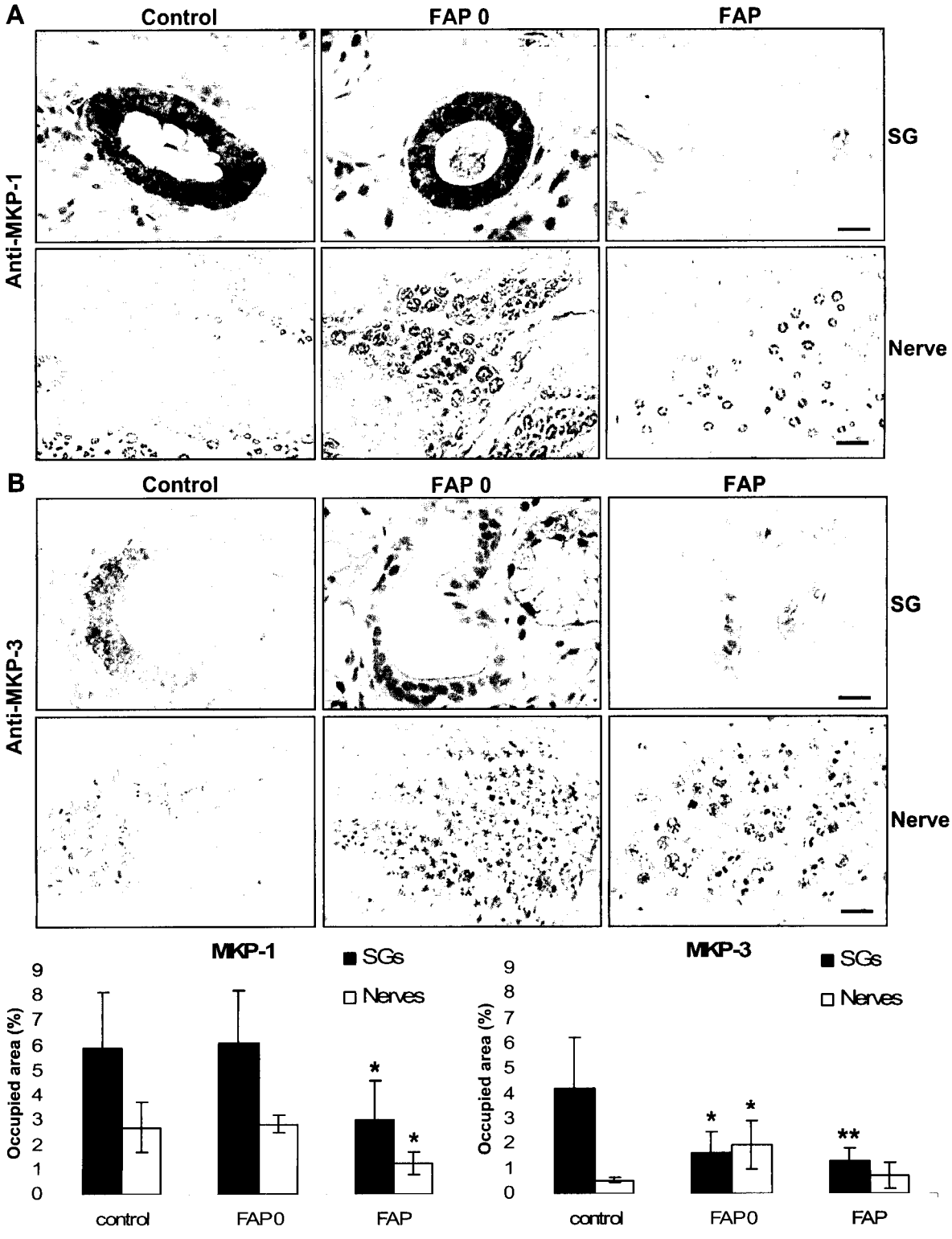

Figure 1. MKP-1 and MKP-3 expression in FAP.
A, MKP-1 immunohistochemistry of representative SG (upper panels) and nerves (lower panels) from control individuals (left panels), FAP 0 (middle panels) and FAP patients (right panels). Bar, 20 µm. **Chart (MKP-1)**, Quantitation of immunohistochemical images of MKP-1 staining in SG excretory ducts and nerves. **B**, MKP-3 immunohistochemistry of representative SG (upper panels) and nerves (lower panels) from control individuals (left panels), FAP 0 (middle panels) and FAP patients (right panels). Bar, 20 µm. **Chart (MKP-3)**, Quantitation of immunohistochemical images of MKP-3 staining in SG excretory ducts and nerves. Data are represented as percentage of occupied area ± SD for SG controls (n=6), FAP 0 (n=4) and FAP patients (n=6), and for nerves controls (n=4), FAP 0 (n=6) and FAP patients (n=5). $^{*}P < 0.05$ and $^{**}P < 0.02$, compared to control groups.

ERK1/2 activation is up-regulated in FAP

The diminished expression of MKPs in FAP suggests that MAPKs cascades might be up-regulated in FAP. Semi-quantification of MAPKs by immunohistochemistry of FAP SG did not show activation of p38 and JNK MAPKs when compared to control SG (data not shown). However, ERK1/2 MAPK activation in FAP SG showed a marked up-regulation beginning at FAP 0 and persisting in the FAP stage. Often phosphorylated ERK1/2 (pERK1/2) translocation to the nucleus of stratified cuboidal epithelial lining in excretory ducts was observed, whereas in controls a cytoplasmic localization was present (Figure 2A and chart). MAPKs were also assessed in human FAP nerve biopsies. Consistently with the analyses of human SG, intensity of immunostaining for phosphorylated forms of p38 and JNK was not statistically different in FAP and control nerves (data not shown). However, increased ERK1/2 phosphorylation was evident in human FAP nerves. In asymptomatic carriers (FAP 0), activated ERK1/2 was approximately 3-fold increased in axons, whereas pERK1/2 was almost absent in controls. Total ERK1/2 (tERK1/2) levels were similar in the two types of samples (Figure 2B and chart). At a later symptomatic stage, phosphorylation levels of ERK1/2 were lower, however tERK1/2 levels also decreased, leading to a sustained ERK1/2 activation, when compared to normal specimens (Figure 2B and chart). Although ERK1/2 was observed in several cell types, neuronal axons were the main cellular structure with positive staining. These results correlate well with the decreased expression of MKP-1 seen in nerves from FAP patients. Up-regulation of ERK1/2 detected in asymptomatic carriers is not explained by the actions of MKP-1 and -3 and additional mechanisms might intervene at this stage, such as MEK1/2 activation.

In an attempt to analyze ERK1/2 activation *in vivo*, we used a transgenic mouse model that expresses human TTR V30M in a TTR-knockout background. These mice when older than 9 months of age develop TTR amyloid deposits in several organs within the gastrointestinal tract, and at the age of 24 months the pattern of amyloid deposition is similar to the one seen in FAP autopsies except for the absence of TTR deposition in the peripheral nerve (Takaoka et al. 1997). When we analyzed protein extracts from TTR V30M mice peripheral nerve, we found a 2-fold increased activation of ERK1/2 in older animals (17 months of age) when compared with younger ones (2 months of age; Figure 2C). The observed activation was not age-dependent, since age-matched wild-type and TTR-knockout mice did not show differences on ERK1/2 activation (data not shown). It is possible that low amounts of pre-fibrillar TTR species are present in old transgenic TTR V30M mice not detected by previous immunohistochemical methods. Taken together, the human and mice data indicate ERK1/2 up-regulation in FAP tissues.

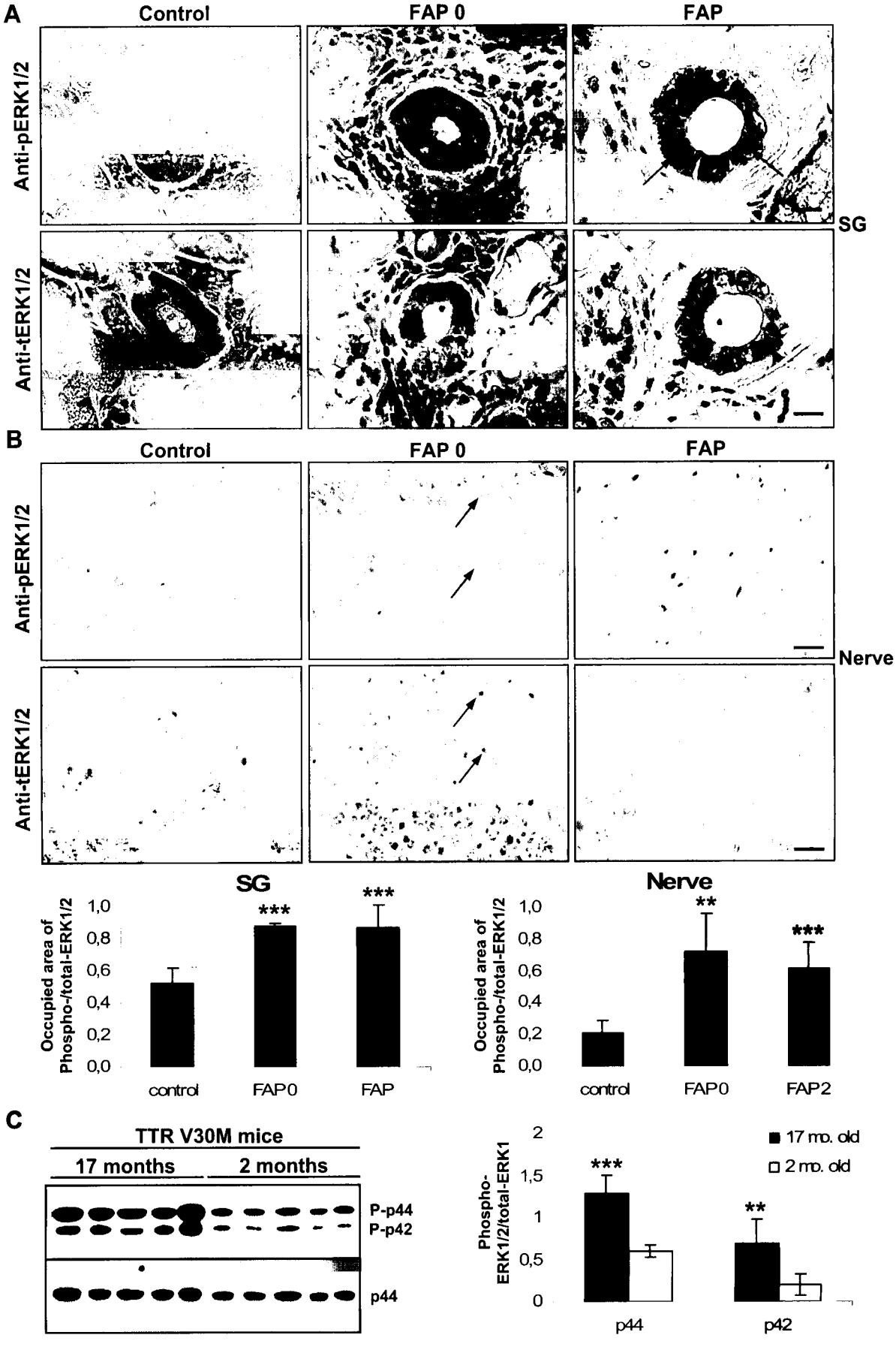

Figure 2. ERK1/2 increased activation in FAP.
A, Representative pERK1/2 (upper panels) and tERK1/2 (lower panels) immunohistochemistry of SG biopsies from control individuals (left panels), FAP 0 (middle panels) and FAP patients (right

panels). Arrows, nuclear translocation. Arrow heads, cytoplasmic localization. Bar, 20 µm. **Chart (SG)**, Quantitation of immunohistochemical images of the ratio between pERK1/2 and tERK1/2 staining in control individuals (n=5), FAP 0 (n=3) and FAP patients (n=6) SG excretory ducts. Data are represented as occupied area in squared pixels ± SD. ***$P < 0.001$. **B**, Representative pERK1/2 (upper panels) and tERK1/2 (lower panels) immunohistochemistry of nerves from control individuals (left panels), FAP 0 (middle panels) and FAP patients (right panels). Bar, 20 µm. **Chart (Nerve)**, Quantitation of immunohistochemical images of the ratio between pERK1/2 and tERK1/2 staining in control individuals (n=5), FAP 0 (n=7) and FAP patients (n=5) nerves. Data are represented as occupied area in squared pixels ± SD. **$P < 0.002$, ***$P < 0.001$. **C**, ERK1/2 activation in TTR V30M mice peripheral nerve; Immunoblots representing stimulation of pERK1/2 (top lanes) and expression of tERK1 (bottom lane) from peripheral nerve extracts of TTR V30M mice. 20 µg of total protein was loaded per lane. **Chart**, Quantitation of immunoblot images of the ratio between phospho-ERK1/2 (P-p44/42) and total-ERK1 (p44). **$P < 0.007$ and ***$P < 0.0001$, comparing older (n=6) to younger (n=6) TTR V30M mice.

Despite the fact that this transgenic mouse model was reported to lack TTR deposition in the peripheral nerve (Takaoka et al. 1997), we performed TTR immunohistochemistry using a rabbit polyclonal anti-human TTR and a biotin-extravidin-peroxidase system that is more sensitive for antigen detection. Indeed, using these improvements, we observed TTR immunostaining in the peripheral nerve (i.e. braquial plexus and sciatic nerve) in an extracellular distribution between nerve fibers and near Schwann cells (Figure 3A, upper panels); in DRG, TTR was located in the stroma in a close contact with satellite cells that surround neuronal cell bodies (Figure 3A, lower panels), as it was described for FAP patients. Table 1 shows the increased penetrance of TTR deposition with advancing age of these mice.

Table 1. TTR deposition in sciatic nerve and DRG of TTR V30M transgenic mice in a TTR-knockout background ranging from 1 to 21 months of age as evaluated by TTR immunohistochemistry.

Tissue/Age	1-6 months	7-12 months	13-21 months
Sciatic nerve	4 (n=23)	3 (n=11)	9 (n=19)
DRG	5 (n=22)	3 (n=11)	12 (n=18)

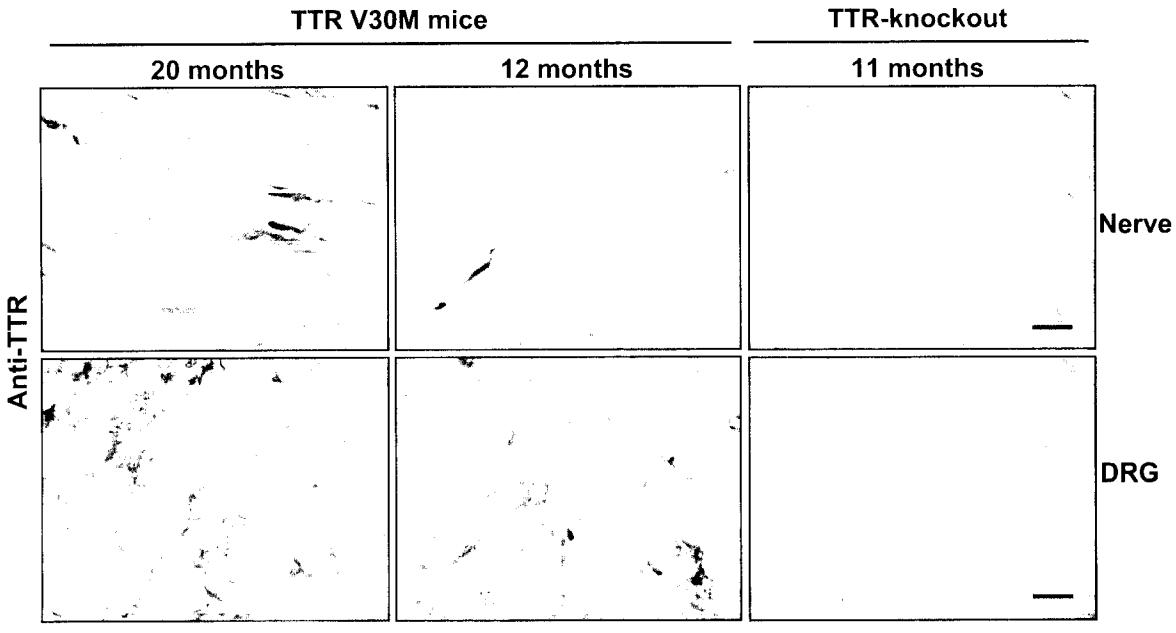

Figure 3. Analysis of TTR deposition in peripheral nerve and DRG of TTR V30M transgenic mice in a TTR-knockout background.
TTR immunohistochemistry of representative nerves (upper panels) and DRG (lower panels) from 20 months of age (left panels) and 12 months of age (middle panels) of TTR V30M mice, and 11 months of age TTR-knockout mice (right panels). Bar, 20 μm.

MEK1/2 activation is up-regulated in FAP

One of the signaling mechanisms that up-regulates ERK1/2 activity are upstream kinases. The immediate upstream ERK1/2 kinase is MEK1/2. Consistent with the human nerve ERK1/2 data, we found MEK1/2 activation (phospho/total levels) up-regulated in FAP nerves both from asymptomatic carriers and patients, relatively to controls (Figure 4 and chart). As observed for ERK1/2, in a later symptomatic stage, phosphorylation levels of MEK1/2 decreased; however tMEK1/2 levels were also lower, leading to sustained MEK1/2 activation, when compared to normal specimens. To note that axonal staining is significantly decreased for tERK1/2 and tMEK1/2 due to severe loss of nerve fibers in patients.

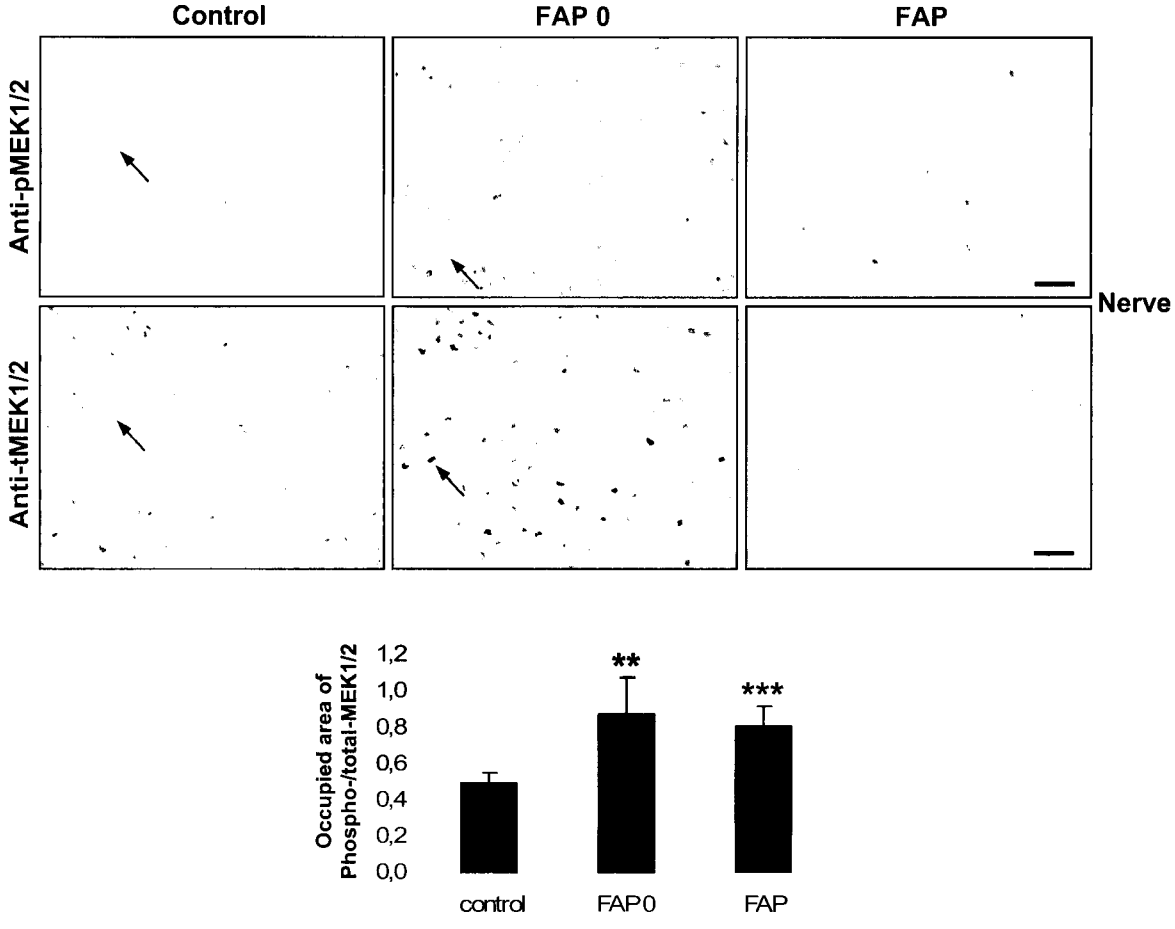

Figure 4. MEK1/2 increased activation in FAP nerves.
pMEK1/2 (upper panels) and tMEK1/2 (lower panels) immunohistochemistry of representative nerves from control individuals (left panels), FAP 0 (middle panels) and FAP patients (right panels). Bar, 20 μm. **Chart**, Quantitation of immunohistochemical images of the ratio between pMEK1/2 and tMEK1/2 staining in control individuals (n=5), FAP 0 (n=7) and FAP patients (n=6). Data are represented as occupied area in squared pixels ± SD. $^{**}P < 0.01$ and $^{***}P < 0.001$.

ERK1/2 activation is RAGE mediated

The RN22 cellular system, that presents a Schwann cell like phenotype and was previously demonstrated to display RAGE mediated neurotoxicity triggered by TTR aggregates (Sousa et al. 2001b), was used to determine whether TTR aggregates could activate the ERK1/2 MAPK cascade. We found that treatment of RN22 cells with TTR aggregates triggered a rapid and sustained ERK1/2 phosphorylation after 15 min, while soluble TTR had no effect (Figure 5A). Then, we posed the question whether RAGE was mediating ERK1/2 activation stimulated by TTR aggregates. In fact, we found that TTR aggregate-induced ERK1/2 activation was RAGE mediated, as anti-RAGE IgG had a significant inhibitory effect in ERK1/2 activation, when compared with nonimmune IgG at the same concentration (Figure 5B and charts (i), (ii)). Previous studies demonstrated that prolonged exposure of RN22 cells to TTR aggregates (24 h) leads to a RAGE-dependent activation of caspase-3 (Sousa et al. 2001b). Here, we investigated whether ERK1/2 is mediating intracellular signaling leading to induction of apoptosis stimulated by TTR aggregates. Using the described cell culture apoptosis assay (Sousa et al. 2001b) we blocked the ERK1/2 signaling pathway with U0126, a MEK1/2 pharmacological inhibitor. U0126 completely abolished TTR aggregate-dependent caspase-3 activation, whereas control U0126 and soluble TTR did not activate caspase-3 (Figure 5C).

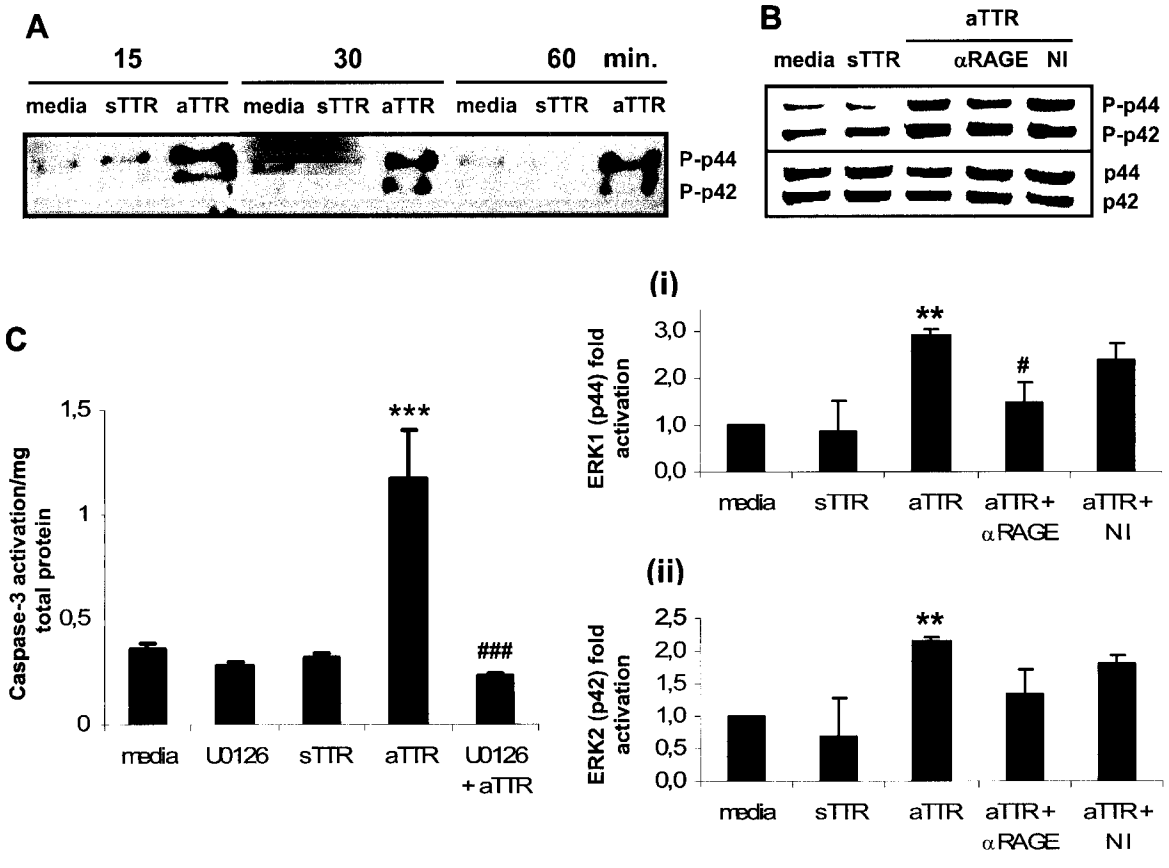

Figure 5. ERK1/2 activation triggered by TTR aggregates.
A, TTR aggregates trigger ERK1/2 MAPK activation. Immunoblot representing pERK1/2 (P-p44/42) induction in RN22 cells exposed for the indicated time periods to either 1 μM soluble TTR (sTTR) or 1 μM TTR aggregates (aTTR). **B**, TTR aggregates activate ERK1/2 MAPK cascade via RAGE. Immunoblots representing stimulation of phospho-ERK1/2 (P-p44/42) and expression of total-ERK1/2 (p44/42) from RN22 cell lysates. Cells were exposed 30 min to either 1 μM soluble TTR (sTTR) or 1 μM TTR aggregates (aTTR). Where indicated, cells were pre-incubated with polyclonal anti-RAGE (αRAGE) or non-immune IgG (NI). **Chart (i)**, Quantitation of immunoblot images of the ratio between phospho- and total-ERK1 (p44), and **(ii)** phospho- and total-ERK2 (p42). Data are represented as fold activation relatively to non-treated cells (media), which was set as 1. Results derive from three independent experiments. $^{**}P < 0.003$, compared with non-treated cells and $^{\#}P < 0.05$, compared with cells treated with aTTR in the presence of non-immune IgG (aTTR + NI). **C**, TTR aggregates induction of caspase-3 is ERK1/2 MAPK mediated. Activation of caspase-3 in RN22 cells exposed for 24 h to either 2 μM soluble TTR (sTTR) or 2 μM aggregated TTR (aTTR). Where indicated cells were pre-incubated with 1 μM U0126 for 1 h. Then these cultures were exposed for 24 h to aTTR (2 μM) along with 5 μM U0126. $^{***}P < 0.001$, compared with non-treated cells (media). $^{\#\#\#}P < 0.001$, compared with cells treated with TTR aggregates.

Discussion

This study addresses early intracellular signaling events occurring as a consequence of TTR deposition in FAP. We propose that the MEK-ERK MAPK signaling pathway is involved in FAP pathogenesis. Supporting this hypothesis, we show that cultured Schwann-like cells treated with TTR aggregates elicit a sustained ERK1/2 activation, which is transduced in part by RAGE. It is possible that other still unknown receptors intervene in the TTR aggregate-induced signaling cascades. It is well characterized that RAGE signaling induces oxidative stress and activates ERK cascades, leading to downstream increased NFκB activity (Yan et al. 1994; Lander et al. 1997). In addition, the RAGE promoter contains 2 functional NFκB binding sites (Li and Schmidt 1997), therefore both the increased NFκB activation and increased RAGE expression observed in FAP (Sousa et al. 2000c; Sousa et al. 2001b) most likely contribute to the observed ERK sustained activation observed in this cellular system. Moreover, it was demonstrated that the cytosolic domain of RAGE directly binds to ERK by a D-domain docking site (Ishihara et al. 2003). *In vivo*, using transgenic mice expressing a signaling transduction deficient RAGE in peripheral neurons, a diminished phosphorylation of ERK1/2 after nerve crush injury has been observed (Rong et al. 2004b). As shown previously, long exposure of RN22 cells to TTR aggregates leads to increased activation of caspase-3, which was mediated by RAGE (Sousa et al. 2001b). When we posed the question whether ERK cascade could play a role in this process, we found that in fact blockade of ERK activation, using the MEK inhibitor U0126, abolished caspase-3 activation. These evidences point to ERK1/2 as an important player in mediating the cytotoxic effects of TTR aggregates.

Data with clinical samples revealed a chronic MEK-ERK activation starting at early asymptomatic stage (FAP 0) and persisting throughout the course of the disease. Moreover, in a FAP animal model, we show an increased ERK1/2 activation in total protein extracts of peripheral nerve from older mice, which are more prone to have TTR deposits, as compared to younger animals and control mice. In fact, we show here, for the first time, that this FAP animal model has TTR deposited in the peripheral nerve. The cellular localization of pERK differed depending on the tissue analyzed. In FAP SG, pERK nuclear translocation was visualized. In FAP nerves, pERK was sequestered in axons where ERK acts in neuronal cytoplasmic substrates that might ultimately contribute to axon degeneration. The possibility of pERK nuclear translocation in dorsal root ganglia has to be considered, as TTR deposition in the stroma of sensitive ganglia most likely affects the cell body and probably leads to the nuclear regulation of specific gene products that then circulate in axons.

While ERK activation occurred at the asymptomatic and symptomatic levels both in SG and nerve, expression of the two phosphatases investigated differed. The down-regulation of MKP-1 (as shown by immunohistochemistry in SG and nerve, and microarray data) in symptomatic individuals correlated with the observed ERK up-regulation in the same tissues, but was not evident for the asymptomatic level. Immunohistochemical analysis of MKP-3 expression (a more specific ERK1/2 phosphatase as compared with the other MAPKs) differed between SG and nerves; while in SG, MKP-3 expression was down-regulated in accordance with the observed ERK activation in FAP 0 and FAP individuals, in nerves MKP-3 was over-expressed at the asymptomatic level (FAP 0). These results might derive from differences between the two tissues analyzed, including cell specific phosphatase expression and modulation which in FAP might have different responses at different clinical stages. It has been proposed that growth factors, cytokines, cell stressors or activated oncogenes induce MKPs gene transcription via both ERK-dependent and independent pathways (Camps et al. 2000; Colucci-D'Amato et al. 2003). In this context, active ERK can generate a negative feedback loop leading to the up-regulation of MKPs expression. Modulation of ERK activity by MKPs entails not only MKP expression level but also activity. In fact, recently, several phosphatases have been shown to be redox-sensitive and can be either reversibly or irreversibly inhibited, depending on the extension and mechanism of oxidation (Meng et al. 2002; Tonks 2003). Possible down-regulation of MKPs activity caused by oxidative stress, which occurs in FAP tissues both at the asymptomatic and symptomatic levels, can also modulate ERK activity.

Although ERK signaling pathways are generally thought to promote neuronal survival, there is a growing number of recent studies implicating ERK activation mediating neuronal injury. Neuronal cell lines and primary cultures exposed to oxidative stressors were protected by inhibition of ERK phosphorylation (Oh-hashi et al. 1999; Satoh et al. 2000; Stanciu et al. 2000; Kulich and Chu 2001). Moreover, animal models of cerebral ischemia-reperfusion treated with MEK inhibitors, developed neuroprotection (Alessandrini et al. 1999; Namura et al. 2001). In neurodegenerative diseases such as Alzheimer's disease (AD), Parkinson's disease (PD) and Lewy body dementias, pERK appears to be located within discrete, cytoplasmic granules (Pei et al. 2002; Zhu et al. 2002a), and this pattern was also observed in 6-hydroxydopamine-treated neuronal cells (Zhu et al. 2002a). Despite the existence of discrete active ERK accumulations in the cytoplasm, ERK may not be available to phosphorylate possible downstream pro-survival substrates. Conversely, substrates participating in pro-apoptotic pathways could be accessible to active ERK. For example, death associated protein kinase (DAPK) participates in various apoptotic paradigms and was shown to interact with ERK. ERK functions as the upstream

activating kinase of DAPK, which promotes the cytoplasmic retention of ERK, thereby inhibiting ERK signaling in the nucleus and promoting DAPK activity (Chen et al. 2005). The molecular signaling mechanisms in FAP neurodegeneration are not fully understood. In this study we pursued to unravel these signaling mechanisms and we found that ERK signaling cascade is abnormally activated. Finally, chronic ERK activation might be an early and sustained signaling amplifier of TTR deposits-induced cytotoxicity leading to NFκB activation, up-regulation of pro-inflammatory cytokines (i.e. IL-1β, TNFα, M-CSF), oxidative stress, and ultimately to neurodegeneration in FAP.

ACKNOWLEDGEMENTS

We thank Paul Moreira for the production and purification of recombinant TTR, Rossana Correia, Fernanda Malhão and Maria José Ferreira (Molecular Neurobiology, IBMC, Porto, Portugal) for tissue processing, and Rui Fernandes (Advanced Tissue Analysis Facility, IBMC), and António Guimarães (Hospital de Santo António, Porto) for analysis of pathological findings. We are indebted to Dr. Shuishiro Maeda (Yamanashi University) for providing human TTR V30M transgenics. This work was supported by grants from POCTI program of Fundação para a Ciência e Tecnologia – FCT, Saúde XXI and Gulbenkian Foundation, Portugal and fellowships SFRH/BPD/9416/2002 (to I. C.) and SFRH/BD/4563/2001 (to F. A. M.) from Fundação para a Ciência e Tecnologia, Portugal.

CHAPTER 3 – PART II

Study of Selected Transcription Factors in Familial Amyloidotic Polyneuropathy

Study of Selected Transcription Factors in Familial Amyloidotic Polyneuropathy

Filipe Almeida Monteiro[1,2] and Maria João Saraiva[1,2]

[1]Molecular Neurobiology, Instituto de Biologia Molecular e Celular, Porto, Portugal;

[2]Instituto de Ciências Biomédicas de Abel Salazar, University of Porto, Portugal.

Corresponding author: Maria João Saraiva; Molecular Neurobiology; Instituto de Biologia Molecular e Celular; R. Campo Alegre, 823. 4150-180 Porto, Portugal.

Tel. 351-226074900; Fax 351-226099157. E-mail: mjsaraiv@ibmc.up.pt

Running title: Transcription factors in familial amyloidotic polyneuropathy.

Abstract

Recently, we have shown that among mitogen-activated protein kinase (MAPK) related pathways, solely the extracellular-regulated protein kinases 1/2 (ERK1/2) are up-regulated in familial amyloidotic polyneuropathy (FAP). Besides nuclear transcription factor κB (NFκB), MAPKs downstream targets, such as transcription factors, have not yet been studied in FAP. Here, we show that activation of ETS-domain transcription factor 1 (Elk-1) is down-regulated in FAP salivary glands (SG) and nerves from asymptomatic carriers, which is possibly related to ERK1/2 negative feedback modulation. Other transcription factors, such as activating transcription factor-2 (ATF-2) and c-Jun, presented different activations in FAP SG and nerve from asymptomatic carriers, suggesting tissue specific pathways to be further investigated in the future. Finally, no differences in expression were found for phosphorylated (active) forms of both p53 and signal transducer and activator of transcription 3 (STAT3) transcription factors. These preliminary data suggest a complex interplay between selected transcription factors in FAP, but give guidance for further investigation on pathways not addressed herein.

Abbreviations: AP-1, activator protein 1; ATF-2, activating transcription factor 2; Elk-1, ETS-domain transcription factor 1; ERK, extracellular signal-regulated kinase; FAP, familial amyloidotic polyneuropathy; MKP-1, MAP kinase phosphatase 1; NFκB, nuclear transcription factor κB; SAPK/JNK, stress-activated protein kinase or jun amino-terminal kinase; SG, salivary gland; STAT3, signal transducer and activator of transcription 3; TTR, transthyretin.

Introduction

Several transduction pathways have been involved with the pathology of amyloid related disorders. Mitogen-activated protein kinases (MAPKs) signaling cascades were shown to have a key role in the regulation of gene expression, cell proliferation and programmed cell death. At least three different MAPKs pathways are expressed in mammals: extracellular signal-related kinases (ERKs), Jun amino-terminal kinases or stress-activated protein kinases (JNKs/SAPKs) and p38 proteins (Chang and Karin 2001).
Following the study of MAPKs and MAPK phosphatases (i.e. MKP-1 and MKP-3) in the first part of this chapter, we pursued with the study of MAPKs downstream transcription factors. The identification of transcription factors abnormally regulated, leading to altered gene expression, might be of great importance in FAP. Several transcription factors have been described to be activated upon phosphorylation by MAPKs, such as Elk-1 (ETS-domain transcription factor), ATF-2 (activating transcription factor 2), c-Jun, and p53.

Elk-1 has been reported to be phosphorylated by all MAPKs (i.e. ERK1/2, JNKs and p38), promoting *c-fos* gene transcription. ATF-2 is phosphorylated by both JNK and p38 and induces transcription of *c-jun*. Regarding c-Jun, it is phosphorylated by JNK (Karin 1995; Davis 2000; Shaulian and Karin 2002). Activated c-Jun functions as either a homodimer or a heterodimer with other members of the Jun, Fos or ATF families to form activator protein 1 (AP-1) dimeric complex. Thus, AP-1 is composed of dimeric basic region-leucine zipper (bZIP) proteins, which recognize either 12-*O*-tetradecanoylphorbol-13-acetate (TPA) response elements (TRE, 5′-TGAG/CTCA-3′) or cAMP response elements (CRE, 5′-TGACGTCA-3′). AP-1 activity is induced by a variety of physiological stimuli and environmental stresses. In addition, AP-1 regulates a wide range of cellular processes, such as cell proliferation, death, survival and differentiation. Despite the increasing knowledge regarding the physiological functions of AP-1, the target-genes mediating these functions are not always obvious (Shaulian and Karin 2002). Finally, the tumour suppressor, p53, acts mainly as a transcription factor on a number of genes whose products regulate cell cycle arrest and apoptosis (Muller et al. 2000). Its stability and activity is enhanced through phosphorylation by JNK and p38 (Sionov and Haupt 1999).
As shown in FAP tissues, increased expression of pro-inflammatory and oxidative stress-related molecules is present (Sousa et al. 2001a; Sousa et al. 2001b). An important signaling pathway induced by cytokines and reactive oxygen species (ROS) involves the Janus family tyrosine kinases (Jak kinases) and signal transducers and activators of transcription (STATs) (Heim 1999). It was shown that after peripheral nerve injury, only

STAT3, among all the STAT proteins, is significantly increased (Schwaiger et al. 2000). It is presently unknown whether this pathway is involved in FAP-related nerve injury.
In the present work we investigated the activation of selected transcription factors in FAP clinical samples by semi-quantitative immunohistochemical analysis.

Materials and methods

Subjects

Labial minor SG biopsies were obtained from V30M FAP patients prior to performing liver transplantation, the only available treatment for this disorder. Control SG were from age- and gender-matched non-FAP volunteer individuals that had no evidence of infection. The collection of biopsies material was approved by ethical committee of Hospital Geral de Santo António, Porto, Portugal, and participant subjects were volunteers. SG collection and characterization was described previously (Sousa *et al* 2005). For immunohistochemical analysis, SG were collected to 4% paraformaldehyde in phosphate-buffered saline (PBS). The general characterization of SG consisted of TTR immunohistochemistry and analysis of presence of amyloid deposits by Congo red staining. SG with TTR amyloid deposits were classified as FAP. Sural nerve biopsy specimens from asymptomatic carriers (FAP 0) and controls (near relatives of FAP patients who ultimately turned out not to have mutations in TTR) were available at the Hospital Geral de Santo António, Porto, Portugal, since this material was obtained as part of the clinical diagnosis and evaluation of FAP, prior to the current use of molecular diagnostic methods. Human skins were obtained from biopsies of control individuals and FAP patients and were classified for the presence of TTR and amyloid deposition as follows: positive for the presence of non-fibrillar TTR and negative for amyloid (+/-), and positive for non-fibrillar TTR and amyloid (+/+) (Sousa et al. 2004b).

Immunohistochemistry

For immunohistochemical analysis, nerve and SG paraffin sections were deparaffinated and hydrated in a modified alcohol series. Antigens were unmasked by microwaving in 10 mM sodium citrate buffer pH 6.0, endogenous peroxidase activity was blocked with 3% hydrogen peroxide in methanol for 15 min and sections were subsequently incubated in blocking buffer (4% fetal bovine serum (FBS) and 1% bovine serum albumin (BSA) in PBS) for 30 min at 37ºC in a moist chamber. Incubation with primary antibody, at the appropriate dilution in blocking buffer, was performed overnight at 4ºC in a humidified chamber. Primary antibodies used and incubation dilutions are depicted in table 1. Subsequent immunohistochemistry was performed with either mouse or rabbit biotin-conjugated secondary antibodies (Sigma). Antigen visualization was performed with either biotin-extravidin-alkaline phosphatase or biotin-extravidin-peroxidase kits (Sigma), using Fast Red (Sigma) or 3-amino-9-ethyl carbazole (Sigma), respectively, as substrates. On parallel control sections, primary antibody was replaced by blocking buffer alone. Semi-

quantitative immunohistochemistry (SQ-IHC) analysis was performed using Scion Image software (freely downloaded from Scion Corporation website). This application enables the measurement of the area occupied by pixels corresponding to the immunohistochemical substrate color that is normalized relatively to the total area. Each slide used in the SQ-IHC was analyzed in 5 different representative areas. Results are shown as % of occupied area (± SD).

Table 1. Summary of primary antibodies, with respective working dilutions, used in immunohistochemical analysis of human nerve, SG and skin biopsies.

Antibody	Host	Working dilutions			Company
		Nerve	SG	Skin	
Phospho-Elk-1 (Ser 383)	Rb	1:50	1:50	1:50	C. S.
Elk-1 [I-20]	Rb	1:50	1:50	N.P.	S. C.
Phospho-ATF-2 (Thr 69/71)	Rb	1:25	1:25	1:25	C. S.
ATF-2 [C-19]	Rb	1:50	1:50	N.P.	S. C.
Phospho-c-Jun [KM-1] (Ser 63)	Mo	1:40	1:40	1:40	S. C.
c-Jun [N]	Rb	N.P.	1:50	N.P.	S. C.
Phospho-p53 (Ser 15)	Rb	1:50	1:50	1:50	S. C.
Phospho-STAT3 (Ser 727)	Rb	N.P.	1:50	N.P.	C. S.

Legend: C.S., Cell Signaling Tecn; S. C., Santa Cruz Biotech; Rb, rabbit; Mo, mouse; N.P., not performed.

Statistical analysis

Group values, expressed as the mean ± SD, were compared by Student's *t* test, and *P* values of less than 0.05 were considered significant.

Results

Activation of Elk-1, ATF-2 and c-Jun is down-regulated in FAP SG

Previously, we found that MAP kinase phosphatase -1 and -3 (MKP-1 and MKP-3) expression is down-regulated and that ERK1/2 MAPKs display an abnormally sustained activation in FAP SG (Monteiro et al. 2006); thus we pursued to study MAPKs pathways by analysing their downstream transcription factors such as Elk-1, ATF-2, c-Jun and p53. By SQ-IHC, amyloid laden SG from FAP patients showed a significant down-regulation of the phosphorylated forms of Elk-1, ATF-2 and c-Jun (Figure 1 and charts). Phosphorylated Elk-1, ATF-2 and c-Jun (*p*-Elk-1, *p*-ATF-2 and *p*-c-Jun) immunostaining when present was almost exclusively cytoplasmic, whereas in controls besides predominant cytoplasmic immunostaining, nuclear translocation was often observed in the stratified cuboidal epithelial lining of excretory ducts (Figure 1). When these SG biopsies were probed with an antibody that recognizes phosphorylated and non-phosphorylated forms, we observed that total levels of each transcription factor did not differ between FAP and control groups (Figure 1). The immunostaining of phosphorylated-p53 (*p*-p53) transcription factor was without difference between patients and controls (Figure 1).

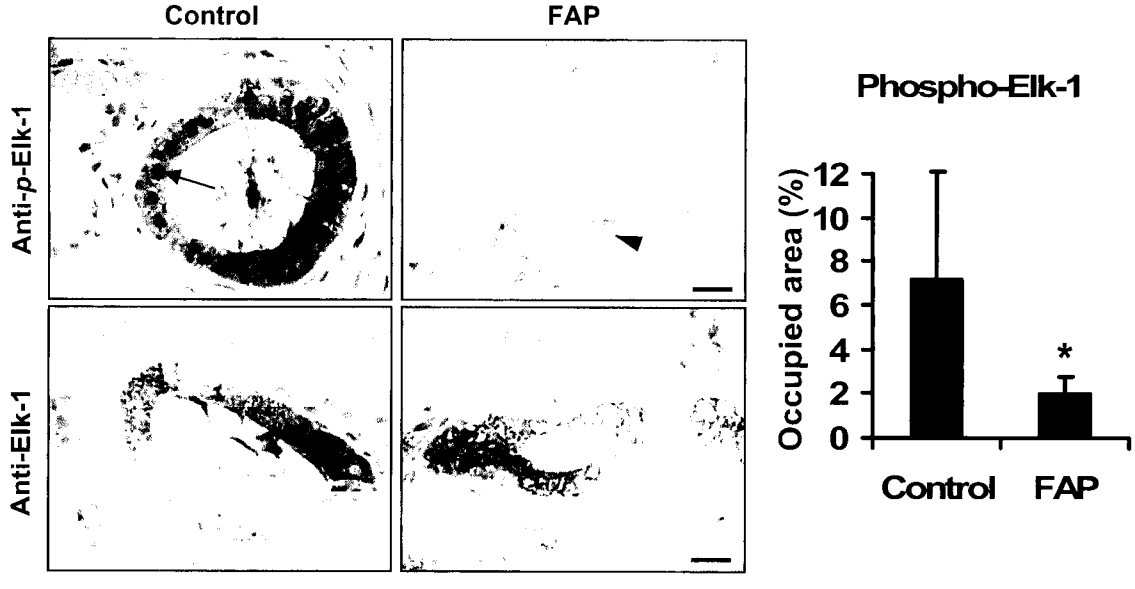

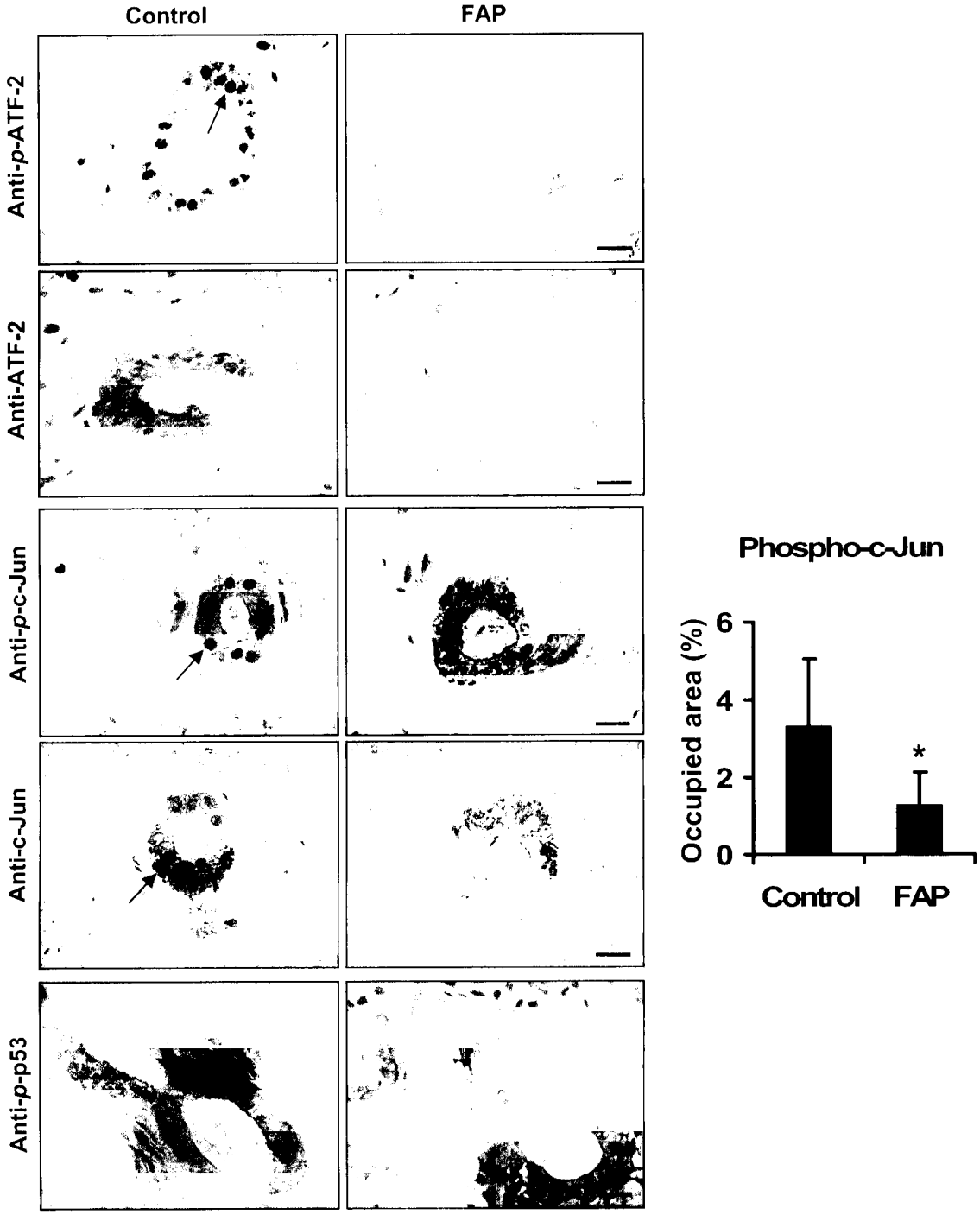

Figure 1. MAPKs-dependent transcription factors expression in FAP SG.
Phospho-Elk-1 (*p*-Elk-1), Elk-1, phospho-ATF-2 (*p*-ATF-2), ATF-2, phospho-c-Jun (*p*-c-Jun), c-Jun and phospho-p53 (*p*-p53) immunohistochemistry of representative SG excretory ducts from control individuals (left panels) and FAP patients (right panels). Arrows, nuclear localization. Arrow heads, cytoplasmic localization. Bar, 20 µm. **Chart (phospho-Elk-1)**, Quantitation of immunohistochemical images of phospho-Elk-1 staining in SG excretory ducts. Data are represented as percentage of occupied area ± SD for SG controls (n=6) and FAP patients (n=6). $^*P < 0.05$. **Chart (phospho-c-Jun)**, Quantitation of immunohistochemical images of phospho-c-Jun staining in SG excretory ducts. Data are represented as percentage of occupied area ± SD for SG controls (n=5) and FAP patients (n=6). $^*P < 0.05$.

STAT3, a transcription factor not related to MAPKs signaling, was described as being induced by cytokines and oxidative stress (Heim 1999), which are known to occur in FAP (Sousa et al. 2001b). However, immnunohistochemical analysis of STAT3 active form (*p*-STAT3) revealed no differences when comparing FAP and control groups (Figure 2).

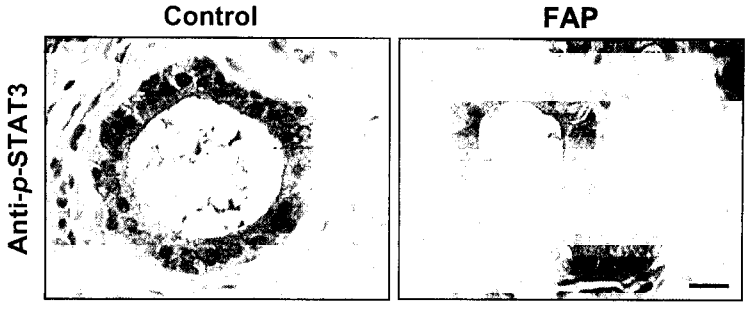

Figure 2. STAT3 expression in FAP SG.
Phospho-STAT3 (*p*-STAT3) immunohistochemistry of representative SG excretory ducts from control individuals (left panel) and FAP patients (right panel). Bar, 20 μm.

Activation of Elk-1 is down-regulated in nerves from asymptomatic carriers

We then performed immunohistochemical analysis for the same transcription factors in FAP nerve biopsies corresponding to an early stage of the disease progression (nerve with TTR deposition but without amyloid deposits), named FAP 0. Previously, we reported that among MAPKs cascades, only MEK-ERK was up-regulated in FAP nerves, displaying specific increase of axonal staining when compared to normal specimens (Monteiro et al. 2006). In the present study we observed that activation of Elk-1 is significantly down-regulated in FAP 0 nerves. Other transcription factors, such as ATF-2 was up-regulated in FAP 0 nerves (Figure 3). The observed immunostaining was almost exclusively axonal. Furthermore, phosphorylated forms of c-Jun and p53 displayed no differences between carriers and control individuals (data not shown).

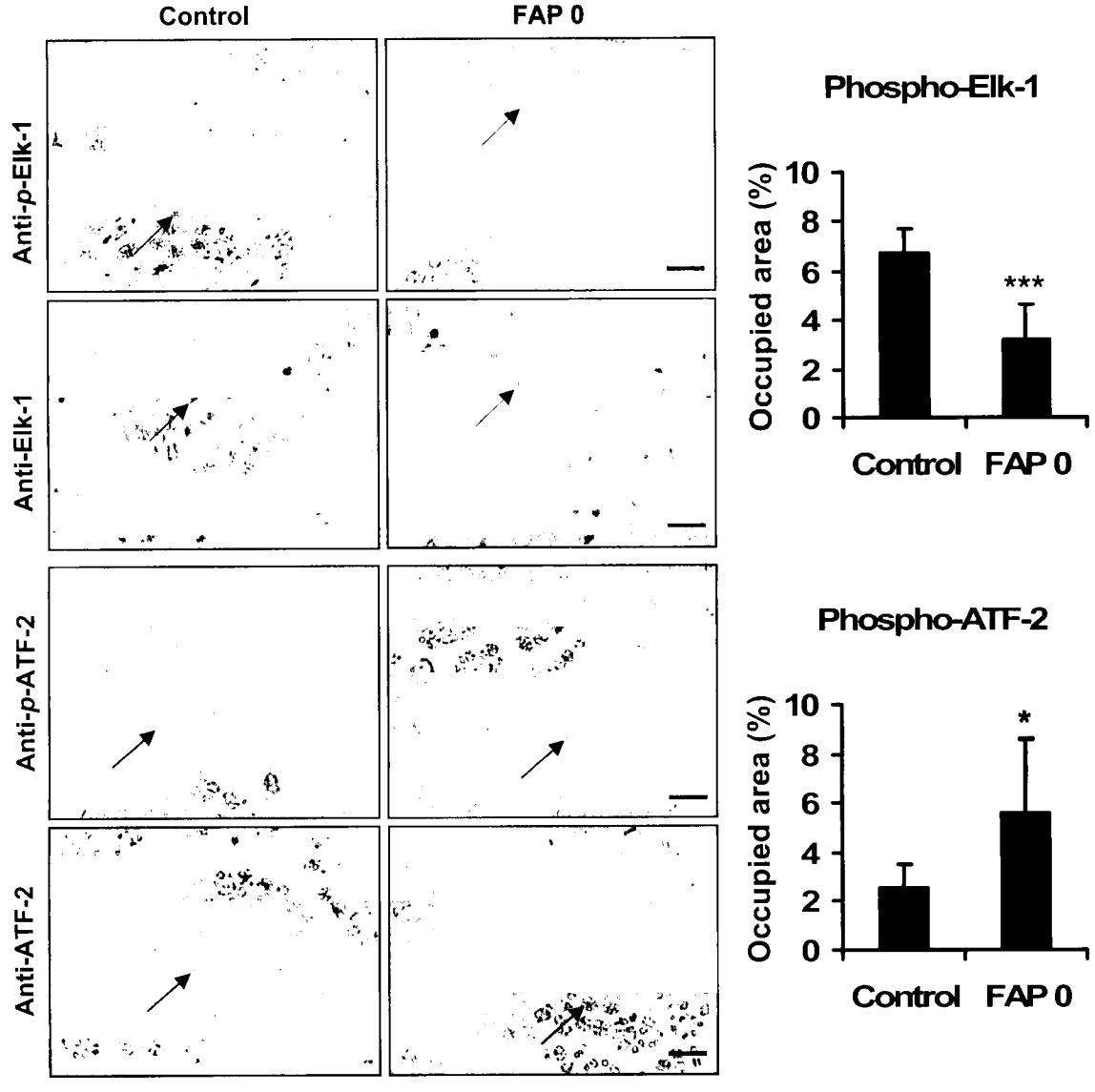

Figure 3. Transcription factors expression in FAP asymptomatic nerves.
Phospho-Elk-1 (*p*-Elk-1), Elk-1, phospho-ATF-2 (*p*-ATF-2) and ATF-2 immunohistochemistry of representative nerves from control individuals (left panels) and FAP 0 carriers (right panels). Arrows, axonal localization. Bar, 15 µm. **Chart (phospho-Elk-1)**, Quantitation of immunohistochemical images of phospho-Elk-1 staining in nerves. Data are represented as percentage of occupied area ± SD for nerve controls (n=7) and FAP 0 carriers (n=8). ***$P < 0.0001$. **Chart (phospho-ATF-2)**, Quantitation of immunohistochemical images of phospho-ATF-2 staining in nerves. Data are represented as percentage of occupied area ± SD for nerve controls (n=6) and FAP 0 carriers (n=9). *$P < 0.05$.

Phosphorylated Elk-1, ATF-2, c-Jun and p53 expression in FAP skins

Immunohistochemical analysis to study the expression of *p*-Elk-1, *p*-ATF-2, *p*-c-Jun and *p*-p53 transcription factors was also performed in FAP skin biopsies either (+/-) or (+/+) (i.e. non-fibrillar TTR/amyloid TTR deposits). None of the active forms of these transcription factors showed any immunohistochemical difference between patient and control skins (data not shown). The skin is a tissue that is exposed to large environmental stresses, therefore, this fact might account for this result.

Discussion

Transcription factors most likely have a crucial role in cell death observed in neurodegenerative diseases. The potential requirement of transcription for proper execution of apoptotic death induced by cytotoxic stimuli, including oxidative stress, led us to search for transcription factors that are activated or inhibited in FAP. These transcription factors might govern the expression balance between putative death and survival proteins towards neuronal cell death, which occurs in FAP.

Currently, NFκB is the only transcription factor known to have increased activation in FAP tissues. *In vitro*, using PC12 cells over-expressing the receptor for advanced glycation end products (RAGE) it was shown a RAGE-dependent activation of NFκB elicited by TTR aggregates (Sousa et al. 2000c; Sousa et al. 2005b). In FAP, TTR-RAGE interaction appears to contribute to NFκB activation, which is likely to induce the observed increased expression of both pro-inflammatory cytokines and RAGE, thereby propagating cytotoxic effects of TTR deposits transduced by RAGE (Sousa et al. 2000c; Sousa et al. 2001b). Activation of NFκB is associated with chronic neurodegenerative disorders such as Alzheimer's, Parkinson's and Huntington's diseases; however, increased NFκB activity has been suggested to represent an early protective response to ongoing oxidative stress, thus having a neuroprotective function (Mattson and Camandola 2001). Therefore, still unknown transcription factors might intervene in FAP neurodegeneration.

Here we studied by semi-quantitative immunohistochemical analysis the activation of transcription factors downstream of MAPKs. We found that activation of Elk-1 is down-regulated in FAP SG and asymptomatic FAP nerves. Elk-1 down-regulation was unexpected, since Elk-1 is one among the downstream targets of ERK1/2, which was shown to have abnormal sustained activation in FAP (Monteiro et al. 2006). It is possible that Elk-1 is not accessible to active ERK1/2 or alternatively the rapid dephosphorylation of Elk-1 by a protein phosphatase might occur. In fact, calcineurin (protein serine/threonine phosphatase 2B) was found to specifically down-regulate the transcriptional activity of Elk-1, following stimulation of this activity by the ERK, JNK or p38 MAPK pathways (Tian and Karin 1999). Calcineurin consists of a catalytic subunit, CnA, and a regulatory subunit, CnB. It is known that cellular calcium (Ca^{2+}) and Ca^{2+}-binding protein calmodulin (CaM) regulate the activities of both CaM-dependent protein kinases (CaM-Ks) and calcineurin. Calcineurin has a narrow substrate specificity comparing to other protein phosphatases. Calcineurin substrates include DARP32 and inhibitor-1, two potent inhibitors of phosphatase 1, NF-AT's (nuclear factor of activated transcription), a family of transcription factors involved in the activation of T-cells, the *N*-methyl-D-

aspartate receptor (NMDA), the IP_3 receptors (Guerini 1997), and Elk-1 (Sugimoto et al. 1997). A functional cooperation between MAPKs and CaM-Ks has also been reported (Tian and Karin 1999). Whether calcineurin is abnormally activated in FAP is unknown. Thus, this hypothesis needs to be addressed in future analyses as this may represent a mechanism to specifically prevent the activation of Elk-1 by TTR deposits but without affecting the other targets of ERK signaling pathway and, therefore, alter cellular responses.

Other transcription factors, such as c-Jun and ATF-2, were differentially activated in FAP depending on the tissue analyzed, despite the absence of JNK and p38 MAPKs activation (Monteiro et al. 2006). The differential activation probably derives from changes in cytotoxicity of TTR deposits according to the tissue analyzed and the stage of disease progression. Thus, these transcription factors may represent tissue specific pathways that will be addressed in the future.

To note that in this study, we have used only asymptomatic FAP nerves (FAP 0), corresponding to an early stage of disease progression, therefore, we do not know what could be the outcome in terms of activation of these transcription factors at latter stages of FAP.

Taken these data together and with the available clinical samples, at this point a scenario involving the interplay between transcription factors is hard to draw. However, these new insights might be pieces of a FAP signaling pathway puzzle waiting for new advances to be put into place. Finally, a more complete understanding of the panoply of transcriptional regulators activated by apoptotic stimuli in neurons may guide attempts to shift the balance of transcriptional activities in favour of survival.

ACKNOWLEDGEMENTS

We thank Dr Barbas do Amaral (Estomatology, Maxillofacial Surgery, Hospital Geral de Santo António, Porto, Portugal) for SG collection, Rossana Correia (Molecular Neurobiology, IBMC) and Rui Fernandes (Advanced Tissue Analysis Facility, IBMC) for tissue processing.

CHAPTER 4

High-Mobility Group Box 1 protein (HMGB1): a Marker of Cytotoxicity in Familial Amyloidotic Polyneuropathy?

High Mobility Group Box 1 protein (HMGB1): a Marker of Cytotoxicity in Familial Amyloidotic Polyneuropathy?

Filipe Almeida Monteiro[1,2] and Maria João Saraiva[1,2]

[1]Molecular Neurobiology, Instituto de Biologia Molecular e Celular, Porto, Portugal; [2]Instituto de Ciências Biomédicas de Abel Salazar, University of Porto, Portugal.

Corresponding author: Maria João Saraiva; Molecular Neurobiology; Instituto de Biologia Molecular e Celular; R. Campo Alegre, 823. 4150-180 Porto, Portugal.

Tel. 351-226074900; Fax 351-226099157. E-mail: mjsaraiv@ibmc.up.pt

Running title: High mobility group box 1 protein in familial amyloidotic polyneuropathy.

Abstract

Familial amyloidotic polyneuropathy (FAP) is an autosomal dominantly inherited disease, characterized by the extracellular deposition of transthyretin (TTR) amyloid fibrils in several organs particularly in the peripheral nervous system (PNS) with progressive distal axonal loss of fibers lading to neuropathy. An increased expression of high mobility group box 1 (HMGB1) protein was recently found in brains of Alzheimer's disease (AD) patients, another amyloid-related disorder. Extracellular HMGB1 was shown to bind and colocalize with amyloid β peptide (Aβ) in senile plaques where it is associated with microglia, inhibiting phagocytosis. In this study we investigated whether HMGB1 is altered in FAP pathology. By immunohistochemical analysis of FAP SG, we found that HMGB1 was located in the cytosol of epithelial cells; by immunoblot analysis, total HMGB1 levels did not differ between control and FAP SG extract pools. In FAP nerves, HMGB1 expression was up-regulated in axons. To access HMGB1 subcellular localization in sensorial neurons, we used dorsal root ganglia (DRG) from a FAP transgenic mouse model. In this model, neuronal cell bodies in DRG affected with TTR deposition revealed HMGB1 up-regulation in the cytoplasm when compared with non-affected DRG. HMGB1 was not detected in serum of FAP patients, whereas it was found in saliva from a small number of FAP patients. Finally, in cell lines treated with TTR cytotoxic species we did not succeed to recapitulate the findings of FAP biopsies, probably due to insufficient noxious stimuli. Taken together, HMGB1 appears to be an early marker for cytotoxicity elicited by deposited TTR in FAP.

Abbreviations: AD, Alzheimer's disease; DRG, dorsal root ganglia; ERK, extracellular signal-regulated kinase; FAP, familial amyloidotic polyneuropathy; HMGB1, high mobility group box 1 protein or amphoterin; JNK, jun amino-terminal kinase; MAPK, mitogen-activated protein kinase; NFκB,: nuclear transcription factor κB; RAGE, receptor for advanced glycation end products; TTR, transthyretin.

Introduction

FAP is an autosomal dominantly inherited disease, characterized by the extracellular deposition of TTR amyloid fibrils particularly in the PNS leading to a progressive neuropathy ultimately resulting in sensory and autonomic dysfunction as a consequence of axonal loss (Coimbra and Andrade 1971b, 1971a). TTR aggregates and amyloid fibrils deposit throughout the connective tissue of several organs, and in the nerve, mainly in the endoneurium in proximity of blood vessels and near Schwann cells and collagen fibrils (Coimbra and Andrade 1971b, 1971a). It is of major importance the search of markers of cytotoxicity associated with this disorder to sought possible new therapeutical approaches besides liver transplantation, the only known treatment for FAP.

In AD, another amyloid-related disorder, HMGB1 is increased and associated with senile plaques (Takata et al. 2003). In addition, it was suggested that HMGB1 release from dying neurons may inhibit microglial amyloid-β (Aβ) peptides clearance and enhance Aβ neurotoxicity (Takata et al. 2003; Takata et al. 2004). Currently, it is not known whether HMGB1 plays a role in FAP neurodegeneration.

HMGB1 was characterized as a 30 kDa, abundant, non-histone nuclear protein, which is expressed in almost all eukaryotic cells and is highly conserved in evolution (99% identity in mammals) (Muller et al. 2004). Structurally, HMGB1 consists of 125 residues organized in two DNA-binding domains, the A and B HMG boxes, and a negatively charged C-terminus (Bianchi and Manfredi 2004). Nuclear HMGB1 is important for regulation of transcription by enabling physical interactions between DNA and various factors, such as p53, nuclear transcription factor κB (NFκB), homeobox-containing proteins, recombinant-activating gene 1/2 (RAG1/2) proteins and steroid hormone receptors (Bianchi 2004). *Hmgb1* gene-knockout mice die of hypoglycaemia shortly after birth indicating that nuclear functions of HMGB1 are essential (Calogero et al. 1999). Phenotypic features include small size, long hind paws and absence of fat. In addition to the nuclear location, some cells display HMGB1 on the plasma membrane. Membrane-associated HMGB1, also referred to as amphoterin (Huttunen and Rauvala 2004), is involved in the mediation of neurite outgrowth (Parkkinen et al. 1993), smooth muscle cell chemotaxis (Degryse et al. 2001) and tumour cell metastasis (Taguchi et al. 2000). There are two ways by which HMGB1 can be released into the extracellular environment. One is a passive process where biologically active HMGB1 is released from cells undergoing necrosis (Scaffidi et al. 2002); the other is an active process in cells of the innate immune system that occurs after HMGB1 acetylation in the nucleus followed by cell secretion (Gardella et al. 2002; Bonaldi et al. 2003). HMGB1 released from necrotic cells evokes inflammatory responses

both *in vitro* and *in vivo*; in contrast, apoptotic cells sequester HMGB1 in the nucleus preventing its release (Scaffidi et al. 2002). Active release of HMGB1 from monocytes or macrophages occurs in response to injury, infection or other inflammatory stimuli, such as cytokines (i.e. tumor necrosis factor α (TNFα), interleukin-1β (IL-1β) and interferon-γ) (Wang et al. 1999; Bonaldi et al. 2003). HMGB1 continually traffics between nucleus and cytosol (Bonaldi et al. 2003) and upon inflammatory stimuli, acetylation of HMGB1 occurs at lysine residues, which prevents its re-entry to the nucleus (Bonaldi et al. 2003; Lotze and Tracey 2005). Subsequently, acetylated HMGB1 is packed into cytoplasmic secretory lysosomes, which are exocytosed when cells receive a second signal, i.e. ATP or lysophosphatidylcholine (LPC), a lipid generated at inflammation sites (Gardella et al. 2002; Rendon-Mitchell et al. 2003).

HMGB1 has been reported to transduce signals through receptor for advanced glycation end products (RAGE) (Hori et al. 1995; Huttunen et al. 1999) and other multiligand receptors, such as Toll-like receptor 2 (TLR2) and TLR4 (Park et al. 2004). Nevertheless, it was suggested that other unknown receptors may intervene, since many functions of HMGB1 are not related to the interaction with known receptors (Lotze and Tracey 2005).

Signaling transduced by HMGB1 and TTR aggregates binding to RAGE have in common the activation of extracellular signal-regulated kinase 1/2 (ERK1/2) and NFκB, and the induction of cytokine expression, namely TNFα (Sousa et al. 2000c; Sousa et al. 2001b; Park et al. 2003; Monteiro et al. 2006). Given that signal transduction through RAGE is believed to play a detrimental role in FAP pathogenesis we questioned whether HMGB1 could be amplifying the cytotoxic effects of extracellular TTR aggregates.

In this study, we investigated the changes of HMGB1 protein levels in both biopsies (i.e. nerve and SG) and fluids (i.e. serum and saliva) from FAP patients and in DRG of a FAP transgenic mouse model. *In vitro* using Schwannoma and neuronal cell lines we sought to characterize HMGB1 subcellular location upon cell treatment with TTR cytotoxic species.

Materials and methods

Subjects

Labial minor SG biopsies were obtained from V30M FAP patients prior to performing liver transplantation. Control SG were from age- and gender-matched non-FAP volunteer individuals that had no evidence of infection. The collection of biopsies material was approved by the ethical committee of Hospital Geral de Santo António, Porto, Portugal, and participants were volunteers. SG collection and characterization was previously described (Sousa et al. 2005b). For protein extracts, SG were collected and immediately frozen at -80ºC until usage. For immunohistochemical analysis, SG were collected in 4% paraformaldehyde in phosphate-buffered saline (PBS). The general characterization of SG consisted of TTR immunohistochemistry and analysis for the presence of amyloid deposits by Congo red staining. SG biopsies from controls (n=6), FAP 0 (SG with TTR deposition but without amyloid deposits; n=4) and FAP patients (SG with TTR deposition along with amyloid deposits; n=6) were used for immunohistochemical analysis. Sural nerve biopsy specimens from FAP patients, asymptomatic carriers (FAP 0) and controls (near relatives of FAP patients who ultimately turned out not to have mutations in TTR) were available at the Hospital Geral de Santo António, Porto, Portugal, since this material was obtained as part of the clinical diagnosis and evaluation of FAP, prior to the current use of molecular diagnostic methods. Skin biopsies from control (n=9), FAP 0 (n=5) and FAP patients (n=4) were available at the Hospital Geral de Santo António, Porto, Portugal. Serum was available from control individuals (n=3) and TTR V30M heterozygotic carriers either asymptomatic (n=3) or symptomatic FAP patients (n=3). Saliva was collected from FAP patients (n=3) and control volunteers (n=3) and immediately frozen at -80ºC until usage. Subsequently, salivas were defrosted on ice and a final concentration of 1 mM PMSF was added. Salivas were then centrifuged at 11,000 *g* for 10 min at 4ºC and total protein in the supernatant was quantified with the Bio-Rad protein assay. Next, salivas were concentrated to ~2 mg/mL prior to Western blot analysis.

Animals

Transgenic mice bearing the human TTR V30M in a TTR and heat shock transcription factor 1 (HSF1) double-knockout background (Santos 2005; Santos and Saraiva 2005) with TTR deposition in the DRG were compared to age-matched mice (6-12 months of age) without TTR deposition in DRG. Presence or absence of TTR deposition was assessed by TTR immunohistochemistry of DRG paraffin sections as previously described (Santos 2005).

Immunohistochemistry

For immunohistochemical analysis, paraffin sections were deparaffinated, hydrated in a modified alcohol series, antigens were unmasked by microwaving in 10 mM sodium citrate buffer pH 6.0, endogenous peroxidase activity was blocked with 3% hydrogen peroxide in methanol for 15 min and incubated in blocking buffer (4% fetal bovine serum (FBS) and 1% bovine serum albumin (BSA) in PBS) for 30 min at 37°C in a moist chamber. Incubation with primary antibody, at the appropriate dilution in blocking buffer, was performed overnight at 4°C in a humidified chamber. Primary antibody was rabbit polyclonal anti-HMGB1 (1:100 for nerve, SG, skin and DRG), purchased from BD Biosciences Pharmingen. On parallel control sections, primary antibody was replaced by blocking buffer alone. Antigen visualization was performed with biotin-extravidin-peroxidase kits (Sigma), using 3-amino-9-ethyl carbazole (Sigma) as substrate. Semi-quantitative immunohistochemistry (SQ-IHC) analysis was performed using Scion Image software (freely downloaded from the Scion Corporation website). This application enables the measurement of the area occupied by pixels corresponding to the immunohistochemical substrate color that is normalized relatively to the total area. Each slide used in the SQ-IHC was analyzed in 5 different representative areas. Results shown represent % occupied area (± SD). For statistical analysis, group values, expressed as the mean ± SD, were compared by Student's *t* test, and *P* values of less than 0.05 were considered significant.

SG preparation

SG protein extracts were obtained by homogenizing SG biopsies into 2 pools of either normal controls (n=4) or FAP patients (n=6) in extraction buffer (Sigma # E 0655). Following homogenization, SG extracts were centrifuged at 11,000 *g* for 10 min at 4°C and protein in the supernatant was quantified with the Bio-Rad protein assay.

Immunoblots

Samples were loaded in 15% SDS-PAGE and transferred to nitrocellulose Hybond-C Extra (Amersham Biosciences) using a semidry transfer system. Blots were incubated with blocking buffer [5% nonfat dried milk in Tris-buffered saline (TBS) with 0.1% tween-20 (T)] for 1 h at room temperature (RT). Subsequently, incubation with primary antibodies, at the appropriate dilution, was performed overnight at 4°C in 5% BSA/TBS-T. The primary antibodies used were rabbit polyclonal anti-HMGB1 (1:2000), purchased from BD Biosciences Pharmingen, and mouse monoclonal anti-β-actin (1:5000) from Sigma. After

incubation with secondary sheep anti-rabbit IgGs horseradish peroxidase conjugate (1:5000) (The Binding Site) or goat anti-mouse IgG horseradish peroxidase conjugate (Pierce) in 1% nonfat dried milk TBS-T for 30 min at RT, blots were developed using the SuperSignal West Pico Chemiluminescent Substrate kit (Pierce) and exposed to Hyperfilm ECL (Amersham Biosciences).

Preparation of TTR species

Recombinant wild-type (wt) TTR was produced in an *E. coli* expression system and purified as previously described (Almeida et al. 1997). Purified soluble TTR was detoxified using Endotoxin Removing Gel (Pierce, Rockford, IL, USA). For preparation of TTR aggregates, TTR was dialyzed against water, pH 7.0, and then incubated with 0.05 M sodium acetate, pH 3.6, for 48 h at RT. The preparation was then centrifuged at 15,000 *g* for 30 min, the pellet washed and resuspended in filtered PBS, pH 7.4. TTR oligomers were produced under aseptic conditions by agitating soluble wt TTR (0.25 mg/mL) with a magnetic stirrer at 500 rpm for 7 days at RT. Protein concentrations were determined by the Lowry method (Lowry et al. 1951). TTR aggregates are composed of short fibrils and amorphous aggregates as assessed by ultrastructural analysis (Cardoso et al. 2002). TTR aggregates and oligomers were positive by Thioflavin T spectrofluorometric assays.

Cell culture assays

RN22 (rat Schwannoma cell line) and ND7/23 (mouse neuroblastoma x rat neurone hybrid) cells were from the European Collection of Cell Cultures. RN22 and ND7/23 cells were propagated in 25 cm^2 dishes in monolayer and maintained at 37°C in a 95% humidified atmosphere and 5% CO_2. Cells were grown in Dulbecco's minimal essential media (DMEM) (Gibco, Rockville, MD, USA) supplemented with 10% FBS (Gibco), 2 mM glutamine (Sigma) and 100 U/mL penicillin/streptavidin (Gibco) (complete media). For immunofluorescence, cells (either RN22 or ND7/23) were grown on a lab-tek chamber slide (Nalgene Nunc International) in complete media. For cell fractionation, ND7/23 cells were grown in 25 cm^2 flasks in complete media. When cells reached ~50% confluence they were incubated for 20h in assay media (DMEM containing either 1% or 2% of dialyzed FBS, for RN22 or ND7/23 cells, respectively) with 2 μM of either soluble, aggregated or oligomeric TTR. Conditioned media was collected after treatment, for assessment of secreted HMGB1. Briefly, conditioned media samples were supplemented with 1 mM PMSF and centrifuged at 3,000 *g* for 5 min at 4°C. Resulting supernatants were centrifuged at 16,000 *g* for 20 min at 4°C. Subsequently, supernatants were concentrated 50 times using Microcon YM-10 (Milipore) to a final volume of 40 μL and 12.5 μL of 4x

SDS sample buffer was subsequently added. After boiling, 5 µL was loaded per lane in a 15% SDS-PAGE gel.

Fluorescence immunocytochemistry

After treatment, RN22 and ND7/23 cells were fixed on a lab-tek with 4% paraformaldehyde in PBS for 10 min at RT. Next, fixed cells were permeabilized with 0.2% triton X-100 for 5 min at RT and quenched in fresh 0.1% sodium borohydrate in PBS for 5 min. Subsequently, lab-teks were washed in PBS and incubated in blocking buffer (4% FBS and 1% BSA in PBS) for 30 min at 37°C. Incubation with rabbit polyclonal anti-HMGB1 (1:1000; BD Biosciences Pharmingen) in blocking buffer was performed overnight at 4°C. After washing twice with PBS for 15 min, slides were incubated with donkey anti-rabbit IgG Alexa Fluor 488 (1:1000) in blocking buffer was incubated for 30 min at RT, in the dark. Next, slides were washed with PBS, mounted with vectashield with DAPI (Vector), and visualized in a Zeiss Cell Observer System (Carl Zeiss, Germany) equipped with a filter for FITC like dye.

Cell fractionation

Cytosolic and nuclear subcellular fractionation was performed after treatment of ND7/23 cells with TTR species. Briefly, cells were washed twice with ice-cold PBS, scraped into 0.5 mL of PBS and centrifuged at 15,000 *g* for 5 min at 4°C. Cell pellets were resuspended in 0.25 mL of buffer A (10 mM Tris-HCl, pH 7.6, 1.5 mM $MgCl_2$, 10 mM KCl, 0.5 mM DTT, 0.5 mM PMSF) and incubated on ice for 10 min. Then samples were gently lysed with a dounce homogenizer performing 50 strokes and centrifuged at 2,300 *g* for 5 min at 4°C. Supernatants consisting of the cytoplasmic fraction were saved. The pellets were completely resuspended in 0.1 mL of buffer B (20 mM Tris-HCl, pH 7.6, 25% glycerol, 0.3 M NaCl, 1.5 mM $MgCl_2$, 0.2 mM EDTA, 0.5 mM DTT, 0.5 mM PMSF) and incubated for 30 min at 4°C under gentle agitation. Subsequently, nuclear lysates were centrifuged at 9,300 *g* for 15 min at 4°C and supernatants were collected and saved as the nuclear fraction. Cytoplasmic and nuclear fractions were subjected to immunoblot analysis as described above, after total protein quantification by the Bio-Rad method.

Results

Translocation of HMGB1 to the cytoplasm in FAP

To test the hypothesis that HMGB1 is released into the extracellular space, we performed HMGB1 SQ-IHC in FAP SG biopsies. Despite the similar amount of immunostaining, the pattern of subcellular localization differed between control, FAP 0 and amyloid laden FAP SG. The later displayed predominant staining in the cytoplasm of the stratified cuboidal epithelial lining of excretory ducts, whereas in control SG staining was similar in the cytoplasm and nucleus and/or predominantly nuclear (Figure 1A, upper panels). In the case of the FAP 0 stage, we analyzed a total of 4 samples in which 2 had predominant HMGB1 staining in the cytoplasm and the other 2 had cytoplasmic along with nuclear staining (Figure 1A, upper-middle panel). Thus, FAP 0 may represent a transition phase between the predominant nuclear localization observed in controls towards predominant cytoplasmic staining in excretory ducts of later FAP stages. Immunoblot analysis of SG extracts confirmed the immunohistochemical observation that the total amount of HMGB1 protein did not differ between control and FAP SG, as documented in figure 1B. We then performed HMGB1 immunohistochemical analysis in FAP nerve biopsies corresponding to different stages of disease progression. FAP nerves showed an up-regulation of HMGB1 expression in axons when compared to controls; however the increase was only significant for asymptomatic carriers (FAP 0) (Figure 1A, lower panels and chart). The apparent decrease of HMGB1 in FAP nerves compared with FAP 0 most likely derives from severe loss of nerve fibers at this later stage of the disease (Figure 1A, lower panels and chart). In addition to axons, which were the main cellular structure presenting immunostaining, we could also observe nuclear staining of Schwann cells and endothelia of blood vessels that did not differ among the analyzed groups. To note that immunohistochemical analysis of skin biopsies showed that HMGB1 staining in FAP 0 and FAP did not differ from controls (data not shown). Taken together, the human nerve and SG data suggest that HMGB1 translocates from the nucleus to the cytoplasm in FAP tissues; extracellular HMGB1 was not evident.

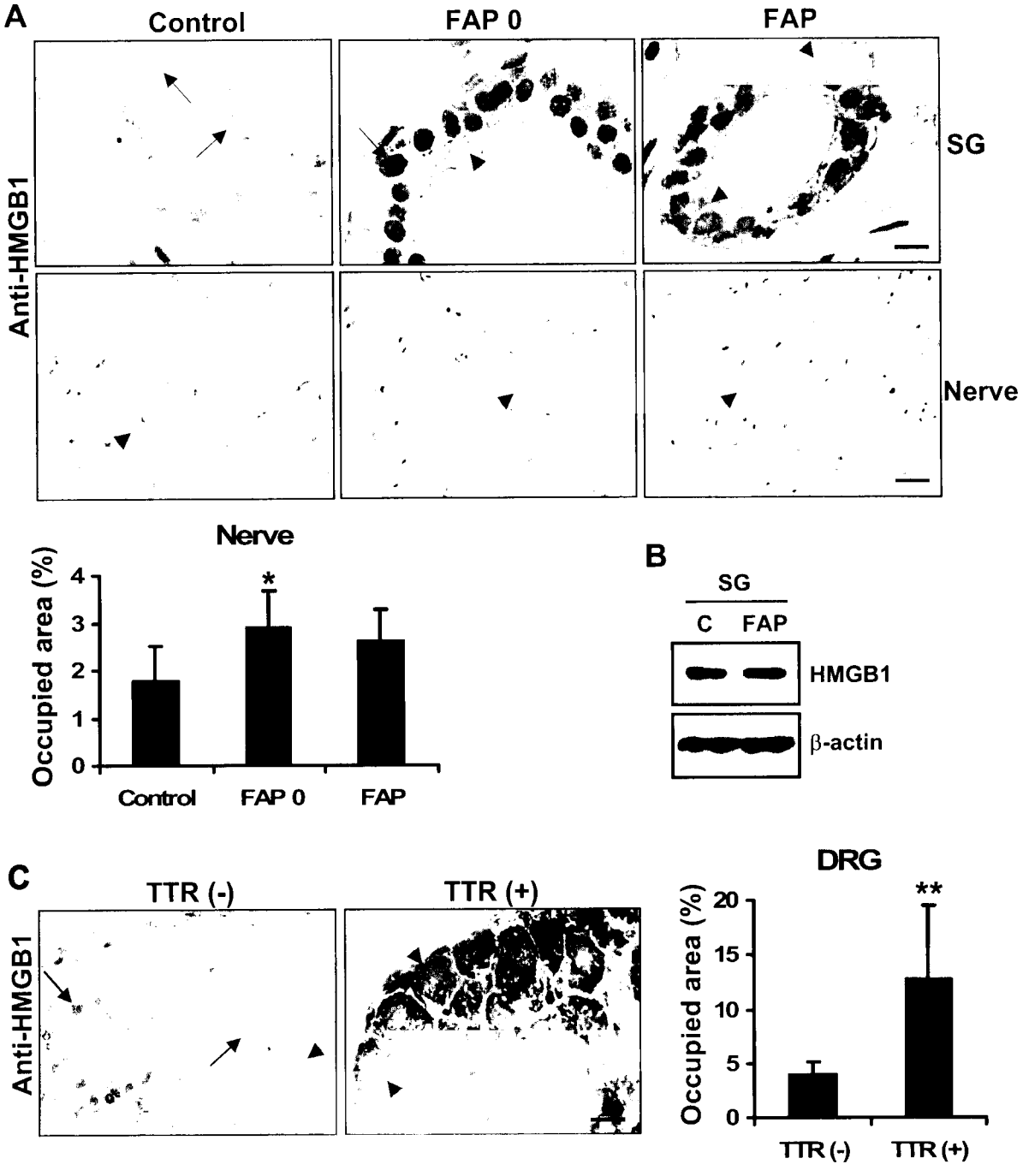

Figure 1. HMGB1 expression in FAP.
A, HMGB1 immunohistochemistry of representative SG (upper panels) and nerves (lower panels) from control individuals (left panels), FAP 0 (middle panels) and FAP patients (right panels). Arrows, nuclear localization. Arrow heads, cytoplasmic translocation. Bar (SG), 10 μm. Bar (Nerve), 20 μm. **Chart (Nerve)**, Quantification of immunohistochemical images of HMGB1 staining in human nerves. Data are represented as percentage of occupied area ± SD for nerve controls (n=5), FAP 0 (n=6) and FAP patients (n=6). *$P < 0.05$ compared to control group. **B**, HMGB1 expression in human SG lysates. Immunoblots representing expression of HMGB1 (top lane) and β-actin (bottom lane) in SG pool extracts from control and FAP individuals. 40 μg of total protein was loaded per lane. **C**, HMGB1 immunohistochemistry of representative DRG from human TTR V30M mice either negative (TTR (-), left panel) or positive (TTR (+), right panel) for TTR deposition. Arrows, nuclear localization. Arrowheads, cytoplasmic localization. Bar, 20 μm. **Chart (DRG)**, Quantification of immunohistochemical images of HMGB1 staining in mouse DRGs. Data are represented as percentage of occupied area ± SD for mouse DRGs either negative (TTR (-); n=5) or positive (TTR (+), n=7) for human TTR deposition. **$P < 0.02$.

As access to FAP DRG is nearly impossible, we used DRG from a FAP transgenic mouse model that expresses human TTR V30M in a TTR and HSF1 double-knockout background to analyze HMGB1 subcellular location in neuronal cell bodies. These mice, besides presenting TTR deposition in distinct organs and in the PNS, also display inflammatory and oxidative stress in the PNS, similarly to what is observed in FAP asymptomatic carriers (Santos 2005; Santos and Saraiva 2005). By comparative immunohistochemical analysis of age-matched mice with and without TTR deposition, we found an approximately 3-fold increased expression of HMGB1 in DRG neurons of animals affected with TTR deposition (Figure 1C and chart). These DRG presented a strong HMGB1 immunostaining that was almost exclusively cytoplasmic in neuronal cell bodies, whereas DRG without TTR deposition presented much fainter immunostaining that when present occurred both in the nucleus and cytoplasm of cell bodies. This result correlates with the observed up-regulation of HMGB1 expression in axons of human FAP nerves.

Assessment of HMGB1 secretion in FAP fluids

It was previously reported that serum HMGB1 was significantly increased in sepsis patients when compared with healthy individuals (Wang et al. 1999). So, we questioned whether higher levels of serum HMGB1 could be detected in FAP patients. However, we did not detect HMGB1 in asymptomatic and symptomatic FAP or control sera (Figure 2A). Interestingly, we found secreted HMGB1 in two out of three saliva samples from FAP patients, which was absent in control individuals (Figure 2B). This finding suggests that cytoplasmic translocation of HMGB1 observed in epithelial cells of excretory ducts from FAP SG biopsies might result in HMGB1 release into the lumen of excretory ducts, being then released in the saliva.

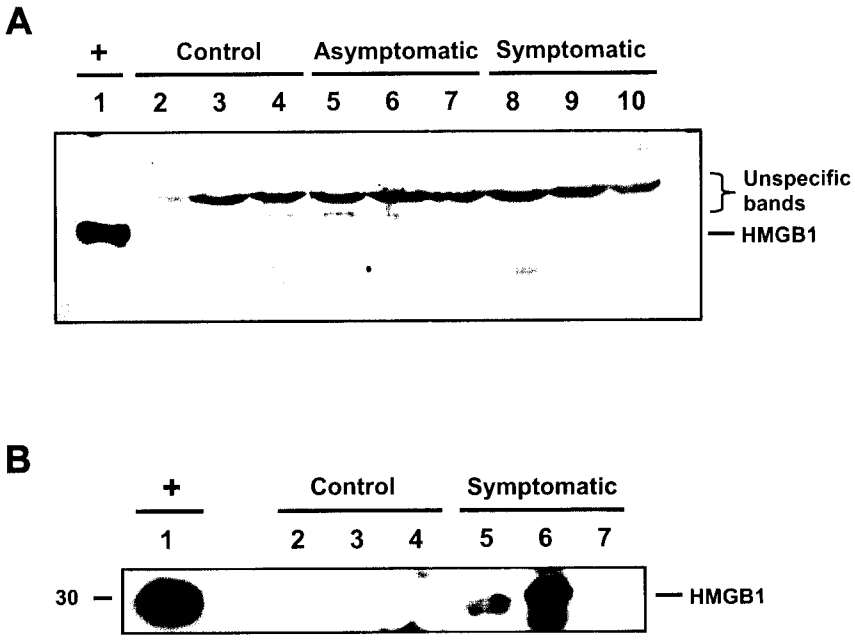

Figure 2. Analysis of HMGB1 secretion in FAP fluids.
A, Serum samples from controls (lanes 2-4), asymptomatic carriers (lanes 5-7) and symptomatic FAP patients (lanes 8-10) were subjected to immunoblot analysis to assess the presence of HMGB1. 10 µL of serum were loaded per lane. **B**, Saliva samples from controls (lanes 2-4) and symptomatic FAP patients (lanes 5-7) were subjected to immunoblot analysis to assess the presence of HMGB1. 50 µg of total protein were loaded per lane. + (lane 1): ND7/23 cell lysate sample as an immunoblot positive control was loaded.

Expression of HMGB1 in cell lines exposed to cytotoxic TTR species

We posed the question whether cytotoxic TTR species could promote RN22 and/or a ND7/23 cell lines to relocate HMGB1 to the cytoplasm. Immunofluorescence analysis of both RN22 (data not shown) and ND7/23 cells after prolonged exposure to cytotoxic TTR species (aggregates or oligomers) showed no alteration in HMGB1 nuclear localization (Figure 3A). Subsequently, we performed the same experiment using ND7/23 cells and assessed HMGB1 levels in nuclear and cytoplasmic fractions, and conditioned media. Immunoblot analysis showed no differences of HMGB1 expression in nuclear and cytoplasmic extracts (Figure 3B), as well as in corresponding conditioned media (data not shown). To note that equal amounts of total protein were loaded in each lane as shown by β-actin immunoblot of cytoplasmic and nuclear extracts. In summary, we did not succeed to recapitulate in cellular assays the translocation and/or over-expression of HMGB1 in the cytosol observed in FAP biopsies.

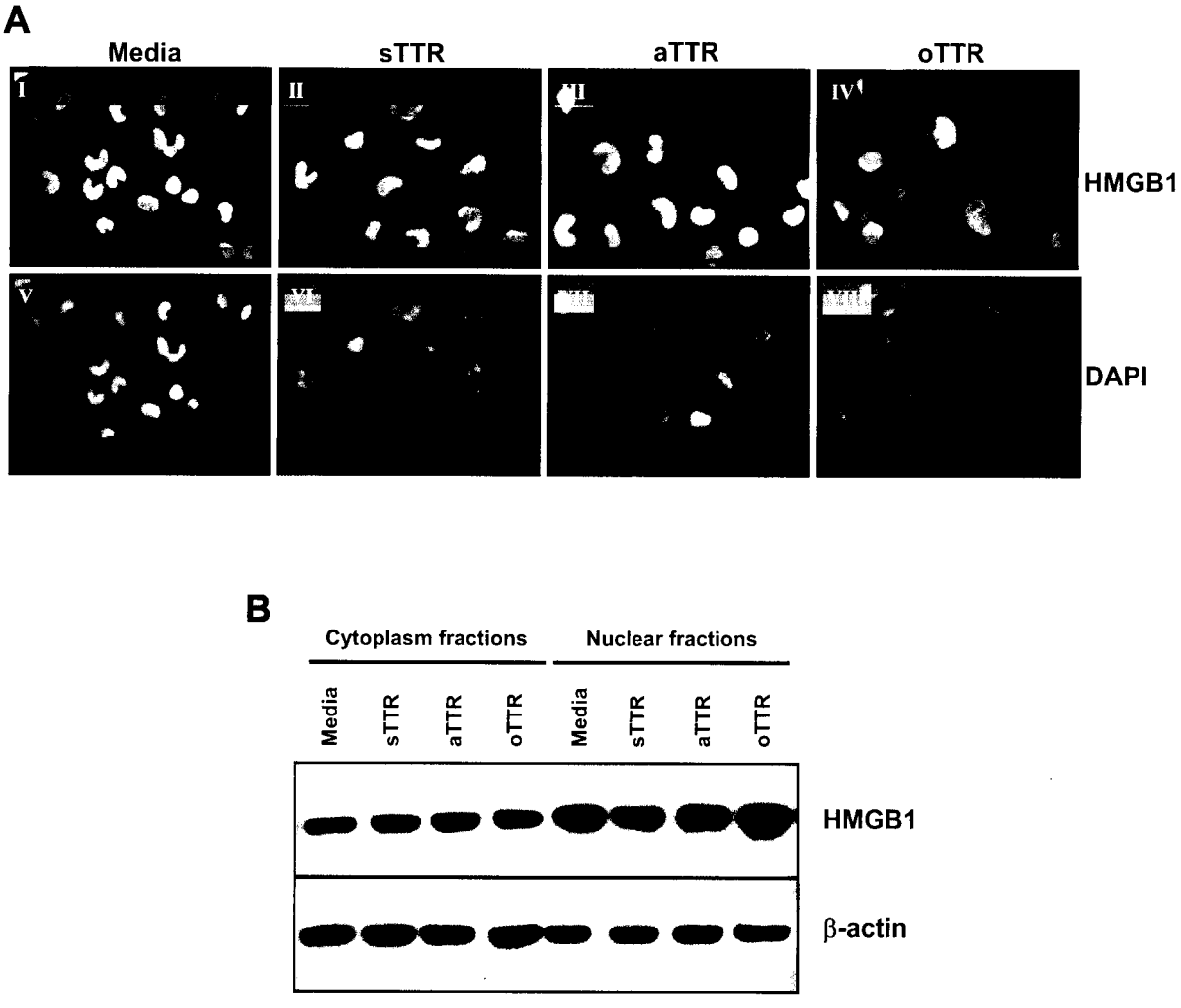

Figure 3. HMGB1 subcellular localization in ND7/23 cells exposed to TTR species.
A, Immunofluorescent labelling of HMGB1 (panels I–VIII; green) in ND7/23 cells either non-treated (I and V) or treated with 2 μM soluble TTR (II and VI) or 2 μM aggregated TTR (III and VII) or 2 μM oligomeric TTR (IV and VIII) for 20 h. DAPI-stained nuclei (panels V-VIII; blue). **B**, Immunoblots representing expression of HMGB1 (top lanes) and β-actin (bottom lanes) in ND7/23 cell lysates from cytoplasm and nuclear fractions. ND7/23 cells were either non-treated (Media) or treated with 2 μM soluble TTR (sTTR), 2 μM aggregated TTR (aTTR) or 2 μM oligomeric TTR (oTTR) for 20 h. 10 μg of total protein was loaded per lane.

Discussion

Recently, extracellular HMGB1 was found associated with senile plaques in the brains of AD patients (Takata et al. 2003; Takata et al. 2004). It was previously shown that extracellular HMGB1 signals through cell surface RAGE leading to the activation of several responses, depending on the cell type: inflammatory cells are activated, stem cells proliferate, and several cell types migrate towards the source of HMGB1 (Bianchi and Manfredi 2004). RAGE is a multiligand receptor that binds β-sheet fibrils composed of subunits such as Aβ, TTR, among others (Sousa et al. 2000c; Schmidt et al. 2001). In the view that different amyloid related disorders can be underlined by a common mechanism, we investigated whether HMGB1 is associated with TTR amyloid fibril deposits in FAP clinical samples. Immunohistochemical analysis for HMGB1 localization showed that HMGB1 is not concentrated in the extracellular milieu of both SG and nerves biopsies. Instead, we visualized a progressive HMGB1 relocation from the nucleus to the cytosol in the epithelial cells of excretory ducts during the course of FAP, in contrast to the predominant nuclear localization observed in controls. This change in the subcellular location was not accompanied by changes in HMGB1 expression levels (as shown by immunohistochemistry and immunoblot analysis of SG). Strikingly, we found HMGB1 in saliva of some FAP patients (2 out of 3) suggesting that HMGB1 is indeed secreted extracellularly into the excretory ducts of SG. FAP nerves, at early asymptomatic stages (FAP 0) displayed an increased expression of HMGB1 in axons, showing that FAP neurons have increased HMGB1 in the cytosol when compared to controls. HMGB1 was also up-regulated in axons of symptomatic nerves, although not statistically significant probably due to severe loss of nerve fibers at this later stage of the disease. In fact, this observation in human FAP nerves was reinforced with the analysis of DRG neurons from a FAP transgenic mouse model where HMGB1 expression was ~3-fold up-regulated in cell bodies of neurons located in DRG affected with TTR deposits as compared with DRG without TTR deposits. To note that HMGB1 was almost exclusively located in the cytoplasm of DRG neurons. Our cell studies *in vitro* did not succeed to recapitulate the HMGB1 relocation observed in FAP tissues, possibly due to insufficient noxious stimuli, duration of treatment or cell type used.

HMGB1 has been shown to be released extracellularly in two different ways: either by active secretion from living inflammatory cells or by passive release from necrotic cells (Erlandsson Harris and Andersson 2004). Recently, the mechanism through which monocyte cells relocate HMGB1 from the nuclei to the cytoplasm was demonstrated: activation by inflammatory signals shifts the balance towards chromatin acetylation, and

HMGB1 becomes hyperacetylated (Bonaldi et al. 2003). *In vitro*, HMGB1 can be acetylated by the most abundant histone acetyltransferases (HATs) and it was suggested that monocytic cells respond to pro-inflammatory stimuli by shifting the acetylation/deacetylaton balance in favour of acetylation (Bonaldi et al. 2003). Acetylation of two specific clusters of lysines interferes with nuclear import signals, but not with nuclear export, and HMGB1 is accumulated in the cytoplasm into secretory lysosomes, which are then exocytosed (Gardella et al. 2002). However, it is not known how developing neurons secrete HMGB1, since these contain no secretory lysosomes (Bianchi and Manfredi 2004). In biological settings of chronic inflammation, active NFκB recruits HATs and induce histone acetylation at NFκB-response regulatory elements leading to chromatin remodelling and induction of gene transcription (Adcock et al. 2004). In addition, oxidative stress activates MAPKs (i.e. ERKs, JNKs and p38 kinases) and the redox-sensitive transcription factor NFκB resulting in the expression of pro-inflammatory mediators through the activation of HAT and inhibition of histone deacetylase (HDAC) activity (Rahman et al. 2004). Thus, it is conceivable that ongoing oxidative stress and up-regulation of pro-inflammatory cytokines in conjunction with abnormal activation of ERK/MAPK and NFκB pathways observed during FAP progression (Sousa et al. 2001b; Monteiro et al. 2006) might tilt the acetylation/deacetylation balance in favour of acetylation; therefore, HMGB1 relocation to the cytosol might derive from a more general acetylation wave. We tried to immunoprecipitate HMGB1 protein from SG samples and subsequently perform an immunoblot with anti-acetyl-lysines antibody to assess HMGB1 acetylation level in FAP SG; however, we did not succeed to immunoprecipitate HMGB1.
The molecular mechanisms leading to FAP neurodegeneration are largely unknown. We propose that chromatin remodelling towards acetylation might control gene expression in FAP, a hypothesis to be further tested. At any rate, HMGB1 translocation to the cytoplasm of DRG neurons and epithelia in excretory ducts of SG appears to be a marker of TTR deposit-induced cytotoxicity in FAP; furthermore, released HMGB1 in saliva might be useful to assess the level of dysfunction in SG of FAP patients.

ACKNOWLEDGEMENTS

We thank Dr Barbas do Amaral (Estomatology, Maxillofacial Surgery, Hospital Geral de Santo António, Porto, Portugal) for SG collection.

We are grateful to Rui Fernandes (Advanced Tissue Analysis Facility, IBMC, Porto, Portugal) and Rossana Correia (Molecular Neurobiology, IBMC) for tissue processing, and Sofia Santos (Molecular Neurobiology, IBMC) for providing DRG paraffin sections already characterized for the deposition of TTR.

GENERAL DISCUSSION

AND

PERSPECTIVES

General discussion and future perspectives

Although TTR has an intrinsic propensity to self assemble into amyloid fibrils, amyloidogenic mutations facilitate this process probably due to TTR tetramer dissociation into partial unfolded intermediates. These intermediates are thought to aggregate into non-fibrillar aggregates and protofibrils that will grow and form amyloid fibrils, the hallmark of amyloid-related disorders. TTR amyloidogenesis is considered a dynamic process that is believed to be facilitated by other factors, such as SAP and proteoglycans (PGs), which are universal components of amyloid deposits *in vivo*.

In this regard, we found up-regulation of chondroitin sulfate PGs (CSPGs) expression in amyloid laden SG from FAP patients. CSPGs might play a dual role in FAP by facilitating TTR amyloidogenesis and/or tissue-specific deposition and by participating together with other ECM-related proteins (i.e. biglycan, NGAL) as both pro- and anti-inflammatory mediators in the inflammation process (see figure 1). One therapeutical approach currently under investigation for inhibiting amyloid fibril formation is the use of glycosaminoglycans (GAGs) mimetics. These are small molecules that compete with GAGs for interacting with amyloidogenic precursors and fibrils and thereby inhibit fibril formation and tissue deposition (Dember 2005). It would be interesting to test this therapeutical strategy in our FAP animal models in the case that CSPGs role in FAP amyloidogenesis is confirmed.

Recently, Sousa et al. (2001a) provided evidence for the presence of toxic non-fibrillar TTR aggregates in FAP nerves prior to the appearance of amyloid fibrils and nerve fiber degeneration. At this stage (asymptomatic), nerves already display signs of inflammatory (i.e. TNFα, IL-1β and M-CSF) and oxidative stress (i.e. tyrosine nitration of proteins), which were sustained or even augmented throughout the course of the disease, where toxic aggregates co-exist with amyloid fibrils. Two mechanisms have been proposed to neurotoxicity exerted by these non-fibrillar aggregates. The first underlies the binding of TTR aggregates/fibrils to plasma membrane causing altered membrane fluidity. The second, implies the interaction of TTR aggregates with cell surface receptors, namely RAGE (see figure 1). However, one should not exclude the possibility that other receptors may intervene (see figure 1). RAGE involvement in FAP pathology was shown by the observation of its increasing expression during the course of disease, in a distribution juxtaposed to TTR deposition. In cell culture, RAGE has been implicated in neuronal cell stress exerted by TTR aggregates. Given that RAGE is a multiligand receptor and structural basis of RAGE-ligand interaction is poorly understood due to lack of

crystallographic data, we sought to unravel structural determinants underlying RAGE-TTR interaction. By screening several TTR mutants we found that human Leu55Pro variant has decreased binding affinity towards RAGE, indicating that β-strand D, which is disrupted in this mutant, is important for RAGE-TTR interaction. Moreover, we also found a RAGE motif comprising residues 102-118, localized within V-domain responsible to RAGE ligand binding, that is involved in binding of TTR. Furthermore, this RAGE peptide was able to suppress TTR aggregate-induced caspase-3 activity in a Schwannoma cell line as well as non-glycosylated sRAGE. Knowing the beneficial effects of sRAGE administration in several animal models of pathologies by blocking interaction of ligands with cellular RAGE and possibly with other receptors, and the potential inhibitory effect in fibrillogenesis as suggested for Aβ, future investigation should aim at administrating RAGE counteracting agents in FAP transgenic mouse models. These findings may have consequences not only in TTR-related but also in other amyloidoses, including AD, for future therapeutic strategies.

Upon ligand engagement, RAGE triggers oxidative stress and activates several signaling pathways, including the MAPK pathways and the redox-sensitive transcription factor NFκB. In addition, in neurodegenerative diseases including AD, a growing body of evidence implicates chronic activation of MAPKs in diseased neurons. Moreover, gene expression microarray data from human FAP SG displayed a down-regulation of MKP-1, a phosphatase able to dephosphorylate ERK1/2, p38 and JNK MAPKs, that was further confirmed by semi-quantitative immunohistochemical analysis of FAP SG and nerves. Therefore, we studied MAPK pathways (i.e. ERK1/2, JNK and p38) involvement in FAP. From all MAPK pathways, we demonstrated that only ERK1/2 pathway is significantly activated at early asymptomatic stage and persisting throughout the course of the disease. Abnormally sustained ERK1/2 activation might result from several inputs: 1) RAGE interaction with TTR aggregates, as demonstrated in cell culture (see figure 1); 2) RAGE over-expression, found in FAP tissues (see figure 1); 3) direct RAGE interaction with ERKs (see figure 1); 4) unknown receptor interaction with TTR aggregates, as suggested by partial blockade of ERK1/2 activation by anti-RAGE antibody (see figure 1); 5) abnormal activation of redox-sensitive upstream kinases (see figure 1); 6) impaired degradation of phospho-ERK1/2 due to alterations in ubiquitin-proteasome system (Ub-P), which occur in neurodegenerative diseases upon oxidative stress (see figure 1); 7) down-regulation of MKPs expression, as we demonstrated for MKP-1 at symptomatic FAP stage (see figure 1); and 8) inhibition of redox-sensitive ERK protein phosphatases by reversible or irreversible oxidation (see figure 1). Indeed, the later can explain both why ERK-dependent induction of MKPs transcriptional expression did not produce a negative feedback loop on ERK signaling and why MKP-3 increased expression in asymptomatic

FAP nerves was found together with active ERK up-regulation. It is well accepted that neurodegenerative diseases underlie oxidative stress and such is the case of FAP. Taken together, oxidative stress is expected to play a major role for pathologically sustained ERK1/2 activity observed in FAP.

Active ERK can phosphorylate cytoplasmic substrates ranging from cytoskeletal proteins, kinases, phosphatases and enzymes and/or active ERK1/2 translocates to the nucleus where it phosphorylates transcription factors (TFs) (see figure 1). Given the variety of substrates, the outcome of ERK activity might depend on several factors such as cell type, cellular context of gene expression that determines the subset of potential substrates available and subcellular compartmentalization that can also regulate the accessibility of substrates. Although some controversial data on beneficial or detrimental role of ERK1/2 activation exist, our data suggests a detrimental role for ERK1/2, as upon treatment with TTR aggregates, cells that had blocked ERK1/2 signaling were significantly protected from activation of caspase-3, a critical protease in the late apoptosis.

Our preliminary data on TFs activity in FAP suggests a complex interplay between the selected TFs. Among them, we found a decrease in Elk-1 phosphorylation probably due to ERK1/2 signaling negative feedback modulation. A possible mechanism is the rapid dephosphorylation of Elk-1 by calcineurin (or serine/threonine protein phosphatase 2B (PP2B); see figure 1). Thus, calcineurin activity should be evaluated in FAP. In the case of calcineurin up-regulation, this opens a new window for FAP therapeutics, since it is well known that immunosuppressants such as cyclosporine A (CsA) and FK506 polypeptides exert a neuroprotective and neurotrophic action in traumatic brain injury, sciatic nerve injury, focal and global ischemia in several animal models (Kaminska et al. 2004). Conversely, down-regulation can also be the outcome since calcineurin was reported to be redox-sensitive (Ferri et al. 2004).

Currently, NFκB is the only TF known to be involved in FAP and activation of NFκB has been suggested to represent an early protective response to ongoing oxidative stress in chronic neurodegenerative diseases. NFκB is a dimeric TF that regulates a large number of genes involved in immune response, cell proliferation, development and apoptosis. Activation of NFκB is induced by a variety of stimuli, including cytokines and oxidative stress (see figure 1). NFκB activity has two levels of regulation. Activation at the cytoplasm leads to proteosome-dependent generation of DNA-binding subunits. Another level of regulation occurs within the nucleus, activity of this TF is regulated by several mechanisms such as posttranslational modifications of the transactivating p65 subunit by phosphorylation, acetylation, among others. The complexity of this regulation is exemplified by observation that individual phosphorylation sites of p65 are targeted either

by single or by several kinases. Among the reported kinases are MSK1 and RSK1, which phosphorylate p65 at serines 276 and 536, respectively (Schmitz et al. 2004). MSK1 and RSK1 are known as ERK1/2 downstream kinase substrates; therefore, it is possible that a cross-talk between ERK1/2 and NFκB pathways occurs in FAP. Future experiments should aim to disclose whether MSK1 and RSK1 are up-regulated in FAP clinical samples and whether inhibition of ERK1/2 pathway by pharmacological inhibitors leads to a decrease of NFκB transactivation activity upon incubation of cells with TTR aggregates.

We analyzed HMGB1, a non-histone nuclear protein, in FAP tissues and fluids. Our observations were the following: in FAP SG, HMGB1 was translocated from the nucleus to the cytosol in epithelial cells; in FAP nerves, HMGB1 was up-regulated in axons; and in DRG neurons affected by TTR deposition from a FAP mouse model, HMGB1 was up-regulated in the cytosol. These led us to investigate what was promoting this feature. In fact, HMGB1 relocation from the nucleus to the cytoplasm was demonstrated in monocyte cells, where inflammatory stimuli shift the balance towards chromatin acetylation, and HMGB1 becomes hyperacetylated. Thus, future studies should assess whether HMGB1 is highly acetylated in FAP and whether HMGB1 ends to be released into the extracellular milieu as suggested by detection of HMGB1 in saliva of 2 out of 3 FAP patients (see figure 1). Recent studies have shown that biological settings of inflammation and oxidative stress activate MAPKs and NFκB pathways resulting in the activation of histone acetyltransferases (HATs) and inhibition of histone deacetylases (HDAC) activities leading to chromatin remodeling and gene transcription. Similarly, it is possible that in FAP, HMGB1 relocation might be a sign of a more general wave of acetylation triggered by the presence of inflammatory/oxidative stimuli leading to NFκB and ERK1/2 chronic activation, chromatin remodeling and active gene transcription (see figure 1). Indeed, ERK1/2 is capable of modulating gene expression both by phosphorylating TFs directly and activating other protein kinases (i.e. RSK and MSK), which then phosphorylate proteins involved in gene expression (see figure 1). For instance, RSK can phosphorylate histone H3, a protein regulator of chromatin structure (Sassone-Corsi et al. 1999). MSK1 is also able to phosphorylate histone H3 and high mobility group (HMG-14) protein (Thomson et al. 1999). Since these proteins are involved in packing DNA into chromatin, activation of histone and HMG proteins via the ERK pathway can result in increased TF accessibility to DNA binding sites (Whitmarsh and Davis 2000). In addition, ERK has been shown to phosphorylate steroid receptor coactivator-1 (SRC-1), which possesses an intrinsic histone acetyltransferase activity and is a coactivator that enhances the activation of

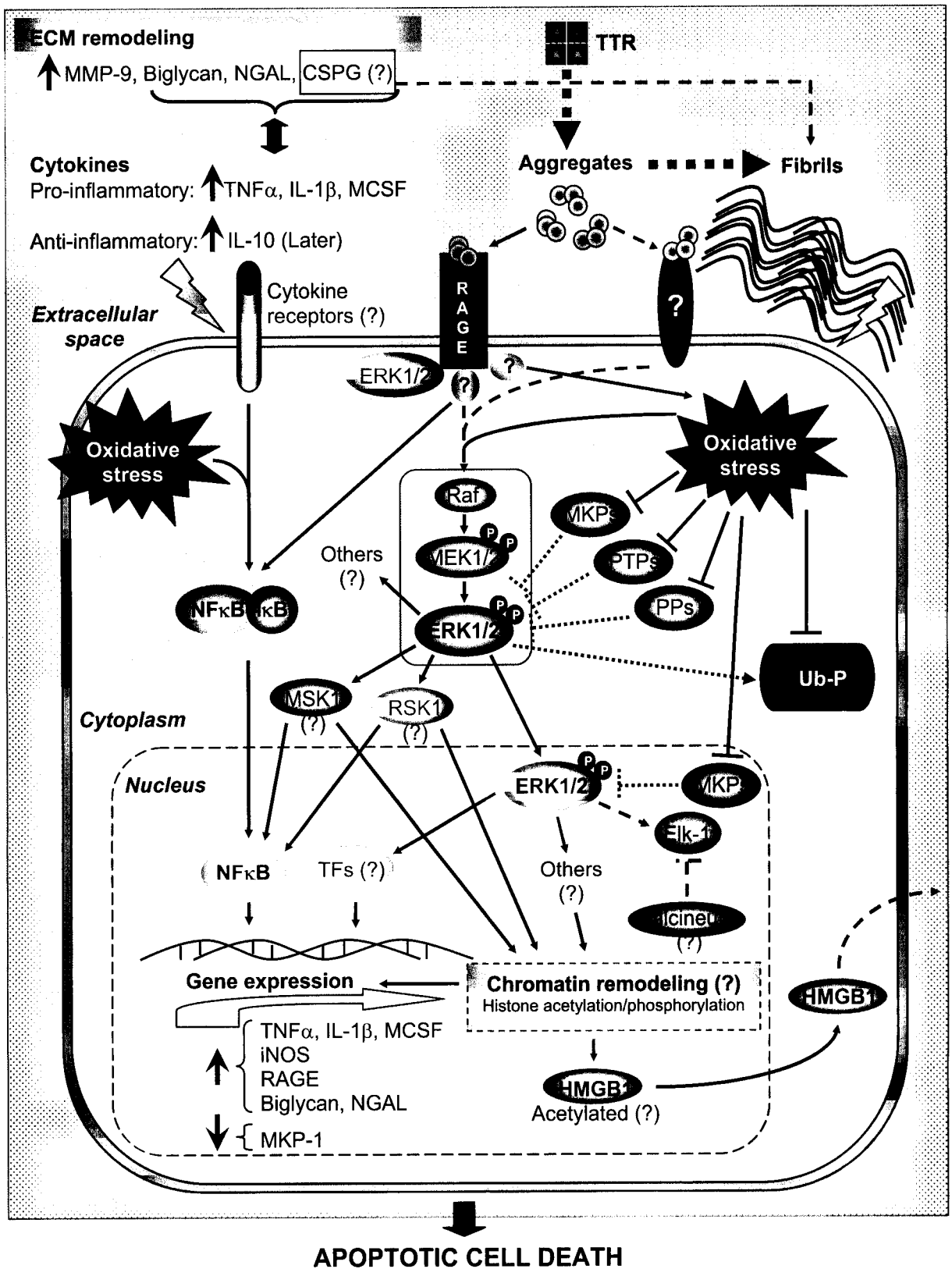

Figure 1. Hypothetical model for the molecular signaling mechanisms possibly elicited by toxic non-fibrillar TTR aggregates.
Legend: the three-tiered ERK signaling module is shown in a pink rectangle; arrows: activation/ translocation; —| : inhibition; ····· : blocked actions; – – – : possible action or unknown intermediates; (?): possible mediators.

steroid nuclear receptors (Rowan et al. 2000). All together, these downstream effects of ERK1/2 and NFκB might influence chromatin remodeling and activation of gene expression in FAP, and HMGB1 relocation appears to be an early marker of cytotoxicity exerted by deposited TTR (see figure 1).

Since ERK signaling participates in several physiological functions, it is probably not a good candidate as a therapeutical target. However, further studies aimed at clarifying the underlying molecular mechanisms for chronic activation of ERK1/2 will help to elucidate not only FAP but also the pathogenesis of other neurodegenerative diseases and may provide the molecular basis for therapeutical intervention. Furthermore, antioxidants and anti-inflammatory drugs, namely glucocorticoids, probably can ameliorate the symptomatology associated with FAP. For instance, glucocorticoids have been reported to have major anti-inflammatory effects apparently due to interaction between the activated glucocorticoid receptor and TFs, namely NFκB, impairing their ability to induce gene expression. Interestingly, among the genes transcriptionally down-regulated by glucocorticoids are the cytokines TNFα, IL-1β and M-CSF, and the inducible enzyme iNOS; regarding up-regulated genes, one can find MKP-1 and IL-10 (Adcock et al. 2004). IL-10 expression is thought to be insufficient to oppose pro-inflammatory stimuli in FAP (see figure 1). Therefore, it would be interesting to test glucocorticoids as a therapeutical strategy to counteract ongoing inflammation and oxidative stress in FAP.

Future investigation on FAP related signaling pathways must be pursued, in order to further elucidate molecular signaling mechanisms ultimately leading to neurodegeneration. Finally, a more complete understanding of FAP signaling pathways puzzle should provide guidance for future attempts to shift the death/survival balance in favour of neuronal survival.

REFERENCES

References

Achen M. G., Duan W., Pettersson T. M., Harms P. J., Richardson S. J., Lawrence M. C., Wettenhall R. E., Aldred A. R. and Schreiber G. (1993) Transthyretin gene expression in choroid plexus first evolved in reptiles. *Am J Physiol* **265,** R982-989.

Adcock I. M., Ito K. and Barnes P. J. (2004) Glucocorticoids: effects on gene transcription. *Proc Am Thorac Soc* **1,** 247-254.

Alessandrini A., Namura S., Moskowitz M. A. and Bonventre J. V. (1999) MEK1 protein kinase inhibition protects against damage resulting from focal cerebral ischemia. *Proc Natl Acad Sci U S A* **96,** 12866-12869.

Alessi D. R., Gomez N., Moorhead G., Lewis T., Keyse S. M. and Cohen P. (1995) Inactivation of p42 MAP kinase by protein phosphatase 2A and a protein tyrosine phosphatase, but not CL100, in various cell lines. *Curr Biol* **5,** 283-295.

Almeida M. R. and Saraiva M. J. (1996) Thyroxine binding to transthyretin (TTR) variants--two variants (TTR Pro 55 and TTR Met 111) with a particularly low binding affinity. *Eur J Endocrinol* **135,** 226-230.

Almeida M. R., Damas A. M., Lans M. C., Brouwer A. and Saraiva M. J. (1997) Thyroxine binding to transthyretin Met 119. Comparative studies of different heterozygotic carriers and structural analysis. *Endocrine* **6,** 309-315.

Almeida M. R., Gales L., Damas A. M., Cardoso I. and Saraiva M. J. (2005) Small transthyretin (TTR) ligands as possible therapeutic agents in TTR amyloidoses. *Curr Drug Targets CNS Neurol Disord* **4,** 587-596.

Alves I. L., Altland K., Almeida M. R., Winter P. and Saraiva M. J. (1997) Screening and biochemical characterization of transthyretin variants in the Portuguese population. *Hum Mutat* **9,** 226-233.

Anderson K., Potter A., Baban D. and Davies K. E. (2003) Protein expression changes in spinal muscular atrophy revealed with a novel antibody array technology. *Brain* **126,** 2052-2064.

Andersson K., Olofsson A., Nielsen E. H., Svehag S. E. and Lundgren E. (2002) Only amyloidogenic intermediates of transthyretin induce apoptosis. *Biochem Biophys Res Commun* **294,** 309-314.

Andersson U. and Tracey K. J. (2003) HMGB1 in sepsis. *Scand J Infect Dis* **35,** 577-584.

Ando Y., Nyhlin N., Suhr O., Holmgren G., Uchida K., el Sahly M., Yamashita T., Terasaki H., Nakamura M., Uchino M. and Ando M. (1997) Oxidative stress is found in amyloid deposits in systemic amyloidosis. *Biochem Biophys Res Commun* **232,** 497-502.

Ando Y. (2005) Liver transplantation and new therapeutic approaches for familial amyloidotic polyneuropathy (FAP). *Med Mol Morphol* **38,** 142-154.

Andrade C. (1952) A peculiar form of peripheral neuropathy; familiar atypical generalized amyloidosis with special involvement of the peripheral nerves. *Brain* **75,** 408-427.

Andrea T. A., Cavalieri R. R., Goldfine I. D. and Jorgensen E. C. (1980) Binding of thyroid hormones and analogues to the human plasma protein prealbumin. *Biochemistry* **19,** 55-63.

Arancio O., Zhang H. P., Chen X., Lin C., Trinchese F., Puzzo D., Liu S., Hegde A., Yan S. F., Stern A., Luddy J. S., Lue L. F., Walker D. G., Roher A., Buttini M., Mucke L., Li W., Schmidt A. M., Kindy M., Hyslop P. A., Stern D. M. and Du Yan S. S. (2004) RAGE potentiates Abeta-induced perturbation of neuronal function in transgenic mice. *Embo J* **23,** 4096-4105.

Avnur Z. and Geiger B. (1984) Immunocytochemical localization of native chondroitin-sulfate in tissues and cultured cells using specific monoclonal antibody. *Cell* **38,** 811-822.

Bamberger M. E. and Landreth G. E. (2002) Inflammation, apoptosis, and Alzheimer's disease. *Neuroscientist* **8,** 276-283.

Barinaga M. (1995) A new twist to the cell cycle. *Science* **269,** 631-632.

Bianchi M. E. (2004) Significant (re)location: how to use chromatin and/or abundant proteins as messages of life and death. *Trends Cell Biol* **14,** 287-293.

Bianchi M. E. and Manfredi A. (2004) Chromatin and cell death. *Biochim Biophys Acta* **1677,** 181-186.

Bierhaus A., Haslbeck K. M., Humpert P. M., Liliensiek B., Dehmer T., Morcos M., Sayed A. A., Andrassy M., Schiekofer S., Schneider J. G., Schulz J. B., Heuss D., Neundorfer B., Dierl S., Huber J., Tritschler H., Schmidt A. M., Schwaninger M., Haering H. U., Schleicher E., Kasper M., Stern D. M., Arnold B. and Nawroth P. P. (2004) Loss of pain perception in diabetes is dependent on a receptor of the immunoglobulin superfamily. *J Clin Invest* **114,** 1741-1751.

Bierhaus A., Humpert P. M., Morcos M., Wendt T., Chavakis T., Arnold B., Stern D. M. and Nawroth P. P. (2005) Understanding RAGE, the receptor for advanced glycation end products. *J Mol Med* **83,** 876-886.

Biswas S. C. and Greene L. A. (2002) Nerve growth factor (NGF) down-regulates the Bcl-2 homology 3 (BH3) domain-only protein Bim and suppresses its proapoptotic activity by phosphorylation. *J Biol Chem* **277,** 49511-49516.

Blake C. C., Geisow M. J., Swan I. D., Rerat C. and Rerat B. (1974) Strjcture of human plasma prealbumin at 2-5 A resolution. A preliminary report on the polypeptide chain conformation, quaternary structure and thyroxine binding. *J Mol Biol* **88,** 1-12.

Blake C. C. and Oatley S. J. (1977) Protein-DNA and protein-hormone interactions in prealbumin: a model of the thyroid hormone nuclear receptor? *Nature* **268,** 115-120.

Blake C. C., Geisow M. J., Oatley S. J., Rerat B. and Rerat C. (1978) Structure of prealbumin: secondary, tertiary and quaternary interactions determined by Fourier refinement at 1.8 A. *J Mol Biol* **121,** 339-356.

Blaner W. S. (1989) Retinol-binding protein: the serum transport protein for vitamin A. *Endocr Rev* **10,** 308-316.

Bokemeyer D., Sorokin A., Yan M., Ahn N. G., Templeton D. J. and Dunn M. J. (1996) Induction of mitogen-activated protein kinase phosphatase 1 by the stress-activated protein kinase signaling pathway but not by extracellular signal-regulated kinase in fibroblasts. *J Biol Chem* **271,** 639-642.

Bonaldi T., Talamo F., Scaffidi P., Ferrera D., Porto A., Bachi A., Rubartelli A., Agresti A. and Bianchi M. E. (2003) Monocytic cells hyperacetylate chromatin protein HMGB1 to redirect it towards secretion. *Embo J* **22,** 5551-5560.

Bonifacio M. J., Sakaki Y. and Saraiva M. J. (1996) 'In vitro' amyloid fibril formation from transthyretin: the influence of ions and the amyloidogenicity of TTR variants. *Biochim Biophys Acta* **1316,** 35-42.

Bonni A., Brunet A., West A. E., Datta S. R., Takasu M. A. and Greenberg M. E. (1999) Cell survival promoted by the Ras-MAPK signaling pathway by transcription-dependent and -independent mechanisms. *Science* **286,** 1358-1362.

Boomsma F., Man in 't Veld A. J. and Schalekamp M. A. (1991) Not norepinephrine but its oxidation products bind specifically to plasma proteins. *J Pharmacol Exp Ther* **259,** 551-557.

Brett J., Schmidt A. M., Yan S. D., Zou Y. S., Weidman E., Pinsky D., Nowygrod R., Neeper M., Przysiecki C., Shaw A. and et al. (1993) Survey of the distribution of a newly characterized receptor for advanced glycation end products in tissues. *Am J Pathol* **143,** 1699-1712.

Brett M., Persey M. R., Reilly M. M., Revesz T., Booth D. R., Booth S. E., Hawkins P. N., Pepys M. B. and Morgan-Hughes J. A. (1999) Transthyretin Leu12Pro is associated with systemic, neuropathic and leptomeningeal amyloidosis. *Brain* **122 (Pt 2),** 183-190.

Brondello J. M., Brunet A., Pouyssegur J. and McKenzie F. R. (1997) The dual specificity mitogen-activated protein kinase phosphatase-1 and -2 are induced by the p42/p44MAPK cascade. *J Biol Chem* **272,** 1368-1376.

Brouwer A. (1989) Inhibition of thyroid hormone transport in plasma of rats by polychlorinated biphenyls. *Arch Toxicol Suppl* **13,** 440-445.

Bucciarelli L. G., Wendt T., Rong L., Lalla E., Hofmann M. A., Goova M. T., Taguchi A., Yan S. F., Yan S. D., Stern D. M. and Schmidt A. M. (2002) RAGE is a multiligand receptor of the immunoglobulin superfamily: implications for homeostasis and chronic disease. *Cell Mol Life Sci* **59,** 1117-1128.

Calogero S., Grassi F., Aguzzi A., Voigtlander T., Ferrier P., Ferrari S. and Bianchi M. E. (1999) The lack of chromosomal protein Hmg1 does not disrupt cell growth but causes lethal hypoglycaemia in newborn mice. *Nat Genet* **22,** 276-280.

Camps M., Nichols A. and Arkinstall S. (2000) Dual specificity phosphatases: a gene family for control of MAP kinase function. *Faseb J* **14,** 6-16.

Cardoso I., Goldsbury C. S., Muller S. A., Olivieri V., Wirtz S., Damas A. M., Aebi U. and Saraiva M. J. (2002) Transthyretin fibrillogenesis entails the assembly of monomers: a molecular model for in vitro assembled transthyretin amyloid-like fibrils. *J Mol Biol* **317,** 683-695.

Cardoso I., Merlini G. and Saraiva M. J. (2003) 4'-iodo-4'-deoxydoxorubicin and tetracyclines disrupt transthyretin amyloid fibrils in vitro producing noncytotoxic species: screening for TTR fibril disrupters. *Faseb J* **17,** 803-809.

Cha Y. K., Kim Y. H., Ahn Y. H. and Koh J. Y. (2000) Epidermal growth factor induces oxidative neuronal injury in cortical culture. *J Neurochem* **75,** 298-303.

Chaney M. O., Stine W. B., Kokjohn T. A., Kuo Y. M., Esh C., Rahman A., Luehrs D. C., Schmidt A. M., Stern D., Yan S. D. and Roher A. E. (2005) RAGE and amyloid beta interactions: atomic force microscopy and molecular modeling. *Biochim Biophys Acta* **1741,** 199-205.

Chang L. and Karin M. (2001) Mammalian MAP kinase signalling cascades. *Nature* **410,** 37-40.

Chavakis T., Bierhaus A., Al-Fakhri N., Schneider D., Witte S., Linn T., Nagashima M., Morser J., Arnold B., Preissner K. T. and Nawroth P. P. (2003) The pattern recognition receptor (RAGE) is a counterreceptor for leukocyte integrins: a novel pathway for inflammatory cell recruitment. *J Exp Med* **198,** 1507-1515.

Chen C. H., Wang W. J., Kuo J. C., Tsai H. C., Lin J. R., Chang Z. F. and Chen R. H. (2005) Bidirectional signals transduced by DAPK-ERK interaction promote the apoptotic effect of DAPK. *Embo J* **24,** 294-304.

Cheng A. M., Saxton T. M., Sakai R., Kulkarni S., Mbamalu G., Vogel W., Tortorice C. G., Cardiff R. D., Cross J. C., Muller W. J. and Pawson T. (1998) Mammalian Grb2 regulates multiple steps in embryonic development and malignant transformation. *Cell* **95,** 793-803.

Chu C. T., Levinthal D. J., Kulich S. M., Chalovich E. M. and DeFranco D. B. (2004) Oxidative neuronal injury. The dark side of ERK1/2. *Eur J Biochem* **271,** 2060-2066.

Coimbra A. and Andrade C. (1971a) Familial amyloid polyneuropathy: an electron microscope study of the peripheral nerve in five cases. II. Nerve fibre changes. *Brain* **94,** 207-212.

Coimbra A. and Andrade C. (1971b) Familial amyloid polyneuropathy: an electron microscope study of the peripheral nerve in five cases. I. Interstitial changes. *Brain* **94,** 199-206.

Colucci-D'Amato L., Perrone-Capano C. and di Porzio U. (2003) Chronic activation of ERK and neurodegenerative diseases. *Bioessays* **25,** 1085-1095.

Combs C. K., Karlo J. C., Kao S. C. and Landreth G. E. (2001) beta-Amyloid stimulation of microglia and monocytes results in TNFalpha-dependent expression of inducible nitric oxide synthase and neuronal apoptosis. *J Neurosci* **21,** 1179-1188.

Costa P. P., Figueira A. S. and Bravo F. R. (1978) Amyloid fibril protein related to prealbumin in familial amyloidotic polyneuropathy. *Proc Natl Acad Sci U S A* **75,** 4499-4503.

Costa R. H., Lai E. and Darnell J. E., Jr. (1986) Transcriptional control of the mouse prealbumin (transthyretin) gene: both promoter sequences and a distinct enhancer are cell specific. *Mol Cell Biol* **6,** 4697-4708.

Costa R. H., Van Dyke T. A., Yan C., Kuo F. and Darnell J. E., Jr. (1990) Similarities in transthyretin gene expression and differences in transcription factors: liver and yolk sac compared to choroid plexus. *Proc Natl Acad Sci U S A* **87,** 6589-6593.

Davis R. J. (2000) Signal transduction by the JNK group of MAP kinases. *Cell* **103,** 239-252.

Deane R., Du Yan S., Submamaryan R. K., LaRue B., Jovanovic S., Hogg E., Welch D., Manness L., Lin C., Yu J., Zhu H., Ghiso J., Frangione B., Stern A., Schmidt A. M., Armstrong D. L., Arnold B., Liliensiek B., Nawroth P., Hofman F., Kindy M., Stern D. and Zlokovic B. (2003) RAGE mediates amyloid-beta peptide transport across the blood-brain barrier and accumulation in brain. *Nat Med* **9,** 907-913.

Degryse B., Bonaldi T., Scaffidi P., Muller S., Resnati M., Sanvito F., Arrigoni G. and Bianchi M. E. (2001) The high mobility group (HMG) boxes of the nuclear protein HMG1 induce chemotaxis and cytoskeleton reorganization in rat smooth muscle cells. *J Cell Biol* **152,** 1197-1206.

Dember L. M. (2005) Emerging treatment approaches for the systemic amyloidoses. *Kidney Int* **68,** 1377-1390.

Dermietzel R. and Spray D. C. (1993) Gap junctions in the brain: where, what type, how many and why? *Trends Neurosci* **16,** 186-192.

Dickson P. W., Aldred A. R., Marley P. D., Bannister D. and Schreiber G. (1986) Rat choroid plexus specializes in the synthesis and the secretion of transthyretin (prealbumin). Regulation of transthyretin synthesis in choroid plexus is independent from that in liver. *J Biol Chem* **261,** 3475-3478.

Divino C. M. and Schussler G. C. (1990) Receptor-mediated uptake and internalization of transthyretin. *J Biol Chem* **265,** 1425-1429.

Du S., McLaughlin B., Pal S. and Aizenman E. (2002) In vitro neurotoxicity of methylisothiazolinone, a commonly used industrial and household biocide, proceeds via a zinc and extracellular signal-regulated kinase mitogen-activated protein kinase-dependent pathway. *J Neurosci* **22,** 7408-7416.

Du Yan S., Zhu H., Fu J., Yan S. F., Roher A., Tourtellotte W. W., Rajavashisth T., Chen X., Godman G. C., Stern D. and Schmidt A. M. (1997) Amyloid-beta peptide-receptor for advanced glycation endproduct interaction elicits neuronal expression of macrophage-colony stimulating factor: a proinflammatory pathway in Alzheimer disease. *Proc Natl Acad Sci U S A* **94,** 5296-5301.

Eneqvist T., Andersson K., Olofsson A., Lundgren E. and Sauer-Eriksson A. E. (2000) The beta-slip: a novel concept in transthyretin amyloidosis. *Mol Cell* **6,** 1207-1218.

Eneqvist T., Lundberg E., Nilsson L., Abagyan R. and Sauer-Eriksson A. E. (2003) The transthyretin-related protein family. *Eur J Biochem* **270,** 518-532.

Episkopou V., Maeda S., Nishiguchi S., Shimada K., Gaitanaris G. A., Gottesman M. E. and Robertson E. J. (1993) Disruption of the transthyretin gene results in mice with depressed levels of plasma retinol and thyroid hormone. *Proc Natl Acad Sci U S A* **90,** 2375-2379.

Erlandsson Harris H. and Andersson U. (2004) Mini-review: The nuclear protein HMGB1 as a proinflammatory mediator. *Eur J Immunol* **34,** 1503-1512.

Ernstrom U., Pettersson T. and Jornvall H. (1995) A yellow component associated with human transthyretin has properties like a pterin derivative, 7,8-dihydropterin-6-carboxaldehyde. *FEBS Lett* **360,** 177-182.

Farooq A. and Zhou M. M. (2004) Structure and regulation of MAPK phosphatases. *Cell Signal* **16,** 769-779.

Farrow S. N., White J. H., Martinou I., Raven T., Pun K. T., Grinham C. J., Martinou J. C. and Brown R. (1995) Cloning of a bcl-2 homologue by interaction with adenovirus E1B 19K. *Nature* **374,** 731-733.

Ferrao-Gonzales A. D., Souto S. O., Silva J. L. and Foguel D. (2000) The preaggregated state of an amyloidogenic protein: hydrostatic pressure converts native transthyretin into the amyloidogenic state. *Proc Natl Acad Sci U S A* **97,** 6445-6450.

Ferrell J. E., Jr. (1996) MAP kinases in mitogenesis and development. *Curr Top Dev Biol* **33,** 1-60.

Ferrer I., Barrachina M., Tolnay M., Rey M. J., Vidal N., Carmona M., Blanco R. and Puig B. (2003) Phosphorylated protein kinases associated with neuronal and glial tau deposits in argyrophilic grain disease. *Brain Pathol* **13,** 62-78.

Ferri A., Nencini M., Battistini S., Giannini F., Siciliano G., Casali C., Damiano M. G., Ceroni M., Chio A., Rotilio G. and Carri M. T. (2004) Activity of protein phosphatase calcineurin is decreased in sporadic and familial amyotrophic lateral sclerosispatients. *J Neurochem* **90,** 1237-1242.

Fleming C. E., Saraiva M. J. and Sousa M. M. (2005) Transthyretin is involved in nerve regeneration. Abstract Viewer/Itinerary Planner. Washington, DC: Society for Neuroscience. On-line.

Gabbita S. P., Robinson K. A., Stewart C. A., Floyd R. A. and Hensley K. (2000) Redox regulatory mechanisms of cellular signal transduction. *Arch Biochem Biophys* **376,** 1-13.

Gardella S., Andrei C., Ferrera D., Lotti L. V., Torrisi M. R., Bianchi M. E. and Rubartelli A. (2002) The nuclear protein HMGB1 is secreted by monocytes via a non-classical, vesicle-mediated secretory pathway. *EMBO Rep* **3,** 995-1001.

Goldsteins G., Andersson K., Olofsson A., Dacklin I., Edvinsson A., Baranov V., Sandgren O., Thylen C., Hammarstrom S. and Lundgren E. (1997) Characterization of two highly amyloidogenic mutants of transthyretin. *Biochemistry* **36,** 5346-5352.

Gomez-Santos C., Ferrer I., Reiriz J., Vinals F., Barrachina M. and Ambrosio S. (2002) MPP+ increases alpha-synuclein expression and ERK/MAP-kinase phosphorylation in human neuroblastoma SH-SY5Y cells. *Brain Res* **935,** 32-39.

Goova M. T., Li J., Kislinger T., Qu W., Lu Y., Bucciarelli L. G., Nowygrod S., Wolf B. M., Caliste X., Yan S. F., Stern D. M. and Schmidt A. M. (2001) Blockade of receptor for advanced glycation end-products restores effective wound healing in diabetic mice. *Am J Pathol* **159,** 513-525.

Gorevic P. D., Prelli F. C., Wright J., Pras M. and Frangione B. (1989) Systemic senile amyloidosis. Identification of a new prealbumin (transthyretin) variant in cardiac tissue: immunologic and biochemical similarity to one form of familial amyloidotic polyneuropathy. *J Clin Invest* **83,** 836-843.

Grewal S. S., York R. D. and Stork P. J. (1999) Extracellular-signal-regulated kinase signalling in neurons. *Curr Opin Neurobiol* **9,** 544-553.

Grumont R. J., Rasko J. E., Strasser A. and Gerondakis S. (1996) Activation of the mitogen-activated protein kinase pathway induces transcription of the PAC-1 phosphatase gene. *Mol Cell Biol* **16,** 2913-2921.

Guerini D. (1997) Calcineurin: not just a simple protein phosphatase. *Biochem Biophys Res Commun* **235,** 271-275.

Gurjar M. V., Deleon J., Sharma R. V. and Bhalla R. C. (2001) Role of reactive oxygen species in IL-1 beta-stimulated sustained ERK activation and MMP-9 induction. *Am J Physiol Heart Circ Physiol* **281,** H2568-2574.

Gustavsson A., Jahr H., Tobiassen R., Jacobson D. R., Sletten K. and Westermark P. (1995) Amyloid fibril composition and transthyretin gene structure in senile systemic amyloidosis. *Lab Invest* **73,** 703-708.

Hamilton J. A., Steinrauf L. K., Braden B. C., Liepnieks J., Benson M. D., Holmgren G., Sandgren O. and Steen L. (1993) The x-ray crystal structure refinements of normal human transthyretin and the amyloidogenic Val-30-->Met variant to 1.7-A resolution. *J Biol Chem* **268,** 2416-2424.

Hanford L. E., Enghild J. J., Valnickova Z., Petersen S. V., Schaefer L. M., Schaefer T. M., Reinhart T. A. and Oury T. D. (2004) Purification and characterization of mouse soluble receptor for advanced glycation end products (sRAGE). *J Biol Chem* **279,** 50019-50024.

Hanyu N., Ikeda S., Nakadai A., Yanagisawa N. and Powell H. C. (1989) Peripheral nerve pathological findings in familial amyloid polyneuropathy: a correlative study of proximal sciatic nerve and sural nerve lesions. *Ann Neurol* **25,** 340-350.

Harms P. J., Tu G. F., Richardson S. J., Aldred A. R., Jaworowski A. and Schreiber G. (1991) Transthyretin (prealbumin) gene expression in choroid plexus is strongly conserved during evolution of vertebrates. *Comp Biochem Physiol B* **99,** 239-249.

Harper J. D. and Lansbury P. T., Jr. (1997) Models of amyloid seeding in Alzheimer's disease and scrapie: mechanistic truths and physiological consequences of the time-dependent solubility of amyloid proteins. *Annu Rev Biochem* **66,** 385-407.

Harper S. J. and Wilkie N. (2003) MAPKs: new targets for neurodegeneration. *Expert Opin Ther Targets* **7,** 187-200.

Hashimoto K., Guroff G. and Katagiri Y. (2000) Delayed and sustained activation of p42/p44 mitogen-activated protein kinase induced by proteasome inhibitors through p21(ras) in PC12 cells. *J Neurochem* **74,** 92-98.

Hatterer J. A., Herbert J., Hidaka C., Roose S. P. and Gorman J. M. (1993) CSF transthyretin in patients with depression. *Am J Psychiatry* **150,** 813-815.

Heffetz D., Fridkin M. and Zick Y. (1991) Generation and use of antibodies to phosphothreonine. *Methods Enzymol* **201,** 44-53.

Heim M. H. (1999) The Jak-STAT pathway: cytokine signalling from the receptor to the nucleus. *J Recept Signal Transduct Res* **19,** 75-120.

Hennebry S. C., Wright H. M., Likic V. A. and Richardson S. J. (2006) Structural and functional evolution of transthyretin and transthyretin-like proteins. *Proteins.*

Hetman M., Kanning K., Cavanaugh J. E. and Xia Z. (1999) Neuroprotection by brain-derived neurotrophic factor is mediated by extracellular signal-regulated kinase and phosphatidylinositol 3-kinase. *J Biol Chem* **274,** 22569-22580.

Hetman M., Hsuan S. L., Habas A., Higgins M. J. and Xia Z. (2002) ERK1/2 antagonizes glycogen synthase kinase-3beta-induced apoptosis in cortical neurons. *J Biol Chem* **277,** 49577-49584.

Hetman M. and Gozdz A. (2004) Role of extracellular signal regulated kinases 1 and 2 in neuronal survival. *Eur J Biochem* **271,** 2050-2055.

Hofer P. A. and Anderson R. (1975) Postmortem findings in primary familial amyloidosis with polyneuropathy. *Acta Pathol Microbiol Scand [A]* **83,** 309-322.

Hofmann M. A., Drury S., Fu C., Qu W., Taguchi A., Lu Y., Avila C., Kambham N., Bierhaus A., Nawroth P., Neurath M. F., Slattery T., Beach D., McClary J., Nagashima M., Morser J., Stern D. and Schmidt A. M. (1999) RAGE mediates a novel proinflammatory axis: a central cell surface receptor for S100/calgranulin polypeptides. *Cell* **97,** 889-901.

Hori O., Brett J., Slattery T., Cao R., Zhang J., Chen J. X., Nagashima M., Lundh E. R., Vijay S., Nitecki D. and et al. (1995) The receptor for advanced glycation end products (RAGE) is a cellular binding site for amphoterin. Mediation of neurite outgrowth and co-expression of rage and amphoterin in the developing nervous system. *J Biol Chem* **270,** 25752-25761.

Hosler J. P. (2004) The influence of subunit III of cytochrome c oxidase on the D pathway, the proton exit pathway and mechanism-based inactivation in subunit I. *Biochim Biophys Acta* **1655,** 332-339.

Hou X., Richardson S. J., Aguilar M. I. and Small D. H. (2005) Binding of amyloidogenic transthyretin to the plasma membrane alters membrane fluidity and induces neurotoxicity. *Biochemistry* **44,** 11618-11627.

Hsu Y. T. and Youle R. J. (1997) Nonionic detergents induce dimerization among members of the Bcl-2 family. *J Biol Chem* **272,** 13829-13834.

Huang J. S., Guh J. Y., Chen H. C., Hung W. C., Lai Y. H. and Chuang L. Y. (2001) Role of receptor for advanced glycation end-product (RAGE) and the JAK/STAT-signaling pathway in AGE-induced collagen production in NRK-49F cells. *J Cell Biochem* **81,** 102-113.

Hudson B. I., Bucciarelli L. G., Wendt T., Sakaguchi T., Lalla E., Qu W., Lu Y., Lee L., Stern D. M., Naka Y., Ramasamy R., Yan S. D., Yan S. F., D'Agati V. and Schmidt A. M. (2003) Blockade of receptor for advanced glycation endproducts: a new target for therapeutic intervention in diabetic complications and inflammatory disorders. *Arch Biochem Biophys* **419,** 80-88.

Hurshman A. R., White J. T., Powers E. T. and Kelly J. W. (2004) Transthyretin aggregation under partially denaturing conditions is a downhill polymerization. *Biochemistry* **43,** 7365-7381.

Huttunen H. J., Fages C. and Rauvala H. (1999) Receptor for advanced glycation end products (RAGE)-mediated neurite outgrowth and activation of NF-kappaB require the cytoplasmic domain of the receptor but different downstream signaling pathways. *J Biol Chem* **274,** 19919-19924.

Huttunen H. J., Fages C., Kuja-Panula J., Ridley A. J. and Rauvala H. (2002a) Receptor for advanced glycation end products-binding COOH-terminal motif of amphoterin inhibits invasive migration and metastasis. *Cancer Res* **62,** 4805-4811.

Huttunen H. J., Kuja-Panula J. and Rauvala H. (2002b) Receptor for advanced glycation end products (RAGE) signaling induces CREB-dependent chromogranin expression during neuronal differentiation. *J Biol Chem* **277,** 38635-38646.

Huttunen H. J. and Rauvala H. (2004) Amphoterin as an extracellular regulator of cell motility: from discovery to disease. *J Intern Med* **255,** 351-366.

Ichijo H., Nishida E., Irie K., ten Dijke P., Saitoh M., Moriguchi T., Takagi M., Matsumoto K., Miyazono K. and Gotoh Y. (1997) Induction of apoptosis by ASK1, a mammalian MAPKKK that activates SAPK/JNK and p38 signaling pathways. *Science* **275,** 90-94.

Ikeda S., Hanyu N., Hongo M., Yoshioka J., Oguchi H., Yanagisawa N., Kobayashi T., Tsukagoshi H., Ito N. and Yokota T. (1987) Hereditary generalized amyloidosis with polyneuropathy. Clinicopathological study of 65 Japanese patients. *Brain* **110 (Pt 2),** 315-337.

Ingenbleek Y. and De Visscher M. (1979) Hormonal and nutritional status: critical conditions for endemic goiter epidemiology? *Metabolism* **28,** 9-19.

Inoue S., Kuroiwa M., Saraiva M. J., Guimaraes A. and Kisilevsky R. (1998) Ultrastructure of familial amyloid polyneuropathy amyloid fibrils: examination with high-resolution electron microscopy. *J Struct Biol* **124,** 1-12.

Ischiropoulos H., Zhu L. and Beckman J. S. (1992a) Peroxynitrite formation from macrophage-derived nitric oxide. *Arch Biochem Biophys* **298,** 446-451.

Ischiropoulos H., Zhu L., Chen J., Tsai M., Martin J. C., Smith C. D. and Beckman J. S. (1992b) Peroxynitrite-mediated tyrosine nitration catalyzed by superoxide dismutase. *Arch Biochem Biophys* **298,** 431-437.

Ishihara K., Tsutsumi K., Kawane S., Nakajima M. and Kasaoka T. (2003) The receptor for advanced glycation end-products (RAGE) directly binds to ERK by a D-domain-like docking site. *FEBS Lett* **550,** 107-113.

Jacobson D. R., McFarlin D. E., Kane I. and Buxbaum J. N. (1992) Transthyretin Pro55, a variant associated with early-onset, aggressive, diffuse amyloidosis with cardiac and neurologic involvement. *Hum Genet* **89,** 353-356.

Jacobson D. R., Alves I. L., Saraiva M. J., Thibodeau S. N. and Buxbaum J. N. (1995) Transthyretin Ser 6 gene frequency in individuals without amyloidosis. *Hum Genet* **95,** 308-312.

Jacobsson B. (1989) In situ localization of transthyretin-mRNA in the adult human liver, choroid plexus and pancreatic islets and in endocrine tumours of the pancreas and gut. *Histochemistry* **91,** 299-304.

Jarvis J. A., Munro S. L. and Craik D. J. (1994) Structural analysis of peptide fragment 71-93 of transthyretin by NMR spectroscopy and electron microscopy: insight into amyloid fibril formation. *Biochemistry* **33,** 33-41.

Johan K., Westermark G., Engstrom U., Gustavsson A., Hultman P. and Westermark P. (1998) Acceleration of amyloid protein A amyloidosis by amyloid-like synthetic fibrils. *Proc Natl Acad Sci U S A* **95,** 2558-2563.

Jornvall H., Carlstrom A., Pettersson T., Jacobsson B., Persson M. and Mutt V. (1981) Structural homologies between prealbumin, gastrointestinal prohormones and other proteins. *Nature* **291,** 261-263.

Kabat E. A., Moore D. H. and Landow H. (1942) An electrophoretic study of the protein components in cerebrospinal fluid and their relationship to the serum proteins. *J Clin Invest* **21,** 571-577.

Kamata H. and Hirata H. (1999) Redox regulation of cellular signalling. *Cell Signal* **11,** 1-14.

Kaminska B., Gaweda-Walerych K. and Zawadzka M. (2004) Molecular mechanisms of neuroprotective action of immunosuppressants--facts and hypotheses. *J Cell Mol Med* **8,** 45-58.

Kanai M., Raz A. and Goodman D. S. (1968) Retinol-binding protein: the transport protein for vitamin A in human plasma. *J Clin Invest* **47,** 2025-2044.

Kanda Y., Goodman D. S., Canfield R. E. and Morgan F. J. (1974) The amino acid sequence of human plasma prealbumin. *J Biol Chem* **249,** 6796-6805.

Karin M. (1995) The regulation of AP-1 activity by mitogen-activated protein kinases. *J Biol Chem* **270,** 16483-16486.

Keyse S. M. (2000) Protein phosphatases and the regulation of mitogen-activated protein kinase signalling. *Curr Opin Cell Biol* **12,** 186-192.

Kisilevsky R. and Boudreau L. (1983) Kinetics of amyloid deposition. I. The effects of amyloid-enhancing factor and splenectomy. *Lab Invest* **48,** 53-59.

Kisilevsky R. (2000) Review: amyloidogenesis-unquestioned answers and unanswered questions. *J Struct Biol* **130,** 99-108.

Kislinger T., Fu C., Huber B., Qu W., Taguchi A., Du Yan S., Hofmann M., Yan S. F., Pischetsrieder M., Stern D. and Schmidt A. M. (1999) N(epsilon)-(carboxymethyl)lysine adducts of proteins are ligands for receptor for advanced glycation end products that activate cell signaling pathways and modulate gene expression. *J Biol Chem* **274,** 31740-31749.

Klotz I. M. and Hunston D. L. (1984) Mathematical models for ligand-receptor binding. Real sites, ghost sites. *J Biol Chem* **259,** 10060-10062.

Kohno K., Palha J. A., Miyakawa K., Saraiva M. J., Ito S., Mabuchi T., Blaner W. S., Iijima H., Tsukahara S., Episkopou V., Gottesman M. E., Shimada K., Takahashi K., Yamamura K. and Maeda S. (1997) Analysis of amyloid deposition in a transgenic mouse model of homozygous familial amyloidotic polyneuropathy. *Am J Pathol* **150,** 1497-1508.

Kohrle J. (1994) Thyroid hormone deiodination in target tissues--a regulatory role for the trace element selenium? *Exp Clin Endocrinol* **102,** 63-89.

Kornhauser J. M. and Greenberg M. E. (1997) A kinase to remember: dual roles for MAP kinase in long-term memory. *Neuron* **18,** 839-842.

Krieger M. (2001) Scavenger receptor class B type I is a multiligand HDL receptor that influences diverse physiologic systems. *J Clin Invest* **108,** 793-797.

Kulich S. M. and Chu C. T. (2001) Sustained extracellular signal-regulated kinase activation by 6-hydroxydopamine: implications for Parkinson's disease. *J Neurochem* **77,** 1058-1066.

Kulich S. M. and Chu C. T. (2003) Role of reactive oxygen species in extracellular signal-regulated protein kinase phosphorylation and 6-hydroxydopamine cytotoxicity. *J Biosci* **28,** 83-89.

Kuperstein F. and Yavin E. (2002) ERK activation and nuclear translocation in amyloid-beta peptide- and iron-stressed neuronal cell cultures. *Eur J Neurosci* **16,** 44-54.

Lagna G., Hata A., Hemmati-Brivanlou A. and Massague J. (1996) Partnership between DPC4 and SMAD proteins in TGF-beta signalling pathways. *Nature* **383,** 832-836.

Lander H. M., Tauras J. M., Ogiste J. S., Hori O., Moss R. A. and Schmidt A. M. (1997) Activation of the receptor for advanced glycation end products triggers a p21(ras)-dependent mitogen-activated protein kinase pathway regulated by oxidant stress. *J Biol Chem* **272,** 17810-17814.

Lansbury P. T., Jr. (1997) Structural neurology: are seeds at the root of neuronal degeneration? *Neuron* **19,** 1151-1154.

Lashuel H. A., Lai Z. and Kelly J. W. (1998) Characterization of the transthyretin acid denaturation pathways by analytical ultracentrifugation: implications for wild-type, V30M, and L55P amyloid fibril formation. *Biochemistry* **37,** 17851-17864.

Lechapt-Zalcman E., Authier F. J., Creange A., Voisin M. C. and Gherardi R. K. (1999) Labial salivary gland biopsy for diagnosis of amyloid polyneuropathy. *Muscle Nerve* **22,** 105-107.

Li J. and Schmidt A. M. (1997) Characterization and functional analysis of the promoter of RAGE, the receptor for advanced glycation end products. *J Biol Chem* **272,** 16498-16506.

Li J., Qu X. and Schmidt A. M. (1998) Sp1-binding elements in the promoter of RAGE are essential for amphoterin-mediated gene expression in cultured neuroblastoma cells. *J Biol Chem* **273,** 30870-30878.

Liang P. and Pardee A. B. (1992) Differential display of eukaryotic messenger RNA by means of the polymerase chain reaction. *Science* **257,** 967-971.

Liang P., Averboukh L. and Pardee A. B. (1993) Distribution and cloning of eukaryotic mRNAs by means of differential display: refinements and optimization. *Nucleic Acids Res* **21,** 3269-3275.

Liang P., Bauer D., Averboukh L., Warthoe P., Rohrwild M., Muller H., Strauss M. and Pardee A. B. (1995) Analysis of altered gene expression by differential display. *Methods Enzymol* **254,** 304-321.

Liliensiek B., Weigand M. A., Bierhaus A., Nicklas W., Kasper M., Hofer S., Plachky J., Grone H. J., Kurschus F. C., Schmidt A. M., Yan S. D., Martin E., Schleicher E., Stern D. M., Hammerling G. G., Nawroth P. P. and Arnold B. (2004) Receptor for advanced glycation end products (RAGE) regulates sepsis but not the adaptive immune response. *J Clin Invest* **113,** 1641-1650.

Liu F., Pouponnot C. and Massague J. (1997) Dual role of the Smad4/DPC4 tumor suppressor in TGFbeta-inducible transcriptional complexes. *Genes Dev* **11,** 3157-3167.

Liz M. A., Faro C. J., Saraiva M. J. and Sousa M. M. (2004) Transthyretin, a new cryptic protease. *J Biol Chem* **279,** 21431-21438.

Longo Alves I., Hays M. T. and Saraiva M. J. (1997) Comparative stability and clearance of [Met30]transthyretin and [Met119]transthyretin. *Eur J Biochem* **249,** 662-668.

Lotze M. T. and Tracey K. J. (2005) High-mobility group box 1 protein (HMGB1): nuclear weapon in the immune arsenal. *Nat Rev Immunol* **5,** 331-342.

Lowry O. H., Rosebrough N. J., Farr A. L. and Randall R. J. (1951) Protein measurement with the Folin phenol reagent. *J Biol Chem* **193,** 265-275.

Lue L. F., Walker D. G., Brachova L., Beach T. G., Rogers J., Schmidt A. M., Stern D. M. and Yan S. D. (2001) Involvement of microglial receptor for advanced glycation endproducts (RAGE) in Alzheimer's disease: identification of a cellular activation mechanism. *Exp Neurol* **171,** 29-45.

Lueprasitsakul W., Alex S., Fang S. L., Pino S., Irmscher K., Kohrle J. and Braverman L. E. (1990) Flavonoid administration immediately displaces thyroxine (T4) from serum transthyretin, increases serum free T4, and decreases serum thyrotropin in the rat. *Endocrinology* **126,** 2890-2895.

Magnus J. H., Stenstad T., Kolset S. O. and Husby G. (1991) Glycosaminoglycans in extracts of cardiac amyloid fibrils from familial amyloid cardiomyopathy of Danish origin related to variant transthyretin Met 111. *Scand J Immunol* **34,** 63-69.

Makover A., Moriwaki H., Ramakrishnan R., Saraiva M. J., Blaner W. S. and Goodman D. S. (1988) Plasma transthyretin. Tissue sites of degradation and turnover in the rat. *J Biol Chem* **263,** 8598-8603.

Malek S. N., Yang C. H., Earnshaw W. C., Kozak C. A. and Desiderio S. (1996) p150TSP, a conserved nuclear phosphoprotein that contains multiple tetratricopeptide repeats and binds specifically to SH2 domains. *J Biol Chem* **271,** 6952-6962.

Malherbe P., Richards J. G., Gaillard H., Thompson A., Diener C., Schuler A. and Huber G. (1999) cDNA cloning of a novel secreted isoform of the human receptor for advanced glycation end products and characterization of cells co-expressing cell-surface scavenger receptors and Swedish mutant amyloid precursor protein. *Brain Res Mol Brain Res* **71,** 159-170.

Mansour S. J., Matten W. T., Hermann A. S., Candia J. M., Rong S., Fukasawa K., Vande Woude G. F. and Ahn N. G. (1994) Transformation of mammalian cells by constitutively active MAP kinase kinase. *Science* **265,** 966-970.

Martell K. J., Seasholtz A. F., Kwak S. P., Clemens K. K. and Dixon J. E. (1995) hVH-5: a protein tyrosine phosphatase abundant in brain that inactivates mitogen-activated protein kinase. *J Neurochem* **65,** 1823-1833.

Martone R. L., Herbert J., Dwork A. and Schon E. A. (1988) Transthyretin is synthesized in the mammalian eye. *Biochem Biophys Res Commun* **151,** 905-912.

Matsubara K., Mizuguchi M., Igarashi K., Shinohara Y., Takeuchi M., Matsuura A., Saitoh T., Mori Y., Shinoda H. and Kawano K. (2005) Dimeric transthyretin variant assembles into spherical neurotoxins. *Biochemistry* **44,** 3280-3288.

Mattson M. P. and Camandola S. (2001) NF-kappaB in neuronal plasticity and neurodegenerative disorders. *J Clin Invest* **107,** 247-254.

McCutchen S. L., Colon W. and Kelly J. W. (1993) Transthyretin mutation Leu-55-Pro significantly alters tetramer stability and increases amyloidogenicity. *Biochemistry* **32,** 12119-12127.

Meng T. C., Fukada T. and Tonks N. K. (2002) Reversible oxidation and inactivation of protein tyrosine phosphatases in vivo. *Mol Cell* **9,** 387-399.

Miller S. R., Sekijima Y. and Kelly J. W. (2004) Native state stabilization by NSAIDs inhibits transthyretin amyloidogenesis from the most common familial disease variants. *Lab Invest* **84,** 545-552.

Miroy G. J., Lai Z., Lashuel H. A., Peterson S. A., Strang C. and Kelly J. W. (1996) Inhibiting transthyretin amyloid fibril formation via protein stabilization. *Proc Natl Acad Sci U S A* **93,** 15051-15056.

Misra-Press A., Rim C. S., Yao H., Roberson M. S. and Stork P. J. (1995) A novel mitogen-activated protein kinase phosphatase. Structure, expression, and regulation. *J Biol Chem* **270,** 14587-14596.

Misu K., Hattori N., Nagamatsu M., Ikeda S., Ando Y., Nakazato M., Takei Y., Hanyu N., Usui Y., Tanaka F., Harada T., Inukai A., Hashizume Y. and Sobue G. (1999) Late-onset familial amyloid polyneuropathy type I (transthyretin Met30-associated familial amyloid polyneuropathy) unrelated to endemic focus in Japan. Clinicopathological and genetic features. *Brain* **122 (Pt 10),** 1951-1962.

Mita S., Maeda S., Shimada K. and Araki S. (1984) Cloning and sequence analysis of cDNA for human prealbumin. *Biochem Biophys Res Commun* **124,** 558-564.

Monaco H. L., Rizzi M. and Coda A. (1995) Structure of a complex of two plasma proteins: transthyretin and retinol-binding protein. *Science* **268,** 1039-1041.

Monteiro F. A., Sousa M. M., Cardoso I., Amaral J. B., Guimaraes A. and Saraiva M. J. (2006) Activation of ERK1/2 MAP kinases in Familial Amyloidotic Polyneuropathy. *J Neurochem* **97,** 151-161.

Mori T., Wang X., Jung J. C., Sumii T., Singhal A. B., Fini M. E., Dixon C. E., Alessandrini A. and Lo E. H. (2002) Mitogen-activated protein kinase inhibition in traumatic brain injury: in vitro and in vivo effects. *J Cereb Blood Flow Metab* **22,** 444-452.

Muller S., Berger M., Lehembre F., Seeler J. S., Haupt Y. and Dejean A. (2000) c-Jun and p53 activity is modulated by SUMO-1 modification. *J Biol Chem* **275,** 13321-13329.

Muller S., Ronfani L. and Bianchi M. E. (2004) Regulated expression and subcellular localization of HMGB1, a chromatin protein with a cytokine function. *J Intern Med* **255,** 332-343.

Murakami T., Yasuda Y., Mita S., Maeda S., Shimada K., Fujimoto T. and Araki S. (1987) Prealbumin gene expression during mouse development studied by in situ hybridization. *Cell Differ* **22,** 1-9.

Nagata Y., Tashiro F., Yi S., Murakami T., Maeda S., Takahashi K., Shimada K., Okamura H. and Yamamura K. (1995) A 6-kb upstream region of the human transthyretin gene can direct

developmental, tissue-specific, and quantitatively normal expression in transgenic mouse. *J Biochem (Tokyo)* **117,** 169-175.

Nakamura M., Ando Y., Nagahara S., Sano A., Ochiya T., Maeda S., Kawaji T., Ogawa M., Hirata A., Terazaki H., Haraoka K., Tanihara H., Ueda M., Uchino M. and Yamamura K. (2004) Targeted conversion of the transthyretin gene in vitro and in vivo. *Gene Ther* **11,** 838-846.

Namura S., Iihara K., Takami S., Nagata I., Kikuchi H., Matsushita K., Moskowitz M. A., Bonventre J. V. and Alessandrini A. (2001) Intravenous administration of MEK inhibitor U0126 affords brain protection against forebrain ischemia and focal cerebral ischemia. *Proc Natl Acad Sci U S A* **98,** 11569-11574.

Naylor H. M. and Newcomer M. E. (1999) The structure of human retinol-binding protein (RBP) with its carrier protein transthyretin reveals an interaction with the carboxy terminus of RBP. *Biochemistry* **38,** 2647-2653.

Neeper M., Schmidt A. M., Brett J., Yan S. D., Wang F., Pan Y. C., Elliston K., Stern D. and Shaw A. (1992) Cloning and expression of a cell surface receptor for advanced glycosylation end products of proteins. *J Biol Chem* **267,** 14998-15004.

Newcomer M. E., Jones T. A., Aqvist J., Sundelin J., Eriksson U., Rask L. and Peterson P. A. (1984) The three-dimensional structure of retinol-binding protein. *Embo J* **3,** 1451-1454.

Nilsson S. F. and Peterson P. A. (1971) Evidence for multiple thyroxine-binding sites in human prealbumin. *J Biol Chem* **246,** 6098-6105.

Nordvag B. Y., Husby G., Ranlov I. and el-Gewely M. R. (1992) Molecular diagnosis of the transthyretin (TTR) Met111 mutation in familial amyloid cardiomyopathy of Danish origin. *Hum Genet* **89,** 459-461.

Noshita N., Sugawara T., Hayashi T., Lewen A., Omar G. and Chan P. H. (2002) Copper/zinc superoxide dismutase attenuates neuronal cell death by preventing extracellular signal-regulated kinase activation after transient focal cerebral ischemia in mice. *J Neurosci* **22,** 7923-7930.

Nunes A. F., Saraiva M. J. and Sousa M. M. (2006) Transthyretin knockouts are a new mouse model for increased neuropeptide Y. *Faseb J* **20,** 166-168.

Nyhlin N., Anan I., El S. M., Ando Y. and Suhr O. B. (2002) Reduction of free radical activity in amyloid deposits following liver transplantation for familial amyloidotic polyneuropathy. *J Intern Med* **251,** 136-141.

Oh-hashi K., Maruyama W., Yi H., Takahashi T., Naoi M. and Isobe K. (1999) Mitogen-activated protein kinase pathway mediates peroxynitrite-induced apoptosis in human dopaminergic neuroblastoma SH-SY5Y cells. *Biochem Biophys Res Commun* **263,** 504-509.

Olofsson A., Ippel H. J., Baranov V., Horstedt P., Wijmenga S. and Lundgren E. (2001) Capture of a dimeric intermediate during transthyretin amyloid formation. *J Biol Chem* **276,** 39592-39599.

Olofsson A., Ostman J. and Lundgren E. (2002) Amyloid: morphology and toxicity. *Clin Chem Lab Med* **40,** 1266-1270.

Palha J. A., Episkopou V., Maeda S., Shimada K., Gottesman M. E. and Saraiva M. J. (1994) Thyroid hormone metabolism in a transthyretin-null mouse strain. *J Biol Chem* **269,** 33135-33139.

Palha J. A., Moreira P., Wisniewski T., Frangione B. and Saraiva M. J. (1996) Transthyretin gene in Alzheimer's disease patients. *Neurosci Lett* **204,** 212-214.

Palha J. A., Hays M. T., Morreale de Escobar G., Episkopou V., Gottesman M. E. and Saraiva M. J. (1997) Transthyretin is not essential for thyroxine to reach the brain and other tissues in transthyretin-null mice. *Am J Physiol* **272,** E485-493.

Palha J. A., Ballinari D., Amboldi N., Cardoso I., Fernandes R., Bellotti V., Merlini G. and Saraiva M. J. (2000a) 4'-Iodo-4'-deoxydoxorubicin disrupts the fibrillar structure of transthyretin amyloid. *Am J Pathol* **156,** 1919-1925.

Palha J. A., Fernandes R., de Escobar G. M., Episkopou V., Gottesman M. and Saraiva M. J. (2000b) Transthyretin regulates thyroid hormone levels in the choroid plexus, but not in the brain parenchyma: study in a transthyretin-null mouse model. *Endocrinology* **141,** 3267-3272.

Palha J. A., Nissanov J., Fernandes R., Sousa J. C., Bertrand L., Dratman M. B., Morreale de Escobar G., Gottesman M. and Saraiva M. J. (2002) Thyroid hormone distribution in the mouse brain: the role of transthyretin. *Neuroscience* **113,** 837-847.

Park J. S., Arcaroli J., Yum H. K., Yang H., Wang H., Yang K. Y., Choe K. H., Strassheim D., Pitts T. M., Tracey K. J. and Abraham E. (2003) Activation of gene expression in human neutrophils by high mobility group box 1 protein. *Am J Physiol Cell Physiol* **284,** C870-879.

Park J. S., Svetkauskaite D., He Q., Kim J. Y., Strassheim D., Ishizaka A. and Abraham E. (2004) Involvement of toll-like receptors 2 and 4 in cellular activation by high mobility group box 1 protein. *J Biol Chem* **279,** 7370-7377.

Park L., Raman K. G., Lee K. J., Lu Y., Ferran L. J., Jr., Chow W. S., Stern D. and Schmidt A. M. (1998) Suppression of accelerated diabetic atherosclerosis by the soluble receptor for advanced glycation endproducts. *Nat Med* **4,** 1025-1031.

Parkkinen J., Raulo E., Merenmies J., Nolo R., Kajander E. O., Baumann M. and Rauvala H. (1993) Amphoterin, the 30-kDa protein in a family of HMG1-type polypeptides. Enhanced expression in transformed cells, leading edge localization, and interactions with plasminogen activation. *J Biol Chem* **268,** 19726-19738.

Pearson G., Robinson F., Beers Gibson T., Xu B. E., Karandikar M., Berman K. and Cobb M. H. (2001) Mitogen-activated protein (MAP) kinase pathways: regulation and physiological functions. *Endocr Rev* **22,** 153-183.

Pei J. J., Braak H., An W. L., Winblad B., Cowburn R. F., Iqbal K. and Grundke-Iqbal I. (2002) Up-regulation of mitogen-activated protein kinases ERK1/2 and MEK1/2 is associated with the progression of neurofibrillary degeneration in Alzheimer's disease. *Brain Res Mol Brain Res* **109,** 45-55.

Pepys M. B., Rademacher T. W., Amatayakul-Chantler S., Williams P., Noble G. E., Hutchinson W. L., Hawkins P. N., Nelson S. R., Gallimore J. R., Herbert J. and et al. (1994) Human serum

amyloid P component is an invariant constituent of amyloid deposits and has a uniquely homogeneous glycostructure. *Proc Natl Acad Sci U S A* **91,** 5602-5606.

Pepys M. B. (2001) Pathogenesis, diagnosis and treatment of systemic amyloidosis. *Philos Trans R Soc Lond B Biol Sci* **356,** 203-210; discussion 210-201.

Pepys M. B., Herbert J., Hutchinson W. L., Tennent G. A., Lachmann H. J., Gallimore J. R., Lovat L. B., Bartfai T., Alanine A., Hertel C., Hoffmann T., Jakob-Roetne R., Norcross R. D., Kemp J. A., Yamamura K., Suzuki M., Taylor G. W., Murray S., Thompson D., Purvis A., Kolstoe S., Wood S. P. and Hawkins P. N. (2002) Targeted pharmacological depletion of serum amyloid P component for treatment of human amyloidosis. *Nature* **417,** 254-259.

Peterson P. A., Nilsson S. F., Ostberg L., Rask L. and Vahlquist A. (1974) Aspects of the metabolism of retinol-binding protein and retinol. *Vitam Horm* **32,** 181-214.

Quintas A., Saraiva M. J. and Brito R. M. (1997) The amyloidogenic potential of transthyretin variants correlates with their tendency to aggregate in solution. *FEBS Lett* **418,** 297-300.

Quintas A., Saraiva M. J. and Brito R. M. (1999) The tetrameric protein transthyretin dissociates to a non-native monomer in solution. A novel model for amyloidogenesis. *J Biol Chem* **274,** 32943-32949.

Quintas A., Vaz D. C., Cardoso I., Saraiva M. J. and Brito R. M. (2001) Tetramer dissociation and monomer partial unfolding precedes protofibril formation in amyloidogenic transthyretin variants. *J Biol Chem* **276,** 27207-27213.

Rahman I., Marwick J. and Kirkham P. (2004) Redox modulation of chromatin remodeling: impact on histone acetylation and deacetylation, NF-kappaB and pro-inflammatory gene expression. *Biochem Pharmacol* **68,** 1255-1267.

Ramachandiran S., Huang Q., Dong J., Lau S. S. and Monks T. J. (2002) Mitogen-activated protein kinases contribute to reactive oxygen species-induced cell death in renal proximal tubule epithelial cells. *Chem Res Toxicol* **15,** 1635-1642.

Ramasamy R., Vannucci S. J., Yan S. S., Herold K., Yan S. F. and Schmidt A. M. (2005) Advanced glycation end products and RAGE: a common thread in aging, diabetes, neurodegeneration, and inflammation. *Glycobiology* **15,** 16R-28R.

Rask L., Anundi H. and Peterson P. A. (1979) The primary structure of the human retinol-binding protein. *FEBS Lett* **104,** 55-58.

Raz A., Shiratori T. and Goodman D. S. (1970) Studies on the protein-protein and protein-ligand interactions involved in retinol transport in plasma. *J Biol Chem* **245,** 1903-1912.

Redondo C., Damas A. M., Olofsson A., Lundgren E. and Saraiva M. J. (2000a) Search for intermediate structures in transthyretin fibrillogenesis: soluble tetrameric Tyr78Phe TTR expresses a specific epitope present only in amyloid fibrils. *J Mol Biol* **304,** 461-470.

Redondo C., Damas A. M. and Saraiva M. J. (2000b) Designing transthyretin mutants affecting tetrameric structure: implications in amyloidogenicity. *Biochem J* **348 Pt 1,** 167-172.

Reixach N., Deechongkit S., Jiang X., Kelly J. W. and Buxbaum J. N. (2004) Tissue damage in the amyloidoses: Transthyretin monomers and nonnative oligomers are the major cytotoxic species in tissue culture. *Proc Natl Acad Sci U S A* **101,** 2817-2822.

Rendon-Mitchell B., Ochani M., Li J., Han J., Wang H., Yang H., Susarla S., Czura C., Mitchell R. A., Chen G., Sama A. E., Tracey K. J. and Wang H. (2003) IFN-gamma induces high mobility group box 1 protein release partly through a TNF-dependent mechanism. *J Immunol* **170,** 3890-3897.

Reszka A. A., Bulinski J. C., Krebs E. G. and Fischer E. H. (1997) Mitogen-activated protein kinase/extracellular signal-regulated kinase 2 regulates cytoskeletal organization and chemotaxis via catalytic and microtubule-specific interactions. *Mol Biol Cell* **8,** 1219-1232.

Rethinasamy P., Muthuchamy M., Hewett T., Boivin G., Wolska B. M., Evans C., Solaro R. J. and Wieczorek D. F. (1998) Molecular and physiological effects of alpha-tropomyosin ablation in the mouse. *Circ Res* **82,** 116-123.

Richardson S. J., Bradley A. J., Duan W., Wettenhall R. E., Harms P. J., Babon J. J., Southwell B. R., Nicol S., Donnellan S. C. and Schreiber G. (1994) Evolution of marsupial and other vertebrate thyroxine-binding plasma proteins. *Am J Physiol* **266,** R1359-1370.

Riisoen H. (1988) Reduced prealbumin (transthyretin) in CSF of severely demented patients with Alzheimer's disease. *Acta Neurol Scand* **78,** 455-459.

Ritthaler U., Deng Y., Zhang Y., Greten J., Abel M., Sido B., Allenberg J., Otto G., Roth H., Bierhaus A. and et al. (1995) Expression of receptors for advanced glycation end products in peripheral occlusive vascular disease. *Am J Pathol* **146,** 688-694.

Robbins J. (1991) Thyroid hormone transport proteins and the physiology of hormone binding. In: The thyroid. Braverman LE and Utiger RD (eds). JB Lippincott Company, Philadelphia, pp 111-125.

Robinson M. J., Tessier P., Poulsom R. and Hogg N. (2002) The S100 family heterodimer, MRP-8/14, binds with high affinity to heparin and heparan sulfate glycosaminoglycans on endothelial cells. *J Biol Chem* **277,** 3658-3665.

Rong L. L., Trojaborg W., Qu W., Kostov K., Yan S. D., Gooch C., Szabolcs M., Hays A. P. and Schmidt A. M. (2004a) Antagonism of RAGE suppresses peripheral nerve regeneration. *Faseb J* **18,** 1812-1817.

Rong L. L., Yan S. F., Wendt T., Hans D., Pachydaki S., Bucciarelli L. G., Adebayo A., Qu W., Lu Y., Kostov K., Lalla E., Yan S. D., Gooch C., Szabolcs M., Trojaborg W., Hays A. P. and Schmidt A. M. (2004b) RAGE modulates peripheral nerve regeneration via recruitment of both inflammatory and axonal outgrowth pathways. *Faseb J* **18,** 1818-1825.

Rowan B. G., Weigel N. L. and O'Malley B. W. (2000) Phosphorylation of steroid receptor coactivator-1. Identification of the phosphorylation sites and phosphorylation through the mitogen-activated protein kinase pathway. *J Biol Chem* **275,** 4475-4483.

Said G., Ropert A. and Faux N. (1984) Length-dependent degeneration of fibers in Portuguese amyloid polyneuropathy: a clinicopathologic study. *Neurology* **34,** 1025-1032.

Sakaguchi T., Yan S. F., Yan S. D., Belov D., Rong L. L., Sousa M., Andrassy M., Marso S. P., Duda S., Arnold B., Liliensiek B., Nawroth P. P., Stern D. M., Schmidt A. M. and Naka Y. (2003) Central role of RAGE-dependent neointimal expansion in arterial restenosis. *J Clin Invest* **111,** 959-972.

Sakon S., Xue X., Takekawa M., Sasazuki T., Okazaki T., Kojima Y., Piao J. H., Yagita H., Okumura K., Doi T. and Nakano H. (2003) NF-kappaB inhibits TNF-induced accumulation of ROS that mediate prolonged MAPK activation and necrotic cell death. *Embo J* **22,** 3898-3909.

Santos C. R. and Power D. M. (1999) Identification of transthyretin in fish (Sparus aurata): cDNA cloning and characterisation. *Endocrinology* **140,** 2430-2433.

Santos S. D. (2005) The stress response in transthyretin amyloidosis. PhD thesis. Instituto de Ciências Biomédicas de Abel Salazar, University of Porto.

Santos S. D. and Saraiva M. J. (2005) HSF1-KO mice expressing human mutant transthyretin V30M: a novel model for familial myloidotic polyneuropathy affecting the peripheral nervous system. Abstract Viewer/Itinerary Planner. Washington, DC: Society for Neuroscience. On-line.

Saraiva M. J., Birken S., Costa P. P. and Goodman D. S. (1984) Amyloid fibril protein in familial amyloidotic polyneuropathy, Portuguese type. Definition of molecular abnormality in transthyretin (prealbumin). *J Clin Invest* **74,** 104-119.

Saraiva M. J. (2001) Transthyretin mutations in hyperthyroxinemia and amyloid diseases. *Hum Mutat* **17,** 493-503.

Saraiva M. J. (2004) Transthyretin mutations in familial amyloidotic polyneuropathy. Hot Thyroidology, http://www.hotthyroidology.com.

Sasaki H., Yoshioka N., Takagi Y. and Sakaki Y. (1985) Structure of the chromosomal gene for human serum prealbumin. *Gene* **37,** 191-197.

Sasaki H., Tone S., Nakazato M., Yoshioka K., Matsuo H., Kato Y. and Sakaki Y. (1986) Generation of transgenic mice producing a human transthyretin variant: a possible mouse model for familial amyloidotic polyneuropathy. *Biochem Biophys Res Commun* **139,** 794-799.

Sasaki H., Nakazato M., Saraiva M. J., Matsuo H. and Sakaki Y. (1989) Activity of a metallothionein-transthyretin fusion gene in transgenic mice. Possible effect of plasmid sequences on tissue-specific expression. *Mol Biol Med* **6,** 345-353.

Sasaki N., Takeuchi M., Chowei H., Kikuchi S., Hayashi Y., Nakano N., Ikeda H., Yamagishi S., Kitamoto T., Saito T. and Makita Z. (2002) Advanced glycation end products (AGE) and their receptor (RAGE) in the brain of patients with Creutzfeldt-Jakob disease with prion plaques. *Neurosci Lett* **326,** 117-120.

Sassone-Corsi P., Mizzen C. A., Cheung P., Crosio C., Monaco L., Jacquot S., Hanauer A. and Allis C. D. (1999) Requirement of Rsk-2 for epidermal growth factor-activated phosphorylation of histone H3. *Science* **285,** 886-891.

Satoh T., Nakatsuka D., Watanabe Y., Nagata I., Kikuchi H. and Namura S. (2000) Neuroprotection by MAPK/ERK kinase inhibition with U0126 against oxidative stress in a mouse neuronal cell line and rat primary cultured cortical neurons. *Neurosci Lett* **288,** 163-166.

Scaffidi P., Misteli T. and Bianchi M. E. (2002) Release of chromatin protein HMGB1 by necrotic cells triggers inflammation. *Nature* **418,** 191-195.

Schlueter C., Hauke S., Flohr A. M., Rogalla P. and Bullerdiek J. (2003) Tissue-specific expression patterns of the RAGE receptor and its soluble forms--a result of regulated alternative splicing? *Biochim Biophys Acta* **1630,** 1-6.

Schmidt A. M., Vianna M., Gerlach M., Brett J., Ryan J., Kao J., Esposito C., Hegarty H., Hurley W., Clauss M. and et al. (1992) Isolation and characterization of two binding proteins for advanced glycosylation end products from bovine lung which are present on the endothelial cell surface. *J Biol Chem* **267,** 14987-14997.

Schmidt A. M., Yan S. D., Yan S. F. and Stern D. M. (2000) The biology of the receptor for advanced glycation end products and its ligands. *Biochim Biophys Acta* **1498,** 99-111.

Schmidt A. M., Yan S. D., Yan S. F. and Stern D. M. (2001) The multiligand receptor RAGE as a progression factor amplifying immune and inflammatory responses. *J Clin Invest* **108,** 949-955.

Schmitz M. L., Mattioli I., Buss H. and Kracht M. (2004) NF-kappaB: a multifaceted transcription factor regulated at several levels. *Chembiochem* **5,** 1348-1358.

Schwaiger F. W., Hager G., Schmitt A. B., Horvat A., Hager G., Streif R., Spitzer C., Gamal S., Breuer S., Brook G. A., Nacimiento W. and Kreutzberg G. W. (2000) Peripheral but not central axotomy induces changes in Janus kinases (JAK) and signal transducers and activators of transcription (STAT). *Eur J Neurosci* **12,** 1165-1176.

Schwarzman A. L., Gregori L., Vitek M. P., Lyubski S., Strittmatter W. J., Enghilde J. J., Bhasin R., Silverman J., Weisgraber K. H., Coyle P. K. and et al. (1994) Transthyretin sequesters amyloid beta protein and prevents amyloid formation. *Proc Natl Acad Sci U S A* **91,** 8368-8372.

Sebastiao M. P., Saraiva M. J. and Damas A. M. (1998) The crystal structure of amyloidogenic Leu55 --> Pro transthyretin variant reveals a possible pathway for transthyretin polymerization into amyloid fibrils. *J Biol Chem* **273,** 24715-24722.

Seibert F. B. and Nelson J. W. (1942) Electrophoretic study of the blood protein response in tuberculosis. *J Biol Chem* **143,** 29-38.

Seo S. R., Chong S. A., Lee S. I., Sung J. Y., Ahn Y. S., Chung K. C. and Seo J. T. (2001) Zn2+-induced ERK activation mediated by reactive oxygen species causes cell death in differentiated PC12 cells. *J Neurochem* **78,** 600-610.

Serag A. A., Altenbach C., Gingery M., Hubbell W. L. and Yeates T. O. (2001) Identification of a subunit interface in transthyretin amyloid fibrils: evidence for self-assembly from oligomeric building blocks. *Biochemistry* **40,** 9089-9096.

Shaulian E. and Karin M. (2002) AP-1 as a regulator of cell life and death. *Nat Cell Biol* **4,** E131-136.

Sionov R. V. and Haupt Y. (1999) The cellular response to p53: the decision between life and death. *Oncogene* **18,** 6145-6157.

Skundric D. S. and Lisak R. P. (2003) Role of neuropoietic cytokines in development and progression of diabetic polyneuropathy: from glucose metabolism to neurodegeneration. *Exp Diabesity Res* **4,** 303-312.

Slevin M., Krupinski J., Slowik A., Rubio F., Szczudlik A. and Gaffney J. (2000) Activation of MAP kinase (ERK-1/ERK-2), tyrosine kinase and VEGF in the human brain following acute ischaemic stroke. *Neuroreport* **11,** 2759-2764.

Smith T. J., Davis F. B., Deziel M. R., Davis P. J., Ramsden D. B. and Schoenl M. (1994) Retinoic acid inhibition of thyroxine binding to human transthyretin. *Biochim Biophys Acta* **1199,** 76-80.

Snow A. D., Willmer J. and Kisilevsky R. (1987) A close ultrastructural relationship between sulfated proteoglycans and AA amyloid fibrils. *Lab Invest* **57,** 687-698.

Soares M. L., Centola M., Chae J., Saraiva M. J. and Kastner D. L. (2003) Human transthyretin intronic open reading frames are not independently expressed in vivo or part of functional transcripts. *Biochim Biophys Acta* **1626,** 65-74.

Sobue G., Nakao N., Murakami K., Yasuda T., Sahashi K., Mitsuma T., Sasaki H., Sakaki Y. and Takahashi A. (1990) Type I familial amyloid polyneuropathy. A pathological study of the peripheral nervous system. *Brain* **113 (Pt 4),** 903-919.

Soprano D. R., Herbert J., Soprano K. J., Schon E. A. and Goodman D. S. (1985) Demonstration of transthyretin mRNA in the brain and other extrahepatic tissues in the rat. *J Biol Chem* **260,** 11793-11798.

Sousa J. C., Grandela C., Fernandez-Ruiz J., de Miguel R., de Sousa L., Magalhaes A. I., Saraiva M. J., Sousa N. and Palha J. A. (2004a) Transthyretin is involved in depression-like behaviour and exploratory activity. *J Neurochem* **88,** 1052-1058.

Sousa J. C., de Escobar G. M., Oliveira P., Saraiva M. J. and Palha J. A. (2005a) Transthyretin is not necessary for thyroid hormone metabolism in conditions of increased hormone demand. *J Endocrinol* **187,** 257-266.

Sousa M. M., Berglund L. and Saraiva M. J. (2000a) Transthyretin in high density lipoproteins: association with apolipoprotein A-I. *J Lipid Res* **41,** 58-65.

Sousa M. M., Norden A. G., Jacobsen C., Willnow T. E., Christensen E. I., Thakker R. V., Verroust P. J., Moestrup S. K. and Saraiva M. J. (2000b) Evidence for the role of megalin in renal uptake of transthyretin. *J Biol Chem* **275,** 38176-38181.

Sousa M. M., Yan S. D., Stern D. and Saraiva M. J. (2000c) Interaction of the receptor for advanced glycation end products (RAGE) with transthyretin triggers nuclear transcription factor kB (NF-kB) activation. *Lab Invest* **80,** 1101-1110.

Sousa M. M., Cardoso I., Fernandes R., Guimaraes A. and Saraiva M. J. (2001a) Deposition of transthyretin in early stages of familial amyloidotic polyneuropathy: evidence for toxicity of nonfibrillar aggregates. *Am J Pathol* **159,** 1993-2000.

Sousa M. M., Du Yan S., Fernandes R., Guimaraes A., Stern D. and Saraiva M. J. (2001b) Familial amyloid polyneuropathy: receptor for advanced glycation end products-dependent triggering of neuronal inflammatory and apoptotic pathways. *J Neurosci* **21,** 7576-7586.

Sousa M. M. and Saraiva M. J. (2001) Internalization of transthyretin. Evidence of a novel yet unidentified receptor-associated protein (RAP)-sensitive receptor. *J Biol Chem* **276,** 14420-14425.

Sousa M. M. and Saraiva M. J. (2003) Neurodegeneration in familial amyloid polyneuropathy: from pathology to molecular signaling. *Prog Neurobiol* **71,** 385-400.

Sousa M. M., Ferrao J., Fernandes R., Guimaraes A., Geraldes J. B., Perdigoto R., Tome L., Mota O., Negrao L., Furtado A. L. and Saraiva M. J. (2004b) Deposition and passage of transthyretin through the blood-nerve barrier in recipients of familial amyloid polyneuropathy livers. *Lab Invest* **84,** 865-873.

Sousa M. M., do Amaral J. B., Guimaraes A. and Saraiva M. J. (2005b) Up-regulation of the extracellular matrix remodeling genes, biglycan, neutrophil gelatinase-associated lipocalin, and matrix metalloproteinase-9 in familial amyloid polyneuropathy. *Faseb J* **19,** 124-126.

Srikrishna G., Huttunen H. J., Johansson L., Weigle B., Yamaguchi Y., Rauvala H. and Freeze H. H. (2002) N -Glycans on the receptor for advanced glycation end products influence amphoterin binding and neurite outgrowth. *J Neurochem* **80,** 998-1008.

Stanciu M., Wang Y., Kentor R., Burke N., Watkins S., Kress G., Reynolds I., Klann E., Angiolieri M. R., Johnson J. W. and DeFranco D. B. (2000) Persistent activation of ERK contributes to glutamate-induced oxidative toxicity in a neuronal cell line and primary cortical neuron cultures. *J Biol Chem* **275,** 12200-12206.

Stangou A. J. and Hawkins P. N. (2004) Liver transplantation in transthyretin-related familial amyloid polyneuropathy. *Curr Opin Neurol* **17,** 615-620.

Sugimoto T., Stewart S. and Guan K. L. (1997) The calcium/calmodulin-dependent protein phosphatase calcineurin is the major Elk-1 phosphatase. *J Biol Chem* **272,** 29415-29418.

Suzuki K., Yamaguchi T., Tanaka T., Kawanishi T., Nishimaki-Mogami T., Yamamoto K., Tsuji T., Irimura T., Hayakawa T. and Takahashi A. (1995) Activation induces dephosphorylation of cofilin and its translocation to plasma membranes in neutrophil-like differentiated HL-60 cells. *J Biol Chem* **270,** 19551-19556.

Taanman J. W. (1997) Human cytochrome c oxidase: structure, function, and deficiency. *J Bioenerg Biomembr* **29,** 151-163.

Taguchi A., Blood D. C., del Toro G., Canet A., Lee D. C., Qu W., Tanji N., Lu Y., Lalla E., Fu C., Hofmann M. A., Kislinger T., Ingram M., Lu A., Tanaka H., Hori O., Ogawa S., Stern D. M. and Schmidt A. M. (2000) Blockade of RAGE-amphoterin signalling suppresses tumour growth and metastases. *Nature* **405,** 354-360.

Takahashi K., Yi S., Kimura Y. and Araki S. (1991) Familial amyloidotic polyneuropathy type 1 in Kumamoto, Japan: a clinicopathologic, histochemical, immunohistochemical, and ultrastructural study. *Hum Pathol* **22,** 519-527.

Takahashi K., Sakashita N., Ando Y., Suga M. and Ando M. (1997) Late onset type I familial amyloidotic polyneuropathy: presentation of three autopsy cases in comparison with 19 autopsy cases of the ordinary type. *Pathol Int* **47,** 353-359.

Takaoka Y., Tashiro F., Yi S., Maeda S., Shimada K., Takahashi K., Sakaki Y. and Yamamura K. (1997) Comparison of amyloid deposition in two lines of transgenic mouse that model familial amyloidotic polyneuropathy, type I. *Transgenic Res* **6,** 261-269.

Takata K., Kitamura Y., Kakimura J., Shibagaki K., Tsuchiya D., Taniguchi T., Smith M. A., Perry G. and Shimohama S. (2003) Role of high mobility group protein-1 (HMG1) in amyloid-beta homeostasis. *Biochem Biophys Res Commun* **301,** 699-703.

Takata K., Kitamura Y., Tsuchiya D., Kawasaki T., Taniguchi T. and Shimohama S. (2004) High mobility group box protein-1 inhibits microglial Abeta clearance and enhances Abeta neurotoxicity. *J Neurosci Res* **78,** 880-891.

Tanaka Y., Ando Y., Kumamoto T., Miyazaki A., Nakamura M., Nakayama M., Araki S. and Ando M. (1994) Changed affinity of apolipoprotein AII to high density lipoprotein (HDL) in patients with familial amyloidotic polyneuropathy (FAP) type I. *Biochim Biophys Acta* **1225,** 311-316.

Tawara S., Nakazato M., Kangawa K., Matsuo H. and Araki S. (1983) Identification of amyloid prealbumin variant in familial amyloidotic polyneuropathy (Japanese type). *Biochem Biophys Res Commun* **116,** 880-888.

Taylor K. R. and Gallo R. L. (2006) Glycosaminoglycans and their proteoglycans: host-associated molecular patterns for initiation and modulation of inflammation. *Faseb J* **20,** 9-22.

Teng M. H., Yin J. Y., Vidal R., Ghiso J., Kumar A., Rabenou R., Shah A., Jacobson D. R., Tagoe C., Gallo G. and Buxbaum J. (2001) Amyloid and nonfibrillar deposits in mice transgenic for wild-type human transthyretin: a possible model for senile systemic amyloidosis. *Lab Invest* **81,** 385-396.

Terazaki H., Ando Y., Misumi S., Nakamura M., Ando E., Matsunaga N., Shoji S., Okuyama M., Ideta H., Nakagawa K., Ishizaki T., Ando M. and Saraiva M. J. (1999) A novel compound heterozygote (FAP ATTR Arg104His/ATTR Val30Met) with high serum transthyretin (TTR) and retinol binding protein (RBP) levels. *Biochem Biophys Res Commun* **264,** 365-370.

Terazaki H., Ando Y., Fernandes R., Yamamura K., Maeda S. and Saraiva M. J. (2006) Immunization in familial amyloidotic polyneuropathy: counteracting deposition by immunization with a Y78F TTR mutant. *Lab Invest* **86,** 23-31.

Theodosiou A. and Ashworth A. (2002) MAP kinase phosphatases. *Genome Biol* **3,** REVIEWS3009.

Thomson S., Clayton A. L., Hazzalin C. A., Rose S., Barratt M. J. and Mahadevan L. C. (1999) The nucleosomal response associated with immediate-early gene induction is mediated via alternative MAP kinase cascades: MSK1 as a potential histone H3/HMG-14 kinase. *Embo J* **18,** 4779-4793.

Tian J. and Karin M. (1999) Stimulation of Elk1 transcriptional activity by mitogen-activated protein kinases is negatively regulated by protein phosphatase 2B (calcineurin). *J Biol Chem* **274,** 15173-15180.

Tonks N. K. (2003) PTP1B: from the sidelines to the front lines! *FEBS Lett* **546,** 140-148.

Tsuzuki T., Mita S., Maeda S., Araki S. and Shimada K. (1985) Structure of the human prealbumin gene. *J Biol Chem* **260,** 12224-12227.

Tufvesson E. and Westergren-Thorsson G. (2000) Alteration of proteoglycan synthesis in human lung fibroblasts induced by interleukin-1beta and tumor necrosis factor-alpha. *J Cell Biochem* **77,** 298-309.

Tufvesson E. and Westergren-Thorsson G. (2002) Tumour necrosis factor-alpha interacts with biglycan and decorin. *FEBS Lett* **530,** 124-128.

Vahlquist A., Rask L., Peterson P. A. and Berg T. (1975) The concentrations of retinol-binding protein, prealbumin, and transferrin in the sera of newly delivered mothers and children of various ages. *Scand J Clin Lab Invest* **35,** 569-575.

Valencia J. V., Weldon S. C., Quinn D., Kiers G. H., DeGroot J., TeKoppele J. M. and Hughes T. E. (2004) Advanced glycation end product ligands for the receptor for advanced glycation end products: biochemical characterization and formation kinetics. *Anal Biochem* **324,** 68-78.

van Bennekum A. M., Wei S., Gamble M. V., Vogel S., Piantedosi R., Gottesman M., Episkopou V. and Blaner W. S. (2001) Biochemical basis for depressed serum retinol levels in transthyretin-deficient mice. *J Biol Chem* **276,** 1107-1113.

van Jaarsveld P. P., Edelhoch H., Goodman D. S. and Robbins J. (1973) The interaction of human plasma retinol-binding protein and prealbumin. *J Biol Chem* **248,** 4698-4705.

Vatassery G. T., Quach H. T., Smith W. E., Benson B. A. and Eckfeldt J. H. (1991) A sensitive assay of transthyretin (prealbumin) in human cerebrospinal fluid in nanogram amounts by ELISA. *Clin Chim Acta* **197,** 19-25.

Veerhuis R., Janssen I., De Groot C. J., Van Muiswinkel F. L., Hack C. E. and Eikelenboom P. (1999) Cytokines associated with amyloid plaques in Alzheimer's disease brain stimulate human glial and neuronal cell cultures to secrete early complement proteins, but not C1-inhibitor. *Exp Neurol* **160,** 289-299.

Verheij M., Bose R., Lin X. H., Yao B., Jarvis W. D., Grant S., Birrer M. J., Szabo E., Zon L. I., Kyriakis J. M., Haimovitz-Friedman A., Fuks Z. and Kolesnick R. N. (1996) Requirement for ceramide-initiated SAPK/JNK signalling in stress-induced apoptosis. *Nature* **380,** 75-79.

Vieira A. V., Sanders E. J. and Schneider W. J. (1995) Transport of serum transthyretin into chicken oocytes. A receptor-mediated mechanism. *J Biol Chem* **270,** 2952-2956.

Vindis C., Seguelas M. H., Lanier S., Parini A. and Cambon C. (2001) Dopamine induces ERK activation in renal epithelial cells through H2O2 produced by monoamine oxidase. *Kidney Int* **59,** 76-86.

Wallace M. R., Naylor S. L., Kluve-Beckerman B., Long G. L., McDonald L., Shows T. B. and Benson M. D. (1985) Localization of the human prealbumin gene to chromosome 18. *Biochem Biophys Res Commun* **129,** 753-758.

Wang H., Bloom O., Zhang M., Vishnubhakat J. M., Ombrellino M., Che J., Frazier A., Yang H., Ivanova S., Borovikova L., Manogue K. R., Faist E., Abraham E., Andersson J., Andersson U., Molina P. E., Abumrad N. N., Sama A. and Tracey K. J. (1999) HMG-1 as a late mediator of endotoxin lethality in mice. *Science* **285,** 248-251.

Wautier M. P., Chappey O., Corda S., Stern D. M., Schmidt A. M. and Wautier J. L. (2001) Activation of NADPH oxidase by AGE links oxidant stress to altered gene expression via RAGE. *Am J Physiol Endocrinol Metab* **280,** E685-694.

Wei L., Kawano H., Fu X., Cui D., Ito S., Yamamura K., Ishihara T., Tokuda T., Higuchi K. and Maeda S. (2004) Deposition of transthyretin amyloid is not accelerated by the same amyloid in vivo. *Amyloid* **11,** 113-120.

Wei S., Episkopou V., Piantedosi R., Maeda S., Shimada K., Gottesman M. E. and Blaner W. S. (1995) Studies on the metabolism of retinol and retinol-binding protein in transthyretin-deficient mice produced by homologous recombination. *J Biol Chem* **270,** 866-870.

Weisner B. and Roethig H. J. (1983) The concentration of prealbumin in cerebrospinal fluid (CSF), indicator of CSF circulation disorders. *Eur Neurol* **22,** 96-105.

Westermark P., Sletten K., Johansson B. and Cornwell G. G., 3rd (1990) Fibril in senile systemic amyloidosis is derived from normal transthyretin. *Proc Natl Acad Sci U S A* **87,** 2843-2845.

Whitehead A. S., Skinner M., Bruns G. A., Costello W., Edge M. D., Cohen A. S. and Sipe J. D. (1984) Cloning of human prealbumin complementary DNA. Localization of the gene to chromosome 18 and detection of a variant prealbumin allele in a family with familial amyloid polyneuropathy. *Mol Biol Med* **2,** 411-423.

Whitmarsh A. J. and Davis R. J. (2000) A central control for cell growth. *Nature* **403,** 255-256.

Woeber K. A. and Ingbar S. H. (1968) The contribution of thyroxine-binding prealbumin to the binding of thyroxine in human serum, as assessed by immunoadsorption. *J Clin Invest* **47,** 1710-1721.

Xia Z., Dickens M., Raingeaud J., Davis R. J. and Greenberg M. E. (1995) Opposing effects of ERK and JNK-p38 MAP kinases on apoptosis. *Science* **270,** 1326-1331.

Yamamoto K., Hsu S. P., Yoshida K., Ikeda S., Nakazato M., Shiomi K., Cheng S. Y., Furihata K., Ueno I. and Yanagisawa N. (1994) Familial amyloid polyneuropathy in Taiwan: identification of transthyretin variant (Leu55-->Pro). *Muscle Nerve* **17,** 637-641.

Yamamoto K., Ikeda S., Hanyu N., Takeda S. and Yanagisawa N. (1998) A pedigree analysis with minimised ascertainment bias shows anticipation in Met30-transthyretin related familial amyloid polyneuropathy. *J Med Genet* **35,** 23-30.

Yan S. D., Schmidt A. M., Anderson G. M., Zhang J., Brett J., Zou Y. S., Pinsky D. and Stern D. (1994) Enhanced cellular oxidant stress by the interaction of advanced glycation end products with their receptors/binding proteins. *J Biol Chem* **269,** 9889-9897.

Yan S. D., Chen X., Fu J., Chen M., Zhu H., Roher A., Slattery T., Zhao L., Nagashima M., Morser J., Migheli A., Nawroth P., Stern D. and Schmidt A. M. (1996) RAGE and amyloid-beta peptide neurotoxicity in Alzheimer's disease. *Nature* **382,** 685-691.

Yan S. D., Zhu H., Zhu A., Golabek A., Du H., Roher A., Yu J., Soto C., Schmidt A. M., Stern D. and Kindy M. (2000) Receptor-dependent cell stress and amyloid accumulation in systemic amyloidosis. *Nat Med* **6,** 643-651.

Yang D. D., Conze D., Whitmarsh A. J., Barrett T., Davis R. J., Rincon M. and Flavell R. A. (1998) Differentiation of CD4+ T cells to Th1 cells requires MAP kinase JNK2. *Immunity* **9,** 575-585.

Yeh C. H., Sturgis L., Haidacher J., Zhang X. N., Sherwood S. J., Bjercke R. J., Juhasz O., Crow M. T., Tilton R. G. and Denner L. (2001) Requirement for p38 and p44/p42 mitogen-activated

protein kinases in RAGE-mediated nuclear factor-kappaB transcriptional activation and cytokine secretion. *Diabetes* **50,** 1495-1504.

Yonekura H., Yamamoto Y., Sakurai S., Petrova R. G., Abedin M. J., Li H., Yasui K., Takeuchi M., Makita Z., Takasawa S., Okamoto H., Watanabe T. and Yamamoto H. (2003) Novel splice variants of the receptor for advanced glycation end-products expressed in human vascular endothelial cells and pericytes, and their putative roles in diabetes-induced vascular injury. *Biochem J* **370,** 1097-1109.

Yuan J., Lipinski M. and Degterev A. (2003) Diversity in the mechanisms of neuronal cell death. *Neuron* **40,** 401-413.

Zhang P., Wang Y. Z., Kagan E. and Bonner J. C. (2000) Peroxynitrite targets the epidermal growth factor receptor, Raf-1, and MEK independently to activate MAPK. *J Biol Chem* **275,** 22479-22486.

Zhu J. H., Kulich S. M., Oury T. D. and Chu C. T. (2002a) Cytoplasmic aggregates of phosphorylated extracellular signal-regulated protein kinases in Lewy body diseases. *Am J Pathol* **161,** 2087-2098.

Zhu X., Lee H. G., Raina A. K., Perry G. and Smith M. A. (2002b) The role of mitogen-activated protein kinase pathways in Alzheimer's disease. *Neurosignals* **11,** 270-281.